

nuclear fusion

fusion nucléaire

ядерный синтез

fusión nuclear

**ATOMIC AND PLASMA-MATERIAL
INTERACTION DATA FOR FUSION**

(Supplement to the journal Nuclear Fusion)

VOLUME 2



INTERNATIONAL ATOMIC ENERGY AGENCY, VIENNA, 1992
AGENCE INTERNATIONALE DE L'ENERGIE ATOMIQUE, VIENNE, 1992
МЕЖДУНАРОДНОЕ АГЕНТСТВО ПО АТОМНОЙ ЭНЕРГИИ, ВЕНА, 1992
ORGANISMO INTERNACIONAL DE ENERGIA ATOMICA, VIENA, 1992

The following States are Members of the International Atomic Energy Agency:

AFGHANISTAN	HAITI	PANAMA
ALBANIA	HOLY SEE	PARAGUAY
ALGERIA	HUNGARY	PERU
ARGENTINA	ICELAND	PHILIPPINES
AUSTRALIA	INDIA	POLAND
AUSTRIA	INDONESIA	PORTUGAL
BANGLADESH	IRAN, ISLAMIC REPUBLIC OF	QATAR
BELARUS	IRAQ	ROMANIA
BELGIUM	IRELAND	RUSSIAN FEDERATION
BOLIVIA	ISRAEL	SAUDI ARABIA
BRAZIL	ITALY	SENEGAL
BULGARIA	JAMAICA	SIERRA LEONE
CAMBODIA	JAPAN	SINGAPORE
CAMEROON	JORDAN	SOUTH AFRICA
CANADA	KENYA	SPAIN
CHILE	KOREA, REPUBLIC OF	SRI LANKA
CHINA	KUWAIT	SUDAN
COLOMBIA	LEBANON	SWEDEN
COSTA RICA	LIBERIA	SWITZERLAND
COTE D'IVOIRE	LIBYAN ARAB JAMAHIRIYA	SYRIAN ARAB REPUBLIC
CUBA	LIECHTENSTEIN	THAILAND
CYPRUS	LUXEMBOURG	TUNISIA
CZECHOSLOVAKIA	MADAGASCAR	TURKEY
DEMOCRATIC PEOPLE'S REPUBLIC OF KOREA	MALAYSIA	UGANDA
DENMARK	MALI	UKRAINE
DOMINICAN REPUBLIC	MAURITIUS	UNITED ARAB EMIRATES
ECUADOR	MEXICO	UNITED KINGDOM OF GREAT BRITAIN AND NORTHERN IRELAND
EGYPT	MONACO	UNITED REPUBLIC OF TANZANIA
EL SALVADOR	MONGOLIA	UNITED STATES OF AMERICA
ESTONIA	MOROCCO	URUGUAY
ETHIOPIA	MYANMAR	VENEZUELA
FINLAND	NAMIBIA	VIET NAM
FRANCE	NETHERLANDS	YUGOSLAVIA
GABON	NEW ZEALAND	ZAIRE
GERMANY	NICARAGUA	ZAMBIA
GHANA	NIGER	ZIMBABWE
GREECE	NIGERIA	
GUATEMALA	NORWAY	
	PAKISTAN	

The Agency's Statute was approved on 23 October 1956 by the Conference on the Statute of the IAEA held at United Nations Headquarters, New York; it entered into force on 29 July 1957. The Headquarters of the Agency are situated in Vienna. Its principal objective is "to accelerate and enlarge the contribution of atomic energy to peace, health and prosperity throughout the world".

© IAEA, 1992

Permission to reproduce or translate the information contained in this publication may be obtained by writing to the Division of Publications, International Atomic Energy Agency, Wagramerstrasse 5, P.O. Box 100, A-1400 Vienna, Austria.

Printed by the IAEA in Austria
July 1992

ATOMIC AND PLASMA-MATERIAL INTERACTION DATA FOR FUSION

(Supplement to the journal Nuclear Fusion)

VOLUME 2

INTERNATIONAL ATOMIC ENERGY AGENCY, VIENNA, 1992

The volumes of ATOMIC AND PLASMA-MATERIAL INTERACTION DATA FOR FUSION are published by the International Atomic Energy Agency as supplements of the journal NUCLEAR FUSION.

For these supplements, papers, letters and reviews are accepted which deal with the following topics:

- Elementary collision processes in fusion plasmas involving photons, electrons, ions, atoms and molecules;
- Collision processes of plasma particles with surfaces of fusion relevant materials;
- Plasma-material interaction phenomena, including the thermophysical response of materials.

Each submitted contribution should contain fusion relevant data and information in either of the above areas. Original contributions should provide new data, using well established methods. Review articles should give a critical analysis or evaluation of a wider range of data. They are normally prepared on the invitation of the Scientific Editor or on prior mutual consent. Each submitted contribution is assessed by two independent referees.

Every manuscript submitted must be accompanied by a *disclaimer* stating that the paper has not been published and is not being considered for publication elsewhere. If no copyright is claimed by the authors, the IAEA automatically owns the copyright of the paper.

Guidelines for the preparation of manuscripts are given on the inside back cover. Manuscripts and correspondence should be addressed to: The Editor, NUCLEAR FUSION, International Atomic Energy Agency, Wagramerstrasse 5, P.O. Box 100, A-1400 Vienna, Austria.

Publisher:	International Atomic Energy Agency, Wagramerstrasse 5, P.O. Box 100, A-1400 Vienna, Austria	
Scientific Editor:	R.K. Janev, Atomic and Molecular Data Unit, Division of Physical and Chemical Sciences	
Editor:	C. Bobeldijk, Division of Scientific and Technical Information	
Manuscript Editors:	J.W. Weil, Division of Publications Maria Demir, Division of Publications	
Editorial Board:	V.A. Abramov (Russ. Fed.) R. Behrisch (Germany) H.-W. Drawin (France) W.B. Gauster (USA) H.B. Gilbody (UK) A. Kingston (UK) Yu.V. Martynenko (Russ. Fed.)	A. Miyahara (Japan) R.A. Phaneuf (USA) D.E. Post (USA) H.P. Summers (JET) H. Tawara (Japan) W.L. Wiese (USA)

Annual subscription price (one issue): Austrian Schillings 300,—
Airmail delivery (optional): Austrian Schillings 40,— to any destination

ATOMIC AND PLASMA-MATERIAL INTERACTION DATA FOR FUSION, VOLUME 2
IAEA, VIENNA, 1992
STI/PUB/23/APID/2

FOREWORD

The present issue of Atomic and Plasma–Material Interaction Data for Fusion is devoted to the atomic and molecular processes taking place in the edge region of magnetically confined fusion plasmas. The plasma edge region is defined as the region outside the last closed magnetic flux surface (separatrix), i.e. it includes both the scrape-off plasma and the divertor plasma. The fact that the magnetic field lines in the plasma edge region are open (i.e. they strike the containment vessel material structures) leads to a series of important consequences (intense field parallel conductive plasma flow, rapid decrease of plasma energy in the field perpendicular direction, direct plasma interaction with the material walls, etc.) which define the behaviour, parameters and composition of the edge plasma. The typical range of edge plasma temperatures is from 150–300 eV near the separatrix to 10–20 eV near the walls (or even less at the divertor plates). The typical edge plasma densities may range from 10^{12} – 10^{13} cm⁻³ (scrape-off region) to 10^{14} – 10^{15} cm⁻³ (divertor region). Owing to hydrogen recycling in the near-wall region, the neutral gas density in the plasma edge may become comparable to the plasma density. Impurities in the plasma edge, generated by plasma–wall interactions, are usually in a low charge state. The low edge plasma temperatures support the existence of molecular species in the plasma edge, resulting either from plasma–wall interaction (e.g. hydrocarbons) or from plasma fuelling (hydrogen). Under such physical conditions, the atomic physics of the plasma edge region becomes extremely complex and includes various types of atomic (ionic) and molecular radiation processes, energy loss processes (excitation, ionization and dissociation induced by particle impact), momentum transfer processes, processes that change the particle charge state (recombination, ionization, charge transfer), and processes that change the particle number (recombination, dissociation, electron and heavy particle exchange reactions), etc. Moreover, because of the high plasma and neutral particle densities in the edge region, the collision times of excited particles are comparable to their radiative lifetimes, resulting in a radiative–collisional plasma regime. All the above mentioned atomic processes have a significant impact on the plasma impurity and on neutral gas transport in the edge region, on the local plasma energy cooling rates and even on the edge plasma dynamics. There is growing evidence that the edge plasma conditions have a decisive influence on the global plasma energy confinement time, and that they determine the threshold of L-mode to H-mode transition, the features of edge localized plasma instability modes and the disruption density limit in tokamak devices. The collisional atomic and molecular processes, playing a vital role in the neutral particle transport, crucially affect the hydrogen and impurity recycling in the plasma edge, and the helium ash transport and exhaust; furthermore, together with the radiative and plasma–surface interaction processes, they have a determining impact on the divertor performance. Detailed knowledge of the cross-sections and rate coefficients of all these processes is instrumental for a better understanding and modelling of the edge plasma behaviour and for the edge plasma diagnostics.

The articles included in the present volume address the data status for some of the most important classes of plasma edge atomic collision processes and the spectroscopic database for the edge plasma constituents, and provide information on the radiative cooling rates of carbon and oxygen impurities. Most of the articles have been prepared within an IAEA Co-ordinated Research Programme on Atomic and Molecular Data for Fusion Edge Plasmas aimed at enhancing the compilation, critical evaluation and generation of the atomic data information required in plasma edge modelling and diagnostic studies.

Vienna, June 1992

R.K. Janev
Scientific Editor

CONTENTS

W.L. Wiese: Spectroscopic data for fusion edge plasmas	7
S. Trajmar: Electron collision processes with plasma edge neutrals	15
G.H. Dunn: Electron-ion collisions in the plasma edge	25
H. Tawara, Y. Itikawa, H. Nishimura, H. Tanaka, Y. Nakamura: Cross-section data for collisions of electrons with hydrocarbon molecules	41
M.A. Cacciatore, M. Capitelli, R. Celiberto: Dissociative and energy transfer reactions involving vibrationally excited H ₂ /D ₂ molecules	65
R.A. Phaneuf: Assessment of ion-atom collision data for magnetic fusion plasma edge modelling	75
T. Tabata, R. Ito, T. Shirai, Y. Nakai, H.T. Hunter, R.A. Phaneuf: Extended scaling of cross-sections for the ionization of H, H ₂ and He by multiply charged ions	91
P. Reinig, M. Zimmer, F. Linder: Ion-molecule collision processes relevant to fusion edge plasmas	95
X. Bonnin, R. Marchand, R.K. Janev: Radiative losses and electron cooling rates for carbon and oxygen plasma impurities	117

SPECTROSCOPIC DATA FOR FUSION EDGE PLASMAS

W.L. WIESE

National Institute of Standards and Technology,
Gaithersburg, Maryland,
United States of America

ABSTRACT. The status of spectroscopic data for neutral atoms and moderately charged atomic ions of interest to fusion edge plasmas is reviewed. A table is presented which lists references to all current critical compilations on energy levels, wavelengths and transition probabilities. The critical assessment of spectroscopic data is discussed mainly with respect to atomic transition probabilities, since the typical uncertainties for these are still quite large. For the specific case of neutral iron and its low ions (Fe I to Fe V) the scope and quality of evaluated spectroscopic data are discussed in detail.

1. INTRODUCTION

The physical parameters of fusion edge plasmas as well as the range of impurity ions that will be encountered in current or planned fusion plasma devices have been discussed in other papers of this volume and in the recent review paper by Janev et al. [1]. Thus, these facts need not be stated here again, but, generally, related elements and higher ions will be included in the discussion whenever this is practical and convenient.

NIST spectroscopic data centres and their services

At the National Institute of Standards and Technology, NIST (formerly the National Bureau of Standards, NBS), two data centres deal with the subject of atomic spectroscopy: the Atomic Energy Levels and Wavelengths Data Center and the Atomic Transition Probabilities Data Center.

Each of these data centres is engaged in two distinctly different activities: (a) monitoring of the current literature and maintenance of a bibliographic database, and (b) critical compilation of comprehensive numerical data tables.

A related data centre operated at NIST is the Molecular Spectra Data Center, which is primarily engaged in the tabulation of microwave spectral tables.

2. BIBLIOGRAPHICAL DATABASES AND PUBLICATIONS

The two NIST data centres on atomic spectroscopy constantly monitor the current international literature in a search for relevant papers which contain new data. In this comprehensive, all-inclusive search for new

data, all sources are collected, regardless of quality. Included are bibliographical searches for papers which contain significant comments on, or reviews of, existing data, and papers which describe the experimental and theoretical methods for obtaining such data. In each data centre, about 200 journals are scanned for new papers by utilizing the Current Contents journal [2] and, independently, Chemical Abstracts [3]. All papers with pertinent titles are examined for data relevance and content; if found to be relevant, they are classified according to species, i.e. according to chemical element and stage of ionization, and according to the type of data, the experimental or theoretical method applied, etc.

The papers are then entered into bibliographical databases maintained at these two centres. Both databases are in the process of being built up. In each case, approximately 2000 references are included for articles that appeared from the early 1980s onward. References to earlier articles still have to be added to make the databases complete.

The principal *bibliographic* publications for these two subject areas are as follows:

(a) *Atomic energy levels*: General bibliographies were published from time to time. The latest one [4] was published by the National Bureau of Standards in 1985 and a new one [5] is planned for the very near future. Much of the preparatory work has been completed. All literature references pertaining specifically to species of interest to fusion research are collected for the International Bulletin on Atomic and Molecular Data for Fusion, which is issued semi-annually by the IAEA.

(b) *Atomic transition probabilities*: The last general bibliography on atomic transition probabilities [6] was published in 1977; a supplement [7], published in 1980,

covered the period from 1977 to March 1980. No further general bibliographies have been published since then; however, like the NIST data centre for atomic energy levels, the NBS data centre regularly contributed all literature references of interest to fusion research to the semi-annual International Bulletin on Atomic and Molecular Data for Fusion of the IAEA, and it also contributed to the Transactions of the International Astronomical Union (IAU) [8] in three-year intervals. Thus, all papers with transition probabilities of interest to magnetic fusion research or astrophysics can be found in those publications.

3. CRITICAL EVALUATIONS AND COMPILATIONS OF NUMERICAL DATA

The spectroscopic data centres at NIST have operated for many years — the Atomic Energy Levels Data Center since 1946 and the Atomic Transition Probabilities Data Center since 1960. Both centres are parts of active research groups in which spectroscopic data are not only compiled but also produced by various experimental and theoretical techniques. Researchers devote portions of their time to critical data evaluation and utilize their extensive first hand knowledge of various data production approaches in data compilation work. Detailed criteria for the critical assessment of literature data have been developed and refined, of which examples are given below.

Over the years, numerous critical data tables have been produced at NIST which have become widely accepted as standard reference data works. Probably best known among them are the tables on Atomic Energy Levels by Moore [9] (which are now partially superseded by the new compilations listed in Table I).

In Table I, the *most recent* tabulations of critically evaluated wavelengths, atomic energy levels and transition probabilities are compiled, according to chemical element and in the order of increasing atomic number Z . Most of these tabulations [9–11, 13, 15–34] have been prepared at NIST, except for the wavelength tables done by Kelly [12], Striganov and Sventitskij [14] and Odintzova and Striganov [17].

The completeness and quality of the numerical material in these tables varies appreciably from spectrum to spectrum, especially with regard to transition probabilities. As an example, in Table II some statistics on the evaluated numerical material for the lower spectra of iron are given, since these are of strong interest for fusion edge plasmas. It is seen that the numerical data on the three major spectroscopic quantities decrease

TABLE I. REFERENCES FOR THE MOST RECENT CRITICAL DATA TABLES ON WAVELENGTHS, ENERGY LEVELS AND TRANSITION PROBABILITIES

Z	Element	Data tabulations on		
		Wavelengths ^a	Energy levels	Transition probabilities
1	H, D, T	10	10	11
2	He	12, 13, 14	15, 16	11
3	Li	12, 13, 14	9	11
4	Be	12, 13	9	11
5	B	12, 13, 17	17	11
6	C	12–14, 18	18	11
7	N	12–14, 19	19	11
8	O	12–14, 20	20	11
9	F	12, 13, 14	9	11
10	Ne	12, 13, 14	9	11
11	Na	12, 13, 14	21	22
12	Mg	12, 13, 14	23	22
13	Al	12, 13, 14	24	22
14	Si	12, 13, 14	25	22
15	P	12, 13	26	22
16	S	12, 13	27	23
17	Cl	12, 13, 14	9	22
18	Ar	12, 13, 14	9	22
19	K	12, 13, 14	28	22
20	Ca	12, 13, 14	28	22
21	Sc	29	28	30
22	Ti	12, 13, 14	28	30
23	V	12, 13	28	30
24	Cr	12, 13	28	30
25	Mn	12, 13	28	30
26	Fe	12, 13, 14	28	31
27	Co	12, 13	28	31
28	Ni	12, 13	28	31
29	Cu	12, 13, 14	32	33
30	Zn	12, 13	9	33
31	Ga	12, 13	9	33
32	Ge	12, 13	9	33
33	As	12, 13	9	33
34	Se	12, 13	9	33
35	Br	12, 13	9	33
36	Kr	12, 13, 14	9	33

For elements heavier than $Z = 36$:

Wavelength data: Ref. [13].
 Energy level data: Ref. [9] (Vols 2 and 3);
 Ref. [34], molybdenum;
 Ref. [35], rare earths,
 La–Lu ($Z = 57–71$).

Transition probability data: Ref. [33]

^a For many heavier elements, two older wavelength tables by Meggers et al. [36] and by Moore [37] are more extensive than those in Refs [12, 13 and 14] and should therefore also be used. However, the data in the new tables always supersede the older compilations.

TABLE II. EXTENT AND QUALITY OF CRITICALLY EVALUATED SPECTROSCOPIC DATA FOR THE IRON ATOM AND ITS LOWER IONS

Spectrum	Wavelengths			Energy levels		Transition probabilities			
	Number of lines listed			Sugar and Corliss [28] (1985)		Fuhr, Martin and Wiese [31] (1988)			
						Allowed (E1) lines		Forbidden (M1, E2) lines	
	Kelly [12], VUV lines (1987)	Striganov and Sventitskij [14] (1968)	Reader and Corliss [13] (1990)	Number of levels	Highest level listed (quantum numbers)	Total No. of lines	Lines with uncertainties of $\leq 25\%$	Total No. of lines	Lines with uncertainties of $\leq 25\%$
Fe I	54	1165	738	491	5d, 7s	1948	1241	103	0
Fe II	1456	747	405	577	5d, 6s	646	115	356	14
Fe III	922	427	180	550	6h, 7s	60	0	31	0
Fe IV	1285	73	156	276	4p	—	—	88	0
Fe V	1085	145	148	180	4p	—	—	53	0

significantly in volume from the neutral spectrum to the fifth stage of ionization, especially for transition probabilities. For these, no reliable data exist at all for Fe IV and Fe V for the normal electric dipole ('allowed') transitions, but some data are available for magnetic dipole and electric quadrupole ('forbidden') lines. For atomic energy levels, precise experimental data exist only for the low level configurations.

Some of the tabulations cited in Table I are rather old and need to be revised and enlarged with the newly available literature material. Unfortunately, this large task — involving often many thousands of transitions per element, sometimes even per spectrum — will take years to accomplish, considering the small workforce in the NIST data centres and the increasing amounts of accurate data.

Some new literature references [38–44] containing large amounts of good quality data, which are of strong interest for fusion edge plasmas, are collected in Table III and the relevant spectra are identified.

At this point, it should be noted that the above mentioned NIST Molecular Spectra Data Center has compiled tables on the spectra of molecular oxygen [45], nitrogen [46] and carbon monoxide [47]. For other diatomic molecules, the tables by Huber and Herzberg [48] should be used.

4. DATA ASSESSMENT

As noted before, the critical assessment of the literature data is the key step for selecting a 'best' set of evaluated data. With respect to atomic energy levels, it was realized early on that, except for the simplest atomic systems (He- and H-like ions), *experimental* observations of wavelengths in combination with the Ritz principle [49] produce the most accurate, internally fully consistent sets of level data. Therefore, nearly all data for energy levels are selected from spectral observations with laboratory or, sometimes, solar sources.

Atomic transition probabilities are subject to especially large uncertainties; often, these were found to be even worse than the authors' estimates, as seen from numerous discrepancies between supposedly high quality experimental (as well as theoretical) results in the literature. Therefore, all transition probability data need to be critically evaluated according to a uniform set of general criteria.

At the NIST data centre, five main criteria have been developed [11, 22] and are consistently applied:

- (1) A general evaluation of the applied method;
- (2) The authors' consideration of the 'critical factors' in each experimental or theoretical approach;

TABLE III. RECENT HIGH QUALITY DETERMINATIONS OF LARGE AMOUNTS OF ATOMIC SPECTROSCOPY DATA^a

Spectrum	Authors
(a) Wavelengths and energy levels	
V II	Iglesias and Cabeza [38]
Fe I	Brown et al. [39]
Fe II	Johansson and Baschek [40]
(b) Atomic transition probabilities	
He through Ne, all stages of ionization	Results of "Opacity Project"; latest paper by Luo and Pradhan [41] (earlier papers referenced therein)
Ar I	Wiese et al. [42]
Mo I	Whaling and Brault [43]
W I	Den Hartog et al. [44]

^a This listing is limited to spectra of interest for fusion edge plasmas.

- (3) The authors' uncertainty estimates (these are only available for experimental data);
- (4) The extent of agreement or disagreement with other reliable data;
- (5) The degree of fit of the data into systematic trends.

Of key importance is the second criterion, i.e. the 'critical factors' of each method, which are discussed below and which need to be adequately taken into account in order to be sure that uncertainties are minimized.

For the three main approaches to determining transition probabilities or the related atomic lifetimes, the 'critical factors' are as follows (see Ref. [22] for more details and further references):

Emission method

Validity of the plasma model applied for the emission source. Usually, the local thermodynamic equilibrium (LTE) model is used and optically thin conditions for the line emission are assumed. Tests are available to check the validity of these assumptions. Moderate deviations from the optically thin condition, i.e. limited self-absorption, can be accurately corrected.

Accurate plasma diagnostics for the determination of the particle densities and temperature of the emission source.

A well defined and stable emission source, which is homogeneous in the line of sight, with temporal and spatial stability and with small boundary layers.

Accurate absolute line intensity measurements that include contributions from the extended line wings and are based on accurate absolute radiometric standards.

Atomic lifetime determinations

Absence of, or corrections for, radiation trapping and collisional effects. These are usually tested and treated by variation of the density. Density dependent results are extrapolated to zero density.

Absence of, or consideration of, cascading effects, i.e. consideration of possible repopulation of the measured level from higher levels. Cascading must be corrected by such approaches as the arbitrarily normalized direct cascades (ANDC) technique, while fittings to two or three exponential decays are not adequate.

Quantum mechanical calculations

Consideration of configuration interaction due to correlation between the atomic electrons. Correlation effects are especially strong for transitions that involve equivalent electrons in the upper or lower state. In this case, multiconfigurational treatments, such as the multiconfigurational Hartree-Fock (MCHF) method, are required to adequately describe the atomic structure. The quality of the results may be tested by adding interacting configurations in a stepwise manner and by checking for gradual convergence of the data. Close agreement between the results for the length and velocity forms of the transition integral is also a useful (but not sufficient) indicator. Single configuration treatments are adequate only for transitions where the jumping electron is far removed from the core electrons. In semi-empirical approaches, the choice of experimental energy levels accounts partially for multiconfigurational effects.

Unusually small transition integrals, especially among comparable transitions, are sometimes an indication of accidental near-cancellation of positive and negative contributions to the integral which will make the results very unreliable. Thus, the ratio of the positive parts to the negative parts should always be determined and checked.

Strengths of individual lines are difficult to determine when intermediate coupling rather than the usual LS coupling prevails. Comparisons with *relative* experimental line strength data, which are normally quite accurate, are important to assess the coupling situation.

Relativistic effects become significant for highly stripped ions as well as for heavy neutral atoms, as many studies have shown. Therefore, relativistic treatments, such as the Dirac-Hartree-Fock (DHF) approach, have to be applied for these species.

Studies of systematic trends of oscillator strengths for given transitions along isoelectronic sequences often provide additional insight into regular or irregular behaviour as well as added possibilities for comparisons.

As an example, we consider the situation with respect to reliable transition probability data for the neutral iron atom and the lower ions of iron. Table II illustrates that the number of known *reliable* data — i.e. data estimated to be accurate to 25% or better — drastically decreases from the neutral atom to Fe IV, for which no reliable material on ‘allowed’ (electric dipole) lines exists.

For Fe I, good data are available for about 2000 lines of moderate and high line strengths, mainly in the near ultraviolet and visible ranges of the spectrum. Relative transition probability (or oscillator strength) data from several emission and absorption experiments, normalized to the same scale, are usually consistent within the combined error limits, which are typically about $\pm 25\%$. Figure 1 illustrates the satisfactory agreement between the stabilized arc emission experiment of Bridges and Kornblith [50] and the electric furnace absorption work by Blackwell et al. [51, 52] (the latter work has provided especially precise data, with uncertainties within only a few per cent). The absolute scale for these data — as well as for additional material from other emission work — has been based on the mean value of seven atomic lifetime (τ) or oscillator strength determinations [53–59] of the upper level of the principal resonance line, as shown in Table IV. The results have yielded an absolute transition probability with an uncertainty of only $\pm 2\%$ (99% confidence limit), thus producing an excellent normalization point for the relative data.

For Fe II, the available experimental transition probability data are much reduced, because Fe II ions in excited states are more difficult to generate than neutral iron. Most experimental investigations are emission measurements with a variety of radiation sources [60–65], including the sun. The principal data source is the wall stabilized arc experiment by Moity [60], which has provided about two thirds of the data, but is estimated to be only moderately accurate, providing results with uncertainties barely within $\pm 50\%$. For Fe II, some data in the NIST tables were also selected from the large scale semi-empirical calculations by

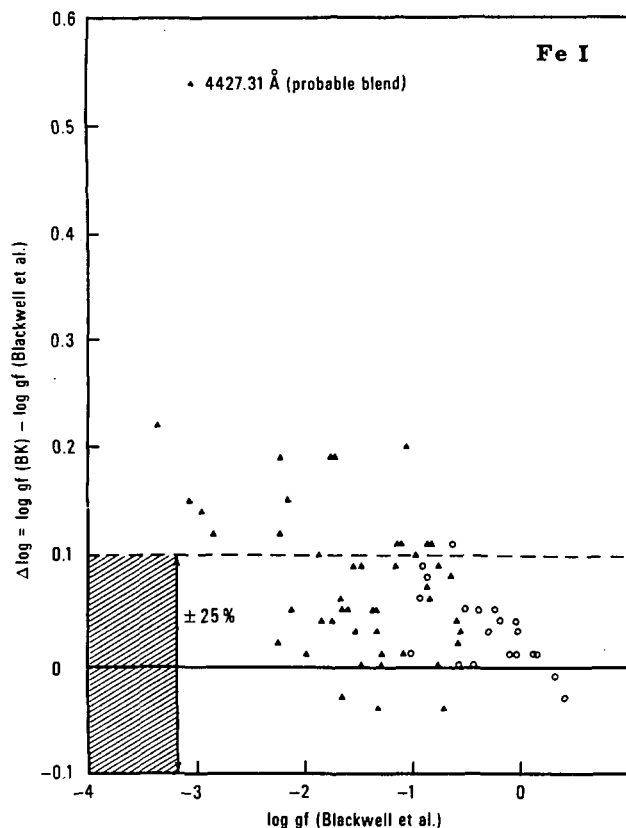


FIG. 1. Comparison between the Fe I emission data of Bridges and Kornblith [50] (BK) and the absorption data of Blackwell et al. [51, 52]. Plotted are the differences $\log gf$ (BK) — $\log gf$ (Blackwell et al.) versus $\log gf$ (Blackwell et al.), where g is the statistical weight of the lower state of the various Fe I lines which are compared and f is the oscillator strength. Open circles are used for all lines for which the f -values of BK are estimated to be accurate within $\pm 10\%$, while solid triangles are used for lines with uncertainties estimated within $\pm 25\%$. Many Blackwell f -value data are estimated to be within $\pm 1\%$ on a relative scale.

Kurucz [66]. Kurucz’s method is especially suited to Fe II, since he could utilize a new, comprehensive set of observed energy level data for his semi-empirical approach. Figure 2 shows the fair agreement between Kurucz’s results for the *stronger* lines and the experimental data that were used in the recent NIST tabulation [31].

For Fe III, only two data sources for transition probabilities are available: the semi-empirical calculations by Kurucz and Peytremann [67] and similar calculations by Biemont [68]. For the stronger lines, the two calculations usually agree within 50%. A limited assessment of these data may be undertaken by comparing them with some lifetime results of Anderson et al. [69]. On average, the beam foil lifetimes are about 14% larger than the relevant inverse transition

TABLE IV. SELECTED LIFETIME OSCILLATOR STRENGTH DATA FOR THE Fe I RESONANCE LEVEL AND LINE

Reference	Lifetime τ (ns) of the $z \ ^3F_5^o$ level	Oscillator strength of the 3719.93 Å line
Wagner and Otten [53]	59.5 ± 1.6	0.0425
Klose [54]	61.5 ± 0.4	0.0413
Hilborn and De Zafra [55]	63.2 ± 3.6	0.0400
Brzozowski et al. [56]	60.5 ± 1.5	0.0418
Marek et al. [57]	62.4 ± 4.2	0.0405
Hannaford and Lowe [58]	61.0 ± 1.0	0.0414
Bell and Tubbs [59]		0.041 ± 0.003

Average f-value = 0.0412 ± 0.000311 .

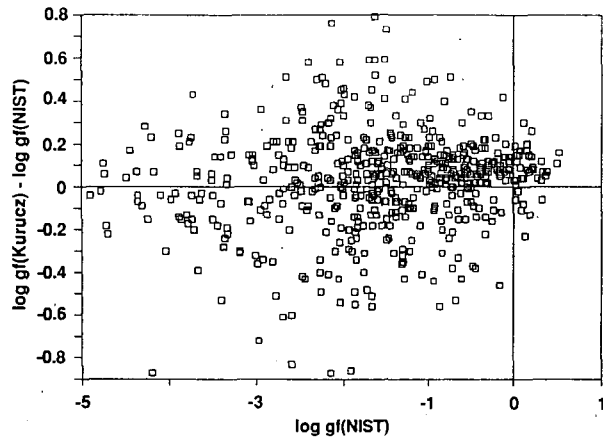


FIG. 2. Plot of $\log gf$ (Kurucz) — $\log gf$ (NIST) for Fe II lines versus $\log gf$ (NIST), where Kurucz is Ref. [66] and NIST is Ref. [31].

probability sums from the calculations, which must be considered good agreement; thus, these lines are included in the critical tables.

For the next two ions, Fe IV and Fe V, no reliable transition probability data are available at all for the allowed (electric dipole) lines. Only the data of Kurucz and Peytremann [67] — which do not compare well with experimental data for similar spectra — are available and are estimated to be of moderate to poor accuracy. (Very recently, new calculated data for numerous Fe IV and Fe V lines have been published by Fawcett [70]; these data are based on a multi-configuration Hartree-Fock-Slater code. In the absence of experimental comparison data, it is difficult to

assess their accuracy, but, in view of a normalization problem [70], typical accuracies are estimated to be no better than $\pm 50\%$ and worse for weak lines.)

5. SUMMARY AND OUTLOOK

Data evaluation and compilation work at the NIST data centres is currently concentrated on the following chemical elements:

Atomic energy levels: Elements of the third period, nuclear charges $Z = 11-18$.

Wavelengths: Elements of the second and third periods.

Transition probabilities: Lightest ten elements, $Z = 1-10$ (H-Ne).

It is planned to publish the data tables in book form and on diskettes. Also, a comprehensive numerical database on spectroscopic data for all elements — which will include data for the three above listed quantities plus various ancillary data — will be constructed and operated. Diskettes containing the numerical data will be made available with retrieval software.

REFERENCES

- [1] JANEV, R.K., HARRISON, M.F.A., DRAWIN, H.W., Nucl. Fusion **29** (1989) 109.
- [2] Current Contents (Physical, Chemical and Earth Sciences), Institute for Scientific Information, Philadelphia, PA.
- [3] Chemical Abstracts, American Chemical Society, Columbus, Ohio (since 1907).
- [4] MUSGROVE, A., ZALUBAS, R., Natl. Bur. Stand. (US), Spec. Publ. 363, Suppl. 3 (1985).
- [5] MUSGROVE, A., ZALUBAS, R., Natl. Bur. Stand. (US), Spec. Publ. 363, Suppl. 4 (1991).
- [6] FUHR, J.R., MILLER, B.J., MARTIN, G.A., Natl. Bur. Stand. (US), Spec. Publ. 505 (1978).
- [7] MILLER, B.J., FUHR, J.R., MARTIN, G.A., Natl. Bur. Stand. (US), Spec. Publ. 505, Suppl. 1 (1980).
- [8] WIESE, W.L., in Reports on Astronomy, Vol. XX A (1988) 117, Vol. XIX A (1985) 122, Vol. XVIII A (1982) 116, Kluwer Acad. Publ., Dordrecht.
- [9] MOORE, C.E., Atomic Energy Levels, Natl. Bur. Stand. (US) Ref. Data Ser. **35** Vols 1-3 (1971) (reprint of NBS Circ. 467), US Govt. Printing Office, Washington, DC.
- [10] MOORE, C.E., Natl. Bur. Stand. (US) Ref. Data Ser. **3** Sect. 6 (1972).
- [11] WIESE, W.L., SMITH, M.W., GLENNON, B.M., Natl. Bur. Stand. (US) Ref. Data Ser. **4** (1966).

- [12] KELLY, R.L., *J. Phys. Chem. Ref. Data* **16**, Suppl. 1 (1987).
- [13] READER, J., CORLISS, C.H. (Eds), *Handbook of Chemistry and Physics*, 71st edn, CRC Press, Boca Raton, FL (1990).
- [14] STRIGANOV, A.R., SVENITSKIJ, N.S., *Tables of Spectral Lines of Neutral and Ionized Atoms*, IFI/Plenum Press, New York (1968).
- [15] MARTIN, W.C., *J. Phys. Chem. Ref. Data* **2** (1973) 257.
- [16] MARTIN, W.C., *Phys. Rev., A* **36** (1987) 3575.
- [17] ODINTZOVA, G.A., STRIGANOV, A.R., *J. Phys. Chem. Ref. Data* **8** (1979) 63.
- [18] MOORE, C.E., *Natl. Bur. Stand. (US) Ref. Data Ser. 3 Sect. 3* (1970).
- [19] MOORE, C.E., *Natl. Bur. Stand. (US) Ref. Data Ser. 3 Sect. 4* (1972) and *Sect. 5* (1975).
- [20] MOORE, C.E., *Natl. Bur. Stand. (US) Ref. Data Ser. 3 Sect. 7* (1976); *Sect. 8* (1979); *Sect. 9* (1998); *Sect. 10* (1982); *Sect. 11* (1985).
- [21] MARTIN, W.C., ZALUBAS, R., *J. Phys. Chem. Ref. Data* **10** (1981) 152.
- [22] WIESE, W.L., SMITH, M.W., MILES, B.M., *Natl. Bur. Stand. (US) Ref. Data Ser. 22* (1969).
- [23] MARTIN, W.C., ZALUBAS, R., *J. Phys. Chem. Ref. Data* **9** (1980) 1.
- [24] MARTIN, W.C., ZALUBAS, R., *J. Phys. Chem. Ref. Data* **8** (1979) 817.
- [25] MARTIN, W.C., ZALUBAS, R., *J. Phys. Chem. Ref. Data* **12** (1983) 323.
- [26] MARTIN, W.C., ZALUBAS, R., MUSGROVE, A., *J. Phys. Chem. Ref. Data* **14** (1985) 751.
- [27] MARTIN, W.C., ZALUBAS, R., MUSGROVE, A., *J. Phys. Chem. Ref. Data* **19** (1990) 821.
- [28] SUGAR, J., CORLISS, C., *J. Phys. Chem. Ref. Data* **14**, Suppl. 2 (1985).
- [29] KAUFMAN, V., SUGAR, J., *J. Phys. Chem. Ref. Data* **17** (1988) 1679.
- [30] MARTIN, G.A., FUHR, J.R., WIESE, W.L., *J. Phys. Chem. Ref. Data* **17**, Suppl. 3 (1988).
- [31] FUHR, J.R., MARTIN, G.A., WIESE, W.L., *J. Phys. Chem. Ref. Data* **17**, Suppl. 4 (1988).
- [32] SUGAR, J., MUSGROVE, A., *J. Phys. Chem. Ref. Data* **19** (1990) 527.
- [33] WIESE, W.L., MARTIN, G.A., *Handbook of Chemistry and Physics*, 70th edn, CRC Press, Boca Raton, FL (1989).
- [34] SUGAR, J., MUSGROVE, A., *J. Phys. Chem. Ref. Data* **17** (1988) 155.
- [35] MARTIN, W.C., ZALUBAS, R., HAGAN, L., *Natl. Bur. Stand. (US) Ref. Data Ser. 60* (1978).
- [36] MEGGERS, W.F., CORLISS, C.H., SCRIBUER, B.F., *Natl. Bur. Stand. (US) Monogr.* **145** (1975).
- [37] MOORE, C.E., *Natl. Bur. Stand. (US) Ref. Data Ser. 40* (1972); *Natl. Bur. Stand. (US) Circ.* **488** (1968) Sect. 1-5.
- [38] IGLESIAS, L., CABEZA, M.I., *Opt. Pura y Apl.* **21** (1988) 139.
- [39] BROWN, C.M., GINTER, M.L., JOHANSSON, S., TILFORD, S.G., *J. Opt. Soc. Am., B* **5** (1988) 2125.
- [40] JOHANSSON, S., BASCHEK, B., *Nucl. Instrum. Methods, B* **31** (1988) 222.
- [41] LUO, D., PRADHAN, A.K., *J. Phys., B* **22** (1989) 3377. (This is No. XI of the Opacity Project papers, and earlier papers of this series are cited therein.)
- [42] WIESE, W.L., BRAULT, J.W., DANZMANN, K., HELBIG, V., KOCK, M., *Phys. Rev., A* **39** (1989) 2461.
- [43] WHALING, W., BRAULT, J.W., *Phys. Scr.* **38** (1988) 707.
- [44] DEN HARTOG, E.A., LAWLER, J.E., DUQUETTE, D.W., *J. Opt. Soc. Am., B* **4** (1987) 48.
- [45] KRUPENIE, P.H., *J. Phys. Chem. Ref. Data* **1** (1972) 423.
- [46] LOFTUS, A., KRUPENIE, P.H., *J. Phys. Chem. Ref. Data* **6** (1977) 113.
- [47] KRUPENIE, P.H., *Natl. Bur. Stand. (US) Ref. Data Ser. 5* (1966).
- [48] HUBER, K.P., HERZBERG, G., *Molecular Spectra and Molecular Structure*, Vol. 4, Van Nostrand Reinhold, New York (1979).
- [49] WHITE, H.E., *Introduction to Atomic Spectra*, McGraw-Hill, New York (1934).
- [50] BRIDGES, J.M., KORNBLITH, R.L., *Astrophys. J.* **192** (1974) 793.
- [51] BLACKWELL, D.E., IBBETSON, P.A., PETFORD, A.D., SHALLIS, M.J., *Mon. Not. R. Astron. Soc.* **186** (1979) 633.
- [52] BLACKWELL, D.E., PETFORD, A.D., SHALLIS, M.J., *Mon. Not. R. Astron. Soc.* **186** (1979) 657.
- [53] WAGNER, R., OTTEN, E.W., *Z. Phys.* **220** (1969) 349.
- [54] KLOSE, J.Z., *Astrophys. J.* **165** (1971) 637.
- [55] HILBORN, R.C., DE ZAFRA, R., *Astrophys. J.* **183** (1973) 347.
- [56] BRZozowski, J., ERMAN, P., LYYRA, M., SMITH, W.H., *Phys. Scr.* **14** (1976) 48.
- [57] MAREK, J., RICHTER, J., STAHNKE, H.-J., *Phys. Scr.* **19** (1979) 325.
- [58] HANNAFORD, P., LOWE, R.M., *J. Phys., B* **14** (1981) L5.
- [59] BELL, G.D., TUBBS, E.F., *Astrophys. J.* **159** (1970) 1093.
- [60] MOITY, J., *Astron. Astrophys., Suppl. Ser.* **52** (1983) 37.
- [61] WHALING, W., *Atomic Transition Probabilities for Fe II*, Tech. Rep. 84A, California Institute of Technology, Pasadena, CA (1984).
- [62] BRIDGES, J.M., in *Phenomena in Ionized Gases* (Proc. 11th Int. Conf. Prague, 1973), contributed papers, Institute of Plasma Physics, Czechoslovak Academy of Sciences, Prague (1973) 418.
- [63] BASCHEK, B., GARZ, T., HOLWEGER, H., RICHTER, J., *Astron. Astrophys.* **4** (1970) 229.
- [64] BLACKWELL, D.E., SHALLIS, M.J., SIMMONS, G.J., *Astron. Astrophys.* **81** (1980) 340.
- [65] KOSTYK, R.I., ORLOVA, T.V., *Astrometriya Astrofiz.* **47** (1982) 32.
- [66] KURUCZ, R.L., *Smithson. Astrophys. Observ. Spec. Rep.* **390** (1981).
- [67] KURUCZ, R.L., PEYTRMANN, E., *Smithson. Astrophys. Observ. Spec. Rep.* **362** (1975).
- [68] BIEMONT, E., *J. Quant. Spectrosc. Radiat. Transfer* **16** (1976) 137.
- [69] ANDERSON, T., PETERSON, P., BIEMONT, E., *J. Quant. Spectrosc. Radiat. Transfer* **17** (1977) 389.
- [70] FAWCETT, B.C., *At. Data Nucl. Data Tables* **41** (1989) 181.

ELECTRON COLLISION PROCESSES WITH PLASMA EDGE NEUTRALS

S. TRAJMAR

Jet Propulsion Laboratory,
California Institute of Technology,
Pasadena, California,
United States of America

ABSTRACT. Experimental techniques for measuring electron-atom (molecule) collision cross-sections, which are needed in studies of fusion edge plasmas, are briefly described. A survey of available data is given and gaps in the required database are pointed out. A few remarks on the present status of the theory for calculating electron collision cross-sections are made and it is emphasized that a joint experimental and theoretical effort is required for substantial progress in satisfying the data needs.

1. INTRODUCTION

In general, the atomic and molecular database needs for studies of fusion edge plasmas have been discussed extensively [1-5]. Here we are concerned with the status of cross-section data for electron impact excitation of neutral atomic and molecular species. The term electron impact excitation is used in a broad sense, including elastic scattering, momentum transfer and total electron scattering, as well as the large variety of specific excitation channels. Excitations to the electronic continua (ionization) are treated by others in this volume. Inner electron shell and multi-electron excitations do not play an important role in edge plasmas and are omitted. The species considered here are: the H, C, O, rare gas (He, Ne, Ar, Kr, Xe) and metal (Li, Be, Al, Si, Ti, V, Cr, Fe, Ni, Cu, Ga, Zr, Mo, Ta, W) atoms, and the H₂, CO, N₂, O₂, H₂O and CO₂ molecules. Electron collision processes involving hydrocarbon molecules are treated separately by H. Tawara in this volume.

2. DEFINITION OF CROSS-SECTIONS

The cross-sections of interest to us are the experimental differential cross-section (DCS_n), the integral cross-section (Q_n), the momentum transfer cross-section (Q^M) and the total electron scattering cross-section (Q_{TOT}) as defined below.

$$\text{DCS}_n(E_0, \theta) = \frac{d\sigma_n(E_0, \Omega)}{d\Omega} \quad (1)$$

$$Q_n(E_0) = 2\pi \int_0^\pi \text{DCS}_n(E_0, \theta) \sin \theta d\theta \quad (2)$$

$$Q^M(E_0) = 2\pi \int_0^\pi \text{DCS}_0(E_0, \theta) (1 - \cos \theta) \sin \theta d\theta \quad (3)$$

$$Q_{\text{TOT}}(E_0) = Q_{\text{ion}}(E_0) + \sum_n Q_n(E_0) \quad (4)$$

where E₀ is the electron impact energy, θ is the scattering polar angle and Ω is the solid angle. The sub-index n specifies the excitation processes and n = 0 refers to elastic scattering; σ designates the ideal experimental or theoretical integral cross-section for a well defined process. The bar above the right hand side of Eq. (1) indicates integration over the energy loss profile, averaging over instrumental energy and angular resolutions and the usual statistical averaging over experimentally indistinguishable sublevels. The azimuthal scattering angle dependence disappears because we are dealing with randomly oriented target species.

Theoretical calculations yield the complex scattering amplitude which is related to the differential cross-sections as

$$\frac{d\sigma_n(E_0, \Omega)}{d\Omega} = \frac{k_n}{k_0} |f_n(E_0, \Omega)|^2 \quad (5)$$

where k₀ and k_n are the initial and final momenta of the free electron.

3. METHODS OF MEASUREMENTS

Differential cross-section measurements are carried out by crossing the target molecular beam (or static gas cell) with a nearly monoenergetic electron beam, usually at 90° , and determining the energy and angular distribution of the scattered electrons. These distributions contain the information on the nature of the electron collision processes, the energy level scheme of the target and the corresponding cross-sections. Sometimes, secondary particles generated in the collision are detected to extract information on a particular process (or the scattered electrons are detected in coincidence with secondary particles to obtain more detailed information). One customary way to represent the scattering data is by the energy loss spectra, which is a representation of the scattering intensity as a function of the energy lost by the electron. The energy loss values of features characterize the energy level scheme of the target, and the scattering intensities are related to the corresponding DCS_n . An energy loss spectrum is similar to a photoabsorption spectrum, and, indeed, it can be shown that at the limit of zero momentum transfer (high impact energy, small scattering angle) these two spectra become equivalent. In general, however, dipole selection rules do not apply to electron impact excitation. Spin- and symmetry-forbidden transitions readily occur in electron collision at low impact energies and high scattering angles. The energy loss spectra of molecules are complex because of vibrational-rotational structure and transitions associated with dissociating electronic states. The major difficulties in extracting DCS_n from energy loss spectra are: (1) the decomposition of the heavily overlapping structure of molecular energy loss spectra into contributions from individual processes, and (2) the determination of the precise scattering geometry and of the target and electron beam fluxes or, equivalently, the establishment of a calibration procedure for converting the measured scattering intensities to absolute DCS_n . This is not a simple task, especially at low impact energies. The most practical method is to carry out relative scattering measurements for the test gas and for a standard gas under identical conditions, and to utilize the known DCS_n for the standard gas to normalize the relative DCS_n of the test gas. The standard gas is usually helium, for which the elastic cross-sections are well established. For more details see Refs [6–8].

From the DCS_n , one can obtain the integral and, in the case of elastic scattering, the momentum transfer cross-sections. Integral cross-sections for excitation processes can also be obtained from measuring the

photon emission subsequent to the electron impact excitation. The line emission (or optical excitation) cross-sections can be converted, with the appropriate branching ratios, into apparent excitation cross-sections which contain both the direct electron impact excitation and all cascade contributions. The apparent excitation cross-sections can be converted to electron impact excitation cross-sections if cascade can be properly accounted for. In ionization measurements (including dissociative ionization and attachment) it is convenient to monitor the ion yield and to extract cross-sections from these signals. Although dissociation processes leading to excited or ionic products have been extensively studied by monitoring photon emission or ion yields, not much information is available on dissociation into neutral ground-state fragments. This is mainly due to the experimental difficulties of detecting low energy neutral fragment species. There are very encouraging developments in this area, however. Dissociations in fast neutral beams produce fast neutral fragments which can be conveniently detected by charge particle detectors [9, 10].

Total electron collision cross-sections have been measured with an accuracy of a few per cent by various types of transmission-attenuation experiments. They are important for modelling efforts and, in addition, because of their high accuracy, they can serve as checks on other cross-sections through Eq. (4).

At very low electron impact energies, beam techniques are difficult. Cross-section information at these energies has been obtained by swarm techniques, which can yield total electron scattering and momentum transfer cross-sections with high accuracy ($\sim 3\%$). Integral inelastic cross-sections can also be deduced from swarm measurements, but this procedure becomes ambiguous when more than a very few channels are open. Unfortunately, this is the case for molecules at a rather low impact energy. The energy ranges amenable to beam and swarm techniques overlap, and the two types of measurement not only yield complementary information but also serve to cross-check each other. The relationship between the single collision beam studies and the multiple collision swarm measurements is discussed in Ref. [11].

4. REVIEW OF CROSS-SECTION DATA

A number of comprehensive reviews on electron collision cross-sections [12–16] and optical excitation functions (optical excitation cross-sections as a func-

tion of electron impact energy) [17–19] have been published in recent years. The International Atomic Energy Agency and several data centres around the world are engaged in data compilations and literature surveys [20]. Here we briefly summarize the status of electron–atom (molecule) collision cross-section data relevant to fusion edge plasmas.

4.1. Atomic species

An indication on the status of atomic data is given in Table I.

For H and the rare gas atoms (He, Ne, Ar, Kr and Xe), extensive sets of differential and integral cross-sections are available for elastic scattering and for excitation of the lower electronic states. Accurate momentum transfer and total electron scattering cross-sections are also available, for impact energies from a few tenths of an electronvolt to a few thousand electronvolts. Surveys on these subjects appeared in Refs [13, 17, 21–23]. Several recent measurements have been reported for H [24–27] and for the rare gases: He [31, 33, 38, 39, 42, 46], Ne [30, 31, 32, 34, 35, 36, 38, 42], Ar [28, 31, 32, 33, 37, 38, 39, 42, 44, 45], Kr [29, 32, 33, 40, 42, 44]; Xe [32, 33, 38, 41, 42, 43, 44]. In the case of H, the coverage for elastic scattering cross-sections can be considered adequate, but inelastic differential cross-sections are available only for the $1s \rightarrow 2s$ and $2p$ excitations, and integral cross-sections are available only for the excitation of the $n = 2$ and 3 manifolds. In the case of rare gases, the situation is quite satisfactory for modelling purposes and is definitely the best as far as atomic (and molecular) species are concerned.

Extensive measurements have been reported for atomic oxygen [47–51], and this subject was recently reviewed [52]. Measurements have been initiated for atomic carbon and nitrogen [53].

Experimental data for metal atoms are scarce. Most of the information is available in the form of optical excitation functions, and this subject was recently reviewed [18]. For Li, total electron scattering cross-sections [54], elastic scattering, momentum transfer and excitation cross-sections [55–57] have been reported. For Cu, elastic scattering and excitation cross-sections have been measured at a few impact energies [58–60]. For other metals listed in Table I, no cross-sections other than the optical excitation functions for Be, Al, Ti, Cr, Fe and Mo have been measured [18]. The absence of data for metal atoms is partly due to problems associated with the normalization of the measurements to the absolute scale and partly due to

TABLE I. SUMMARY OF EXPERIMENTAL ATOMIC EXCITATION CROSS-SECTION DATA

Species	Elastic	Excitation	Q^M	Q_{TOT}	Opt.
H	h	h	h	h	h
He	h	h	h	h	h
Ne, Ar, Kr, Xe	h	m	h	h	m
O	m	m	—	—	ℓ
C	—	—	—	—	—
Li	m	m	m	h	m
Cu	m	ℓ	m	—	m
Be, Al, Ti	—	—	—	—	ℓ
Cr, Fe, Mo					
Si, V, Ni, Ga,					
Zr, Ta, W	—	—	—	—	—

h, m and ℓ refer to high, medium and low degree of data availability. Opt. designates optical excitation functions.

experimental difficulties. For permanent gases, practical and reliable procedures have been established for normalizing the measured relative scattering intensities to He elastic scattering cross-sections, which are accurately known and can be used as secondary standards (see, for example, Ref. [8]). These procedures have not yet been successfully applied to metal atoms.

Up to here, we have discussed electron collisions with ground-state atoms. It may also be necessary, however, to consider electron collisions with excited atoms, especially with metastable rare gases. In this case, stepwise excitation and de-excitation (superelastic scattering) cross-sections are needed. The information in this area is quite limited. Optical excitation functions for metastable He [61–63], Ne [61] and Ar [64] have been reported. Total electron scattering cross-sections are available for metastable He [65] and for Ar [66]. Some DCS_n measurements have been reported for excitation of metastable He [67]. Superelastic (quenching) cross-sections can also be generated from the available inelastic data using the principle of detailed balance [68, 69].

4.2. Molecular species

Here, we briefly summarize elastic, momentum transfer, rotational, vibrational and electronic excitation (including dissociation and dissociative attachment) and total electron scattering cross-sections available for H₂, CO, N₂, O₂, H₂O and CO₂. (Electron collision processes

TABLE II. SUMMARY OF EXPERIMENTAL MOLECULAR EXCITATION CROSS-SECTION DATA

Species	Elastic	Excitation				Q ^M	Q _{TOT}	Opt.
		Rot.	Vibr.	El.D.	El.C.			
H ₂	h	m	h	m	m	h	h	m
CO	h	(m)	h	ℓ	ℓ	h	h	m
N ₂	h	(m)	h	h	m	h	h	m
O ₂	h	—	m	h	ℓ	h	h	m
H ₂ O	h	(m)	m	—	ℓ	h	h	m
CO ₂	h	(m)	h	—	ℓ	h	h	m

h, m and ℓ refer to high, medium and low degree of data availability. El.D. and El.C. refer to electronic discrete and electronic continuum state excitations, respectively. Opt. refers to optical excitation functions. Parentheses indicate data obtained by indirect deduction.

involving hydrocarbon molecules are discussed in another article in this volume.) Table II gives a summary for these molecules. Comprehensive reviews can be found in Refs [11, 13-16, 70-76].

Elastic scattering cross-sections have been measured for all molecular species of interest to us, over a wide range of impact energies. It should be noted, however, that the rotational excitation is not separated from elastic scattering in most of the works and, in this case, elastic scattering cross-sections represent the sum from these two processes. Recent results (not covered by the quoted reviews) have been published for CO₂ [77] and for H₂O [78]. The integral elastic cross-sections are typically in the range 10⁻¹⁶ to 10⁻¹⁵ cm² for impact energies below 50 eV.

Rotational excitation can be resolved with the available techniques, only for H₂. Unresolved rotational structures were unfolded for N₂, CO, H₂O and CO₂ [79]. At very low impact energies, integral rotational excitation cross-sections have been obtained from swarm measurements. For homonuclear diatomic molecules, direct excitation is due to the polarizability or the electric quadrupole moment of the molecule, and the $\Delta J = \pm 2$ (± 4 ...) selection rule applies. Typical cross-sections are about 10⁻¹⁸ cm². For molecules with a permanent dipole, the $\Delta J = \pm 1$ processes dominate over most other processes. For highly polar molecules, cross-sections as large as 10⁻¹⁴ cm² occur.

At low electron energies, resonance processes can greatly increase the rotational excitation cross-sections (to an order of magnitude of 10⁻¹⁶ cm²).

Vibrational excitation is effectively achieved by low energy electrons, especially through resonance processes. Direct excitation cross-sections are typically 10⁻¹⁸ cm², but resonance may enhance them to 10⁻¹⁶ cm². Cross-sections have been measured for all the molecules of interest to us, but gaps in the energy range persist and the coverage for O₂ is rather limited. Cross-sections for N₂ [80] and H₂O [81] have been reported very recently.

Electronic state excitation cross-sections for discrete states have been reported for the diatomic molecules, but only for a few states and over limited energy ranges. In most cases the low energy cross-sections are scarce. N₂ has been the most extensively studied. Measurements on O₂ have been reported very recently [82]. Practically no data exist for H₂O and CO₂. Efforts are now under way to extend the measurements to low energies, but progress is slow because of the difficulties encountered in handling low energy electrons, the breakdown of the Franck-Condon principle, and resonance processes. Optical measurements yield the optical excitation functions, but they face similar experimental problems as electron scattering measurements, and transformation of the data to integral electron impact excitation cross-sections requires the knowledge of branching ratios and correction for cascade effects. Excitation to *continuum states* leads to dissociation (neutral or charged fragments). When the dissociation products are charged or excited, they can be conveniently detected and integral cross-sections can be directly measured. Most of the experimental data fall in this category. For a review on optical measure-

ments see Refs [17] and [19]. An estimation of cross-sections for the production of excited hydrogen atoms following dissociative excitation of molecular hydrogen by electron impact was made very recently by Fujimoto et al. [83]. Measurements on dissociation to neutral fragments are difficult. A technique based on the measurement of pressure changes was applied to N_2 [84]. Recent approaches utilizing fast molecular beam techniques [9, 10] seem very promising and are being applied to N_2 , O_2 , CO and CO_2 . Only fragmentary information is available for the kinetic energy distribution of dissociation fragments despite of its importance in modelling efforts. Resonances do not play a major role in electronic state excitations, except at threshold in certain cases. They act only over a small impact energy range, and even over these energy ranges their effect can be neglected for modelling works. The largest cross-sections for electronic state excitations are associated with dipole allowed transitions at intermediate impact energies (of the order of 10^{-16} cm²).

Momentum transfer cross-sections are available for all molecular species, with good accuracy over a very wide range of impact energies, from combined swarm and beam data and various consistency checks. A comprehensive summary is given in Ref. [13]. The value of the momentum transfer cross-section ranges from 10^{-13} cm² (H_2O) to 10^{-16} cm² (Ne) at low electron energies.

Total electron scattering cross-sections are also available, with high accuracy over a wide energy range for all molecular species [13]. These are the most reliable cross-sections and can serve for consistency checks on integral cross-sections. Very recent results for H_2 are reported in Ref. [85].

Dissociative attachment plays an important role at low electron energies. Since this is a resonance process, the cross-sections peak sharply at the corresponding resonance energies. Dissociative attachment cross-sections depend very strongly on the vibrational state of the molecule. For H_2 , for example, it was found that the dissociative attachment cross-section from the $v = 4$ vibrationally excited state is by a factor of 10^4 larger than that from the $v = 0$ ground vibrational state [76].

Polar dissociation leads to negative and positive ion pairs and plays an important role at energies higher than those associated with dissociative attachment [86].

The importance of electron collisions with excited molecules may need to be considered under certain

conditions. As mentioned above, vibrational excitation has a drastic effect on dissociation type processes. Molecular species in metastable electronic states may have large cross-sections for excitation, ionization and quenching. Unfortunately, no information on cross-sections exists in this area, with the exception of some differential excitation and dissociative attachment cross-sections for O_2 ($a^1\Delta$) [87].

5. SUMMARY AND CONCLUSIONS

The renaissance of low energy electron collision physics, which commenced in the 1960s, produced tremendous progress and a large body of information in this field. This was due partly to advances in techniques and instrumentation and partly to the need for electron collision data for various applications (lasers, plasma devices, planetary ionospheres, etc.). Despite all this progress, only a small fraction of the very large variety of cross-sections needed in realistic modelling of a practical system is available today. Furthermore, one cannot expect, even with the wildest imagination, that the situation could be significantly changed by laboratory activities alone. The data requirement is simply overwhelming, and the measurements are difficult, time consuming, expensive and in some cases simply not feasible.

A great deal of progress has been made in recent years in the theoretical arena also. Theoretical models and approximations developed to such a stage that reliable cross-sections can be calculated for a number of processes over a significant range of impact energies and scattering angles. In the case of atomic species, the situation is actually quite good. Integral elastic and excitation cross-sections and, to some extent, even differential cross-sections can be quite reliably calculated for the purpose of edge plasma modelling. At intermediate and high impact energies (defined as impact energies ranging from the ionization potential to about 20 times the ionization potential and above), distorted wave (and first-order many-body) approaches can now be applied to any atom (in any ionization state) using supercomputers. At low impact energies (from threshold to the first ionization potential), these approaches are not reliable, but various close coupling schemes are practical and can yield reliable cross-sections. At these low energies, resonance processes play an important role and can have a significant effect on the cross-sections. When many inelastic channels are open, problems arise as to how to account for them in the calculation. Further refinements using

coupled channel approaches augmented by optical potential are in progress. From the theoretical side, the situation is not as good in the case of molecules as in the case of atoms. The complexity of the calculations is greatly increased by the nuclear motion and the non-spherical nature of the interaction potentials. There are unresolved discrepancies between theory and experiment, even for as simple a molecule as H_2 [74, 88]. For recent reviews on the status of theory see Refs [15, 72, 89-93].

A critical evaluation of the available data would be rather difficult and is far beyond the limits of this article. A few general remarks are made here, and a specific example is given in Fig. 1.

Electron impact excitation cross-sections are derived either from differential scattering measurements (which yield DCS_n and, by integration, integral cross-sections) or from measurements of integrated photon or fragment yields (which directly give optical excitation or dissociation cross-sections). DCS_n obtained at intermediate and high impact energies are in general accurate to about 15-20% for strong processes and to about a factor of two for weak processes. At low impact energies (within a few electronvolts of threshold energies), quantitative measurements are more difficult and the accuracy of DCS_n data is typically in the range of 30% to a factor of two. Extrapolation of DCS_n to experimentally inaccessible angles and integration usually produce negligible contributions to the integral cross-section errors. However, if the cross-section changes rapidly with angle in the near zero region and/or the 180° region and if theoretical guides are not available, one may encounter significant extrapolation errors. Optical excitation cross-section measurements face, in general, the same type of problems as electron scattering measurements and are uncertain to similar degrees. Conversion of these cross-sections to electron impact excitation cross-sections can be seriously affected by cascade, branching ratios and radiation trapping, and by the extension of calibration, achieved typically at high impact energies, to the low impact energy region. Measurements of dissociation cross-sections leading to charged particle fragments can be made to somewhat higher accuracy than measurements of electron impact excitation cross-sections, but measurements concerning dissociation to neutral fragments are more difficult and have larger errors associated with them.

Figure 1 shows electron impact excitation cross-sections for the ($X^1\Sigma_g^+ - B^1\Sigma_u^+$) excitation in H_2 obtained by various researchers. Both experimental and theoretical results are included for the sake of

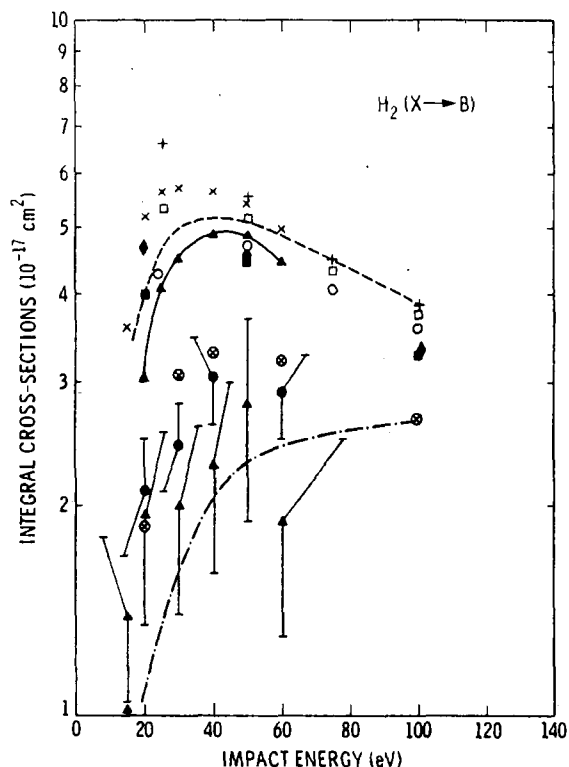


FIG. 1. Integral cross-sections for electron impact excitation of the $B^1\Sigma_u^+$ state in H_2 .

Experimental results: ● [94], ▲ [95], ⊗ [96], - - - [97].

Theoretical results: + [98], □ [98], ◆ [99], ■ [99], ○ [98], × [100], - ▲ - [100], - - - [101]. (When more than one symbol is associated with the same reference, they correspond to different theoretical approximations. For details see Ref. [94].)

completeness. The four sets of experimental data (two from electron scattering [94, 95] and two from optical [96, 97] measurements) form the lower aggregation of points and show a scatter of about $\pm 25\%$. The upper group of points and curves are from theoretical calculations.

It seems to be a natural conclusion that significant progress can be expected only from a joint experimental/theoretical effort. Supercomputers can generate the large amount of data required, but the calculation schemes have to be checked against experiments. The key role of the experiments, therefore, should be the generation of benchmark data.

ACKNOWLEDGEMENTS

The author is grateful to H. Tawara for making unpublished results available to him.

This work was supported by the National Aeronautical and Space Administration, by the United States Department of Energy and by the National Science Foundation.

REFERENCES

- [1] TAWARA, H., PHANEUF, R.A., *Comments At. Mol. Phys.* **21** (1988) 177.
- [2] SUMMERS, H.P., *Comments At. Mol. Phys.* **21** (1988) 277.
- [3] TAWARA, H. (Ed.), *Atomic and Molecular Processes in Edge Plasmas including Hydrocarbon Molecules*, Rep. IPPJ-AM-59, Institute of Plasma Physics, Nagoya University, Nagoya (1988).
- [4] DRAWIN, H.W., *The Application of Atomic and Molecular Physics in Fusion Plasma Diagnostics*, Rep. IPPJ-AM-61, Institute of Plasma Physics, Nagoya University, Nagoya (1988).
- [5] JANEV, R.K., HARRISON, M.F.A., DRAWIN, H.W., *Nucl. Fusion* **29** (1989) 109.
- [6] TRAJMAR, S., REGISTER, D.F., in *Electron Molecule Collisions* (TAKAYANAGI, K., SHIMAMURA, I., Eds), Plenum Press, New York (1984) 427.
- [7] EHRHARDT, H., JUNG, K., KNOTH, G., RADLE, M., in *Atomic and Molecular Physics* (RAI, K., TRIPATHI, D.N., Eds), World Scientific, Singapore (1987) 63.
- [8] NICKEL, J.C., ZETNER, P.W., SHEN, G., TRAJMAR, S., *J. Phys., E* **22** (1189) 730.
- [9] COSBY, P.C., HELM, H., in *41st Annual Gaseous Electronic Conference, Programme and Abstracts*, Univ. of Minnesota, Minneapolis (1988) 158.
- [10] COSBY, P.C., in *26th Int. Conf. on Physics of Electronic and Atomic Collisions, Abstracts of contributed papers*, DATASSIST, New York (1989) 348.
- [11] PICHFORD, L.C., McKOY, B.V., CHUTJIAN, A., TRAJMAR, S. (Eds), *Swarm Studies and Inelastic Electron-Molecule Collisions*, Springer-Verlag, New York (1987).
- [12] BRANDSEN, B.H., Mc DOWELL, M.R.C., *Phys. Rep.* **46** (1978) 249.
- [13] HAYASHI, M., *Recommended Values of Transport Cross Sections for Elastic Collisions and Total Collision Cross Section for Electron in Atomic and Molecular Gases*, Rep. IPPJ-AM-19, Institute of Plasma Physics, Nagoya University, Nagoya (1981).
- [14] TRAJMAR, S., REGISTER, D.F., CHUTJIAN, A., *Phys. Rep.* **97** (1983) 219.
- [15] CHRISTOPHOROU, L.G. (Ed.), *Electron Molecule Interactions and their Applications*, Vols 1 and 2, Academic Press, Orlando, FL (1984).
- [16] SHIMAMURA, I., *Cross Sections for Collisions of Electrons with Atoms and Molecules*, Vol. 82, *Scientific Papers of the Institute of Physical and Chemical Research*, Tokyo (1989) 1.
- [17] Mc CONKEY, J.W., in *Electronic and Ionic Collision Cross Sections Needed in Modeling of Radiation Interaction with Matter* (Proc. Workshop Argonne, IL, 1983), Rep. ANL-84-28, Argonne National Laboratory, Argonne, IL (1983) 129.
- [18] HEDDLE, D.W.O., GALLAGHER, J.W., *Rev. Mod. Phys.* **61** (1989) 221.
- [19] VAN DER BURGT, P.J.M., WESTERWELD, W.B., RISLEY, J.S., *J. Phys. Chem. Ref. Data* **18** (1989) 1757.
- [20] JANEV, R.K., Report on the Activities of the IAEA Atomic and Molecular Data Unit and the International Atomic Data Centre Network for the Period Nov. 1988 — Nov. 1989, Rep. IAEA-NDS-AM18, IAEA, Vienna (1989).
- [21] FABRICANT, I.I., SPHENIC, O.B., SNEGURSKY, A.V., ZAVILOPULO, A.N., *Phys. Rep.* **159** (1988) 1.
- [22] ANDERSEN, N., GALLAGHER, J.W., HERTEL, I.V., *Phys. Rep.* **165** (1988) 1.
- [23] KING, G., TRAJMAR, S., Mc CONKEY, J.W., *Comments At. Mol. Phys.* **23** (1989) 229.
- [24] WILLAMS, J.F., *J. Phys., B* **14** (1981) 1197.
- [25] LOWER, J., Mc CARTHY, I.E., WEIGOLD, E., *J. Phys., B* **20** (1987) 4571.
- [26] DOERING, J.P., VAUGHAN, S.O., *J. Geophys. Res.* **91** (1986) 3279.
- [27] SHYN, T.W., CHO, S.Y., *Phys. Rev., A* **40** (1989) 1315.
- [28] CHUTJIAN, A., CARTWRIGHT, D.C., *Phys. Rev., A* **23** (1981) 2178.
- [29] TRAJMAR, S., SRIVASTAVA, S.K., TANAKA, H., NISHIMURA, H., CARTWRIGHT, D.C., *Phys. Rev., A* **23** (1981) 2167.
- [30] BREWER, D.F., NEWELL, W.R., HARPER, S.F.W., SMITH, A.C.H., *J. Phys., B* **14** (1981) L749.
- [31] KAUPPIA, W.E., STEIN, T.S., SMART, J.H., et al., *Phys. Rev., A* **24** (1981) 725.
- [32] BUCKMAN, S.J., HAMMOD, P., KINGS, G.C., READ, F.H., *J. Phys., B* **16** (1983) 4219.
- [33] WAGENAAR, R., *Small Angle Elastic Scattering by Noble Gas Atoms*, PhD Thesis, FOM-Instituut voor Atoom-en Molecuulfysica, Amsterdam (1984).
- [34] CHARLTON, M., LARICCHIA, G., GRIFFITH, T.C., WRIGHT, G.L., HEYLAND, G.R., *J. Phys., B* **17** (1984) 4945.
- [35] REGISTER, D.F., TRAJMAR, S., *Phys. Rev., A* **29** (1984) 1785.
- [36] REGISTER, D.F., TRAJMAR, S., STEFFENSEN, G., CARTWRIGHT, D.C., *Phys. Rev., A* **29** (1984) 1793.
- [37] FRECH, J., GRANITZA, B., MACHE, C., RAI, N., *J. Phys., B* **18** (1985) 967.
- [38] NICKEL, J.C., IMRE, K., REGISTER, D., TRAJMAR, S., *J. Phys., B* **18** (1985) 125.
- [39] BUCKMAN, S.J., LOHMANN, B., *J. Phys., B* **19** (1986) 2547.
- [40] MITYUREVA, A.A., PENKIN, N.P., SMIRNOV, V.V., *Opt. Spektrosk.* **60** (1986) 144.
- [41] REGISTER, D.F., VUSKOVIC, L., TRAJMAR, S., *J. Phys., B* **19** (1986) 1685.
- [42] MASON, N.J., NEWELL, W.R., *J. Phys., B* **20** (1987) 1357.
- [43] FILIPOVIC, D., MARINKOVIC, B., PEJCEV, V., VUSKOVIC, L., *Phys. Rev., A* **37** (1988) 356.
- [44] WEYHRETER, M.B., BARZIK, M.B., MANN, A., LINDER, F., *Z. Phys., D* **1** (1988) 333.
- [45] FURST, J.E., GOLDEN, D.E., MAHGEREFTECH, M., ZHOU, J., MUELLER, D., *Phys. Rev., A* **40** (1989) 5592.
- [46] CARTWRIGHT, D.C., CSANAK, G., TRAJMAR, S., REGISTER, D.F., *Electron-impact excitation of n¹P states of helium: Theory and experiment*, to be published in *Phys. Rev., A*.
- [47] SHYN, T.W., SHARP, W.E., *J. Geophys. Res.* **91** (1986) 1691.

- [48] SHYN, T.W., CHO, S.Y., SHARP, W.E., *J. Geophys. Res.* **91** (1986) 13751.
- [49] GERMANY, G.A., ANDERSON, R.J., SALAMO, G.J., *J. Chem. Phys.* **89** (1988) 1999.
- [50] DOERING, J.P., GULCICEK, E.E., *J. Geophys. Res.* **94** (1989) 1541 and 2733.
- [51] WILLIAMS, J.F., ALLEN, L.J., *J. Phys.*, B **22** (1989) 3529.
- [52] ITIKAWA, Y., ICHIMURA, A., Cross Sections for Collisions of Electrons and Photons with Atomic Oxygen, Rep. ISAS RN 406, Institute of Space and Astronautical Science, Tokyo (1989).
- [53] DOERING, J.P., DAGDIGIAN, P.J., *Chem. Phys. Lett.* **154** (1989) 234.
- [54] JADUSZLIWER, B.T.A., BEDERSON, B., MILLER, T.M., *Phys. Rev.*, A **24** (1981) 1249.
- [55] WILLIAMS, W., TRAJMAR, S., BOZINIS, D., *J. Phys.*, B **9** (1976) 1529.
- [56] SHUTTLEWORTH, T., BURGESS, D.E., HENDER, M.A., SMITH, A.C.H., *J. Phys.*, B **12** (1979) 3967.
- [57] VUSKOVIC, L., TRAJMAR, S., REGISTER, D.F., *J. Phys.*, B **15** (1982) 2517.
- [58] TRAJMAR, S., WILLIAMS, W., SRIVASTAVA, S.K., *J. Phys.*, B **10** (1977) 3323.
- [59] WINTER, N.W., HAZI, A.V., Review of Electron Impact Excitation Cross Sections for Copper Atom, Rep. UCID-19314, Lawrence Livermore Laboratory, Berkeley, CA (1982).
- [60] SCHEIBER, K.F., HAZI, A.V., HENRY, R.J.W., Electron Impact Excitation Cross Sections for Transitions in Atomic Copper, Rep. UCRL-95991, Lawrence Livermore National Laboratory, Livermore, CA (1987).
- [61] MITYUREVA, A.A., PENKIN, N.P., *Opt. Spectrosc.* **38** (1975) 229.
- [62] GOSTEV, V.A., ELAKHOVSKIJ, D.V., ZAITSEV, V.V., LUIZOVA, L.A., KHAKAEV, A.D., *Opt. Spectrosc.* **48** (1980) 251.
- [63] RALL, D.L.A., SHARPTON, F.A., SCHULMAN, M.B., ANDERSON, L.W., LAWLER, J.E., LIN, C.C., *Phys. Rev. Lett.* **62** (1989) 2253.
- [64] MITYUREVA, A.A., PENKIN, N.P., SMIRNOV, V.V., *Opt. Spectrosc.* **66** (1989) 140.
- [65] WILSON, W.G., WILLIAMS, W.L., *J. Phys.*, B **9** (1976) 423; NEYNABER, R.H., TRUJILLO, S.M., MARINO, L.L., ROTH, E.W., in *Physics of Electronic and Atomic Collisions* (Proc. 3rd Int. Conf. London, 1963), University College London (1963) 1089.
- [66] CELOTTA, R., BROWN, H., MOLOF, R., BEDERSON, B., *Phys. Rev.*, A **3** (1971) 1622; ZUO, M., JIANG, T.Y., VUSKOVIC, L., BEDERSON, B., *Phys. Rev.*, A **41** (1990) 2489.
- [67] MULLER-FIEDLER, R., SCHLEMMER, P., JUNG, K., HOTOP, H., EHRHARDT, H., *J. Phys.*, B **17** (1984) 259.
- [68] BLAGOEV, A.B., IVANOV, I., MISHONOV, T., POPOV, T.K., *J. Phys.*, B **17** (1984) L647.
- [69] TRAJMAR, S., "Estimate of quenching cross sections of metastable Ar and Kr atoms by electron impact", in *Inertial Confinement Fusion in Los Alamos, Progress since 1985*, Rep. LA-UR-89-2675, Los Alamos National Laboratory, Los Alamos, NM (1989).
- [70] ITIKAWA, Y., *Phys. Rep.* **46** (1978) 117.
- [71] GALLAGHER, J.W., BEATY, E.C., DUTTON, J., PITCHFORD, L.C., *J. Phys. Chem. Ref. Data* **12** (1983) 109.
- [72] SHIMAMURA, I., TAKAYANAGI, K. (Eds), *Electron-Molecule Collision*, Plenum Press, New York (1984).
- [73] ITIKAWA, Y., HAYASHI, M., ICHIMURA, A., et al., *J. Phys. Chem. Ref. Data* **15** (1986) 985.
- [74] Mc CONKEY, J.W., TRAJMAR, S., KING, G.C.M., *Comments At. Mol. Phys.* **22** (1988) 17.
- [75] ITIKAWA, Y., ICHIMURA, A., ONDA, K., et al., *J. Phys. Chem. Ref. Data* **18** (1989) 23.
- [76] TAWARA, H., ITIKAWA, Y., NISHIMURA, H., YOSHINO, M., *J. Phys. Chem. Ref. Data* **19** (1990) 617.
- [77] KANIK, I., Mc COLLUM, D.C., NICKEL, J.C., *J. Phys.*, B **22** (1989) 1225.
- [78] SHYN, T.W., CHO, S.Y., *Phys. Rev.*, A **36** (1987) 5138.
- [79] JUNG, K., ANTONI, T., MULLER, R., KOCHER, K.H., EHRHARDT, H., *J. Phys.*, B **15** (1982) 3535.
- [80] BRUNGER, M.J., TEUBNER, P.J.O., WEIGOLD, A.M., BUCKMAN, S.J., *J. Phys.*, B **22** (1989) 1443.
- [81] SHYN, T.W., CHO, S.Y., CRAVANS, T.E., *Phys. Rev.*, A **38** (1988) 678.
- [82] TEILLET-BILLY, D., MALEGAT, L., GAUYACQ, J.P., ABOUAF, E.R., BENOIT, C., *J. Phys.*, B **22** (1989) 1095.
- [83] FUJIMOTO, T., SAWADA, K., TAKAHOTA, K., Res. Rep. NIFS-DATA-4, National Institute for Fusion Science, Nagoya (1990).
- [84] WINTERS, H.F., *J. Chem. Phys.* **44** (1966) 1472.
- [85] SUBRAMANIAN, K.P., KUMAR, V., *J. Phys.*, B **22** (1989) 2387.
- [86] SRIVASTAVA, S.K., ORIENT, O.J., in *Production and Neutralization of Negative Ions and Beams* (Proc. 3rd Int. Symp. Brookhaven, NY, 1983), American Institute of Physics (1983) 56.
- [87] HALL, R.I., TRAJMAR, S., *J. Phys.*, B **8** (1975) L293; KHAKOO, M.A., NEWELL, W.R., SMITH, A.C.H., *J. Phys.*, B **16** (1983) L317; BELIC, D.S., HALL, R.I., *J. Phys.*, B **14** (1981) 365.
- [88] MORRISON, M.A., CROMPTON, R.W., SAHA, B.C., PETROVIC, Z.L., *Aust. J. Phys.* **40** (1987) 239.
- [89] LANE, N., *Rev. Mod. Phys.* **52** (1980) 29.
- [90] GIANTURCO, F.A., JAIN, A., *Phys. Rep.* **143** (1986) 347.
- [91] MORRISON, M.A., *Adv. At. Mol. Phys.* **24** (1988) 51.
- [92] COLLINS, L.A., SCHNEIDER, B.I., in *Electronic and Atomic Collisions* (GIBODY, H.B., NEWELL, W.R., READ, F.H., SMITH, A.C.H., Eds), North-Holland, Amsterdam (1988) 57.
- [93] JOACHAIN, C.J., in *The Physics of Electronic and Atomic Collisions* (Proc. 16th Int. Conf. New York, NY, 1989), American Institute of Physics (1990) 68.
- [94] KHAKOO, M.A., TRAJMAR, S., *Phys. Rev.*, A **34** (1986) 146.
- [95] SRIVASTAVA, S.K., JENSEN, S., *J. Phys.*, B **10** (1977) 3341.
- [96] SHEMANSKY, D.E., AJELLO, J.M., HALL, D.T., *Astrophys. J.* **296** (1985) 765.
- [97] MALCOLM, I.C., DASSÈN, H.W., Mc CONKEY, J.W., *J. Phys.*, B **12** (1979) 1003.

ELECTRON COLLISION PROCESSES WITH PLASMA EDGE NEUTRALS

- [98] CHUNG, S., LIN, C.C., Phys. Rev., A **17** (1978) 1874.
- [99] ARRIGHINI, G.P., BIONDI, F., GUIDOTTI, C.,
BIAGI, A., MARINELLI, F., Chem. Phys. **52** (1980) 133.
- [100] FLIFLET, A.W., Mc KOY, V., Phys. Rev., A **21** (1980)
1963.
- [101] HAZI, A.N., Phys. Rev., A **23** (1981) 2232.

ELECTRON-ION COLLISIONS IN THE PLASMA EDGE

G.H. DUNN*

Joint Institute for Laboratory Astrophysics,
University of Colorado,
and

National Institute of Standards and Technology,
Boulder, Colorado,
United States of America

ABSTRACT. The electron-ion collisional database required for modelling and diagnostics of the fusion plasma edge is briefly examined from the points of view of (1) experimental and theoretical means for obtaining the data, (2) relevant physical processes, (3) limitations on the data, and (4) availability and quality of the data for relevant species. Both molecular and atomic ions are considered.

1. INTRODUCTION

As discussed in some detail in other papers in this volume, the edge plasma plays an important role in the heating and stability of fusion plasmas. The plasma near the walls of the device is typically characterized by low temperatures, in the range of $T \approx 2\text{--}200$ eV, and particle densities in the range of $10^{12}\text{--}10^{15}$ cm⁻³. As is characteristic of the low temperatures and the proximity to the vessel walls, the particle constituents are atoms, molecules and ions of hydrogen, helium, carbon and oxygen, and a host of metal and other constituent impurities of low fractional content coming from walls, limiters and divertors. Ions are in relatively low charge states of less than about 10.

Given charge neutrality and comparable electron and ion temperatures, electron collisions dominate over collisions between heavy particles such as atoms or ions, since the electron collision frequencies are greater than those between heavy particles by the ratio of velocities, $\approx (1836 \times A)^{1/2}$. Only highly resonant particle collisions, such as resonant charge transfer, will have cross-sections large enough to offset the velocity factor and to give a rate comparable to that for electron collisions. The purpose of this paper is to examine the database for electron impact with the ion species found in the edge plasma. We describe briefly how the data are obtained, their accuracies and primary limitations. Actual cross-sections and rates are not presented in the limited space available here, but references are given to compendia, compilations, bibliographies or the original literature, as appropriate.

* Staff member, Quantum Physics Division, National Institute of Standards and Technology, Boulder, CO, USA.

2. METHODS AND THEIR UNCERTAINTIES

It must be borne in mind that because of the vast quantities of data needed for complete modelling, most data may eventually come from theory, and that a primary — though not the sole — function of experiments will be to test the theory. However, experiment has led the way in directing theory towards recognizing important processes and, for molecular ions (particularly polyatomic ions), experiment remains the main source of data, since the theory cannot yet be relied upon to give the needed data. Descriptions of the experimental and theoretical methods, together with broad literature citations, can be found in Refs [1–3].

2.1. Experimental

Three main approaches have been employed to obtain experimental data on electron-ion collisions. One approach uses colliding beams of electrons and ions and appropriate detection of products; another one uses plasmas with the necessary detailed diagnostics and modelling; and the third is a sort of hybrid of these two approaches. The first is most valuable for testing detailed atomic theoretical methods used for calculating the data, and the second is valuable for obtaining data on some species not typically accessible with beams and under conditions characteristic of the fusion environment. The third method employs the electron-beam ion trap (EBIT) or the electron-beam ion source (EBIS) and has recently gained prominence.

In colliding beam experiments, where one is studying the process $e + A^{q+} \rightarrow$ products, a beam of electrons is collided with a beam of ions and the resultant products

are detected. It is necessary to quantitatively measure the strengths of the two beams and the extent of their geometric overlap, and to quantitatively measure the product formation rate. Actually, this class of experiments between charged collision partners often yields the most quantitatively accurate measurements of cross-sections, because the necessary measurables are more accurately obtained than in many other types of cross-section experiments, for example those involving neutral targets. The limitations on electron-ion experiments arise because the target densities are generally low, leading to very low product or signal rates which must be measured in the presence of large backgrounds typically caused by either beam or by both beams. 'False signals' may arise, caused by interactions (e.g. space charge) of one beam with the other, and these are not always recognized nor eliminated. Two standard deviation cross-section total accuracies are often quoted at the 10% level using these methods. In addition to Refs [1-3] noted above, Ref. [4] is excellent, and new beam techniques can be found in Refs [5, 6].

Plasma rate measurements are based primarily on the ability to follow the time evolution of the various species in a plasma — usually spectroscopically — and to measure the temperature. Using a coronal model, a representation of the system involves a set of linear differential equations containing the rate coefficients and the densities. Key rate coefficients are entered from theory or from other measurements, and the remainder is solved for. A serious problem in the method derives from the fact that excited states are often involved, and assumptions must be made about *effective* rates and densities. Experimental uncertainties as low as 20-40% are sometimes quoted. More discussion of the method can be found in Refs [1, 2] and in references cited therein.

The beam-trapped-ion method (EBIT and EBIS) is relatively new, except in the study of ionization. An ion population is established by electron bombardment and the ions are trapped by a combination of longitudinal magnetic field, space charge and applied potentials. In recent applications, the electron energy is changed from that creating the equilibrium population, and a change either in emitted X-rays or in sampled ions is detected. Target densities and target-beam overlaps are not measured, nor are various collection and detection efficiencies, so it is typical to relate the observations to another cross-section which is 'known' either from theory or from another experiment to obtain numerical cross-section values. Measurements can be made on very highly charged states. Populations of ions with noble-gas-like structures dominate; hence such ions are the

easiest to work with, so that essentially all the measurements so far have been made for them. The electron energy resolution is about 50 eV. It is difficult to assess the accuracies of these measurements because of the normalization to other theoretical and experimental data. However, it appears that accuracies of 20-40%, or even better, may not be too optimistic. A good review of this technique with full references has recently been written by Stockli [7].

2.2. Theoretical

A number of approaches of varying accuracies have been used to obtain theoretical data on electron-ion collisions, ranging from semi-empirical estimator formulas to large high speed computer programs that include many coupled-channel effects. As with the experimental methods, we can only discuss these in some generality and try to indicate roughly what one may expect in accuracy from the different approaches.

The estimator formulas which seem to be most familiar and which find the widest usage are the Gaunt factor formula for excitation [8], the Lotz formula for ionization [9], and the Burgess formula for dielectronic recombination [10]. The article by Younger and Märk in Ref. [2] on semi-empirical and semi-classical formulas for ionization indicates that there are at least ten such formulas for ionization, and there are also variations of the formulas cited above for excitation and recombination. Typically, one has the impression that these formulas will produce estimates within a factor of two of the correct value, although in many cases, such as in ionization when indirect processes dominate, in dielectronic recombination when there are field or density effects, or in excitation where resonances are especially important, these formulas may give estimates that are incorrect by a much larger factor. By the same token, however, often the results are within 10-20% of the correct value. Thus a factor of two is a reasonable working number for the usual purpose of these estimators. These formulas were not 'invented' for use with molecular ions, but the expressions for ionization and for excitation have been applied to molecules with the level of accuracy described above.

The radial Schrödinger equation for electron-ion collisions can be expressed in terms of the scattering electron moving in the potential of the target ion and takes the form

$$\left[\frac{d^2}{dr_i^2} - \frac{\ell_i(\ell_i + 1)}{r_i^2} + k_i^2 \right] F(i, r) = 2 \sum_j \{V_{ij} \pm W_{ij}\} F(j, r) \quad (1)$$

where F is the radial function in a given channel, V_{ij} and W_{ij} are respectively direct and exchange potential operators, and the summation is over all discrete and continuum states. Equation (1) represents an infinite set of coupled integro-differential equations.

If one truncates the right-hand side of Eq. (1) to a finite number N of final states of the ion and solves the resultant coupled equations without further approximation, the result is referred to as the N -state close-coupling (or NCC) approximation. A number of large computer programs have been constructed to do this calculation, and when used properly with correct coupling, accurate wave functions, etc., the method yields the most accurate results for electron-ion collisions. The approach directly takes into account the effects of dielectronic resonances, which can substantially affect cross-sections. It sometimes takes a nearly inordinate number of states to get convergent results, however, and other approximations, which originated before the NCC approximation and which are less demanding on computer time, are used. In fact, 'hybrid' calculations are now often made — combining different approaches over different energy ranges. It should be understood that exchange of bombarding and target electrons can play an important role, especially near the threshold, and this needs to be accounted for. All of the approximation methods have been developed to do so; however, the user should be warned that many data calculations in the literature do not take this important effect into account.

An approximation that takes into account only the initial and final channels, but allows for distortion of the scattered wave function from the Coulomb wave is referred to as the distorted wave (DW) approximation. This method, for high enough Z , can give results of an accuracy comparable to that of the NCC approximation and can be far less expensive in computer time. Various fixes allow for additional polarization and for some dielectronic resonances, although most of the DW calculations in the literature do not account for resonances.

If one further neglects the distortion of the Coulomb scattering wave by the ion potential, there results the approximation known as the Coulomb-Born (CB) approximation. Although this approximation is not reliable for ions of low charge or for low energy (errors of factors of two or more) or in cases where dielectronic resonances are important, it can nevertheless yield relatively accurate results for highly charged ions and for high energies where, indeed, the distortion will be negligible. A very large amount of data has been generated using this method.

Although there are other variations, the final approximation we mention here is simply the familiar Born

approximation (BA), in which the Coulomb nature of the scattered wave is not even accounted for and a plane wave is used. This is a valid approximation only at very high energies.

3. DATA: MOLECULAR IONS

Added degrees of freedom of multiple heavy particles, characteristic of molecules, bring a richness to the possible physical processes that is not present for atomic ions. We mention the processes briefly, with a short description of each. In addition to electronic excitation, energy is deposited in the form of vibrational and rotational energy, and the associated states have characteristically long lifetimes. Electronic excitation of molecular ions can lead, as in atoms, to states that can subsequently radiate and to states that may be metastable and thus can collide and transfer energy. In addition, excited electronic states may be repulsive, so that dissociation occurs — usually in times of the order of 10^{-12} – 10^{-14} s, i.e. times short compared to radiative lifetimes. Dissociation products carry away the excess energy as both kinetic and internal energy. The dissociating particle velocities may have a characteristic spatial orientation relative to magnetic fields and the direction of electron velocities, depending on state symmetries. Ionization is similarly diverse: it can lead to bound multiply excited states, which are often unstable against predissociation; or it can lead to dissociative states which again yield particles with possible internal energy, kinetic energy and perhaps also select spatial distributions of velocities. Recombination is dominated by a dielectronic capture process which, for molecules, is called dissociative recombination. Here, an incoming electron excites a bound electron of the ion, and, having lost energy, the electron is captured into a Rydberg state. When the doubly excited Rydberg state is repulsive, stabilization via dissociation may occur in the times noted above, which are very competitive with auto-ionization times, typically in the 10^{-14} s range. The sloped repulsive potential curve and the initial distribution of internuclear separations make the initial dielectronic capture process resonant over a broad range of electron energies. Coming back to vibrational excitation, it is found for the species most carefully studied that the electronic processes discussed can be *extremely* sensitive to internuclear separation and thus to the initial vibrational state populations.

Basic plasma constituents are hydrogen and its isotopes, so the dominant ions present are H_2^+ and H_3^+ , and their isotopic variants. Carbon, as the limiter and

wall material of choice, contributes CO^+ , CO_2^+ and C_nH_m^+ in interactions with the major impurity, oxygen, and the abundant hydrogen. Water will give rise to H_3O^+ , H_2O^+ and OH^+ . Some metallic oxides such as BeO^+ may be present as well. It is highly likely that many of the molecules containing carbon, such as CO^+ , will react to form the very stable molecular ion, HCO^+ , though the latter has apparently not been normally considered as a constituent. We do not consider any further the hydrocarbon molecular ions, as they are treated elsewhere in this volume.

3.1. Collisions with H_2^+

Clearly, because of the high relative concentration, collisions between electrons and H_2^+ are among the most important electron-ion collisions in the wall plasma. Data for these processes have been summarized and treated in compendia [11, 12] of atomic and molecular data for fusion. The discussion here emphasizes important cautions to be exercised in using these data or other data from the original literature.

One important thing to recognize is that, in the edge plasma, molecular H_2 will probably be formed mostly by recombination of H atoms on the walls of the vessel, and recent evidence [13] indicates that molecules so formed may be very highly vibrationally excited — even more so than is projected from the temperature of the surfaces of the vessel. The H_2^+ subsequently formed by electron bombardment of the excited H_2 will likewise be in a vibrational state distribution different from that associated with electron impact of ground state H_2 , normally referred to as the Franck-Condon (FC) distribution.

Excitation. Electronic excitation of this simplest of molecules can be said to always result in dissociation, since any bound levels of the excited molecule are only slightly bound at internuclear separations not 'accessible' in an FC transition from H_2^+ in vibrational levels up to ten or so. The excitation/dissociation has been studied thoroughly from both experimental and theoretical points of view. Theoretical treatments [14] show a rapid increase with internuclear separation of the transition matrix element between the $1s\sigma_g$ and $2p\sigma_u$ states (dissociating to H^+ and $\text{H}(1s)$), and this is the dominant transition. This leads to a very strong dependence of the excitation cross-section on the vibrational level of the H_2^+ target ion (growing by about a factor of 100 between $v = 0$ and $v = 18$). Three independent crossed beam experiments [15] (excitation to the sum of all excited states — they all result in dissociation)

yield results in excellent agreement (10–20%) with each other and in agreement with theoretical predictions (10–20%) when the vibrational levels are assumed to be populated with an FC distribution, as one would expect [16] from a single-collision electron impact ion source. As already noted, this is probably not the case for H_2^+ in the edge plasma. Provided one knows how to treat the vibrational population, one would be advised to 'construct' a net excitation (dissociation) cross-section from the individual cross-sections deduced from theory. Since such good agreement between experiment and theory was found for the case where vibrational populations were known (FC), one may have confidence that such a constructed cross-section will be accurate to $\pm 30\%$. The main inaccuracy will be in estimating the vibrational state distribution. The angular and energy distributions of protons resulting from dissociative excitation have been treated theoretically [17] and the data should be reasonably reliable, though the energy distributions will again be critically dependent on the initial vibrational distribution of the target. Data [14] for excitation to states that dissociate to a proton and an excited atom are entirely theoretical, but can probably be trusted to the 30% level.

Ionization. A very good crossed beam experiment [18] has been performed to measure the cross-section for $e + \text{H}_2^+ \rightarrow 2e + \text{H}^+ + \text{H}^+$, and one should trust these results to $\pm 12\%$. There is no indication that the cross-section will be strongly dependent on vibrational energy level.

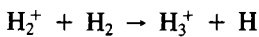
Recombination. By far the dominant recombination mechanism for this ion (as for essentially all molecular ions) is dissociative recombination, $e + \text{H}_2^+ \rightarrow \text{H}_2^{**} \rightarrow \text{H}^* + \text{H}$. The process is both a sink for ions and a source of excited hydrogen atoms in the edge plasma. As with excitation, this process is extremely dependent upon the vibrational level of the target ion, and this must be put into the modelling. Colliding beam experiments yielding cross-sections for total neutral products have been performed both for ions [19] initially in an FC vibrational state distribution [16] and for ions in an unknown distribution [20], thought to be primarily $v = 0, 1$ and 2. Agreement with the difficult theory [21] is qualitatively good, but much remains to be done in order to be able to say that one could construct a reliable cross-section if one only knew the vibrational state populations. Colliding beam experiments [22] have also been performed on ions in an FC distribution to measure the cross-sections for obtaining excited atoms in specific states, namely $n = 2$ and $n = 4$. Each of these gives cross-sections that are about 10% of the total, and evi-

dence indicates that atoms with $n = 3$ will dominate the dissociative recombination process of this ion. Indeed, rationalizing the experimental partial cross-sections in Ref. [22], the total cross-sections Σ of Ref. [19] and the theoretical partial cross-sections of Zhdanov and Chibisov [21], Janev et al. [11] quote values of $\sigma(n=2) = 0.10\Sigma$, $\sigma(n=3) = 0.45\Sigma$, $\sigma(n=4) = 0.22\Sigma$, $\sigma(n=5) = 0.12\Sigma$, $\sigma(n=6) = 0.069\Sigma$ and $\sigma(n \geq 7) = (10/n^3)\Sigma$. Again, this is all for the FC vibrational state distribution, and the uncertain nature of this distribution has been discussed above. There seem to be no data for angular distributions of the dissociation products.

In summary, for H_2^+ the most important need for fusion edge plasmas is a knowledge of the vibrational state populations of the ions in the edge plasmas. This is critical to our ability to construct reliable cross-sections for the various electron-ion processes from quite accurate individual cross-sections. The next most important need is a better knowledge of the partial cross-sections for dissociative recombination into different $H(n)$. Again, for dissociative recombination, essentially no work has been done on the energy and angular distributions of dissociation products.

3.2. Collisions with H_3^+

The simplest triatomic molecule, H_3^+ , is formed rapidly by the reaction



and the ion so formed is vibrationally excited.

Recombination. As with H_2^+ , the cross-sections for recombination are extremely sensitive to vibrational excitation. Because of cosmological implications, the cross-sections for dissociative recombination of H_3^+ in the ground vibrational state have received a lot of attention and have been a source of intense controversy for a number of years, with reputable experimenters finding rates differing by some five orders of magnitude.¹ Ions created in a plasma ion source and recombined with electrons in colliding beam experiments exhibit an about one order of magnitude smaller cross-section for recombination when the ions have been relaxed — as best the experimenters can determine — to low vibrational levels (for D_3^+ see Van der Donk et al. [24]) than when they are taken just as created (and sometimes further excited in extraction from the ion source). There

is still some inconsistency, however. Experiments by Peart and Dolder [25] provided fairly convincing evidence via the threshold for dissociation that the ions were in very low vibrational states, but they were in agreement with the experiments of Mitchell et al. [23, 24] only when the latter did not think they had vibrational relaxation.

For fusion purposes, it seems that the best one can do at this time is to use data resulting from the vibrationally hot ions, even though one has no real idea what the vibrational distribution is in either the wall plasma or the beam experiments. The rates presented by Janev et al. [11] as an average of data obtained for vibrationally hot ions seem at this time about as close as is possible to estimate what the ‘correct’ values would be for the edge plasma situation. Of course, the uncertainty is high (perhaps an order of magnitude, but more realistically about a factor of three) for these rates because the vibrational levels are unknown and also because the experiments are not in agreement. It may be noted that recent evidence [26] suggests that recombination may even depend on environmental parameters such as small ambient electric fields, and there has been some speculation that these can cause disparate results in different experimental situations.

Mitchell et al. [27] measured the branching ratio for dissociative recombination of H_3^+ and found that it proceeds in a way that yields three H atoms with a probability about 2.5 times greater than the probability to produce one H atom and one H_2 molecule. Peart et al. [28] measured the cross-section required to produce H^- and H_2^+ in the recombination and found it to be about 2% of the total recombination rate at the cross-section peak.

Dissociation. The most extensive measurements of dissociation cross-sections are those of Peart and Dolder [29], though Mitchell et al. [23, 24] have also made measurements over a very narrow energy range. It seems that the data of Peart and Dolder are more applicable to fusion modelling, and they have been adopted and cited in the compendium by Janev et al. [11]. There is no good evidence for a strong vibrational state dependence (except, of course, near threshold) of the cross-section, but this point does not seem to have been fully investigated. Allowing for the latter fact, one should probably cautiously apply a factor of two uncertainty in using these data.

Ionization. The measurements of Peart et al. [28] are for proton production by electron impact on H_3^+ ; thus, the measured cross-sections undoubtedly have a component of ionization in them. This has not been

¹ The extensive literature for dissociative recombination of H_3^+ and other ions is summarized and discussed in a recent review by Mitchell [23].

TABLE I. ELECTRON-MOLECULAR ION COLLISION PROCESSES IN THE EDGE PLASMA

Ion	Process(es)	Method ^a	Uncertainty	Ref. ^b	Comments ^b
H ₂ ⁺ D ₂ ⁺	H ₂ ⁺ + e → H ⁺ + products and → H ⁺ + H + e	A T	±10-20% * ±10-20% *	[11], 15 14, 17	* Very sensitive to the vibrational state population. Uncertainties are much larger for edge plasma without vibrational state information (see text).
H ₂ ⁺ /D ₂ ⁺	H ₂ ⁺ + e → H ⁺ + H ⁺ + 2e	A	≈ ±12%	[11], 18	No evidence for strong vibrational state dependence.
H ₂ ⁺ /D ₂ ⁺	H ₂ ⁺ + e → H + H [*] D ₂ ⁺ + e → D + D(nℓ)	A, B T A, T	±60%	[11], 19, 20 21 [11], 22, 21	Uncertainties are possibly much larger if vibrational states are not known (see text). Ref. [11] cites consistent final state distributions
H ₃ ⁺	H ₃ ⁺ + e → H ⁺ + products	A	±12% *	[11], 28, 23, 24	* Data are for 'vibrationally de-excited' ions. No guidance for 'hot' ions, thus the uncertainty is much higher for edge plasma.
H ₃ ⁺	H ₃ ⁺ + e → H + H + H [*] → H + H ₂ [*] → H ⁻ + H ₂ ⁺	A	±300% * ±12%	[11], 23, 24, 25, 27, 2 8 29	* Beam experiments are much more precise than the uncertainty cited, but experiments do not agree well. Strong vibrational state dependence and possible other dependences [26]. H ⁻ channel very small. Other branching measured [27].
D ₃ ⁺				24	
CO ⁺ CO ₂ ⁺ HCO ⁺ H ₂ O ⁺ H ₃ O ⁺ OH ⁺	X _n Y _m ⁺ + e → Z _k + W _j Dissociative recombination	A, B	Not well defined	[23]	The dissociative recombination process is tabulated and discussed in Ref. [23] for a variety of molecules. However, in no case is the vibrational state variation fully articulated. Since the process is typically very sensitive to vibrational excitation, uncertainties are probably very large without this information.
O ₂ ⁺	O ₂ ⁺ + e → O ⁺ + O + e	A	≈ ±15%	30	Vibrational effects not studied; thus, uncertainties are much larger for edge plasma.
CO ⁺	CO ⁺ + e → C ⁺ + O + e → C + O ⁺ + e	A	≈ ±20%	31	Performed only for a deduced mix of electronic (X, A, B) and vibrational states. Therefore, uncertainties are much larger for edge plasma.
H ₃ O ⁺	H ₃ O ⁺ + e → O ⁺ + products → OH ⁺ + products D ₃ O ⁺ + e → D ₂ O ⁺ + products	A	≈ ±20%	32	Performed on an unknown mix of states from the ion source; therefore, uncertainties are larger for edge plasma.
CO ₂ ⁺	CO ₂ ⁺ + e → CO ₂ ²⁺ + 2e	A	≈ ±15%	33	Evidence suggests no highly excited electronic or vibrational levels in target ions.
OH ⁺	OH ⁺ + e → O ²⁺ + H ⁺ + 3e	A	≈ ±20%	34	Cross-section nearly the same as for O + e → O ²⁺ + 3e, a finding similar to that for multiple ionization of other molecular ions.

^a A indicates colliding beam experiments, B indicates plasma rate experiments and T indicates theoretical calculations.

^b [] indicates a recommended compendium of results. Other compendia may be referred to in the text.

Other references are primarily to the original literature.

separated out, so currently there are no data describing ionization of H_3^+ .

3.3. Collisions with other molecular ions

The status of the database for molecular ions, including those already discussed above, is summarized in Table I. As can be seen, the data for other ions are very spotty and incomplete. Dissociative recombination, however, has been studied for a broad range of ions with various combinations of plasma and beam techniques, and a recent review and compendium [23] summarizes the data. The energy range is generally very limited, and, despite probable strong dependences on vibrational state, no serious efforts have been made to sort this out and to obtain data on the dependence, except for the simple ions already discussed above. Normally, some effort is made to try to get ions into the ground state or the low vibrational states, and this may not apply to the edge plasma conditions. Hence, the available data must be used with considerable scepticism.

Experiments on the dissociation of molecular ions have been carried out for a few other ions of interest, namely O_2^+ [30], CO^+ [31] and H_3O^+ [32]. It is very difficult to obtain reliable data for processes of the type $XH_n^+ + e \rightarrow H^+ + \text{products}$, when X is a heavy particle or a composite of particles, because the light H^+ carries away most of the excess energy into large angles and is not collected properly. Thus, few data exist. Ionization of molecular ions of interest has also been carried out only for CO_2^+ [33] and H_3O^+ [34]. Again, for the heavier ions, no serious effort has been made to sort out the vibrational state dependence for dissociation and ionization. Optical excitation of a molecular ion by electron impact has been carried out only for N_2^+ , an ion not particularly of interest for the edge plasma.

4. DATA: ATOMIC IONS

The database for electron collisions with atomic ions is more broadly based than that for collisions with molecular ions. The absence of vibration and rotation makes it easier to define the experimental 'target', and the fewer degrees of freedom make the theory simpler. Of course, even so, in many experiments there is still ambiguity brought about by the possible presence of ions in metastable electronic levels. Similarly, one does not know the densities of metastable ions in the edge plasma. Nevertheless, it has become customary for persons in both theory and experiment to work together to try to unravel the metastable issue. This is not always possible,

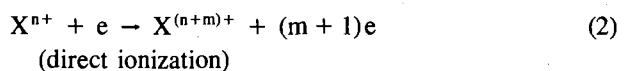
of course, and then one must simply say "this is the best there is, and the plasma may also have metastables in it" — which is, of course, not totally satisfying.

The database for ionization of atomic ions has been given significant attention and scrutiny. A number of evaluations have been performed, and compendia, compilations and bibliographies are available. This is less so for recombination and excitation. In the following, we will discuss the specific collision processes in the order: ionization, recombination, and excitation.

4.1. Ionization

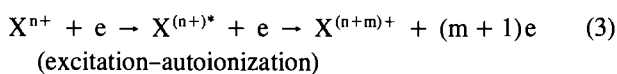
The first crossed-charged beam experiment ever performed was a measurement of the ionization cross-section of He^+ by electron impact, performed by Dolder et al. [35] in 1961. Since then, not only have the laboratories of Dolder and of Harrison been productive in this area, but also laboratories at Giessen, Oak Ridge, JILA, Georgia Institute of Technology and Louvain-la-Neuve have produced prodigious amounts of experimental data and information on ionization of ions by electron impact. The experiments are straightforward conceptually, involving the crossing of beams of the two particles, followed by charge separation either electrostatically or magnetically to detect product ions. The experiments are perhaps the easiest of colliding charged beam experiments, since one can readily collect 100% of the product ions and detect nearly all of them. Once one understands the systematic problems to be avoided, and takes relevant steps to do so, very accurate experiments can be performed — limited primarily by one's patience in obtaining the desired signal-to-background fluctuation ratios. The implementation at Oak Ridge of the Penning ion gauge (PIG) ion source, followed by the use of the electron cyclotron resonance (ECR) ion source there as well as at Giessen and Louvain-la-Neuve, have made the study of multiply charged ions readily accessible with impressive accuracy and, in some cases, astoundingly high precision.

There are at least three fundamental processes occurring in ionizing collisions. The first is *direct ionization*, which can be described by just the knock-on collision between the incident electrons and the target electrons resulting in enough momentum imparted for the target electron(s) to depart:

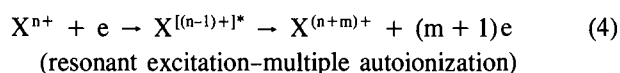


Also frequently occurring and often dominating the direct process is *excitation-autoionization* (EA)

represented by



where the incident electron first excites an inner-shell target electron which in turn shares its excess energy with m other ionic electrons, giving each electron enough energy to depart from the ion, thus leaving it more highly ionized. Finally, the incident electron may have just ϵ less energy than that needed to excite the electron in the above mechanism, but as it approaches the ion in the attractive Coulomb field, it gains kinetic energy so that close to the core it can indeed excite the electron. However, as it starts to leave, it finds itself bound by energy ϵ in a Rydberg state of a once-less-charged ion with an excited core. The ion so formed may proceed to ionize as above, and also to throw off the Rydberg electron:



When $m = 1$, the term coined for this process by LaGattuta and Hahn [36], who hypothesized it, was REDA for *resonant excitation–double autoionization*. Later, Müller et al. [37], who first observed REDA and also observed double and triple net ionization in a resonant process, coined RETA and REQA as obvious generalizations. Now, however, as much as *eightfold* ionization has been observed [38], occurring from identically the same resonances as those leading to single, twofold and threefold ionization. When excitation–autoionization is a major part of the total ionization (as is frequently so), then the resonant process may have meaningful contributions to the total cross-section.

Data on ionization have been compiled and evaluated by several groups [39–44], and we have cited only those most recently published, noting that references to the original literature as well as to earlier compilations and evaluations may be found in those cited. A recent report [45] gives detailed comparisons between rate coefficients given in Refs [40, 44] as well as with those of the Lotz formula, and also points out a few errors in the earlier papers. Reference [40] is comprehensive, giving parametrized cross-sections and rate coefficients, a discussion of uncertainties, and numerous figures.

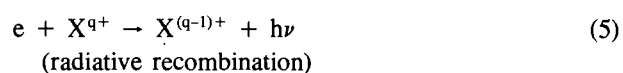
Table II illustrates the present status of the database for single ionization of atomic ions. To a large (though not exclusive) extent, we have relied on the assessment in Ref. [40] in arriving at the indicated uncertainties. In the table, capital letters indicate that the data recommended come primarily from experiment, lower case letters indicate that the data are from theory, and lower

case letters with subscript s indicate that the data are scaled from other isoelectronic species. Since the scaling in Ref. [40] did not include excitation–autoionization, large uncertainties may result for isoelectronic structures where it is important. In Ref. [44], some effort was made to include EA in scaling. Obviously, EA is included in the experiments; it is also included in many of the most recent theoretical calculations. Accuracies are associated with letters of the alphabet according to the schedule at the bottom of the table. Data in Refs [46–52] have not been included in the compendia.²

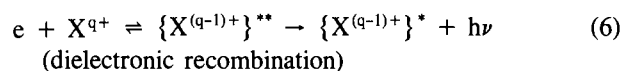
One can see that for a significant number of species/charge states, uncertain scaling has been applied to obtain the data, and that there are no data at all for molybdenum and tungsten ions, the importance of which may once again be high, as these materials are being considered anew for limiters and divertors. Experimental data for these latter are difficult — but not impossible — to obtain, and efforts have not been successful to date. Similarly, the complexities of the atomic structures of these heavy ions make the theory very difficult for the low charge states of interest for the edge plasma, except by simple estimator formulas. On the other hand, the database may be considered excellent for light ions through oxygen, and it is in good shape for iron and nickel for which special efforts have been made to produce data for fusion purposes.

4.2. Recombination

Recombination of atomic ions with electrons is dominated by radiative recombination (RR) at low temperatures for fully stripped ions and by dielectronic recombination (DR) for ions with electrons at high temperatures. The former can be represented by



and the latter by



The first of these is the inverse of photoionization, and the probability clearly involves the ratio of radiative lifetime to the fly-by time of the electron past the ion. The second is the inverse of autoionization. The electron imparts its energy to a bound electron of the ion and is

² In Ref. [41], S. Younger (1982, probably personal communication) is quoted: Distorted wave exchange method; direct ionization only. Since the ion is rubidium-like in structure, it is likely that EA plays a significant role; therefore, we have assigned an accuracy of only “c”.

TABLE II. ELECTRON IMPACT SINGLE IONIZATION OF IONS MOST LIKELY TO BE FOUND IN THE PLASMA EDGE

IONIZATION									
ELEMENT	CHARGE OF TARGET ION								
	+1	+2	+3	+4	+5	+6	+7	+8	+9
Helium	A								
Lithium	A	A							
Beryllium	B	b _s	a _s						
Boron	B	A	B	a _s					
Carbon	A	A	A	B	a _s				
Oxygen	A	A	A	B	A	B	a _s		
Magnesium	B	B	d _s	d _s	c _s	c _s	d _s	c _s	c
Aluminium	B	B	c	d _s	c	c _s	c	c	b
Silicon	d _s	d _s	B	B ⁴⁶	B ⁴⁶	B ⁴⁶	c _s	c _s	d _s
Chlorine	B ⁴⁷	B	d _s	d _s	B	e _s	d _s	d _s	d _s
Titanium	A	A	A	d _s	d _s	d _s	d _s	d _s	d _s
Chromium	A	d _s	e _s	e _s	e _s	A	A	A	d _s
Iron ⁴²	B	B	c	c	B	B	b	b	B
Nickel ⁴³	B	c	B	c	B	B	B	B	b
Copper	B ⁴⁸	B ⁴⁹	B ⁴⁹						
Gallium	A ⁵⁰								
Molybdenum					e ⁵¹				
Tungsten	A ⁵²								

Accuracy: A < 10%; B 10-25%; C 25-50%; D 50-100%; E > 100%; upper case: from experiment; lower case: from theory; lower case with subscript s: scaled using various methods.

Superscript numerals indicate references for original data or compendia; data for iron, Ref. [42]; data for nickel, Ref. [43]. When no numerals are given, then the data are from the evaluation, Ref. [40].

captured into a Rydberg state of a once-less-charged ion which then radiates in competition with autoionization. Both of these processes have lent themselves to detailed experimental study only in the past few years, providing some assessment of the accuracy of the theoretical methods upon which one relies for the bulk of the

data. One can find more than a hundred references to each of these processes from the past six years, so the science of the processes is active and it is not appropriate to try to give a bibliography here. A recent general discussion of the two processes has been presented by Griffin [53].

Radiative recombination. Following the work of Tarter [54] it is common to split the RR rate into two terms: $\alpha_{n_g}^r$, the rate to the ground state, and α_n^r , the rate to all other states, $n \neq n_g$, so that $\alpha^r = \alpha_{n_g}^r + \sum \alpha_n^r$. The first term is related via detailed balance to the photoionization cross-section through the Milne relation, and it is common practice to use the hydrogenic approximation for the higher states n , although, as discussed in Ref. [53], this introduces some uncertainties, which have been shown to be significant.

Parametrized rate coefficients of elements of interest to this report have been tabulated by Shull and Van Steenberg [55] for all ionization stages of C, O, Mg, Si, Fe and Ni, and by Arnaud and Rothenflug [44] for the H, He and Li isoelectronic sequences of these elements. More recent rates are given for C and O ions in Refs [53] and [56]. Hahn [57]³ has tabulated parameters that provide rates for any ion in a 'pure Coulombic' approximation using an effective charge. Detailed calculations of the multitude of oscillator strengths needed for more correctly calculating the cascade matrix for RR than is provided by the hydrogenic approximation have been pursued by a variety of authors (see, for example, Ref. [58]), and the worldwide effort entitled "The Opacity Project" [59] is leading to detailed oscillator strengths, photoionization cross-sections, damping constants, etc., for all ions in the hydrogen through neon isoelectronic sequences going up through iron.

Assessment of the accuracy of the parametrized and tabulated rates is difficult at this time. It has been customary to think "the theoretical task of generating the RR rates is relatively simple" [57]. It was only in 1991, however, that RR has lent itself to direct experimental tests, as reviewed recently by Müller et al. [60], and early results indicate good agreement between experimental and theoretical values of rate coefficients. Andersen and Bolko [61], using a single-pass merged configuration, obtain agreement generally to within a few per cent between their experimental values for fully stripped He, C and F ions and theoretical values. Andersen and Bolko [62] obtained similar agreement for H-like C, O and F, but, for Li-like O, only moderate agreement was obtained. For many-electron Au²⁵⁺ and U²⁸⁺, gigantic discrepancies between experiment and theory have been found at near zero energy by Müller [63], and these remain under investigation to determine

³ The tables in Ref. [57] give the parameter value of $\theta = kt/Z^2$ to as small as 10^{-5} , but the results are not accurate for $\theta \leq 10^{-2}$ (Y. Hahn, personal communication). Thus, the utility of this parameter for low temperatures and high charges is limited.

whether either DR or density effects enter into the disagreements found. On the other hand, with the same apparatus, reasonable agreement has been found for Li-like Ar¹⁵⁺. Some good 'consistency checks' exist for other multiple-electron ions. Thus, the EBIT group [64] has normalized its DR results to observations of RR, and obtained good agreement with theory for Ne-like ions as well as He-like ions, thus giving indirect consistency checks on RR and DR calculations.

One is inclined to believe conservatively that the available rates are accurate to $\pm 50\%$, and many believe the uncertainty to be as low as $\pm 20\%$ or better. However, more extensive and detailed comparisons with experiments are called for, including a broad range of isoelectronic series and charges, before reliable assessments can be made.

Dielectronic recombination. Though hypothesized earlier, DR became a mainstay in ionization balance considerations after 1964 when Burgess [65] showed its importance in resolving discrepancies of temperature measurements of the solar corona. It is the dominant recombination process for high temperatures. Burgess and Summers [66] recognized early that DR could be dramatically affected by the mixing of angular momentum states, and they treated the effect of electron collisions in this context, thus showing density effects for the process. Jacobs et al. [67] recognized that electric fields could mix ℓ -states and strongly influence DR, and they treated dielectronic recombination in fields (DRF) from the special perspective of the influence of plasma microfields. In tokamaks there are, of course, also Lorentz $\vec{v} \times \vec{B}$ fields which can be quite sizeable. This sensitivity to 'environmental effects' makes the discussion of this process less straightforward than that of some of the topics touched on earlier in this paper. Before proceeding, it is worth while to present a brief elementary discussion of the process.

Borrowing from an earlier discussion [68] of DR, let σ_c represent the dielectronic capture cross-section. The fraction undergoing radiative stabilization of the compound state is determined approximately by the branching ratio $[A_r/(A_r + A_a)]$, where A_r and A_a are the transition rates for radiation and autoionization, respectively. The cross-section for DR into a given state is then

$$\sigma = \sigma_c [A_r/(A_r + A_a)] \quad (7)$$

The capture of a free electron into a doubly excited state is the inverse of autoionization. From the principle of detailed balance, it follows that $\sigma_c = kA_a$, where k is a proportionality factor including the ratio of density

of states. The DR cross-section for capture into a state represented by quantum numbers n, ℓ can then be written as

$$\sigma_{n,\ell} = \sigma_0 2(2\ell + 1) \left[\frac{A_a(n, \ell) A_r(n, \ell)}{A_a(n, \ell) + A_r(n, \ell)} \right] \quad (8)$$

where σ_0 involves various constants, includes a reciprocal dependence on the threshold energy ΔE and the energy width δE , and also involves the statistical weights of the initial and core states of the product; $2(2\ell + 1)$ is the statistical weight of the final Rydberg state n, ℓ .

The highly excited Rydberg electron is effectively a 'spectator' as far as the radiative stabilization of the core electron is concerned; thus, $A_r(n, \ell)$ is nearly constant with n and ℓ . One may often make the assumption $A_a \gg A_r$, i.e. for low- Z ions, one normally considers $A_a \approx 10^{14} \text{ s}^{-1}$ and $A_r \approx 10^8 \text{ s}^{-1}$. In such a case, we have from Eq. (8), $\sigma_{n,\ell} \approx 2\sigma_0 A_r(n, \ell) (2\ell + 1)$, and when this is summed over the $n-1$ possible values of ℓ for a given n , we obtain for the DR cross-section to a given n , $\sigma_n \approx Bn^2$. Here, B is a constant, but the point is that σ_n diverges as n^2 . However, it will be recognized that A_a is a strong function of both n and ℓ ; the core excited electron wave function will overlap less with captured electron wave functions for very high n or high ℓ electrons. Thus, $A_a \propto n^{-3}$ is reasonably well established, and one may approximate some behaviour with ℓ , say, $A_a \propto \exp(-\alpha\ell^2)$. Thus, although the number of resonances that could contribute to DR increases as $2n^2$, only values of $\ell \leq \ell_c$ will actually contribute, where ℓ_c is the value of ℓ such that $A_a(n, \ell) = A_r(n, \ell)$. In this case,

$$\sigma_n = \sum_{\ell=0}^{n-1} \sigma_{n,\ell} \approx \sum_{\ell=0}^{\ell_c} \sigma_{n,\ell} = \sigma_0 2(\ell_c + 1)^2 A_r \quad (9)$$

While this limiting of the number of states has little effect for small n 's where $\ell_{\max} = (n-1) < \ell_c$, already for moderate n 's all possible contributions from ℓ 's with $\ell_c \leq \ell \leq (n-1)$ are suppressed because of the strong decrease of A_a with ℓ . There is thus a large 'reservoir' of states that could contribute to DR if their autoionization rates were larger. It is the proclivity of environmental factors to move these states into and out of importance that leads to part of the sensitivity (mentioned earlier) to such things as collisions and ambient electric fields. Thus, an electric field or collisions may mix states with low autoionization rates with those of high rates, thereby increasing the net number of states with $A_a > A_r$ and increasing the DR cross-section. The value of ℓ_c is increased to ℓ_c^* , i.e. more states effectively participate in the recombination process, and the cross-section $\sigma_n^* = \sum_{\ell} \sigma^*(n, \ell)$ is increased. The contributions to DR from high lying Rydberg states is usually less

for transitions in which $\Delta n \neq 0$, thus making cross-sections involving these transitions less susceptible to the external factors mentioned. The sensitivity to environmental factors also depends on the charge of the ion target, since A_r increases with charge, hence decreasing ℓ_c . In the other direction, another sensitivity involves the ability of both collisions and fields to destroy the doubly excited states before radiative stabilization can occur, i.e. impact or field ionization of these states. Thus, careful consideration must be given to these factors in any given situation and locally evaluated parameters must be used.

Over the last decade, cross-sections and rates for DR and DRF have been measured with both beams and plasma rate techniques [69-71]. Recent measurements using electron cooling beams in both heavy ion storage rings and merged beams have a particular advantage in separating out individual final states for study. With this technique, theory and experiment have now been compared for H-like ions [72], He-like ions [73], Li-like ions [73, 74], Be-like ions [75] and B-like ions [75]. In most cases in which environmental conditions are carefully controlled and known, good agreement between theory and experiment has been obtained, thus giving us confidence that the low density rates in the absence of fields can be calculated and used with some assurance. Only for Mg^+ [68] were fields carefully measured and controlled, and in that case quite good agreement with Stark mixing calculations was obtained. However, there are a number of experiments for which agreement between theory and experiment has not been achieved, even when best estimates and fields are taken into account. It seems that a fair amount of caution needs to be exercised in assuming good accuracy after using standard methods for taking field effects into account until further work is done in this area. Pindzola et al. [76] have summarized the cases for which there is disagreement between theory and experiment and have projected advances likely to be forthcoming in the future. Though Bell and Seaton [77] developed a coupled channel formalism for DR calculations, most calculations have been performed in the isolated resonance approximation as a two-step process, as outlined above. There are numerous such calculations in the literature, including those performed with general formulas such as in Ref. [10]. These all give the zero density rate coefficients. Badnell et al. [78] outline how these zero density rate coefficients "can be incorporated [79] into the solution of the collisional dielectronic population rate equations [66] for a finite density plasma by parametrizing raw data calculated with the Burgess General Program [79]". Using the generalized picture [80], the

data can then be incorporated into the solution of the generalized collisional dielectronic rate equations.

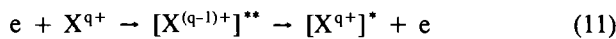
In summary, the evidence is strong that one can readily have access to zero density, zero field rate coefficients for most of the systems of interest in the edge plasma which are generally accurate to something in the neighbourhood of 30%. However, applying these rate coefficients in modelling requires going into detailed evaluations of density and field effects, and the uncertainties in the evaluated rates are probably substantially larger. It appears that the experimental thrust to verify zero density rates has been successful, and now an additional thrust to verify density and field effects should prove valuable.

4.3. Excitation

Just as with ionization and with recombination, there is a direct mechanism and an indirect mechanism for excitation of ions by electrons. The former may be represented by



while the latter has the form



Resonance excitation as represented in expression (11) thus includes resonance dielectronic capture to a doubly excited state, followed by Auger relaxation, not to the ground state, which would be resonant elastic scattering, but to an excited state. The resonance mechanism can often dominate the excitation at specific energies; so it is important that both processes be considered.

For a number of years the only cross-section measurements were performed using the crossed beam method and detecting fluorescence from emitting states. As reviewed by Dunn [81] and Phaneuf [82], *absolute* total emission cross-section measurements were performed on the $\Delta n = 0$ resonance states of Be^+ , Ca^+ , Sr^+ , Ba^+ , Ga^+ , Zn^+ , Mg^+ , Hg^+ , C^{3+} , N^{4+} and Al^{2+} , and for a few non-resonance transitions for the singly charged ions of Ca, Sr, Ba, Zn, Mg and Hg. The only He-like ion and the only intercombination transition for which measurements were made was the $1^1\text{S} \rightarrow 2^3\text{P}$ state of Li^+ . After arduous efforts to improve wave functions and other parts of the theory, it has been possible to obtain agreement between experiment and theory to within something like $\pm 15\%$ or better for the simpler structures. The simple Gaunt factor formula referred to earlier describes the resonance transitions for the singly charged ions to within the advertised factor of two, and most often better than that. Addi-

tional verification of the theory for inner-shell excitation of a variety of ions has come through comparing measured excitation–autoionization cross-sections with the theory which involves excitation calculations.

More recently, two new techniques for measurement of excitation cross-sections have been developed. The first involves the EBIT and EBIS [7]. Again, good agreement with theory has been found for radiating states of highly (more so than of interest to the edge plasma) charged ions. The measurements, as discussed earlier, are not absolute, but are referenced to theory for radiative recombination. The second technique is an electron energy loss method employing trochoidal merge and demerge techniques in crossed electric and magnetic fields. This technique yields absolute cross-sections, and measurements [6] on the $\Delta n = 0$ resonance transition of Si^{3+} with this method again show good agreement with the theory.

The theoretical database for excitation is enormous. Clearly, there is an infinite number of possible transitions for every ion — of course not all calculated and not all important in the edge plasma. There are a number of useful evaluations and compilations (see Refs [83–88]), some motivated by the fusion energy effort. The Opacity Project [59] is working towards obtaining complete collision strengths for all ions of hydrogen through iron, and there is an extremely large database, much of which is not published. Similar projects at Lawrence Livermore National Laboratory and Los Alamos National Laboratory maintain large computer databases, and complete data on titanium have been recently reported [89] from LANL. Many of the data are available in the ALADDIN database system that has been adopted by the IAEA for exchange of fusion relevant atomic and molecular data [90]. Some points of view suggest that so many excitations are needed that it is easier to compute the cross-sections when required than to try to maintain the database. Indeed, the computational capability of the large projects is great enough that this point of view may not be unreasonable.

Accuracies of the data are generally evaluated from a *theoretical point of view*, since, as discussed above, there have been experimental checks for only a limited class of excitations. Even from the theorists' point of view, some are more optimistic about the data than others. Estimated accuracies range all the way from A to E, using the same rating scheme as in Table II. Generally, close coupling calculations performed with care in constructing wave functions, in including the relevant states, etc., obtain ratings of A to B, distorted wave calculations obtain ratings of B to C, and Coulomb

Born calculations obtain ratings of C to E; this is, however, a generalized statement which varies for individual cases.

In summary, the theoretical/computational machinery is in place to obtain excitation cross-sections and rates quoted which one will be told are within 10–20%. In accepting and using such data, however, it must be remembered that the extent to which the calculation methods have been experimentally checked is very limited, as discussed above. It remains one of the challenges in the electron-ion field to make the relevant experimental tests of theory.

ACKNOWLEDGEMENTS

The author is grateful to Dr. Ronald Phaneuf and Dr. Steven Jefferts for helpful comments on the manuscript.

The work was supported in part by the Office of Fusion Energy, United States Department of Energy, under contract with the National Institute of Standards and Technology.

REFERENCES

- [1] BROUILLARD, F. (Ed.), *Atomic Processes in Electron-Ion and Ion-Ion Collisions*, Plenum Press, New York (1986).
- [2] MÄRK, T.D., DUNN, G.H. (Eds), *Electron Impact Ionization*, Springer-Verlag, Berlin (1985).
- [3] BROUILLARD, F., MCGOWAN, J.W. (Eds), *Physics of Ion-Ion and Electron-Ion Collisions*, Plenum Press, New York (1983).
- [4] DOLDER, K.T., PEART, B., *Rep. Prog. Phys.* **39** (1976) 693.
- [5] KILGUS, G., BERGER, J., BLATT, P., et al., *Phys. Rev. Lett.* **64** (1990) 737.
- [6] WÄHLIN, E.K., THOMPSON, J.S., DUNN, G.H., PHANEUF, R.A., GREGORY, D.C., SMITH, A.C.H., *Phys. Rev. Lett.* **66** (1991) 157.
- [7] STOCKLI, M.P., *Z. Phys., D* **21** (1991) 111.
- [8] BURGESS, A., *Mém. Soc. R. Sci. Liège* **4** (1961) 299; SEATON, M.J., BURGESS, A., in *Atomic and Molecular Processes* (BATES, D.R., Ed.), Academic Press, New York (1962) 374; VAN REGEMORTER, H., *Astrophys. J.* **136** (1962) 906.
- [9] LOTZ, W., *Astrophys. J., Suppl.* **14** (1967) 207; *Z. Phys.* **206** (1967) 205; **216** (1968) 241; **232** (1970) 101.
- [10] BURGESS, A., *Astrophys. J.* **141** (1965) 141.
- [11] JANEV, R.K., LANGER, W.D., EVANS, K., POST, D.E., *Elementary Processes in Hydrogen-Helium Plasmas*, Springer Series on Atoms and Plasmas, Vol. 4, Springer-Verlag, Berlin (1987).
- [12] TAWARA, H., ITIKAWA, Y., ITOH, Y., et al., *Atomic Data Involving Hydrogens Relevant to the Edge Plasmas*, Rep. IPPJ-AM-46, Institute of Plasma Physics, Nagoya University (1986).
- [13] EENSHUISTRA, P.J., BONNIE, J.H.M., LOS, J., HOPMAN, H.J., *Phys. Rev. Lett.* **60** (1988) 341; HALL, R.I., ČADEZ, I., et al., *Phys. Rev. Lett.* **60** (1988) 337; ČADEZ, I., HALL, R.I., et al., *J. Phys., B* (London) **21** (1988) 3271; STUTSON, J., PhD Thesis, Univ. of California, Berkeley (1990).
- [14] PEEK, J.M., *Phys. Rev., A* **140** (1965) 11; **154** (1967) 154; **10** (1974) 539; PEEK, J.A., GREEN, T.A., *Phys. Rev.* **183** (1969) 202; COLLINS, L.A., SCHNEIDER, B.I., *Phys. Rev., A* **27** (1983) 101; KIMURA, M., *Phys. Rev., A* **35** (1987) 4101.
- [15] DUNN, G.H., VAN ZYL, B., *Phys. Rev.* **154** (1967) 40; DANCE, D.F., HARRISON, M.F.A., RUNDEL, R.D., SMITH, A.C.H., *Proc. Phys. Soc.* **92** (1967) 577; PEART, B., DOLDER, K.T., *J. Phys., B* (London) **4** (1971) 1496; **5** (1972) 1554.
- [16] DUNN, G.H., *J. Chem. Phys.* **44** (1966) 2592; BUSCH, F. von, DUNN, G.H., *Phys. Rev., A* **5** (1972) 1726.
- [17] ZARE, R.N., *J. Chem. Phys.* **47** (1967) 204; GREEN, T.A., PEEK, J.M., *Phys. Rev.* **183** (1969) 166.
- [18] PEART, B., DOLDER, K.T., *J. Phys., B* (London) **6** (1973) 2409.
- [19] PEART, B., DOLDER, K.T., *J. Phys., B* (London) **7** (1974) 236; AUERBACH, D., CACAK, R., CAUDANO, R., et al., *J. Phys., B* (London) **10** (1977) 3797; MATHÜR, D., KAHN, S.U., HASTED, J.B., *J. Phys., B* (London) **11** (1978) 3615.
- [20] HUS, H., et al., *Phys. Rev. Lett.* **60** (1988) 1006; MCGOWAN, W.M., CAUDANO, R., KEYSER, C.J., *Phys. Rev. Lett.* **36** (1976) 1447.
- [21] NAKASHIMA, K., TAKAGI, H., NAKAMURA, H., *J. Chem. Phys.* **86** (1987) 726; GIUSTISUZOR, A., BARDSLEY, J.N., DERKITZ, C., *Phys. Rev., A* **28** (1983) 682; ZHDANOV, V.P., CHIBISOV, M.I., *Sov. Phys. — JETP* **47** (1978) 38.
- [22] VOGLER, M., DUNN, G.H., *Phys. Rev., A* **11** (1975) 1983; PHANEUF, R.A., CRANDALL, D.H., DUNN, G.H., *Phys. Rev., A* **11** (1975) 528.
- [23] MITCHELL, J.B.A., *Phys. Rep.* **186** (1990) 217.
- [24] HUS, H., YOUSIF, F., SEN, A., MITCHELL, J.B.A., *Phys. Rev., A* **38** (1988) 658; VAN DER DONK, P., YOUSIF, F.B., MITCHELL, J.B.A., *Phys. Rev., A* **43** (1991) 5971.
- [25] PEART, B., DOLDER, K.T., *J. Phys., B* (London) **14** (1974) 1948.
- [26] BORDAS, C., HELM, H., *Phys. Rev., A* **43** (1991) 3645.
- [27] MITCHELL, J.B.A., FORAND, J.L., NG, C.T., et al., *Phys. Rev. Lett.* **51** (1983) 885.
- [28] PEART, B., FORREST, R.A., DOLDER, K.T., *J. Phys., B* (London) **12** (1979) 3441.
- [29] PEART, B., DOLDER, K.T., *J. Phys., B* (London) **8** (1975) L143.
- [30] VAN ZYL, B., DUNN, G.H., *Phys. Rev.* **163** (1967) 43.
- [31] MITCHELL, J.B.A., HUS, H., *J. Phys., B* (London) **18** (1985) 547.

- [32] SCHULZ, P.A., GREGORY, D.C., MEYER, F.W., PHANEUF, R.A., *J. Chem. Phys.* **85** (1986) 3386.
- [33] MÜLLER, A., SALZBORN, E., FRODL, R., BECKER, R., KLEIN, H., *J. Phys.*, B (London) **13** (1980) L221.
- [34] STENKE, M., MÜLLER, A., DUNN, G.H., HOFMAN, G., WEISSBECKER, B., SALZBORN, E., paper presented at Spring Meeting of the German Physical Society, 1990 (unpublished).
- [35] DOLDER, K.T., HARRISON, M.F.A., THONEMAN, P.C., *Proc. Phys. Soc.*, A **264** (1961) 367.
- [36] LaGATTUTA, K.J., HAHN, Y., *Phys. Rev.*, A **24** (1981) 2273.
- [37] MÜLLER, A., TINSCHERT, K., HOFMANN, G., SALZBORN, E., DUNN, G.H., *Phys. Rev. Lett.* **61** (1988) 70.
- [38] HOFMANN, G., MÜLLER, A., NEUMANN, J., et al., in *Physics of Electronic and Atomic Collisions (Proc. 7th Int. Conf. Brisbane, 1991)*, Abstracts (1991) 295.
- [39] BELL, K.L., GILBODY, H.B., HUGHES, J.G., KINGSTON, A.E., SMITH, F.J., *J. Phys. Chem. Ref. Data* **12** (1983) 891.
- [40] LENNON, M.A., BELL, K.L., GILBODY, H.B., et al., *J. Phys. Chem. Ref. Data* **17** (1988) 1285.
- [41] TAWARA, H., KATO, T., *At. Data Nucl. Data Tables* **36** (1987) 167.
- [42] PINDZOLA, M.S., GRIFFIN, D.C., BOTTCHEER, C., YOUNGER, S.M., HUNTER, H.T., *Nucl. Fusion, Special Suppl.* (1987) 21.
- [43] PINDZOLA, M.S., GRIFFIN, D.C., BOTTCHEER, C., BUIE, M.J., GREGORY, D.C., *Phys. Scr.*, T **37** (1991) 35.
- [44] ARNAUD, M., ROTHENFLUG, R., *Astron. Astrophys., Suppl. Ser.* **60** (1985) 425.
- [45] KATO, T., MASAI, K., ARNAUD, M., Comparison of Ionization Rate Coefficients of Ions from Hydrogen through Nickel, Rep. ISSN 0915-6364, National Institute for Fusion Science, Nagoya (1991).
- [46] THOMPSON, J. (JILA, Natl. Bur. Stand., Boulder, CO), GREGORY, D.C. (ORNL), personal communications, 1991.
- [47] DJURIC, N., BELL, R., DUNN, G.H. (JILA, Natl. Bur. Stand., Boulder, CO), personal communications, 1991.
- [48] MÜLLER, A., TINSCHERT, K., HOFMANN, G., SALZBORN, E., DUNN, G.H. (JILA, Natl. Bur. Stand., Boulder, CO), personal communications, 1988.
- [49] GREGORY, D.C., HOWALD, A.M., *Phys. Rev.*, A **34** (1986) 97.
- [50] ROGERS, W.T., STEFANI, G., CAMILLONI, R., DUNN, G.H., *Phys. Rev.*, A **25** (1982) 737.
- [51] TAWARA, H., KATO, T., *At. Data Nucl. Data Tables* **36** (1987) 167 (Figure with reference to S. Younger, 1982).
- [52] MONTAGUE, R.G., HARRISON, M.F.A., *J. Phys.*, B (London) **17** (1984) 2707.
- [53] GRIFFIN, D., *Phys. Scr.*, T **28** (1989) 17.
- [54] TARTER, C.B., *Astrophys. J.* **168** (1971) 313.
- [55] SHULL, J.M., VAN STEENBERG, M., *Astrophys. J., Suppl. Ser.* **48** (1982) 95; errata: *ibid.* **49** (1982) 351.
- [56] HAHN, Y., *Phys. Scr.*, T **28** (1989) 25.
- [57] McLAUGHLIN, D.J., HAHN, Y., *Phys. Rev.*, A **43** (1991) 1313; see also HAHN, Y., *Phys. Scr.*, T **37** (1990) 54.
- [58] VICTOR, G.A., ESCALANTE, V., *At. Data Nucl. Data Tables* **40** (1988) 228.
- [59] PRADHAN, A.K., *Phys. Scr.*, T **35** (1987) 840; BERINGTON, K.A., *Phys. Scr.*, T **37** (1991) 19.
- [60] MÜLLER, A., SCHENNACH, S., WAGNER, M., et al., *Phys. Scr.*, T **37** (1991) 62.
- [61] ANDERSEN, L.H., BOLKO, J., *Phys. Rev.*, A **42** (1990) 1184.
- [62] ANDERSEN, L.H., BOLKO, J., *J. Phys.*, B (London) **23** (1990) 3167.
- [63] MÜLLER, A., in *Recombination of Atomic Ions (Proc. Adv. Res. Workshop Newcastle, 1991)*, Plenum Press, New York, London (1991).
- [64] KNAPP, D.A., MARRS, R.E., LEVINE, M.A., et al., *Phys. Rev. Lett.* **62** (1989) 2104; KNAPP, D.A., BEIERSDORFER, P., SCHNEIDER, M.B., in *Physics of Electronic and Atomic Collisions (Proc. 7th Int. Conf. Brisbane, 1991)*, Abstracts (1991) 303; SCHNEIDER, M.B., KNAP, D.A., CHEN, M., et al., *ibid.*, p. 304.
- [65] BURGESS, A., *Astrophys. J.* **139** (1964) 776.
- [66] BURGESS, A., SUMMERS, H.P., *Astrophys. J.* **157** (1969) 1007.
- [67] JACOBS, V.L., DAVIS, J., KEPPLER, P.C., *Phys. Rev. Lett.* **37** (1976) 1390; see also: JACOBS, V.L., DAVIS, J., *Phys. Rev.*, A **19** (1979) 776.
- [68] MÜLLER, A., BELIĆ, D.S., DEPAOLA, B.D., et al., *Phys. Rev.*, A **36** (1987) 599.
- [69] DUNN, G.H., in *Atomic Processes in Electron-Ion and Ion-Ion Collisions (BROUILLARD, F., Ed.)*, Plenum Press, New York, London (1986).
- [70] ANDERSON, L., MÜLLER, A., KNAPP, D.A., COCKE, L., WOLF, A., DUNN, G., DITTNER, P., in *Recombination of Atomic Ions (Proc. Adv. Workshop Newcastle, 1991)*, Plenum Press, New York, London (1991).
- [71] BITTER, M., HSUAN, H., VON GOELER, S., et al., *Phys. Scr.*, T **37** (1991) 66.
- [72] KILGUS, G., BERGER, J., BLATT, M., et al., *Phys. Rev. Lett.* **64** (1990) 737 (expt. O^{7+}); PINDZOLA, M.S., BADNELL, N.R., GRIFFIN, D.C., *Phys. Rev.*, A **41** (1990) 2422 (theory: C^{5+} , O^{7+} , Si^{13+} , S^{15+}).
- [73] ANDERSEN, L.H., HVELPLUND, P., KNUDSEN, H., KVISTGAARD, P., *Phys. Rev. Lett.* **62** (1989) 2656 (O^{6+}); ANDERSEN, L.H., BOLKO, J., KVISTGAARD, P., *Phys. Rev.*, A **41** (1990) 1293 (C^{4+} , O^{6+} , C^{3+} , O^{5+}); ANDERSEN, L.H., PAN, G.Y., SCHMIDT, H.J., BADNELL, N.R., PINDZOLA, M.S., *Phys. Rev.*, A (1992) (N^{5+} , F^{7+} , Si^{12+}); HAHN, Y., BELLANTONE, R., *Phys. Rev.*, A **40** (1989) 6117 (C^{4+} , O^{6+}); BADNELL, N.R., PINDZOLA, M.S., GRIFFIN, D.C., *Phys. Rev.*, A **41** (1990) 2422 (C^{4+} , O^{6+}).
- [74] GRIFFIN, D.C., PINDZOLA, M.S., KRYLSTEDT, P.G., *Phys. Rev.*, A **40** (1989) 6699 (C^{3+} , O^{5+}); KILGUS, G., HABS, D., SCHWALM, D., et al., *Phys. Rev.*, A (1992) (Cu^{26+}).
- [75] BADNELL, N.R., PINDZOLA, M.S., ANDERSEN, L.H., BOLKO, J., SCHMIDT, H.T., *J. Phys.*, B (London) **24** (1991) 4441 (C^{2+} , O^{4+} , F^{5+} , O^{3+} , F^{4+}).
- [76] PINDZOLA, M.S., BADNELL, N.R., GRIFFIN, D.C., *Recombination of Atomic Ions (Proc. Adv. Res. Workshop Newcastle, 1991)*, Plenum Press, New York, London (1991).

- [77] BELL, R.H., SEATON, M.J., *J. Phys.*, B (London) **18** (1985) 1589.
- [78] BADNELL, N.R., PINDZOLA, M.S., GRIFFIN, D.C., SUMMERS, H.P., *Phys. Scr.*, T **37** (1991) 26.
- [79] SUMMERS, H.P., WOOD, L., Rep. JET-R(88)06, JET Joint Undertaking, Abingdon, Oxfordshire (1988).
- [80] SUMMERS, H.P., HOOPER, M.B., *Plasma Phys.* **25** (1983) 1311.
- [81] DUNN, G., in *The Physics of Ionized Gases* (MATIĆ, M., Ed.), Boris Kidrić, Belgrade (1980) 49.
- [82] PHANEUF, R., in *Atomic Processes in Electron-Ion and Ion-Ion Collisions* (BROUILLARD, F., Ed.), Plenum Press, New York (1986) 117.
- [83] GALLAGHER, J.W., PRADHAN, A.K., An Evaluated Compilation of Data for Electron Impact Excitation of Atomic Ions, Rep. No. 30, JILA Information Center, University of Colorado, Boulder (1985).
- [84] PHANEUF, R.A., JANEV, R.K., PINDZOLA, M.S., Collisions of Carbon and Oxygen Ions with Electrons, H, H₂ and He, *Atomic Data for Fusion*, Vol. 5, ORNL-6090, Oak Ridge National Laboratory, Oak Ridge, TN (1987).
- [85] AGGARWAL, K.M., BERRINGTON, K.A., EISSNER, W.B., KINGSTON, A.E. (Eds), Recommended Data (for Electron Impact Excitation of Ions), Atomic Data Workshop, Daresbury Laboratory (March 1986).
- [86] ITIKAWA, Y., HARA, S., KATO, T., NAKAZAKI, S., PINDZOLA, M.S., CRANDALL, D.H., Recommended Data for Excitation of Carbon and Oxygen Ions by Electron Collisions, Rep. IPPJ-AM-27, Nagoya University (1983); *At. Data Nucl. Data Tables* **33** (1985) 149.
- [87] KATO, T., NAKAZAKI, S., Recommended Data for Excitation Rate Coefficients of Helium Atoms and Helium-like Ions by Electron Impact, Rep. IPPJ-AM-58, Nagoya University (1988).
- [88] MERTS, A.L., MANN, J.B., ROBB, W.D., MAGEE, N.H., Electron Excitation Collision Strengths for Positive Atomic Ions: A Collection of Theoretical Data, Rep. LA-8267-MS, Los Alamos Scientific Laboratory, Los Alamos, NM (1980).
- [89] CLARK, R.E.H., ABDALLAH, J., *Phys. Scr.*, T **37** (1991) 28.
- [90] JANEV, R.K. (Ed.), *Atomic Data Base and Fusion Applications Interface*, INDC(NDS)-211/GA (1988); HULSE, R.A., in *Atomic Processes in Plasmas*, AIP Conf. Proc. **206** (1989) 63.

CROSS-SECTION DATA FOR COLLISIONS OF ELECTRONS WITH HYDROCARBON MOLECULES

H. TAWARA, Y. ITIKAWA*, H. NISHIMURA**,
H. TANAKA⁺, Y. NAKAMURA⁺⁺
National Institute for Fusion Science,
Nagoya, Japan

ABSTRACT. The present status of experimental cross-section data for collisions of electrons with hydrocarbon molecules is described, and the data which can be used for diagnosis and modelling of plasmas containing carbons are evaluated and summarized.

1. INTRODUCTION

Graphites are often used as material for the inner walls of fusion plasma devices to reduce radiation losses from high temperature plasmas. However, they are found to be severely eroded through interactions with hydrogen plasmas. Two major processes are responsible for the erosion of graphites: physical sputtering [1] and chemical sputtering. At extremely high temperatures (> 1200 K), a third mechanism — radiation enhanced sublimation — plays a role. Interactions of graphites with active atomic hydrogens result in abundant production of hydrocarbon molecules.

Carbons released from graphites, in the form of atoms or hydrocarbon molecules, come into contact with plasmas and are excited, dissociated or ionized through collisions with plasma constituents such as electrons or hydrogens. These carbons or their collision products play a key role in determining the behaviour and characteristics of cold plasma near the edge as well as those of hot plasma at the centre.

To provide information for modelling and diagnosis of such plasmas, data on electron collisions with hydrocarbon molecules are needed. Indeed, observation of photons from these molecules provides important information regarding the production mechanisms of these particles and seems to be one of the most powerful

techniques for diagnosing plasmas in which ions, atoms or molecules in excited states, formed through collisions, are abundant. So far, only limited data for hydrocarbons have been compiled for such purposes [2, 3, 3a].

Gianturco and Jain [4] recently reviewed theoretical aspects of electron and polyatomic molecule collisions and discussed the validity of various models. They found that collisions between electron and hydrocarbon molecules are quite complicated. Therefore, most theoretical investigations deal with methane. The calculated total scattering cross-sections and the rotational excitation cross-sections seem to be in reasonable agreement with experimental results if interactions between electrons and molecules (especially target polarization and electron exchange) are properly taken into account.

We survey here the present situation regarding cross-section data for collisions of hydrocarbon molecules with electrons and evaluate some relevant data. Detailed information on these data can be found in a previous report [5].

2. COLLISION DATA FOR HYDROCARBON MOLECULES

2.1. CH₄

2.1.1. Elastic and inelastic electron scattering cross-sections

One of the most common techniques for determining total cross-sections is the measurement of the attenuation of the incident electron beam after it passes through a target of known thickness [6–11]. In some cases, the total cross-sections were determined by summing up the measured differential cross-sections obtained with the

Permanent addresses:

- * Institute for Space and Astronautical Science, Sagamihara 229, Japan.
- ** Physics Department, Niigata University, Niigata 950-21, Japan.
- + Department of General Science, Sophia University, Tokyo 102, Japan.
- ++ Faculty of Science and Technology, Keio University, Hiyoshi, Yokohama 223, Japan.

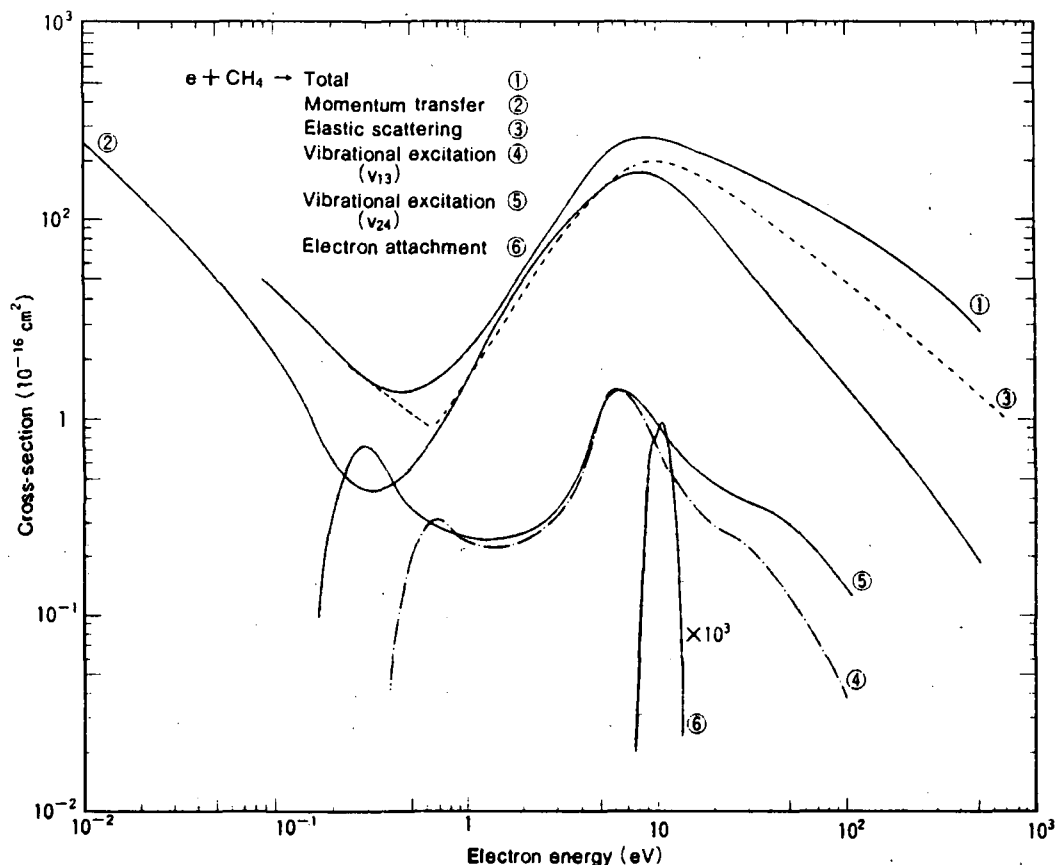


FIG. 1. Cross-sections for scattering of electrons by collisions with CH_4 molecules. The different curves are explained in the text.

crossed beam method. Some of the old data are in general agreement with recent data at low to intermediate energies; a Ramsauer minimum is observed at around 0.4 eV. However, at higher energies, there are some discrepancies. The total cross-sections evaluated from large data sets [6–11] are shown in Fig. 1 (curve 1).

Momentum transfer cross-sections have been determined with two methods: the swarm method (for low energies) [12–15] and the crossed beam method (for high energies) [16–18]. The evaluated data for momentum transfer cross-sections shown in Fig. 1 (curve 2) are based on an analysis by Nakamura [15], with an extrapolation to analyses by Sakae et al. [17] and Shyn and Cravens [18].

Elastic scattering cross-sections obtained in experiments generally include the contribution of rotational and vibrational excitation because of the limited energy resolution of the detection system [16–21]. Such total (or integral) elastic scattering cross-sections obtained

by summing up differential cross-sections over all angles are shown in Fig. 1 (curve 3).

Differential rotational excitation cross-sections for some processes were measured by Müller et al. [22] at 0.5–10 eV over a limited range of angles, but no total cross-sections were given.

CH_4 molecules are known to have nine vibrational modes in their electronic ground state, among which only four have separate energies ($\nu_1 = 363$ meV, $\nu_2 = 190$ meV, $\nu_3 = 374$ meV, $\nu_4 = 162$ meV). The energy separations between the levels ν_1 and ν_3 and between the levels ν_2 and ν_4 are too small and cannot be resolved. Cross-sections for vibrational excitation have been determined from the threshold energy (162 meV) to 20 eV, using the crossed beam method [16, 19, 21, 22], or from the threshold energy to 100 eV, using the swarm technique [12–15]. Data evaluated by Nakamura [15], based upon swarm data, are shown in Fig. 1 (curve 4 for ν_{13} , summed over ν_1 and ν_3 , and curve 5 for ν_{24} , summed over ν_2 and ν_4).

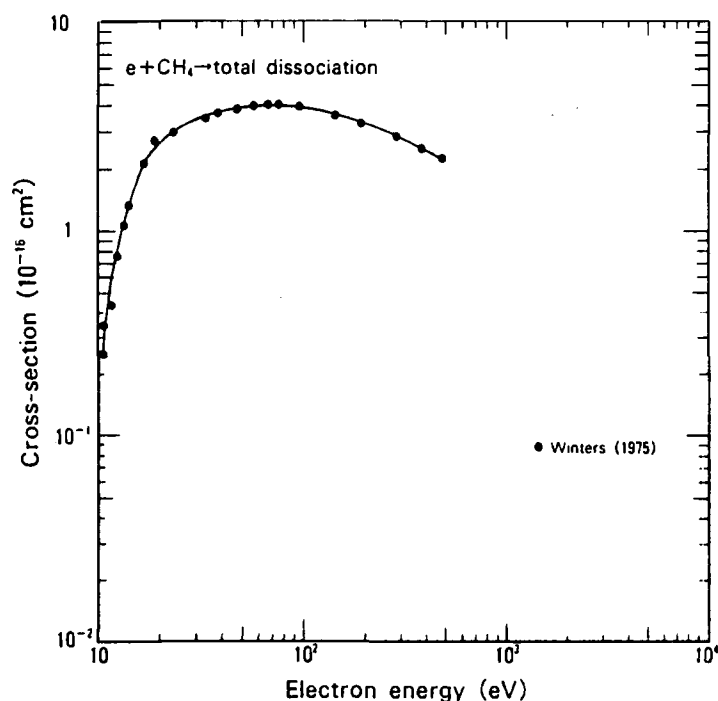


FIG. 2. Total cross-sections of CH_4 for dissociation due to electron impact [24].

The maximum cross-sections at about 7.5 eV are found to be due to enhancement by a broad T_2 symmetry resonance.

Most experiments on electronic excitation concern spectroscopic investigations. Only a few measurements [20] have been reported for electronic excitation cross-sections over a limited energy range.

Cross-sections for dissociative electron attachment, resulting in the production of negative ions (mainly H^- and CH_2^-), were measured by Sharp and Dowell [23] and show a resonance-like behaviour (Fig. 1, curve 6). A strong isotope effect on dissociative attachment was observed (there were practically no CD_2^- ions, only D^- ions for CD_4), although the total negative ion production cross-sections are approximately equal for CH_4 and CD_4 . It is worth mentioning that H^- ion production from CH_4 up to 50 eV electron impact was recently observed by Srivastava and Orient [23a], who suggested that H^- ions might be due to ion pair production through polar dissociation and showed that the integrated cross-sections for H^- ion production above the threshold energy of about 15 eV are much larger than the total dissociative electron attachment cross-sections.

2.1.2. Total dissociation cross-sections

Total dissociation cross-sections were determined by Winters [24] through measurements of the pressure

variation induced when CH_4 dissociates. These results (Fig. 2) include not only dissociation products but also the contribution of all inelastic excitation and ionization processes, indicating that, at relatively high impact energies (> 50 eV), the probabilities of dissociation into ionic and neutral fragments are approximately equal, whereas, at low impact energies, the fragments are mostly uncharged, ground state molecules. Data by Perrin et al. [25], obtained with a different technique, agree reasonably well with those of Winters.

2.1.3. Total and partial ionization cross-sections

Total ionization cross-sections are determined through measurements of all secondary ions produced by electron impact. The agreement among the observed results through this type of measurement is generally good, as seen in Fig. 3(a). The absolute measurements by Rapp and Englander-Golden [26] and by Schram et al. [27] are used as standards. Other measurements are often normalized to one of their absolute values. Rapp et al. [28] determined the cross-sections for the production of charged particles with kinetic energy above 0.25 eV and found that more than 90% of the charged products have near-thermal energies, although the ratios depend on the impact energy.

The cross-sections for CD_4 are practically the same as those for CH_4 , suggesting that the isotope effect is

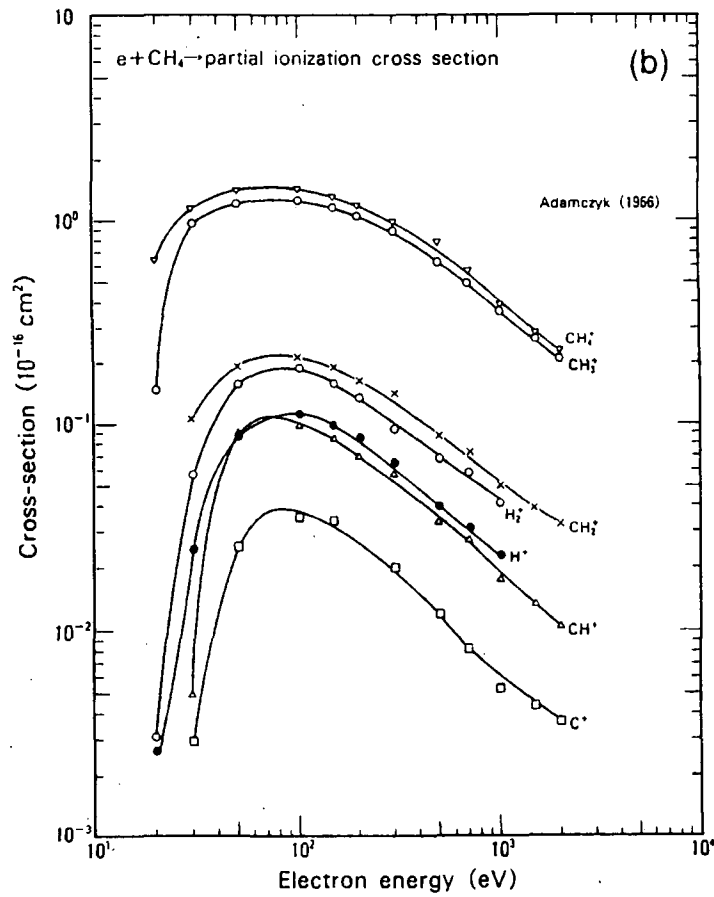
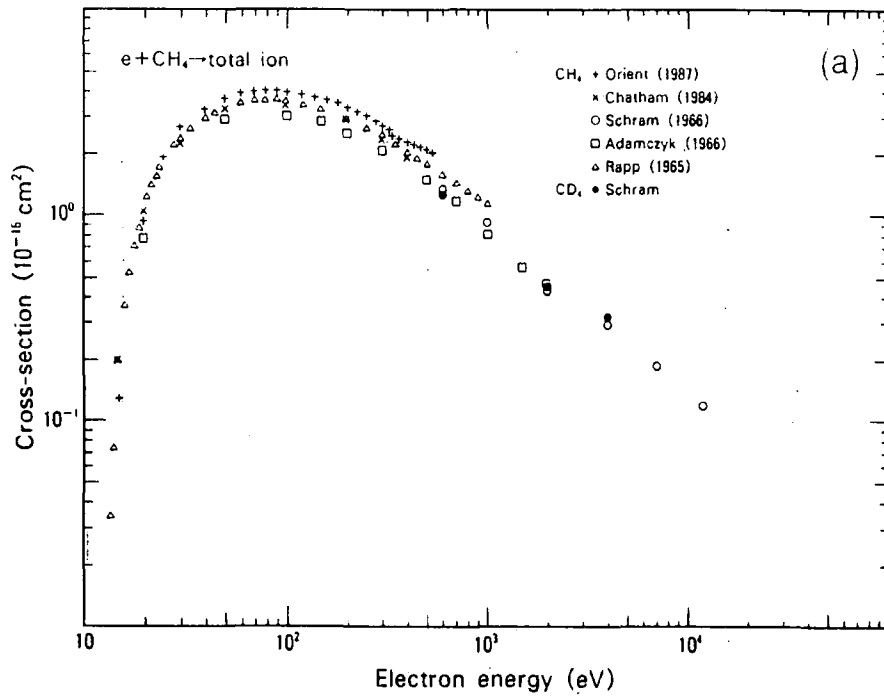


FIG. 3. Cross-sections for (a) total ionization and (b) partial ionization of CH₄ due to electron impact [26, 27, 29-31].

TABLE I. CRACKING PATTERNS OF DISSOCIATIVE IONIZATION OF CH₄ DUE TO 100 eV ELECTRON IMPACT

	CH ₄ ⁺	CH ₃ ⁺	CH ₂ ⁺	Refs
Gas CH ₄	100	85	15	[29, 30]
Neutralized CH ₄	100	400	15	[32]

small in ionization processes, as confirmed experimentally by Schram et al. [27].

Adamczyk et al. [29] determined partial ionization cross-sections for CH₄⁺, CH₃⁺, CH₂⁺, CH⁺, C⁺ and H⁺ over a wide energy range, as shown in Fig. 3(b). Similar data were reported by Chatham et al. [30] and by Orient and Srivastava [31] in a limited energy region. Their partial cross-sections are in agreement with each other at high energies, but there is some disagreement at low energies. The H₂⁺ ions observed by Adamczyk et al. [29] and Chatham et al. [30] seem to be due to double collisions (since they increase quadratically with the pressure).

Note that partial ionization cross-sections of molecules are strongly dependent upon the internal energy of these molecules. Table I compares the relative partial ionization cross-sections (so-called cracking patterns) of the ground state neutral CH₄ gas molecules with those formed through (resonant charge) neutralization of CH₄⁺ ions; the internal energies of the two groups are probably different [32]. It should be noted that part of this difference may be due to discrimination effects on fragmented ions in particle detection systems [32a].

2.1.4. Photon emission cross-sections

Systematic measurements of emission cross-sections for Lyman lines and 2s → 1s transition from hydrogen atoms were made [33–38]. However, the absolute values of these cross-sections and sometimes even their energy dependence curves are scattered because of normalization or calibration procedures of the photon detection systems used. Figure 4 shows the most recent results for Lyman-α and -β line emissions obtained by Pang et al. [38], who normalized their data to the newest cross-sections for Lyman-α emission from H₂ molecules, and those obtained by Vroom and De Heer [33] and by Möhlmann et al. [36], which we renormalized to those of Pang et al. [38] at 400 eV. Also shown are the

renormalized cross-sections for 2s → 2p transitions by Vroom and De Heer [33].

Concerning the isotope effects on Lyman-α emission, Vroom and De Heer [33] found that those for CH₄ are about 20% larger than those for CD₄.

Vroom and De Heer [33] also determined the cross-sections for Balmer-α, -β, -γ and -δ lines of atomic hydrogen. Those for the Balmer-β lines by Aarts et al. [39] and those for the Balmer-β, -γ and -δ lines by Koppe et al. [40] are in reasonable agreement, but the cross-section for the Balmer-β line emission obtained by McLaughlin and Zipf [41] at 100 eV is larger by a factor of four than that obtained by Vroom and De Heer [33], whose results are shown in Fig. 5. The isotope effect for Balmer line emissions leads to cross-sections for CD₄ which are smaller (about 20%) than those for CH₄ [33].

Cross-sections for emissions of carbon atoms (C I: 165.72 nm, 2p3s ³P → 2p² ³P⁰, and 193.09 nm, 2p3s ¹D → 2p² ¹P⁰) were recently determined by Pang et al. [38]. In these emission cross-sections, some structures are seen just above the threshold energy because of different production channels (see Fig. 6). Previous measurements by Sroka [34] (C I: 165.72 nm and 156.1 nm, 2s2p ³D → 2p² ³P) and by Morgan and Metall [35] (C I: 156.1, 165.72 and 193.09 nm) differ (by 20–50%) from the recent results of Pang et al. [38]. Relative cross-sections for some emissions of carbon atoms were reported by Donohue et al. [42]. In most of these measurements, the lines from carbon ions were weak; thus, no cross-sections for emission of lines from carbon ions C⁺ were reported so far, apart from the cross-section for the C II, 133.5 nm (2s2p² ²D → 2s²2p ²P⁰) line measured by Morgan and Metall [35] (2.3 × 10⁻²⁰ cm² at 100 eV).

Emission cross-sections of the molecular band (A²Δ – X²Π: 420–440 nm) of CH⁺ were determined by Aarts et al. [39] (Fig. 6). Koppe et al. [40] also measured these cross-sections, and their results are in reasonable agreement (< 10%) with those of Aarts et al.

2.1.5. Characteristics of neutral and charged products

Information on collision products and their energy distributions is important for estimates of their penetration into plasmas. Only very limited investigations on neutral products from dissociation of CH₄ have been made, because they are difficult to detect. Data by Flesch et al. [43] indicate that the majority of neutral products consist of CH₃ molecules (50% at 20 eV impact energy) and their parent molecules (30%) formed through elastic and inelastic scattering under

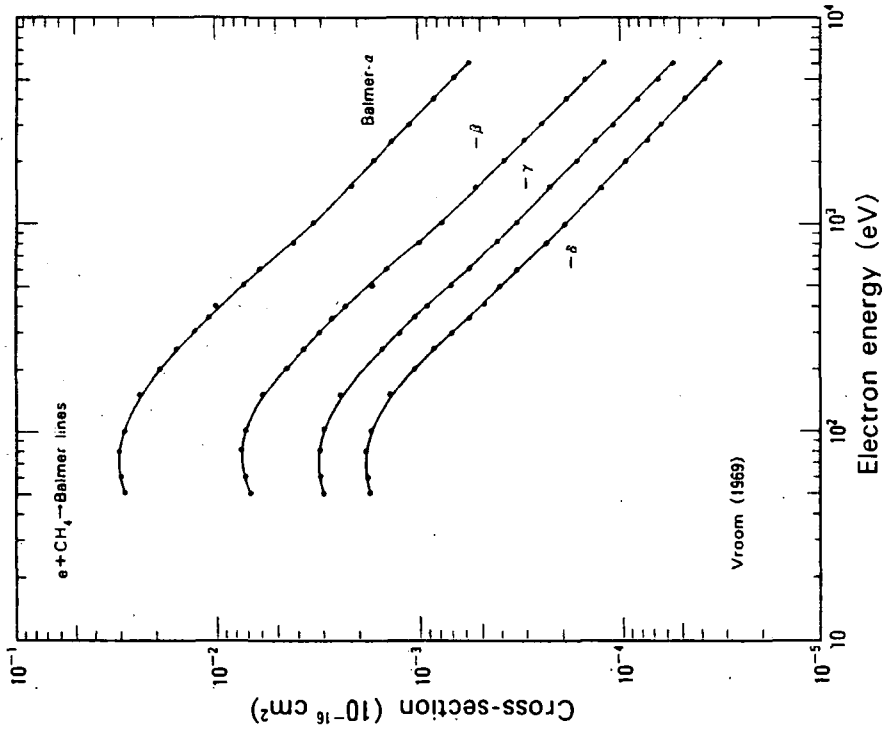


FIG. 5. Emission cross-sections of Balmer lines of hydrogen atoms in $e + CH_4$ collisions [33].

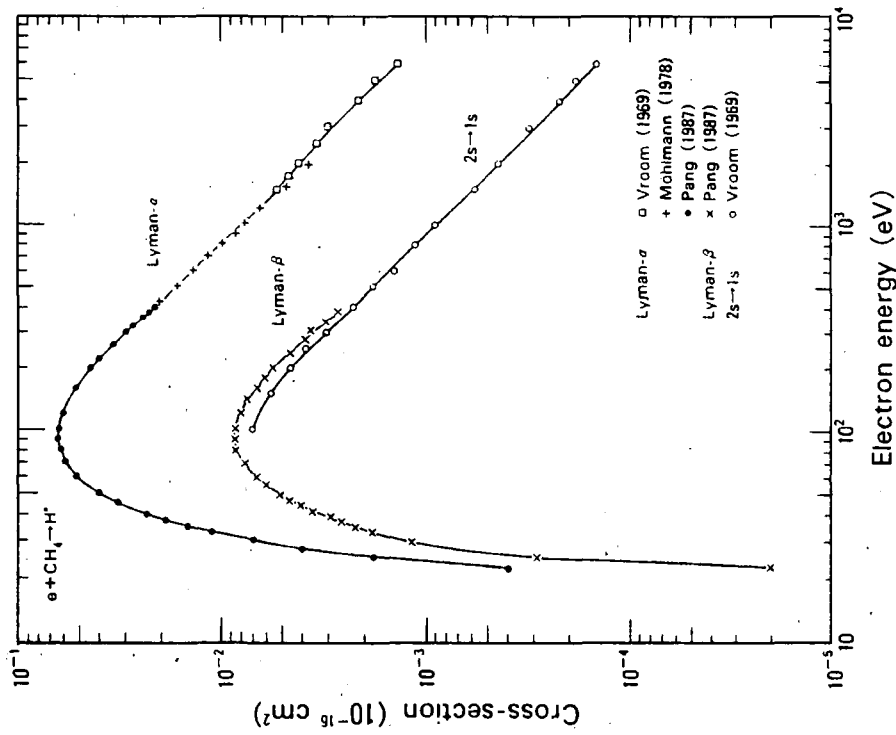


FIG. 4. Emission cross-sections of Lyman lines and $2s - 1s$ transitions of hydrogen atoms in $e + CH_4$ collisions [33, 36, 38].

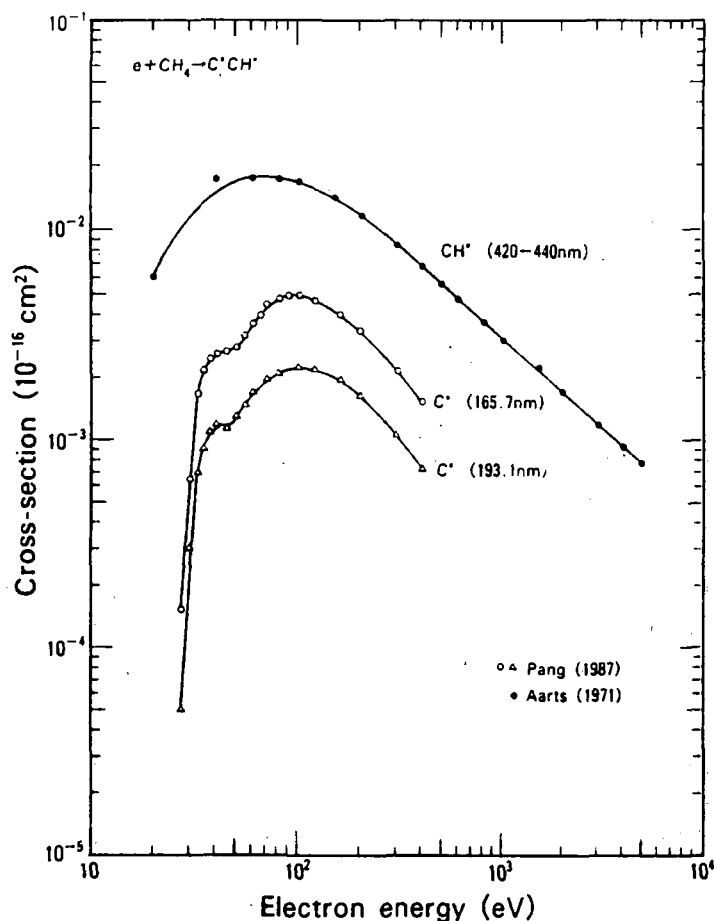


FIG. 6. Emission cross-sections of carbon atom lines and of the CH molecular band in $e + \text{CH}_4$ collisions [38, 39].

electron impact, with the rest (20%) being H_2 . The observed threshold energy of ionization of the CH_3 molecules suggests that they are in vibrationally excited states. If such products are in excited states, they may emit photons and can be detected optically. Observation of the broadening of Balmer or Lyman lines emitted from atomic hydrogens provides information on their initial kinetic energy distributions. For example, the observed Balmer- α lines for H ($n = 3$) resulting from dissociation of CH_4 by electron impact [44] show a broad peak with no particular structure compared with that for H_2 , but the peaks become broader with increasing impact energy, indicating that a number of dissociation channels contribute to this emission. These results show that the average energy of H ($n = 3$) dissociated from CH_4 increases from 2.0 eV to 3.8 eV when the electron impact energy increases from 25 eV to 300 eV. Similar results were obtained for the Balmer- β line of H ($n = 4$) dissociated from CH_4 [45].

Time of flight (TOF) measurements by Finn et al. [46] of energy distributions of atomic hydrogens in high Rydberg states ($E > 5$ eV) from CH_4 indicate that the energy ranges from 1.7 eV to 3.5 eV at 25 eV electron impact; with increasing impact energy, new peaks at higher energies appear. For 100 eV electron impact, the most intense peak of atomic hydrogens is observed at an energy of 4 eV, with the peaks extending up to 14 eV. The TOF results by Schiavone et al. [47] generally agree with those by Finn, but the detailed spectra are found to be largely different, probably because of the variation of the detection efficiencies. However, the ground state atomic hydrogens from CH_4 have not been investigated and no absolute intensities (cross-sections) for the production of these energetic atomic hydrogens have been measured. Measurements of the energy distributions of neutral carbon products are very scarce. In Refs [46, 47] it is suggested that the energy of neutral (possibly metastable) carbon atoms

in high Rydberg states is in the range of 1–2 eV, at 28–48 eV electron impact. Energies for the ground state and for low excited states have not been reported yet.

The detailed energy distributions of protons formed through dissociative ionization of CH_4 were measured by Locht and Momigny [48], who found peaks at 0.0, 0.5, 0.9, 2.35 and 3.97 eV for 25–50 eV electron impact energy (previous measurements often failed to observe the peak at 0 eV). For all impact energies studied, the peak at thermal energy (≈ 0 eV), with threshold energies of 21.3 eV and 22.2 eV, is the most intense, whereas the peak at 2.35 eV occurs at an electron impact energy of about 22 eV. With increasing electron impact energy, other peaks appear and, compared with a number of peaks, the peak at 0.9 eV becomes larger than that at 2.35 eV.

For heavier product ions from dissociation of CH_4 , the initial kinetic energy distributions at 75 eV electron impact are found to be quasi-thermal, but they show no structures. The average energy increases as the product ion becomes lighter (0.05–0.3 eV for $\text{CH}_4^+ > \dots > \text{CH}^+ > \text{C}^+$) [48a].

2.1.6. Recombination and ionization of CH_4^+ by electrons

Total cross-sections for dissociative recombination of CH_4^+ ions in collisions with slow electrons were determined with the merged beam method by Mul et al. [49], who controlled (but not specified) the internal excitation energy of the parent CH_4^+ ions by mixing different gases with CH_4 in the ion source. Note that these cross-sections depend strongly upon the excitation energy of the parent molecular ions. In fact, as shown in Fig. 7, the observed cross-sections decrease approximately as E^{-1} up to 0.1 eV; at higher energies, they drop more rapidly. This rapid drop above 0.1 eV may be due to the presence of ions in vibrationally excited states.

So far, no measurement of ionization of CH_4^+ ions by electrons has been reported, except for preliminary results which indicate that the ionization and dissociation cross-sections are strongly dependent upon the internal excitation energy of the parent CH_4^+ ions [50].

2.2. CH_3 , CH_2 and CH

These radicals are either collision products of hydrocarbon molecules or products from graphites under hydrogen impact. Only limited cross-sections have been reported for ionization and recombination processes.

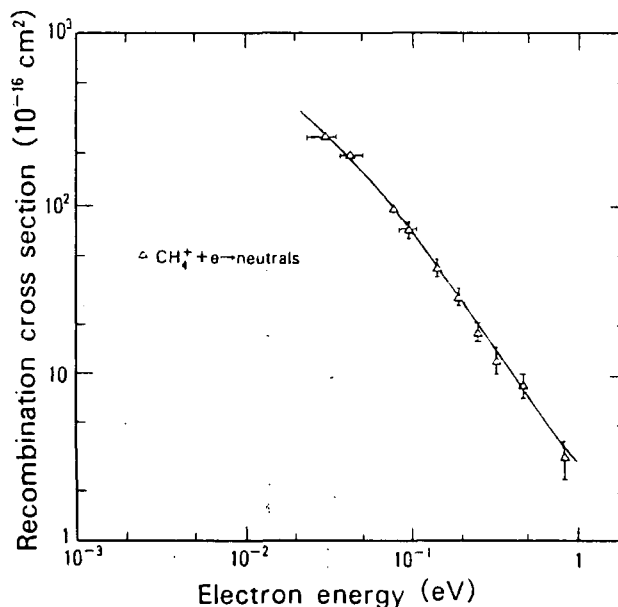


FIG. 7. Total cross-sections of CH_4^+ for dissociative recombination due to electron impact [49].

Cross-sections for pure ionization of CH_3 (CD_3 is used in experiments instead of CH_3) were measured with two different crossed beam methods. In the first method [32], CD_3^+ ions are produced from CD_4 molecules by electron impact and then neutralized to obtain a CD_3 beam. The neutralized CD_3 beam crosses an electron beam with controlled impact energy. The measured cross-sections (Fig. 8(a)) are relatively flat over 50 eV and the peak values are $1.6 \times 10^{-16} \text{ cm}^2$. The second technique is based upon photodissociation of CH_3OH by an ArF excimer laser at 198 nm, and the cross-sections are determined for impact energies of 8–14 eV [51]. Generally, the measurements agree with each other in the energy region studied in Refs [32] and [51]. The first method is also used to determine the cross-sections for dissociative ionization of CD_3 to CD_2^+ (Fig. 8(a)), which are found to be about two thirds of those for the pure ionization process. The cross-sections for CD_2 formed through neutralization of CD_2^+ ions to CD_2^+ and CD^+ (Fig. 8(b)) are found to be of the same order of magnitude as those for CD_3 . It should be borne in mind that these cross-sections are probably strongly dependent upon the internal energy of the parent free radicals. However, the dependence of these cross-sections on their internal energy has not yet been investigated.

No cross-sections have been reported for collision processes involving CH radicals, although this is one of the simplest hydrocarbon molecules.

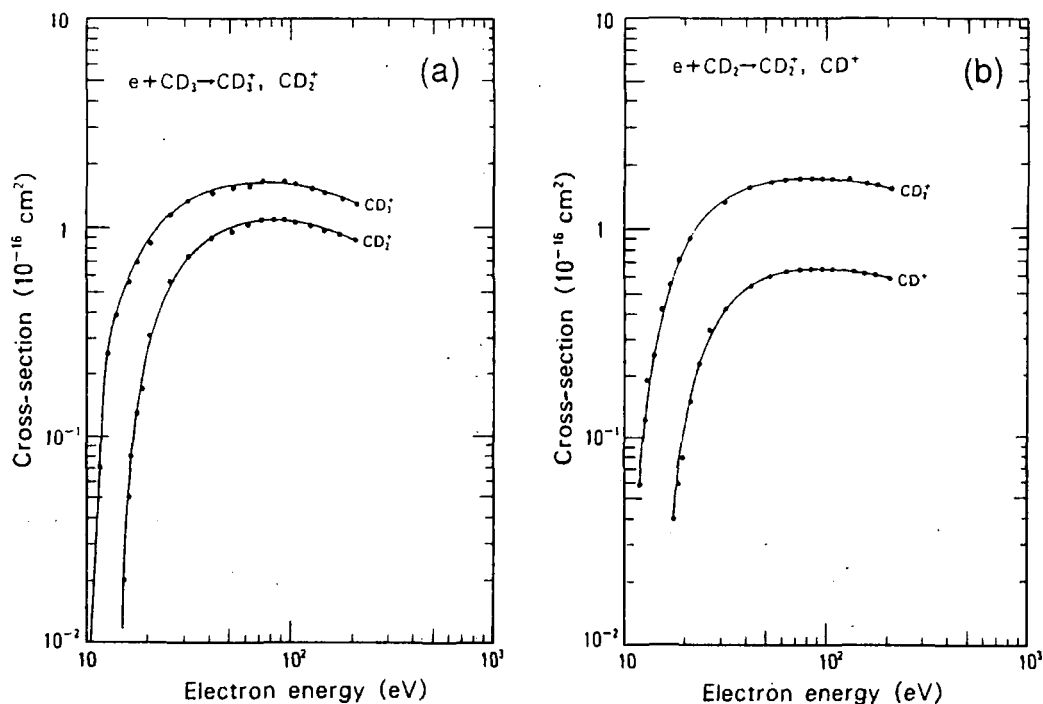


FIG. 8. Cross-sections of (a) CH_3 and (b) CH_2 for pure ionization and dissociative ionization due to electron impact [32].

Total cross-sections for dissociative recombination of CH_3^+ ions with slow electrons were determined by Mul et al. [49] with the merged beam method. In contrast to those for the CH_4^+ ions, the cross-sections were found not to be strongly dependent on how the parent CH_3^+ ions are formed — either in pure CH_4 or in mixtures with other gases. The results of Mul et al. for CH_3^+ (Fig. 9(a)) suggest some contribution of ions in (vibrationally) excited states, as indicated by the rapid drop at higher energies. The cross-sections for CH_3^+ ions are almost of the same size as those for CH_4^+ ions, except at higher energies.

Similar measurements of CH_2^+ ions show no significant dependence on the mixture of the quenching gases in the ion source (Fig. 9(b)), suggesting that the parent CH_2^+ ions are mostly in the ground state. In contrast, measurements of CH^+ ions (Fig. 9(c)) suggest some effect of the excitation energy of the parent ions on the recombination processes.

2.3. C_2H_6

2.3.1. Elastic and inelastic scattering cross-sections

The total cross-sections measured by Floeder et al. [7] and by Sueoka and Mori [10] are in good agree-

ment with each other, within their uncertainties, and are found to agree with the data by Brüche [6], except for those at the lowest energies. The evaluated cross-sections are shown in Fig. 10.

The momentum transfer cross-sections below 1 eV based upon swarm data are found not to be in agreement with each other [52–54]; they are also in disagreement with those obtained by Tanaka et al. [55] with the beam method. At present, it is difficult to give recommended momentum transfer cross-sections for C_2H_6 .

The differential elastic scattering cross-sections measured by Tanaka et al. [55] are found to be in general agreement with those by Curry et al. [21], but they are a factor of two smaller than those by Fink et al. [56] at an energy of 100 eV. Integrated elastic scattering cross-sections were given only by Tanaka et al. [55] (Fig. 10).

Some differential cross-sections for vibrational excitation were obtained by Curry et al. [21] with the beam technique. Total cross-sections, obtained through analysis of the Boltzmann equation, were given by Duncan and Walker [57], but only over a limited energy range. Electronic excitation processes have been investigated spectroscopically [58], but no cross-section is available.

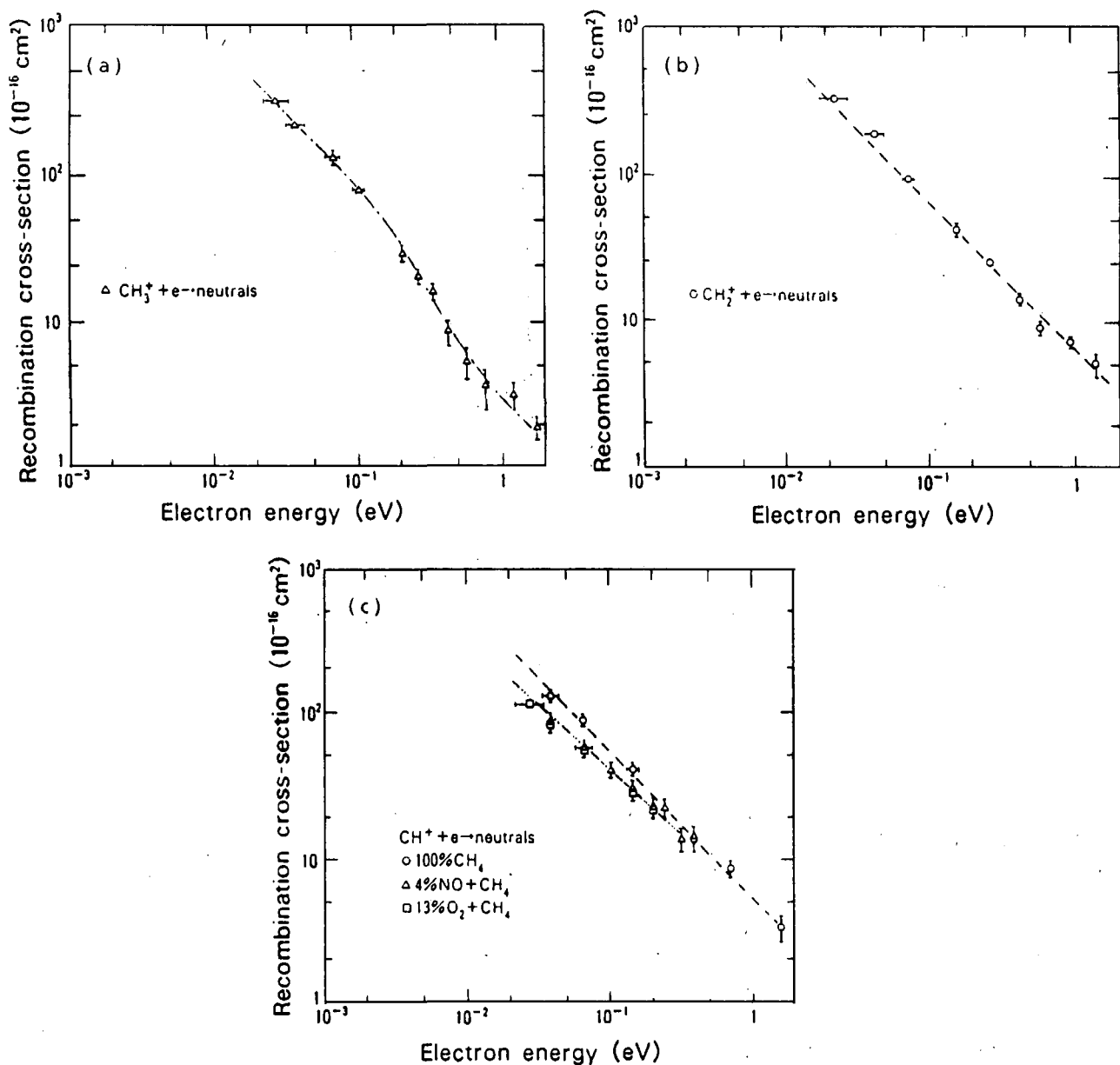


FIG. 9. Total cross-sections of (a) CH_3^+ , (b) CH_2^+ and (c) CH^+ for dissociative recombination due to impact of slow electrons [49].

2.3.2. Dissociation cross-sections

A technique similar to that used for CH_4 dissociation was used by Winters [59] to determine total dissociation cross-sections (Fig. 11). Winters also found that the cross-sections for C_2H_6 are larger (on average by 8% for 50–600 eV electron impact) than those for C_2D_6 . This isotope effect can be explained by the fact that the time required for dissociation depends upon the velocities of particles involved in rotational/vibrational oscillations.

2.3.3. Ionization cross-sections

Total ionization cross-sections were determined by Schram et al. [27], Chatham et al. [30] and Duric et al. [70]. Extrapolated measurements by these groups seem to be in fairly good agreement with each other (see Fig. 12(a)). Partial ionization cross-sections were determined only by Chatham et al. (see Fig. 12(b)). The largest peak is due to C_2H_4^+ , followed by the peak of the parent ions C_2H_6^+ .

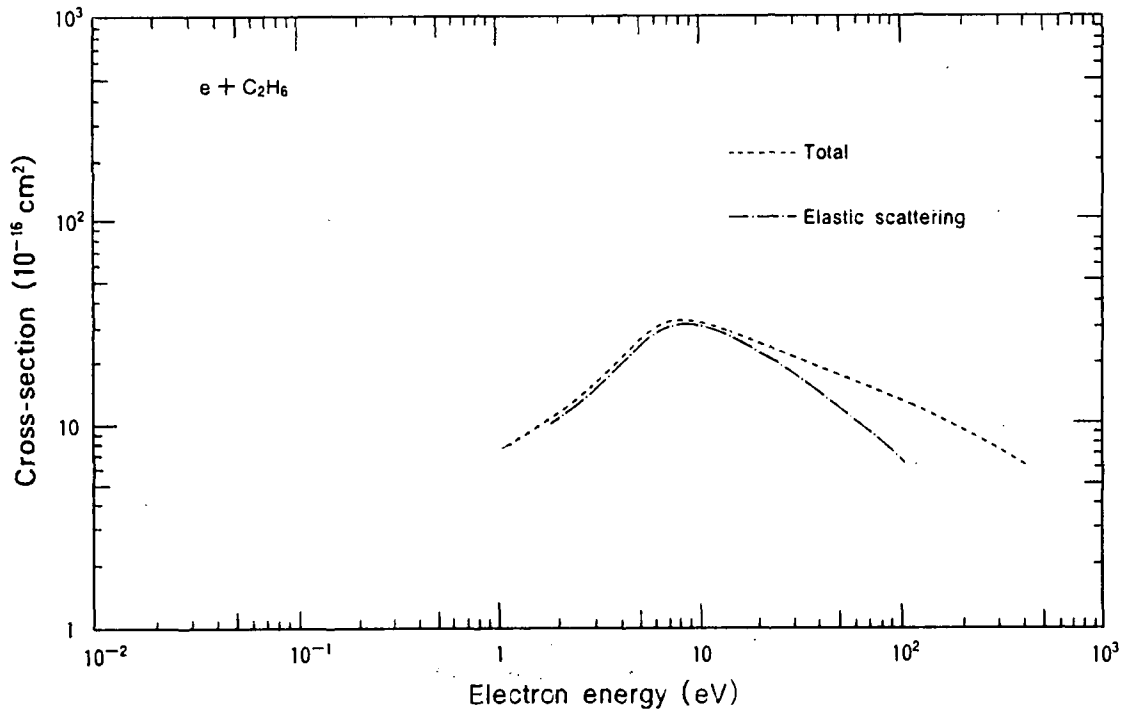


FIG. 10. Cross-sections of C_2H_6 for total and elastic scattering due to electron impact [6, 7, 10].

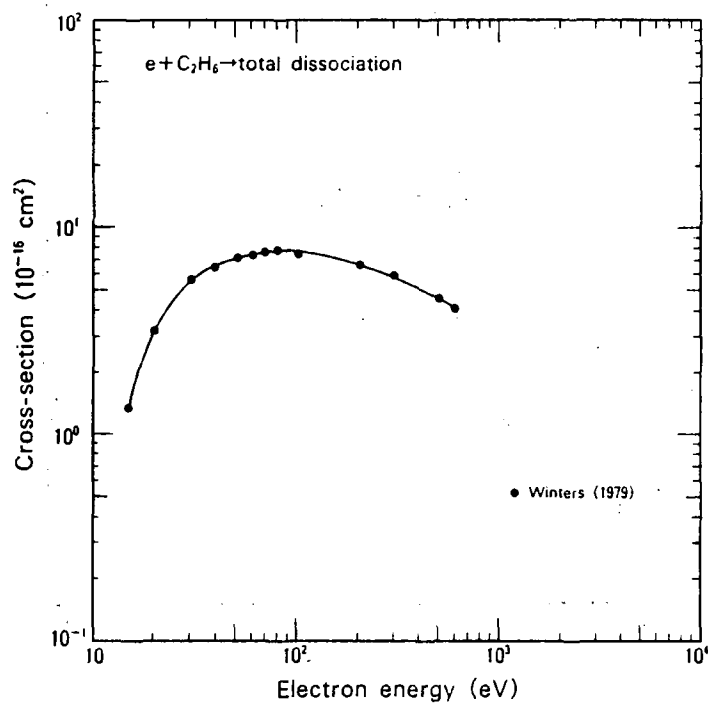


FIG. 11. Total cross-sections of C_2H_6 for dissociation due to electron impact [59].

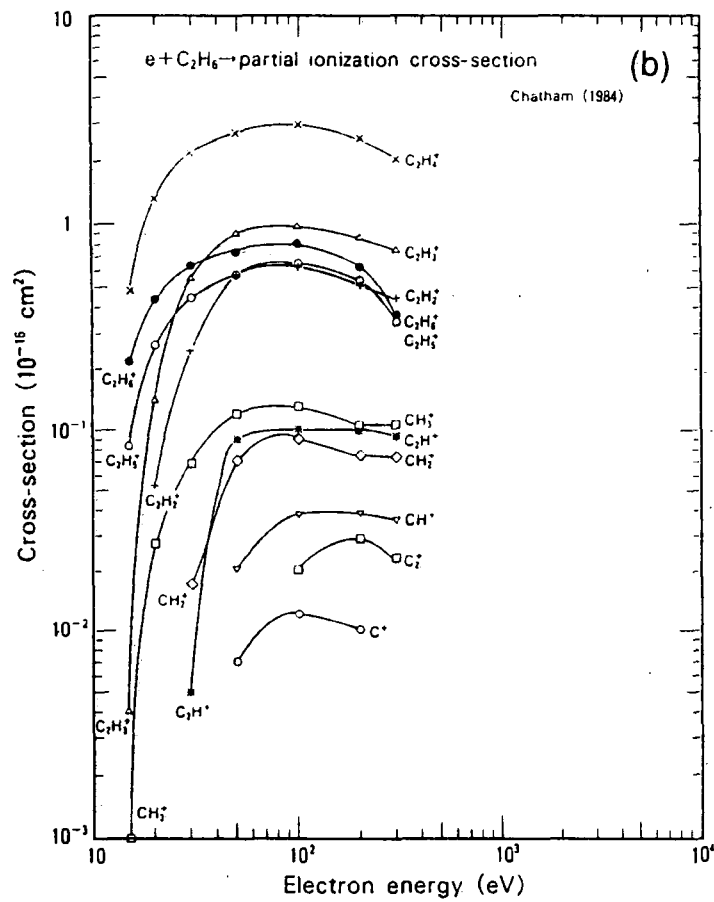
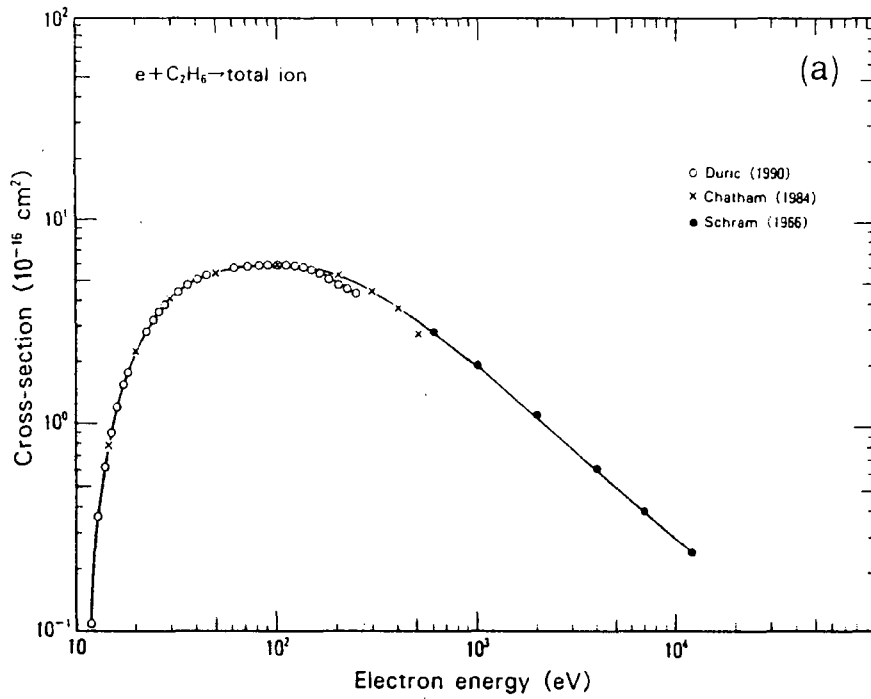


FIG. 12. Cross-sections for (a) total ionization and (b) partial ionization of C_2H_6 due to electron impact [27, 30, 70].

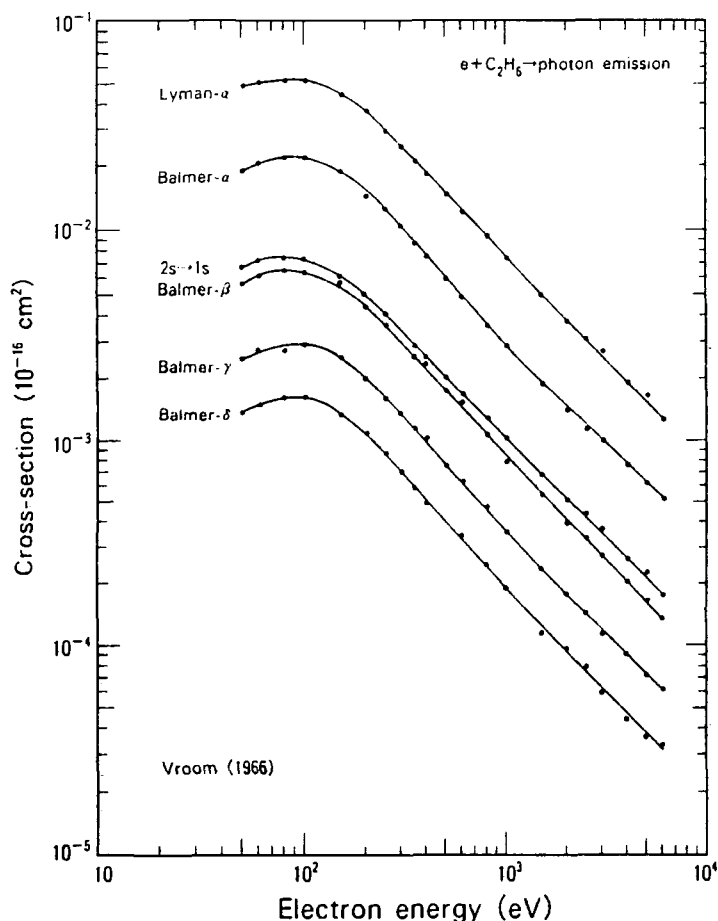


FIG. 13. Emission cross-sections of various lines from C_2H_6 due to electron impact [33].

2.3.4. Photon emission cross-sections

Only a single measurement of the cross-sections for emission of Lyman- α , $2s \rightarrow 1s$ transition and Balmer- α , - β , - γ and - δ lines was reported (Vroom and De Heer [33], see Fig. 13). These Lyman- α data are renormalized to the most recent value of the Lyman- α emission from CH_4 under electron impact (Pang et al. [38]).

2.3.5. Characteristics of neutral and charged products

A technique similar to that applied for CH_4 was used by Flesch et al. [43] to determine the neutral products from C_2H_6 at 20 eV electron impact energy (see Table II). Their ionization energies for these products suggest that H_2 and CH_3 are in vibrationally excited states, whereas other products are in the ground state. Also, the observed appearance energies for these neutrals show that the neutral products are due to dissociative ionization processes. Energy distributions of the charged products were reported by Fuchs and Taubert

TABLE II. NEUTRAL PRODUCTS FROM C_2H_6 DUE TO COLLISIONS WITH 20 eV ELECTRONS [43]

Mass	2	15	26	27	28	29	30
Fraction (%)	3	1	1	1	48	3	43

[48a], who found quasi-thermal distributions with average energies of 0.3 eV (lighter ions) to 0.063 eV (heavier ions). No information is available on the energy distribution of neutral products.

2.4. C_2H_4

2.4.1. Elastic and inelastic scattering cross-sections

Total cross-sections were measured by Floeder et al. [7] and by Sueoka and Mori [10]; the results are in agreement with each other in the energy ranges investigated by the two groups. The peaks at about 2 eV and

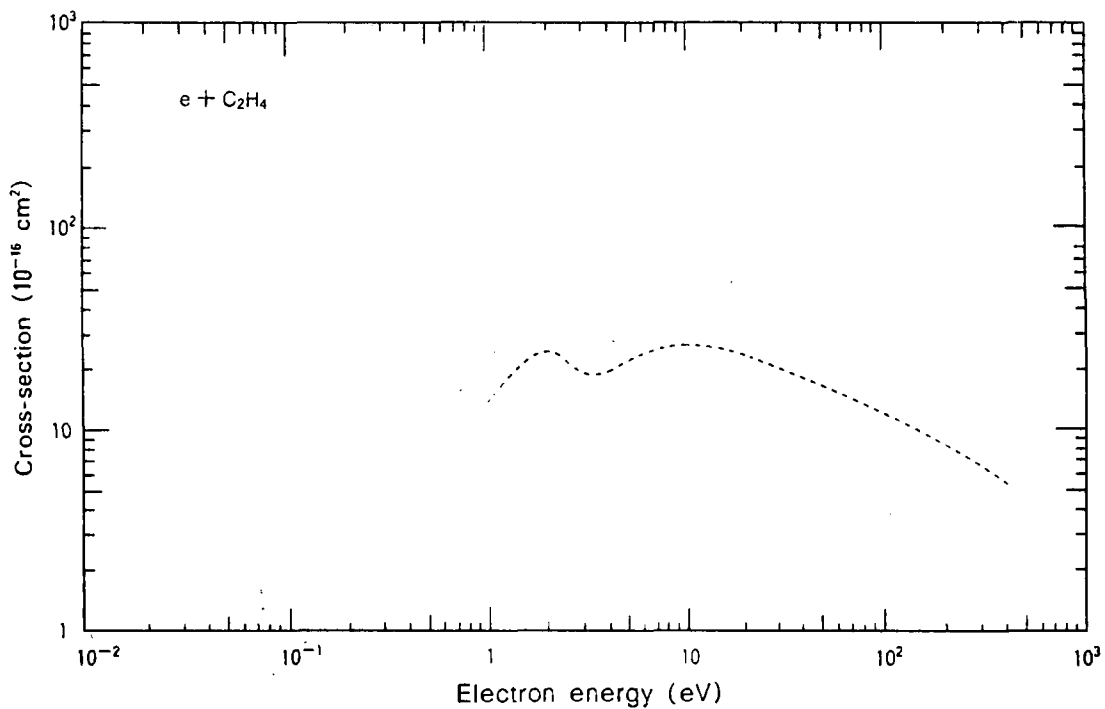


FIG. 14. Evaluated total cross-sections of $e + \text{C}_2\text{H}_4$ collisions.

8 eV are due to shape resonances. The peak observed by Sueoka and Mori at lower energy is slightly broader than peaks observed by Brüche [60], probably because of poor energy resolution. The evaluated cross-sections are shown in Fig. 14.

Cross-sections for momentum transfer, based upon the swarm technique, were measured only below 1 eV. No data are given here because the results are scattered.

Differential elastic scattering cross-sections were determined by Fink et al. [56] over a limited range of angles and energies; no total cross-section was given.

The observed differential cross-sections for vibrational excitation to v_n ($n = 1, 2, 3, 7$) have two strong peaks at 1.8 eV and 7.5 eV which are due to the shape resonances of the ${}^2\text{B}_{2g}$ and ${}^2\text{A}_g$ states, as discussed by Walker et al. [61], who also investigated the isotope effect for C_2H_4 and C_2D_4 .

Most of the measurements for electronic excitation are concerned only with spectroscopic data and no cross-section is available.

2.4.2. Ionization cross-sections

Total ionization cross-sections measured by Rapp and Englander-Golden [26] and by Schram et al. [27] are shown in Fig. 15. Although the measured energy

TABLE III. RELATIVE PARTIAL IONIZATION CROSS-SECTIONS OF C_2H_4 DUE TO 75 eV AND 3500 eV ELECTRON IMPACT [62]

Energy	75 eV	3500 eV
C^+	0.94	0.74
CH^+	1.7	1.3
$\text{C}_2\text{H}_3^{2+}$	0.19	0.09
CH_2^+	3.8	3.6
CH_3^+	0.40	0.36
C_2^+	3.1	1.8
C_2H^+	9.6	5.8
C_2H_2^+	52	51
C_2H_3^+	62	60
C_2H_4^+	100	100

regions did not coincide, the extrapolated values seem to be in good agreement with each other. However, no partial ionization cross-sections are available, except for relative measurements at 75 eV and 3500 eV by Melton [62], as shown in Table III. For these impact energies, there is practically no difference in the relative partial ionization cross-sections.

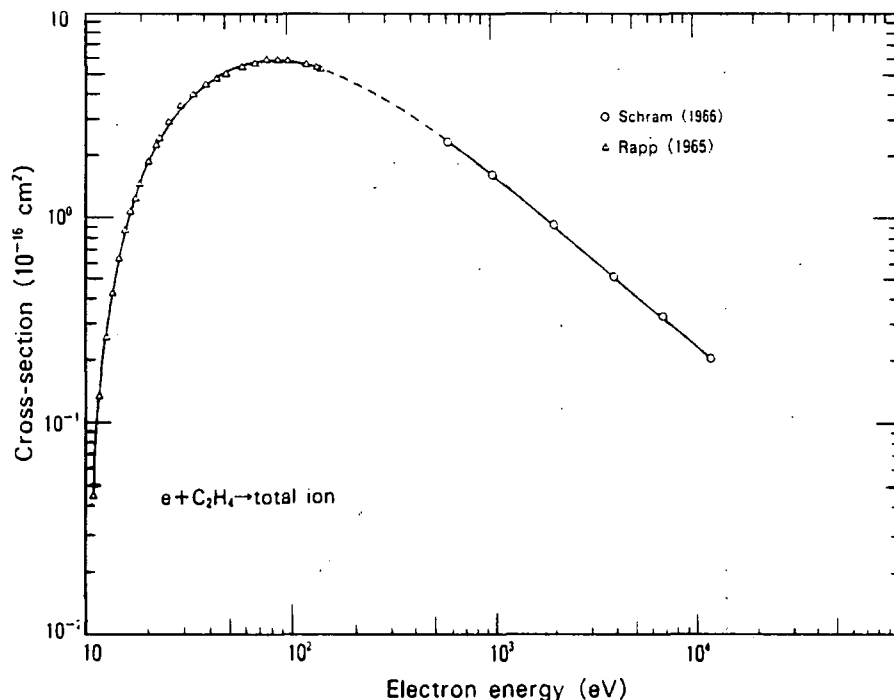


FIG. 15. Total cross-sections for ionization of C_2H_4 due to electron impact [26, 27].

2.4.3. Photon emission cross-sections

Emission cross-sections for the Lyman and Balmer lines from hydrogen atoms were measured by Vroom and De Heer [33] and by Aarts et al. [39]. The cross-section measured by Aarts et al. are about 20% larger than those measured by Vroom and De Heer (see Fig. 16).

Emission cross-sections for the CH^* ($A^2\Delta - X^2\Pi$) molecular band were determined by Aarts et al. [39] (Fig. 16). Relative cross-sections for the CH^* and C_2^* bands as well as for the CH^{++} ($B^1\Delta - A^2\Pi$) band at relatively low energies were reported by Donohue et al. [42].

2.5. C_2H_2

2.5.1. Elastic and inelastic electron scattering cross-sections

Only total cross-sections measured by Brüche [60] are available (see Fig. 17).

The available measured momentum transfer cross-sections are limited, both in quality and in quantity. At present, it is difficult to evaluate these data.

Differential elastic scattering cross-sections were measured by Fink et al. [56] at high energies and by

Kochem et al. [63] at low energies, over a limited range of scattering angles. No total cross-section was given.

Differential cross-sections for vibrational excitation for v_n ($n = 1, 2, 3, 5$) below 3.5 eV were measured in detail by Kochem et al. [63]. No total cross-section for vibrational excitation of C_2H_2 was reported.

For electronic excitation, no data are available, except for some relative measurements [64].

Limited data for dissociative electron detachment to C_2H_2 were given by Azria and Fiquet-Fayard [64a], who observed negative ion peaks of C_2H^- and H^- . The corresponding maximum cross-sections are estimated to be $2.2 \times 10^{-20} \text{ cm}^2$ at 2.3 eV, $3.1 \times 10^{-20} \text{ cm}^2$ at 7.5 eV and $4.4 \times 10^{-21} \text{ cm}^2$ at 11.5 eV. A large isotope effect between H and D was observed for C_2H^- ions.

2.5.2. Total and partial ionization

Total ionization cross-sections were determined by Tate and Smith [65] and by Gaudin and Hagemann [66]. These are shown in Fig. 18, which indicates that the former data are slightly higher (by 20% at 100 eV) than the latter but tend to converge at higher energies. Azria and Fiquet-Fayard [64a] made similar measurements, from the threshold energy to 100 eV, the results of which seem to be very close to those of Tate and

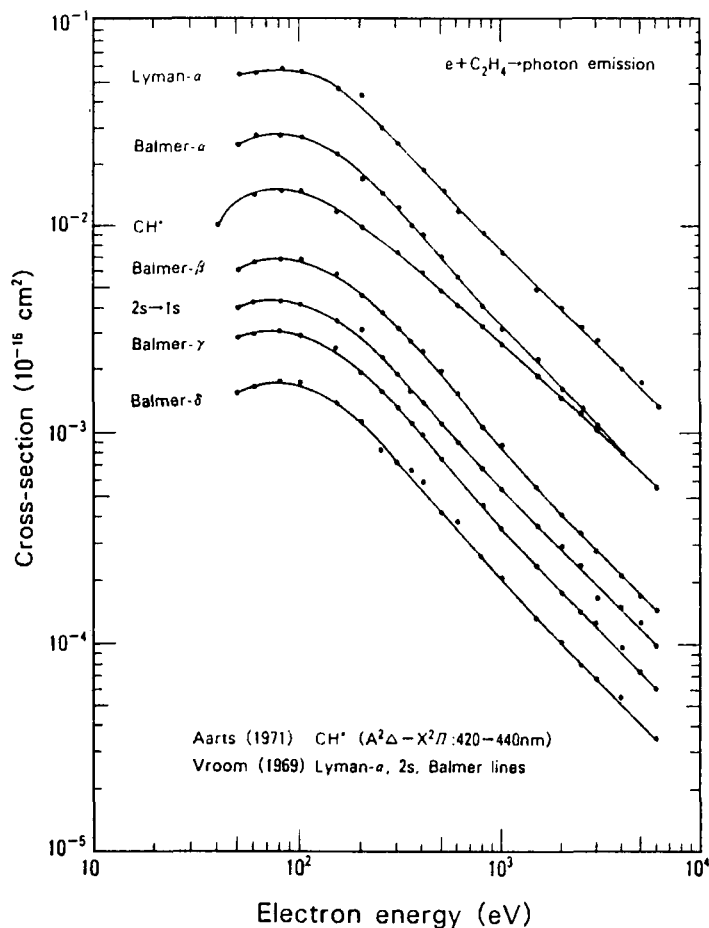


FIG. 16. Emission cross-sections for various lines from C_2H_4 due to electron impact [33, 39].

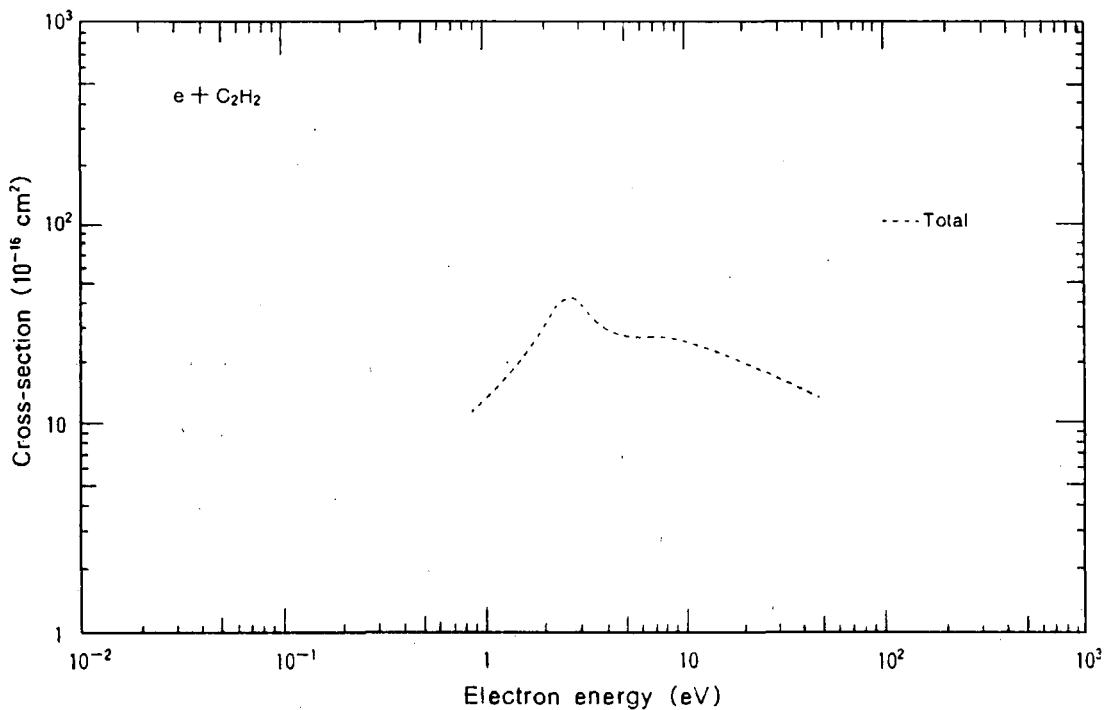


FIG. 17. Total cross-sections of $e + C_2H_2$ collisions [60].

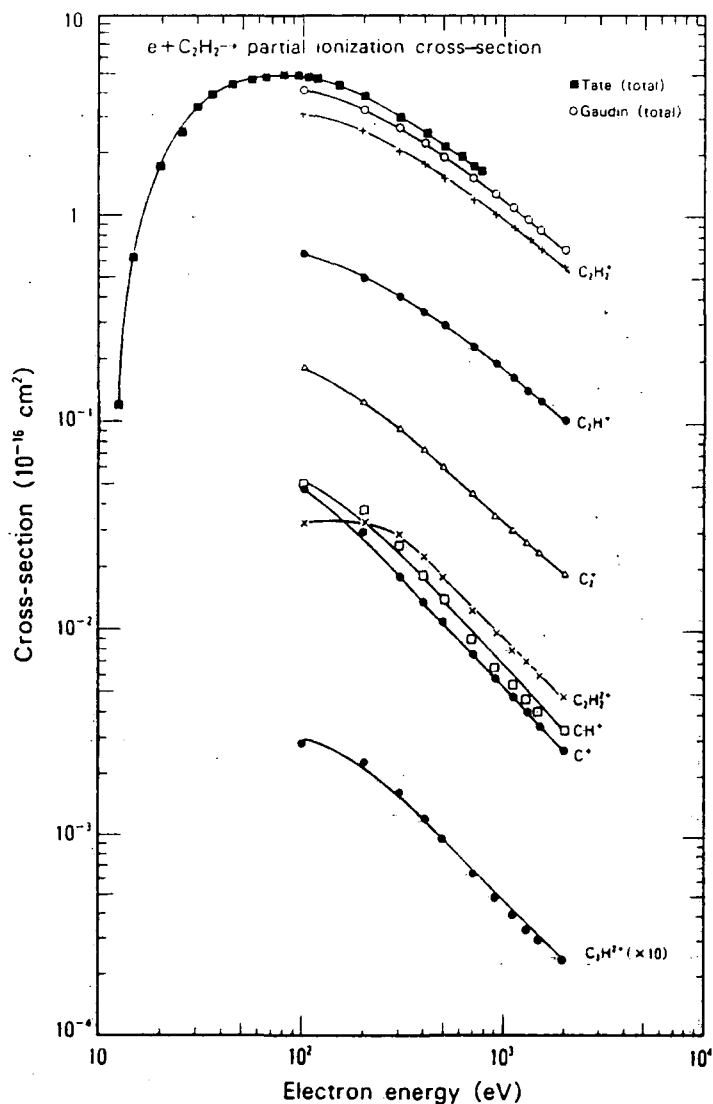


FIG. 18. Cross-sections for total and partial ionization of C_2H_2 due to electron impact. The upper two curves represent the total ionization cross-sections obtained by Tate and Smith [65] (low energy) and those obtained by Gaudin and Hagemann [66] (high energy).

Smith. Partial ionization cross-sections for $C_2H_2^+$, C_2H^+ , C_2^+ , CH^+ , C^+ , $C_2H_2^{2+}$ and C_2H^{2+} were determined by Gaudin and Hagemann (Fig. 18). Melton [62] also measured relative partial cross-sections and his results agree with the data obtained by Gaudin and Hagemann.

2.5.3. Photon emission cross-sections

Measurements of cross-sections for Lyman- α and - β line emissions from atomic hydrogens were reported by

Pang et al. [38], and measurements of cross-sections for the Balmer- β line were reported by Sushanin and Kishko [67]. These results are shown in Fig. 19.

Cross-sections for the emission of the carbon atom (C^*) line at 165.72 nm were studied by Pang et al. [38] and are shown in Fig. 20. A weak structure near the threshold energy can be seen, similar to that for CH_4 . Only a single measurement was reported by Sushanin and Kishko [67] for emission cross-sections for the transition $A^2\Delta - X^2\Pi$ at 431.5 nm of CH^* and for the Swan bands ($d^3\Pi_g - a^3\Pi_u$ transition) for C_2^* at $v = -1, 0$ and 1 (see Fig. 20).

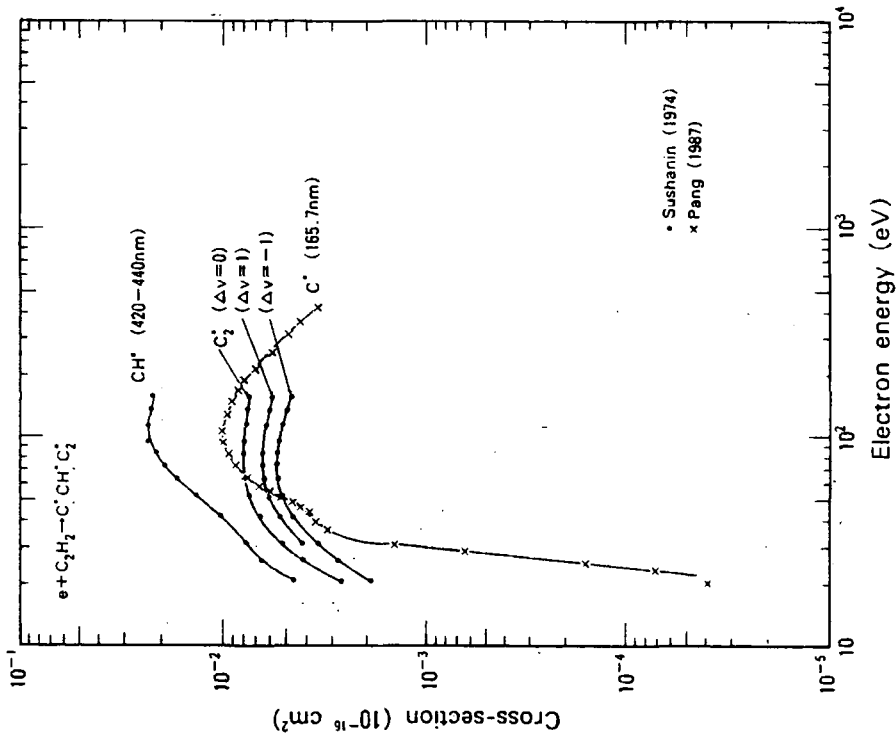


FIG. 20. Cross-sections for the emission of carbon lines and for the emission of molecular bands from C_2H_2 due to electron impact [38, 67].

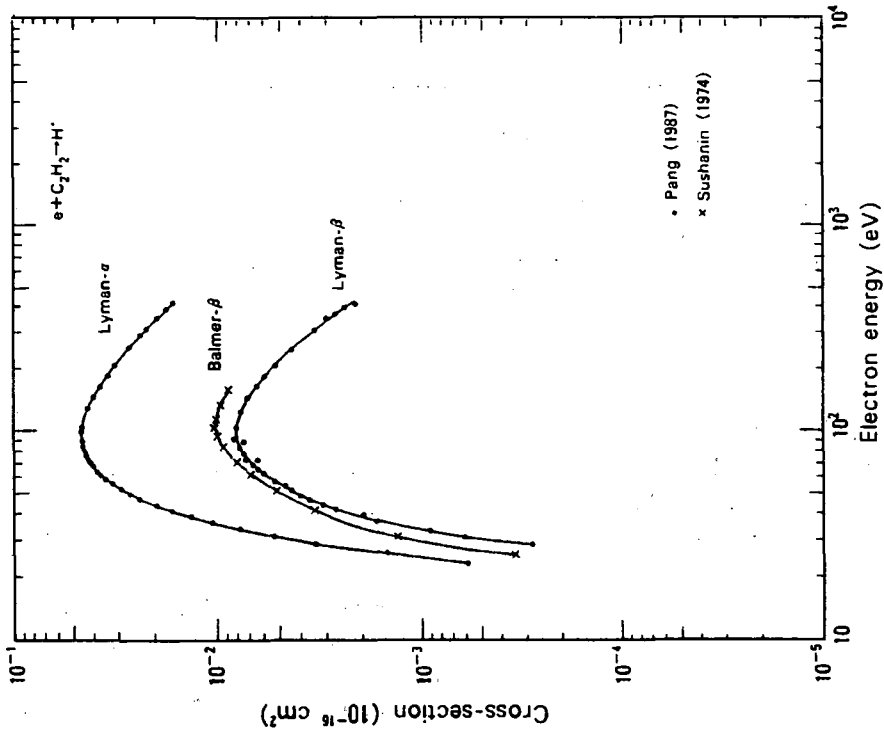


FIG. 19. Emission cross-sections of various lines of atomic hydrogen emitted from C_2H_2 due to electron impact [38, 67].

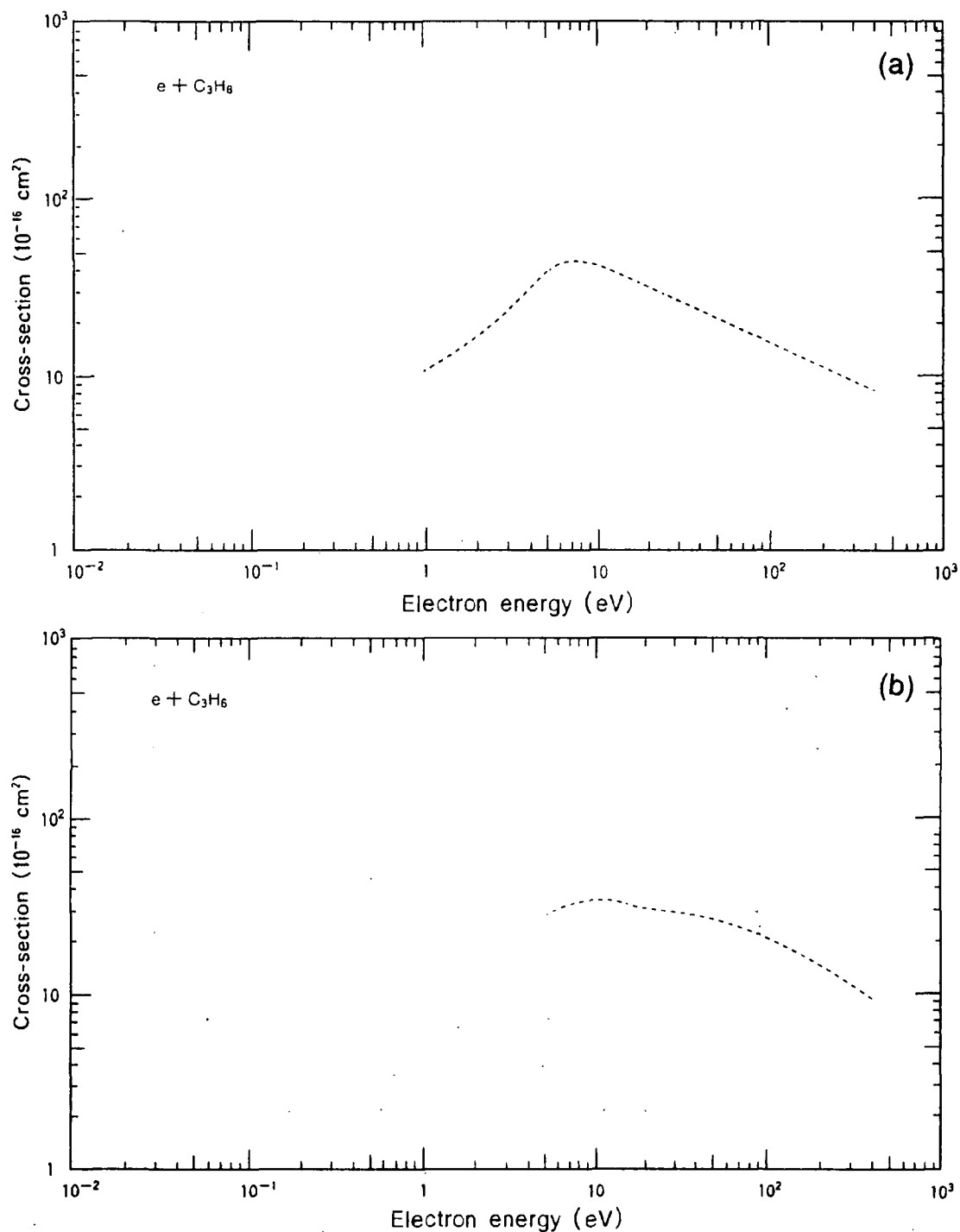


FIG. 21. Total cross-sections of electrons colliding with (a) C_3H_8 and (b) C_3H_6 .

2.6. C_3H_8 and C_3H_6

2.6.1. Elastic and inelastic scattering cross-sections

The total cross-sections for C_3H_8 were redetermined by Floeder et al. [7] and found to be in agreement with the data by Brüche [6] in the energy ranges investigated

in the two studies (see Fig. 21(a)). For cyclopropane and propene (C_3H_6), similar measurements were performed by Floeder et al., who found practically no difference between the two isomers (Fig. 21(b)).¹

¹ A recent study has shown the isomer effect on the total scattering cross-section at low energies (NISHIMURA, H., TAWARA, H., *J. Phys.*, B 24 (1991) L363).

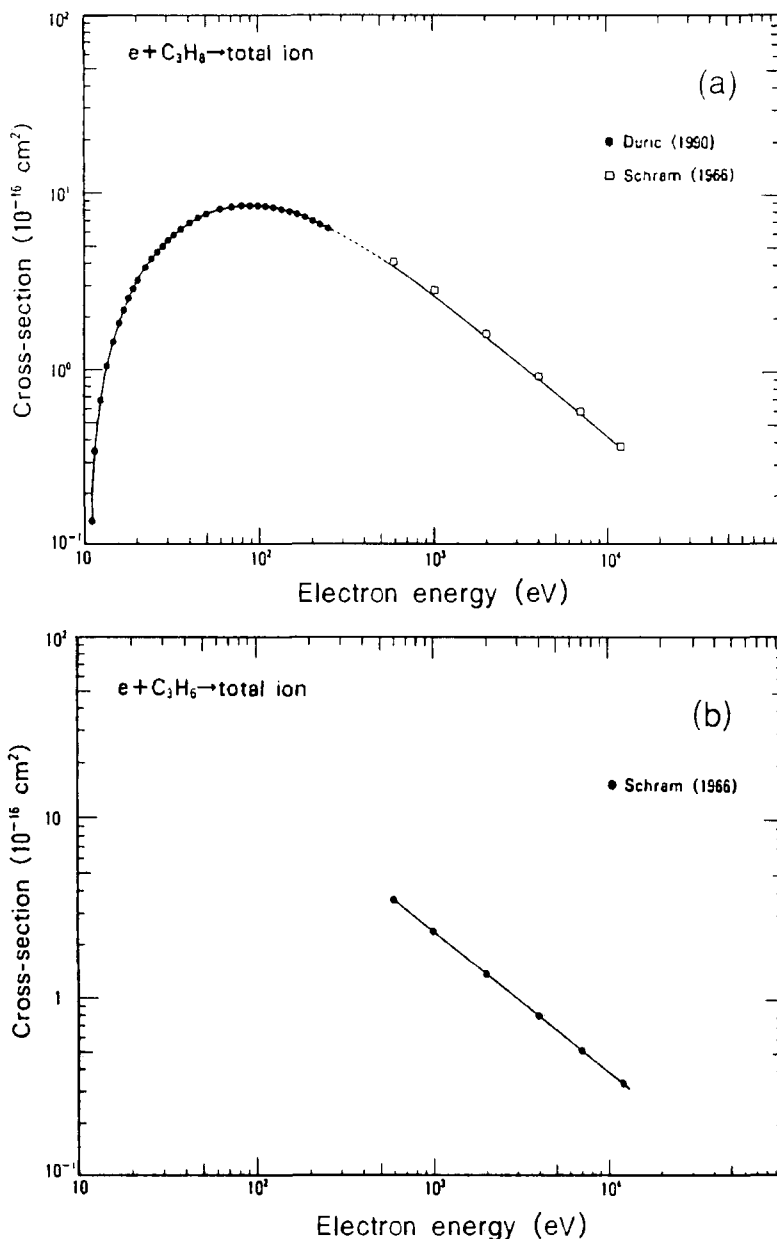


FIG. 22. Cross-sections for total ionization of (a) C_3H_8 and (b) C_3H_6 due to electron impact [27, 70].

The measured cross-sections for momentum transfer based on swarm experiments show a significant variation; therefore, no data are given here.

The cross-sections for cyclopropane and propene were determined below 1 eV with the swarm technique; discrepancies are prominent at lower energies. At present, it is difficult to evaluate these data. Only preliminary differential elastic scattering cross-sections for C_3H_8 were reported by Matsunaga et al. [68].

No vibrational excitation cross-sections for C_3H_8 and C_3H_6 have been reported yet. Relative cross-sections

for electronic excitation of C_3H_8 were investigated only at 50 eV.

Some investigations of electronic excitation for propene were reported by Johnson et al. [69], but no cross-section is available.

2.6.2. Ionization cross-sections

The total ionization cross-sections for C_3H_8 were measured by Schram et al. [27] and by Duric et al. [70] (see Fig. 22(a)). Extrapolations of the two groups of

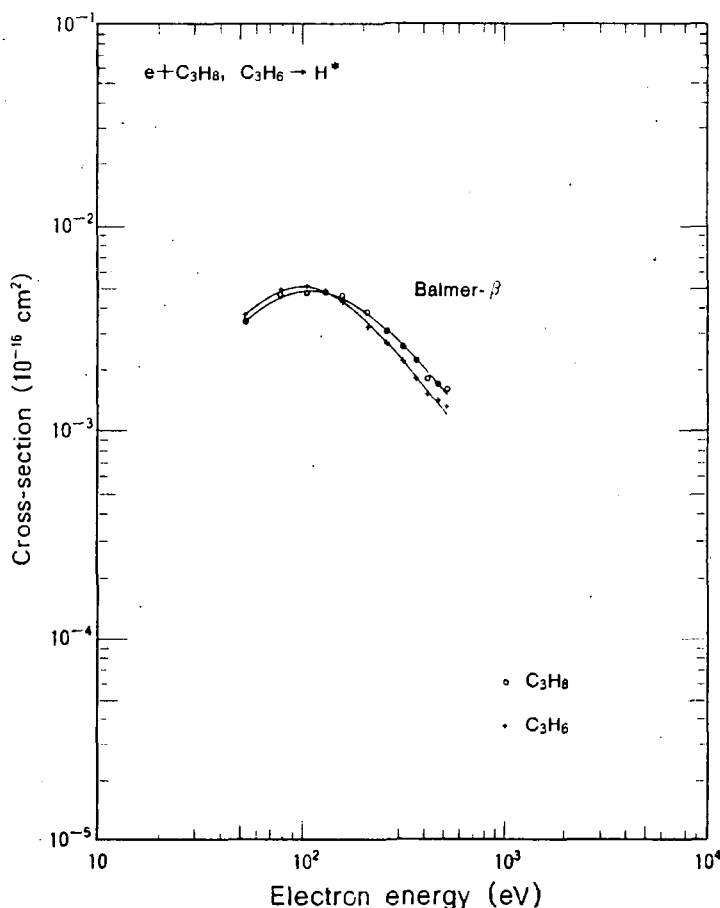


FIG. 23. Cross-sections for the emission of the Balmer- β line from C_3H_8 and C_3H_6 due to electron impact [71].

data seem to be in good agreement with each other. The data for propene (C_3H_6) by Schram et al. (Fig. 22(b)) are about 10% lower than those for cyclopropane. No partial ionization cross-section for these molecules was reported. The energies of product ions from dissociative ionization of C_3H_8 by 75 eV electrons show a smooth, quasi-thermal distribution, with average energies of 0.3 eV (lighter ions) to 0.05 eV (heavier ions) [48a].

2.6.3. Photon emission cross-sections

There are very few photon measurements for C_3H_8 and C_3H_6 . Only Balmer- β line emission cross-sections were reported by Kurepa and Tasic [71] for a relatively narrow electron energy region (see Fig. 23). They compared their results with experimental data for other hydrocarbon molecules and found that the Balmer emission cross-sections slightly decrease as the total number of atoms in a molecule increases, which suggests a reduced probability of dissociation of the parent

TABLE IV. NEUTRAL PRODUCTS FROM C_3H_8 DUE TO COLLISIONS WITH 20 eV ELECTRONS [43]

Mass	2	15	26	27	28	29	30	41	42	43	44
Fraction (%)	1	4	1	1	39	17	1	1	3	13	20

molecules in the superexcited state to fragments in the excited state.

2.6.4. Neutral and charged products

A single observation of neutral products from C_3H_8 was reported by Flesch et al. [43]; their results are shown in Table IV. It is interesting to note that the most abundant product is C_2H_4 , which results from the splitting off of CH_4 from the parent C_3H_8 . No information on the energy distribution of neutrals is available.

3. CONCLUDING REMARKS

We have summarized the present situation regarding cross-section data for hydrocarbon molecules and their ions in collisions with electrons. A considerable amount of collision data are available only for CH₄. For other hydrocarbons, only the total cross-sections for energies above 1 eV seem to be reasonably reliable. Good total ionization cross-sections are also available for most of the hydrocarbons. Cross-sections for other processes (momentum transfer, excitation, partial ionization, photon emission, etc.) are still limited in quality and in quantity. Furthermore, the collision data for radicals are very scarce.

It should be noted that collision data for molecules and molecular ions are strongly dependent upon their internal energy states (see, for example, Table I), and the cross-section data may differ by orders of magnitude, depending on whether the molecule species are in the ground state or in the excited states. Therefore, it is important to specify the internal states of target molecules before measuring the collision cross-sections. In various fields of application of molecule collisions, large fractions of molecules or molecular ions produced in collisions with plasma particles are more likely to be present in excited states than in the ground state.

Thus, a prerequisite for the use of data is a knowledge of the experimental conditions and of where and how the data were obtained. This is especially important when the data are used for plasma modelling. The collision products from molecules or molecular ions and possibly the energy distributions of the products may be different, according to their internal states, and thus the resulting densities and density distributions of species may also be affected.

One of the most important and urgently needed groups of data for both basic collision studies and applications is information on neutral products from hydrocarbons, i.e. their production rates, energy distributions and angular distributions and possibly internal (energy) states.

Another important factor, which is not treated in the present report, is the effect of solid surfaces on collisions of molecules. Collisions of molecules with solid surfaces often lead to inelastic scattering as well as to dissociation or to the breaking up of these molecules into fragments. These fragments can be significantly different from those produced in electron collisions and may also have different internal states. So far, however, products with specified internal states have not been investigated.

Appendix

EMPIRICAL ESTIMATION OF THE IONIZATION CROSS-SECTIONS OF MOLECULES

In some applications of cross-section data, for example in plasma modelling, it is useful to give analytical formulas for the cross-sections. Some empirical formulas were actually proposed and found to reproduce reasonably well the observed ionization cross-sections for atoms and atomic ions as long as direct ionization processes are dominant [72–74]. It should also be possible to estimate the ionization cross-sections for molecules and molecular ions through empirical formulas similar to those used for atomic species. Recently, Margreiter et al. [75] tried to develop an analytical formula based on the Gryzinski (classical binary encounter) approximation modified by the Born–Bethe approximation and an ‘additive rule’ for molecules. Their results are quite promising for total single ionization of some molecules, but, generally, the agreement with experimental data is not always satisfactory. In fact, it seems difficult to justify the use of the so-called additive rule for molecules because this rule assumes that the constituent atoms in a molecule are ionized independently of each other.

Since the origin of partial (dissociative) ionization cross-sections of molecules is complicated, no simple empirical or scaling formula was found to be successful so far. Several proposals were made by Tan and Wu [76] and more recently by Khare et al. [77].

REFERENCES

- [1] MATSUNAMI, N., YAMAMURA, Y., ITIKAWA, Y., ITOH, N., KAZUMATA, Y., MIYAGAWA, S., MORITA, K., SHIMIZU, R., TAWARA, H., *At. Data Nucl. Data Tables* **31** (1984) 1.
- [2] LENNON, M.A., ELLIOTT, D.S., CROWE, A., *Critical Survey of Electron Impact Ionization Data for Selected Molecules*, Department of Computer Science, Queen's University of Belfast (1986).
- [3] EHRHARDT, A.B., LANGER, W.D., *Collisional Processes of Hydrocarbons in Hydrogen Plasmas*, Rep. PPPL-2477, Princeton Plasma Physics Laboratory, Princeton University, Princeton, NJ (1987).
- [3a] De HEER, F.J., *Phys. Scr.* **23** (1981) 170.
- [4] GIANTURCO, F.A., JAIN, A., *Phys. Rep.* **143** (1986) 347.
- [5] TAWARA, H., ITIKAWA, Y., NISHIMURA, N., TANAKA, H., NAKAMURA, Y., *Collision Data Involving Hydrocarbon Molecules*, Rep. NIFS-DATA-6, National Institute for Fusion Science, Nagoya (1990).

- [6] BRÜCHE, E., *Ann. Phys. (Leipzig)* **4** (1930) 387.
- [7] FLOEDER, K., FROMME, D., RAITH, W., SCHWAB, A., SINAPIUS, G., *J. Phys.*, **B 18** (1985) 3347.
- [8] FERCH, J., GRANITZA, B., RAITH, W., *J. Phys.*, **B 18** (1985) L445.
- [9] JONES, R.K., *J. Chem. Phys.* **82** (1985) 5424.
- [10] SUEOKA, D., MORI, S., *J. Phys.*, **B 19** (1986) 4035.
- [10a] DABABNEH, M.S., HSIEH, Y.F., KAUPPILA, W.E., KWAN, C.K., SMITH, S.J., STEIN, T.S., UDDIN, M.N., *Phys. Rev.*, **A 38** (1988) 1207.
- [11] NISHIMURA, H., SAKAE, T., *Jpn. J. Appl. Phys.* **29** (1990) 1372.
- [12] HADDAD, G.N., *Aust. J. Phys.* **38** (1985) 677.
- [13] OHMORI, Y., KITAMORI, K., SHIMOZUMA, M., TAGASHIRA, H., *J. Phys.*, **D 19** (1986) 437.
- [14] DAVIES, D.K., KLINE, L.E., BIES, W.E., *J. Appl. Phys.* **65** (1989) 3311.
- [15] NAKAMURA, Y., in *Gaseous Electronics and its Applications (Proc. 2nd Australia-Japan Workshop Gotemba, Japan, 1990)*, Nagoya Institute of Technology (1990) 41.
- [16] TANAKA, H., OKADA, T., BOESTEN, L., SUZUKI, T., YAMAMOTO, T., KUBO, M., *J. Phys.*, **B 15** (1982) 3305.
- [17] SAKAE, T., SUMIYOSHI, S., MURAKAMI, E., MATSUMOTO, Y., ISHIBASHI, K., KATASE, A., *J. Phys.*, **B 22** (1989) 1385.
- [18] SHYN, T.W., CRAVENS, T.E., *J. Phys.*, **B 23** (1990) 293.
- [19] SOHN, W., JUNG, K., EHRHARDT, H., *J. Phys.*, **B 16** (1983) 891.
- [20] VUSKOVIC, L., TRAJMAR, S., *J. Chem. Phys.* **78** (1983) 4947.
- [21] CURRY, P.J., NEWELL, W.R., SMITH, A.C.H., *J. Phys.*, **B 18** (1985) 2303.
- [22] MÜLLER, R., JUNG, K., KOHEM, K.H., SOHN, W., EHRHARDT, H., *J. Phys.*, **B 18** (1985) 3971.
- [23] SHARP, T.E., DOWELL, J.T., *J. Chem. Phys.* **46** (1967) 1530.
- [23a] SRIVASTAVA, S.K., ORIENT, O.J., *AIP Conference Proceedings No. 111* (1984) 56.
- [24] WINTERS, H.F., *J. Chem. Phys.* **63** (1975) 3462.
- [25] PERRIN, J., SCHMITT, J.P.M., de ROSNY, G., HUC, J., LLORET, A., *Chem. Phys.* **73** (1982) 383.
- [26] RAPP, D., ENGLANDER-GOLDEN, P., *J. Chem. Phys.* **43** (1965) 1464.
- [27] SCHRAM, B.L., Van der WIEL, M.J., De HEER, F.J., MOUSTAFA, H.R., *J. Chem. Phys.* **44** (1966) 49.
- [28] RAPP, D., ENGLANDER-GOLDEN, P., BRIGLIA, D., *J. Chem. Phys.* **42** (1965) 4081.
- [29] ADAMCZYK, B., BOERBOOM, A.J.H., SCHRAM, B.L., KISTEMAKER, J., *J. Chem. Phys.* **44** (1966) 4640.
- [30] CHATHAM, H., HILS, D., ROBERTSON, R., GALLAGHER, A., *J. Chem. Phys.* **81** (1984) 1770.
- [31] ORIENT, O.J., SRIVASTAVA, S.K., *J. Phys.*, **B 20** (1987) 3923.
- [32] BOIOCCHI, F.A., WENTZEL, R.C., FREUND, R.S., *Phys. Rev. Lett.* **53** (1984) 771.
- [32a] MARGREITER, D., WALDER, G., DEUTSCH, H., et al., *Int. J. Mass. Spectrom. Ion Process.* **100** (1990) 143.
- [33] VROOM, D.A., De HEER, F.J., *J. Chem. Phys.* **50** (1969) 573.
- [34] SROKA, W., *Z. Naturforsch.*, **A 24** (1969) 1724.
- [35] MORGAN, H.D., MENTALL, J.E., *J. Chem. Phys.* **60** (1974) 4734.
- [36] MÖHLMANN, G.R., SHIMA, K.H., De HEER, F.J., *Chem. Phys.* **28** (1978) 331.
- [37] ORIENT, O.J., SRIVASTAVA, S.K., *Chem. Phys.* **54** (1981) 183.
- [38] PANG, K.D., AJELLO, J.M., FRANKLIN, B., SHEMANSKY, D.E., *J. Chem. Phys.* **86** (1987) 2750.
- [39] AARTS, J.F.M., BEENAKKER, C.I.M., De HEER, F.J., *Physica* **53** (1971) 32.
- [40] KOPPE, V.T., DANILEVSKIJ, N.P., KOVAL, A.G., *Sov. Phys. — JETP* **43** (1976) 1103.
- [41] McLAUGHLIN, R.W., ZIPF, E.C., *Chem. Phys. Lett.* **55** (1978) 62.
- [42] DONOHUE, D.E., SCHIAVONE, J.A., FREUND, R.S., *J. Chem. Phys.* **67** (1977) 769.
- [43] FLESCH, G.D., UTECHT, R.E., SVEC, H.J., *Int. J. Mass. Spectrom. Ion Process.* **58** (1984) 151.
- [44] ITO, K., ODA, N., HATANO, Y., TSUBOI, T., *Chem. Phys.* **21** (1977) 203.
- [45] OGAWA, T., TOMURA, H., NAKASHIMA, K., KAWAZUMI, H., *Chem. Phys.* **113** (1987) 65.
- [46] FINN, T.G., CARNAHAN, B.L., WELLS, W.C., ZIPF, E.C., *J. Chem. Phys.* **63** (1975) 1596.
- [47] SCHIAVONE, J.A., DONOHUE, D.E., FREUND, R.S., *J. Chem. Phys.* **67** (1977) 759.
- [48] LOCHT, R., MOMIGNY, J., *Chem. Phys.* **49** (1980) 173.
- [48a] FUCHS, R., TAUBERT, R., *Z. Naturforsch.*, **A 19** (1964) 494, 911, 1181.
- [49] MUL, P.M., MITCHELL, J.B.A., D'ANGELO, V.S., DEFRANCE, P., McGOWAN, J.W.M., FROELICH, H.R., *J. Phys.*, **B 14** (1981) 1353.
- [50] GREGORY, D.C., TAWARA, H., in *Physics of Electronic and Atomic Collisions (Abstr. 16th Int. Conf. New York, 1989)*, North-Holland, Amsterdam (1989) 352.
- [51] WANG, D.P., LEE, L.C., SRIVASTAVA, S.K., *Chem. Phys. Lett.* **152** (1988) 513.
- [52] DUNCAN, C.W., WALKER, I.C., *J. Chem. Soc. Faraday Trans. II* **70** (1974) 577.
- [53] McCORKLE, D.L., CHRISTOPHOROU, L.G., MAXEY, D.V., CARTER, J.G., *J. Phys.*, **B 11** (1978) 3067.
- [54] GEE, N., FREEMAN, G.R., *J. Phys.*, **A 22** (1980) 301.
- [55] TANAKA, H., BOETZEN, L., MATSUNAGA, D., KUDO, T., *J. Phys.*, **B 21** (1988) 1255.
- [56] FINK, M., JOST, K., HERMANN, D., *J. Chem. Phys.* **63** (1975) 1985.
- [57] DUNCAN, C.W., WALKER, I.C., *J. Chem. Soc. Faraday Trans. II* **70** (1974) 577.
- [58] DILLON, M.A., TANAKA, H., SPENCE, D., *J. Chem. Phys.* **87** (1987) 1499.
- [59] WINTERS, H.F., *Chem. Phys.* **36** (1979) 353.
- [60] BRÜCHE, E., *Ann. Phys. (Leipzig)* **2** (1929) 909.
- [61] WALKER, I.C., STAMATOVIC, A., WONG, S.F., *J. Chem. Phys.* **69** (1978) 5532.
- [62] MELTON, C., *J. Chem. Phys.* **37** (1962) 562.
- [63] KOHEM, K.H., SOHN, W., JUNG, K., ERHARDT, H., CHANG, E.S., *J. Phys.*, **B 18** (1985) 1253.
- [64] De SOUZA, A.C., De SOUZA, G.G.B., *Phys. Rev.*, **A 38** (1988) 4488.

- [64a] AZRIA, R., FIQUET-FAYARD, F., *J. Phys.* **33** (1972) 663.
- [65] TATE, J.T., SMITH, P.T., *Phys. Rev.* **39** (1932) 270.
- [66] GAUDIN, A., HAGEMANN, R., *J. Chim. Phys.* **64** (1967) 917, 1209.
- [67] SUSHANIN, I.V., KISHKO, S.M., *Sov. Astron.* **18** (1974) 265.
- [68] MATSUNAGA, D., KUBO, M., TANAKA, H., in *Physics of Electronic and Atomic Collisions* (Abstr. 12th Int. Conf. Gatlinburg, 1981), North-Holland, Amsterdam (1981) 358.
- [69] JOHNSON, K.E., JOHNSON, D.B., LIPSKY, S., *J. Chem. Phys.* **70** (1979) 3844.
- [70] DURIC, N., GADEZ, I., KUREPA, M.V., in *Physics of Ionized Gases* (Proc. 15th Summer School and Symp. Dubrovnik, 1990), Institute of Physics, University of Zagreb, Zagreb (1990) 59.
- [71] KUREPA, J.M., TASIC, M.D., *Chem. Phys.* **38** (1979) 361.
- [72] BELL, K.L., GILBODY, H.B., HUGHES, J.G., KINGSTON, A.E., SMITH, F.J., *J. Phys. Chem. Ref. Data* **12** (1983) 891.
- [73] TAWARA, H., KATO, T., *At. Data Nucl. Data Tables* **36** (1987) 167.
- [74] MÄRK, T.D., DUNN, G.H. (Eds), *Electron Impact Ionization*, Springer-Verlag, New York (1985).
- [75] MARGREITER, D., DEUTSCH, H., SCHMIDT, M., MÄRK, T.D., *Int. J. Mass. Spectrom. Ion Process.* **100** (1990) 157.
- [76] TAN, A., WU, S.T., *Chinese J. Phys.* **15** (1977) 56.
- [77] KHARE, S.P., PRAKASH, S., MEATH, W.J., *Int. J. Mass. Spectrom. Ion Process.* **88** (1989) 299; KHARE, S.P., MEATH, W.J., *J. Phys., B* **20** (1987) 2101.

DISSOCIATIVE AND ENERGY TRANSFER REACTIONS INVOLVING VIBRATIONALLY EXCITED H₂/D₂ MOLECULES

M.A. CACCIATORE, M. CAPITELLI, R. CELIBERTO

Centro di Studio per la Chimica dei Plasmi i del CNR,

Dipartimento di Chimica,

Università di Bari,

Bari, Italy

ABSTRACT. Atomic and molecular processes involving vibrationally excited H₂/D₂ molecules relevant to edge plasmas are reviewed. In particular, cross-sections for electron impact dissociation processes of vibrationally excited H₂(v) and D₂(v) molecules (including dissociative attachment and dissociative ionization) as well as dissociation of H₂⁺(v) are presented and discussed. Also discussed are cross-sections for electron impact vibrational excitation of H₂(v) and D₂(v) either by a resonant mechanism or by indirect excitation through electronic excited states radiatively cascading onto the ground state. For heavy particle molecular processes, the most important vibrational energy exchange processes due to the gas phase and to gas-surface collisions are discussed, namely the deactivation of H₂(v) and D₂(v) by H₂/D₂ and by atomic H/D species as well as in collisions with metallic surfaces.

1. INTRODUCTION

It is extremely difficult to understand atomic and molecular processes occurring in edge plasmas because in this medium atomic and molecular species in the ground state and in excited states coexist [1, 2]. This situation is far from being completely understood, even though there are many experimental and theoretical papers on the most important processes (electronic, radiative, charge and excitation exchange processes, involving the atomic species H, H⁺, D, D⁺, H⁻, D⁻). On the other hand, atomic processes involving roto-vibrational H₂⁺/D₂⁺ (as well as H₂/D₂) molecules have been neglected by the plasma physics community for a long time because of the small concentrations of these species in high temperature plasmas. The situation is different in edge plasmas, where large concentrations of molecular species are believed to exist. Fortunately, in the last decade, atomic processes involving roto-vibrational excited states have been studied by researchers who wanted to understand the processes occurring in low energy plasmas ($\epsilon \leq 5$ eV) [3] as well as in multipole magnetic plasmas which are being utilized for the formation of intense H₂/D₂ beams [4].

In the present paper we review the existing database for different elementary processes involving vibrational levels of H₂/D₂ molecules. Basically, we discuss the following topics:

— Energy exchange processes by which vibrational energy is formed in H₂/D₂ through electron impact;

- Direct electronic processes leading to dissociation, dissociative attachment and dissociative ionization from vibrationally excited molecules;
- Vibrational quenching of H₂(v)/D₂(v) in the gas phase;
- Vibrational energy exchange processes between H₂(v)/D₂(v) and metallic surfaces.

The results presented have been obtained by using different theoretical methods, including quantum mechanical, classical and semi-classical ones. We limit our presentation to the atomic and molecular physics of elementary processes. Of course, for a complete understanding of edge plasma properties, one should consider the appropriate Boltzmann equation for the electrons, coupled to the non-equilibrium vibrational kinetics of H₂(v)/D₂(v) interacting in the gas phase and with the surrounding metallic surfaces (see, for example, Refs [3, 4]).

2. ELEMENTARY PROCESSES INDUCED BY ELECTRON IMPACT

2.1. Vibrational excitation by electron impact

Vibrational excitation of H₂/D₂ by electron impact occurs through two distinct mechanisms. The first one (the so-called e-V process) considers excitation as a

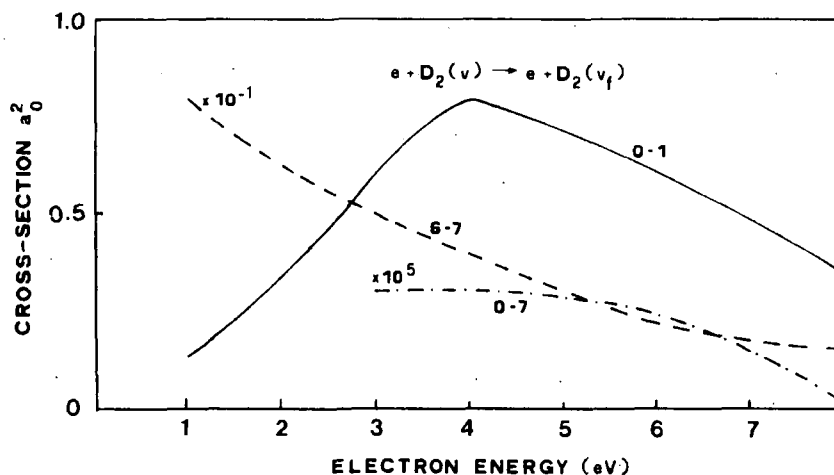
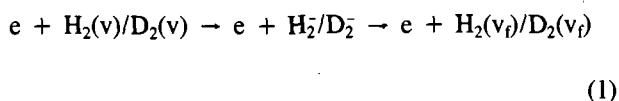
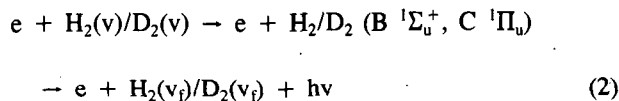


FIG. 1. Cross-sections for vibrational excitation of D_2 (e-V process) as a function of the incident energy for different initial and final vibrational levels.

resonant process of electron capture followed by autodetachment:



(v and v_f indicate the initial and final vibrational quantum numbers, respectively. The second mechanism (the so-called E-V process) considers the excitation of vibrational levels as a result of a two-step process, i.e. excitation of electronically excited states of H_2/D_2 followed by radiative cascade onto the vibrational levels of the ground H_2/D_2 electronic state:



The cross-sections of process (1) have been measured [5] and calculated [6-8] using the resonant scattering theory with local and non-local potentials. In general, the agreement between the different calculations and between calculations and experiments can be considered satisfactory, with the differences not exceeding a factor of two for the 0-1 transition. However, larger differences exist between the calculated values for (0- v_f) transitions ($v_f \geq 2$) and for transitions involving vibrationally excited molecules.

The cross-sections for process (2) have been calculated for the first time by Hiskes [9], who used a phenomenological approach. Actually, Hiskes calculated the cross-sections for process (2) basically by

modulating the total cross-section for the excitation of singlet excited states with the Einstein probabilities linking vibrational states of excited singlet states and vibrational levels of the singlet ground state.

A similar method was recently used for calculating the E-V cross-sections for D_2 [10].¹ Note that the threshold energy of the e-V process is much smaller than the corresponding one for the E-V process.

Figure 1 presents samples of theoretical e-V cross-sections for the excitation of D_2 [11]. Figure 2 shows the excitation of D_2 according to the E-V process from $v = 0$. We note that the excitation of high lying vibrational levels from $v = 0$ by the e-V process strongly decreases with increasing final quantum vibrational number v_f . For excitation by the E-V process, a much smoother dependence of the cross-sections on v_f is observed. Note that there is a large increase in the cross-sections for the e-V process when passing from $v = 0$ to $v = 6$ (see Fig. 1). A comparison of the magnitude of the two kinds of cross-sections shows that the e-V processes dominate the excitation mechanism for $v_f < 2$, while the E-V processes dominate for $v_f > 2$. This statement is true when $v = 0$ and is not true when $v \neq 0$.

Regarding the accuracy of cross-sections, we note that the experimental cross-sections for e-V processes in H_2 agree very well with quantum mechanical calculations. Unfortunately, experimental E-V cross-sections do not exist, so that the numerical results shown in Fig. 2 can only be validated by comparing them with

¹ The scale of the cross-sections in Fig. 4 of Ref. [10] is 10^{-18} cm^2 .

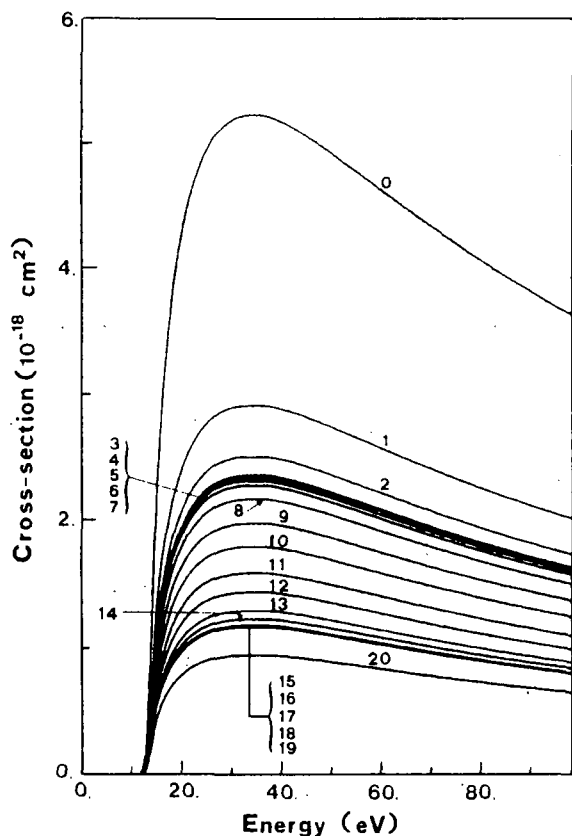


FIG. 2. Cross-sections for vibrational excitation of D₂ (*E-V* process) as a function of the electron energy for different final vibrational levels.

other theoretical results. This was done in the case of H₂, for which three independent calculations [9, 12, 13] of *E-V* cross-sections exist, with the differences not exceeding a factor of two. These differences are due to a different choice of the total excitation cross-section of excited singlet states, as discussed in Ref. [13].

2.2. Dissociative attachment

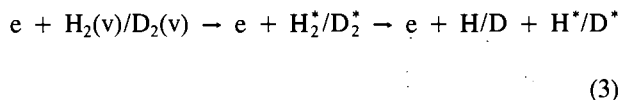
Dissociative attachment cross-sections for vibrationally excited H₂/D₂ have been measured [5] and calculated [6–8] using the resonant scattering theory with local and non-local potentials. The different theoretical results can sensibly differ, especially for low lying vibrational levels.

The most important feature of dissociative attachment cross-sections (common to all calculations as well as to the experimental values) is their dramatic dependence on the initial vibrorotational quantum number. This point can be confirmed in Fig. 3, which shows the cross-section for dissociative attachment of D₂ as a function of energy for different initial vibrational levels. The

cross-sections increase by several orders of magnitude when passing from $v = 0$ to higher values of v . It should be noted that dissociative attachment of H₂/D₂ is a very inefficient process in connection with vibrationally cold H₂/D₂ molecules; however, when the H₂/D₂ molecules are in vibrationally excited states, this process becomes very effective. This point is at the basis of volume sources for the creation of intense beams of H⁻/D⁻ [14].

2.3. Dissociation

Direct electron impact dissociation processes involving H₂(v)/D₂(v), i.e.



were recently calculated [10, 13, 15] by modulating the classical Gryzinski cross-section with the Franck-Condon density to describe the overlap of the vibrational and the continuum wave functions of H₂(v) and H₂^{*}, respectively. Figure 4 shows the cross-sections leading to unexcited D + D atoms from D₂(³Σ_u⁺) for different initial vibrational levels. The threshold energy of process (3) decreases with increasing v . The reverse is true for the maximum of the cross-section, in which

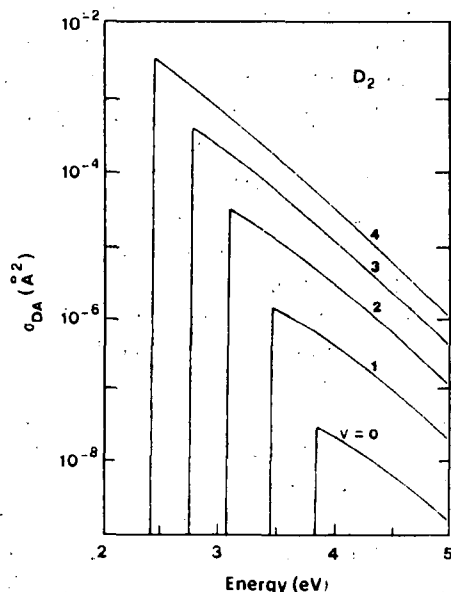


FIG. 3. Cross-sections for dissociative attachment of vibrationally excited D₂(v) (from Ref. [6]) as a function of energy for different initial vibrational levels.

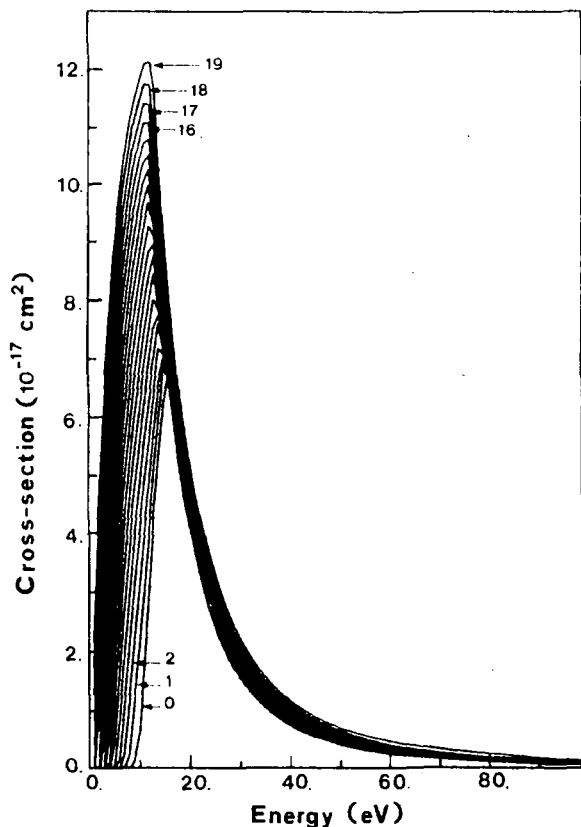


FIG. 4. Electron impact direct dissociation cross-sections of vibrationally excited D_2 over the first repulsive triplet state.

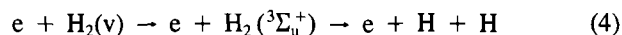
case, however, the cross-section increases only by a factor of two when going from $v = 0$ to $v = 19$.

A more complicated trend is observed for the v -dependence of the cross-section maximum for process (3), leading to excited atomic species, when the interaction takes place on the repulsive part of a bound state (see Ref. [15]). In this case, the cross-section maximum first increases, up to a certain value of v , and then decreases. On the contrary, the behaviour of the threshold energy follows the usual trend, i.e. it decreases with increasing v .

Figure 5 shows the rate coefficients ($\text{cm}^3 \cdot \text{s}^{-1}$) for process (3) as a function of v , calculated by integrating the relevant cross-sections over a Maxwell distribution function for the electron energy. In general, the behaviour of the cross-section at the threshold dominates the rate coefficient at low electron temperatures T_e , while the behaviour of the cross-section near its maximum dominates the rate coefficient at high T_e . As a result, there is a strong increase in the dissociation rate at low T_e , leading to unexcited hydrogen atoms from the completely repulsive ${}^3\Sigma_u^+$ of H_2 , while a smooth dependence on v is observed at high T_e .

The behaviour of the rate coefficients leading to excited $H + H^*$ fragments (Fig. 5(b)–(e)) does not follow a monotonic trend as a function of v ; this is due to the intricate v -dependence of the cross-sections, as discussed in Ref. [15].

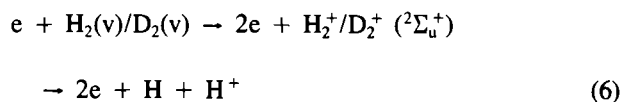
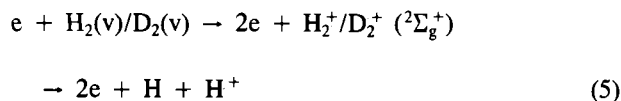
Regarding the accuracy of the method, we are aware of the fact that there are a number of questions regarding the Gryzinski approximation (widely used in plasma physics for obtaining excitation and ionization cross-sections of atoms). However, a comparison of the present results (see Refs [10, 13]) for the process



involving $v = 0$ and $v \neq 0$ vibrational levels, with experimental data and with data obtained by more accurate quantum mechanical scattering methods shows satisfactory agreement between them (differences are within a factor of two), indicating that the present results can be confidently used in modelling H_2/D_2 discharges.

2.4. Dissociative ionization

Another process which can take place in edge plasmas is dissociative ionization, i.e. the processes



Process (5) describes the excitation of the repulsive part of the $H_2^+/D_2^+ ({}^2\Sigma_g^+)$ bound state, while process (6) describes the excitation of the completely repulsive state (${}^2\Sigma_u^+$) of H_2^+/D_2^+ . Cross-sections for this process were calculated by our group [10, 16] by modulating the Gryzinski ionization cross-section with the Franck-Condon density linking the vibrational wave functions of $H_2(v)/D_2(v)$ with the continuum wave functions of H_2^+/D_2^+ . Figure 6 shows the behaviour of the cross-sections of processes (5) and (6) in D_2 for different initial vibrational quantum numbers. With increasing v , there is a monotonic increase in the cross-sections for dissociative ionization involving the completely repulsive $D_2^+ ({}^2\Sigma_u^+)$ state, while the cross-sections for process (5) show a non-monotonic behaviour, reflecting the Franck-Condon matrix linking $D_2(v)$ to D_2^+ .

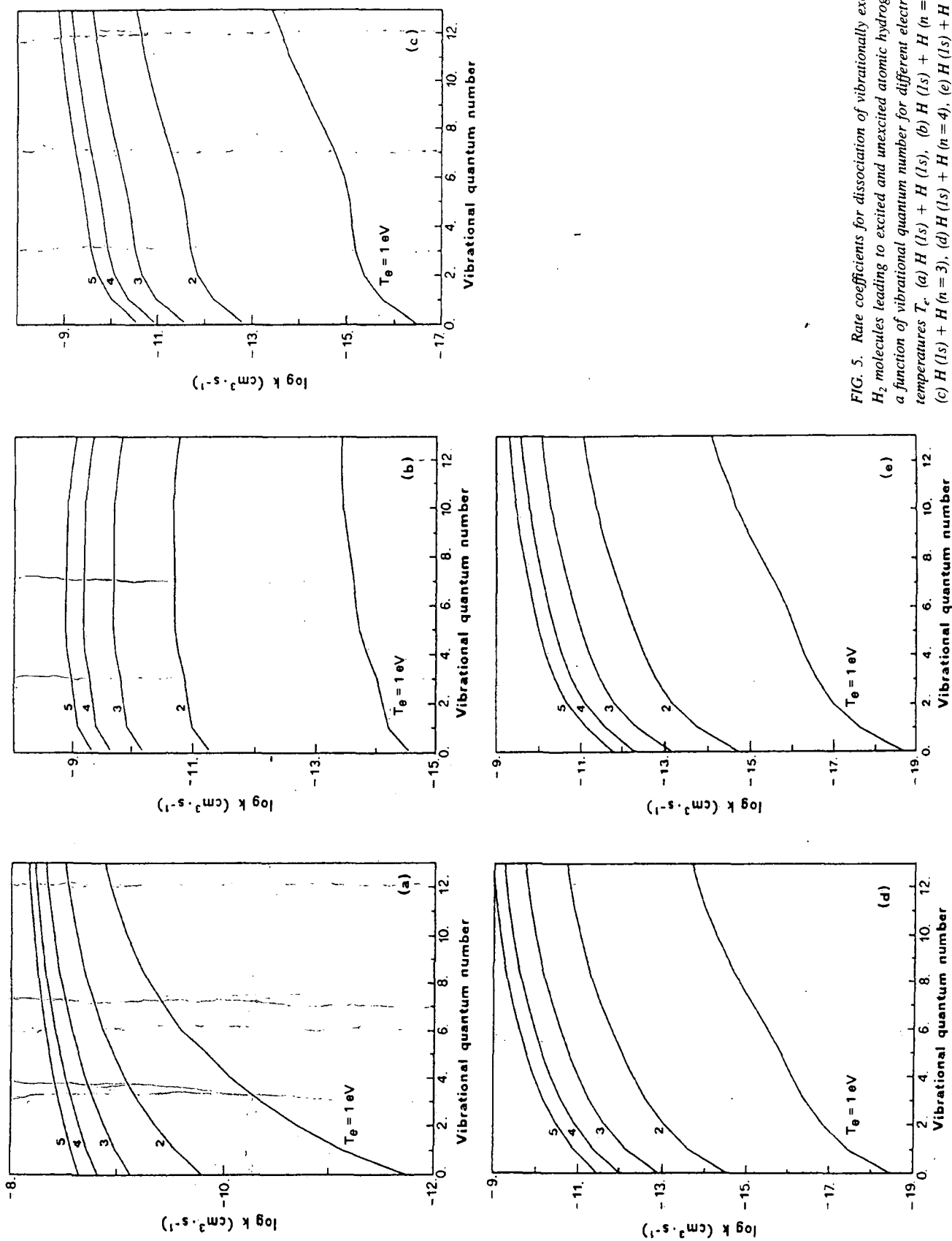


FIG. 5. Rate coefficients for dissociation of vibrationally excited H₂ molecules leading to excited and unexcited atomic hydrogen as a function of vibrational quantum number for different electron temperatures T_e . (a) H(1s) + H(n=3), (b) H(1s) + H(n=2), (c) H(1s) + H(n=4), (d) H(1s) + H(n=5), (e) H(1s) + H(n=5).

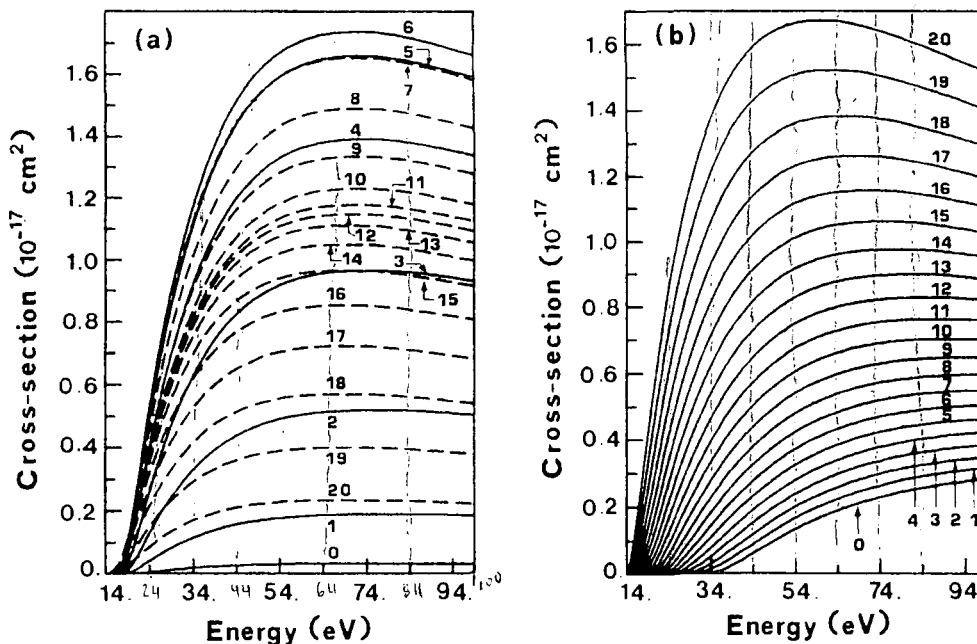
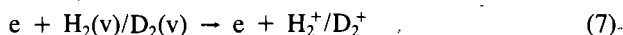


FIG. 6. Cross-sections for dissociative ionization of vibrationally excited D_2 molecules as a function of energy, (a) over the repulsive part of the bound $^2\Sigma_g^+$ state of D_2^+ and (b) over the repulsive state $^2\Sigma_u^+$.

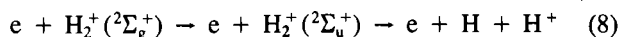
We have recently investigated the accuracy of the present cross-sections for H_2 by comparing the $v = 0$ cross-section with the corresponding experimental one (see Ref. [16]). The results obtained seem to be satisfactory, under the assumption that the direct processes dominate the indirect ones. Moreover, when the method used by us is applied to the process



it gives results for $v = 0$ that are within 10–20% of the corresponding experimental values (see Refs [13, 16]).

2.5. Dissociation of H_2^+ by electron impact

Dissociation of H_2^+ by direct electron impact mainly takes place through the excitation of repulsive H_2^+ ($^2\Sigma_u^+$), i.e. by the process

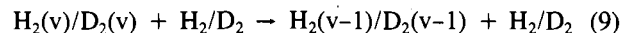


These cross-sections were calculated by Peek [17] using the Born approximation. Figure 7 shows the relevant cross-section for $v = 0$ as well as a cross-section averaged over the vibrationally excited H_2^+ molecules (in this case a Franck–Condon distribution has been considered). A strong enhancement due to the vibrational excitation of H_2^+ can be seen. Also shown in Fig. 7 is

an experimental determination of the averaged cross-section [18], which agrees well with the experimental results. Note that the vibrational excitation of H_2^+ strongly reduces the threshold energy of the process. Regarding the accuracy of the method, it is pointed out that the Born approximation is known to work very well at high electron impact energy, so that the good agreement between theoretical and experimental results may be surprising. When the cross-section is calculated with the Gryzinski method [19] it is in excellent agreement with the $v = 0$ cross-section calculated by Peek [17]. This agreement, however, disappears for high lying vibrational H_2^+ states. It should also be noted that the experimental cross-sections for D_2^+ are very similar to those reported in Fig. 7.

3. VIBRATIONAL RELAXATION IN THE GAS PHASE

So far, we have discussed elementary processes induced by electron impact. The next problem is to understand the relaxation of vibrationally excited molecules colliding with molecules and atoms, i.e. the processes



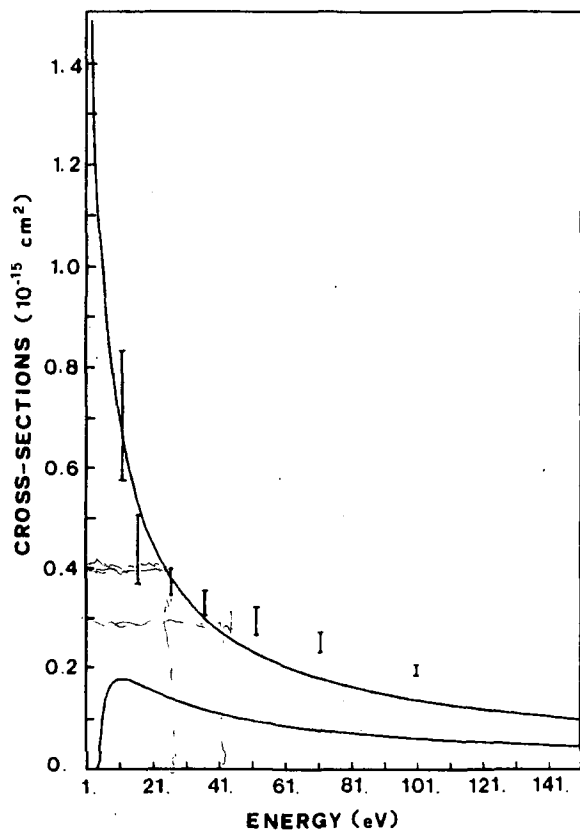
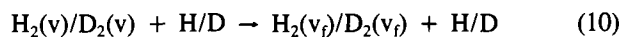


FIG. 7. Comparison between cross-sections of dissociation of H₂⁺, from $v = 0$ (lower curve), from all values of v (upper curve) and from experimental values.



Relaxation process (9) was recently investigated by Cacciatore et al. [20], using a semi-classical model in which the translational and rotational degrees of freedom of the molecule are treated classically and the vibrational energy exchange is treated quantum mechanically. The key issue in these calculations is the description of the interaction potential between the two molecules, which in the case of H₂/H₂ and D₂/D₂ interactions must contain short and long range contributions. The choice of this potential is discussed in detail in Ref. [20], where it is shown that the selected potential is able to reproduce the experimental behaviour of the rate constant for the deactivation of H₂ ($v = 1$) in a wide range of gas temperatures. The same accuracy can be expected for the rate constants involving high lying vibrational excited molecules, even though the accuracy can become worse for vibrational levels close to the continuum.

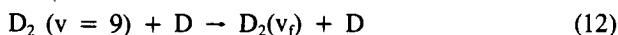
Figure 8 shows the behaviour of relaxation rates ($k_{v,v-1}$) of H₂(v) [20] and D₂(v) [21] as a function of v for a gas temperature of 500 K. It can be seen that

$k_{v,v-1}$ dramatically increases with v . Note also that the gas temperature strongly affects the relaxation rates.

We now discuss the relaxation of H₂(v)/D₂(v) with atomic H/D species (i.e. process (10)). A complete set of rates for both systems were calculated by Gorse et al. [4] and Laganà [22], using a quasi-classical method with the best available H/H₂ potential energy surface. Figure 9 shows a sample of results for D₂. Figure 9(a) shows the relaxation rates for the process



as a function of v . Figure 9(b) shows the relaxation rates for the process



as a function of v_f . For both cases, the two contributions (inelastic and reactive) as well as the total relaxation rate are shown. Moreover, the calculations refer to a translational temperature of atoms ($T_H = 4000$ K) which is much higher than the corresponding one for molecules ($T_{H_2} = 500$ K). It can be seen that the

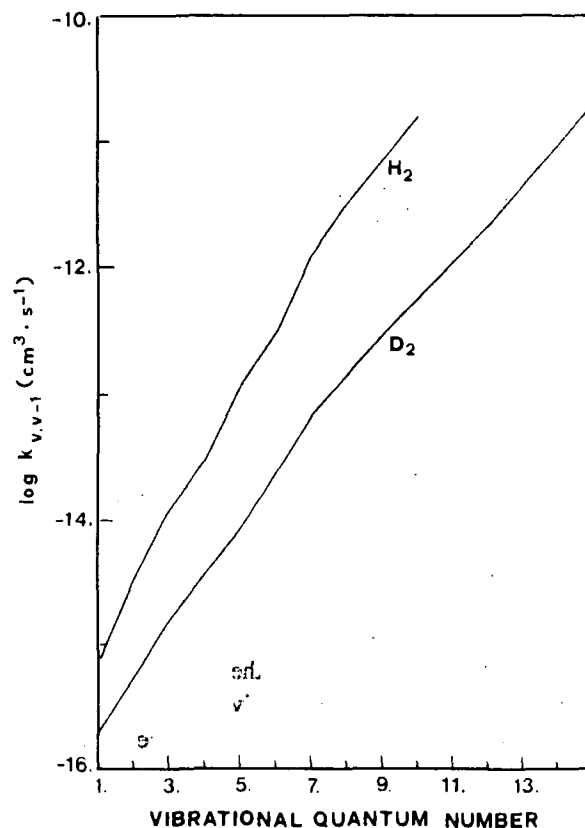


FIG. 8. Vibrational relaxation rates of H₂(v)/D₂(v) with H₂/D₂, as a function of vibrational quantum number ($T = 500$ K).

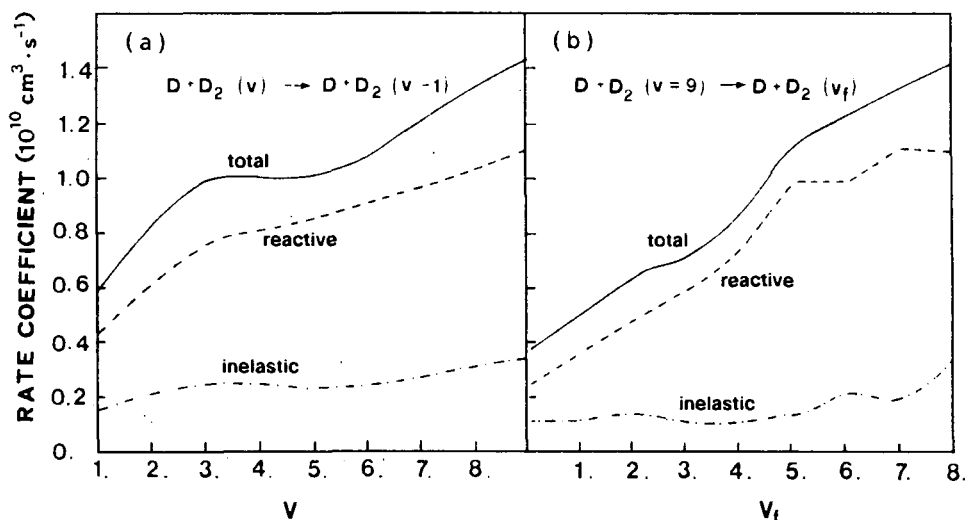


FIG. 9. Vibrational relaxation rates of $D_2(v)$ with D atoms.

relaxation of $D_2(v)$ by atoms can occur through multi-quantum transitions, while the rate constant $k_{v, v-1}$ does not dramatically depend on v . It should also be noted that the relaxation of vibrationally excited H_2 and D_2 molecules with the corresponding atomic species is a very efficient process, since the atomic species are the natural enemies of the vibrationally excited molecules.

4. VIBRATIONAL RELAXATION ON METALLIC SURFACES

Vibrational relaxation and dissociation of highly vibrationally excited $H_2(v)$ and $D_2(v)$ on metallic surfaces can be very important factors in understanding the fate of $H_2(v)/D_2(v)$ after it collides with the container walls.

Two independent calculations have been performed so far — one by Hiskes and Karo [23] for iron surfaces and the other one by Cacciatore et al. [24] for copper surfaces. The last group used a semi-classical theory for atom/diatom surface scattering; in this theory the phonon and electron hole pair dynamics in the solid is coupled with the dynamics of the molecular motions through the definition of an effective potential. The Hamiltonian describing the molecule surface dynamics is then written as

$$H_{\text{eff}} = \sum_i (2m_i)^{-1} (P_{x_i}^2 + P_{y_i}^2 + P_{z_i}^2) + V_{12}(r) + V_{\text{eff}}(x_i, y_i, z_i, t, T_s) + E_{\text{int}}(t, T_s)$$

where $V_{12}(r)$ is the H–H interaction approximated by a Morse potential, x_i is the x co-ordinate of atom i , P_{x_i} is the corresponding momentum in the x component and T_s is the surface temperature. E_{int} is the energy transferred to the surface and V_{eff} is an effective potential expressed as

$$V_{\text{eff}} = V_0(x_i, y_i, z_i) + \langle \Psi_{\text{ph}} | V_{\text{int}} | \Psi_{\text{ph}} \rangle + \langle \Psi_{\text{el}} | V_{\text{C}} / \Psi_{\text{el}} \rangle$$

where V_0 is the static interaction between atoms in the gas phase and surface atoms in their equilibrium positions. Ψ_{ph} and Ψ_{el} are the phonon and electron wave functions. The surface–molecule interaction potential V_{int} was obtained as an analytical fit to recent ab initio calculations for the $H_2/(Cu)_{38}$ system. Hamilton's equations of motion are integrated, using the above Hamiltonian, for a number of initial values of the kinetic and vibrational energies of H_2/D_2 molecules. The surface temperature T_s is set at 300 K.

The main conclusions of these calculations can be summarized as follows:

(a) The dissociation probability of $H_2(v)/D_2(v)$ strongly increases with the kinetic energy of molecules and with the initial vibrational quantum number. It is in any case negligible for kinetic energies less than 0.05 eV.

(b) The vibrational deactivation probability is very small in all cases.

(c) Below the classical energy threshold (~ 1 eV), dissociation occurs through the tunnelling effect. In this case, dissociation probabilities approaching unity

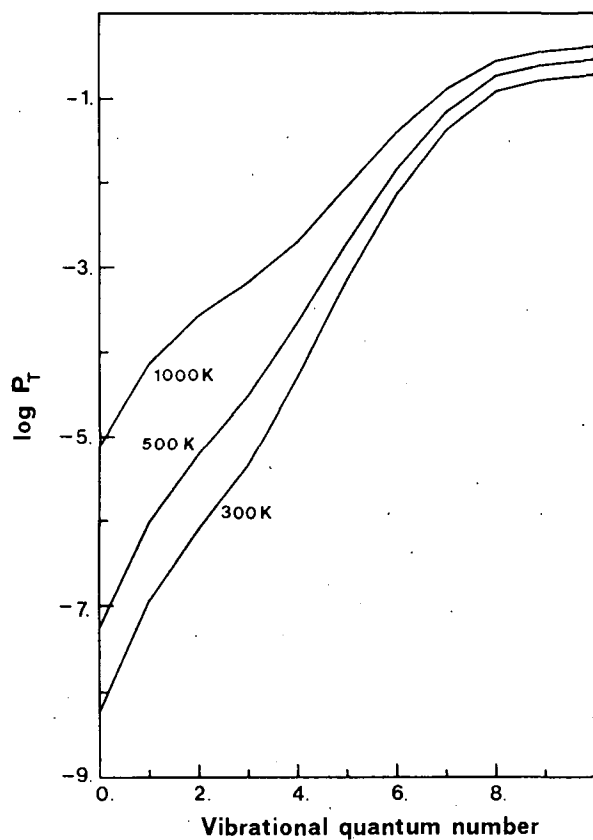


FIG. 10. Tunnelling probabilities, averaged over a Maxwell velocity distribution function for vibrationally excited H₂ molecules colliding with copper surfaces, as a function of vibrational quantum number.

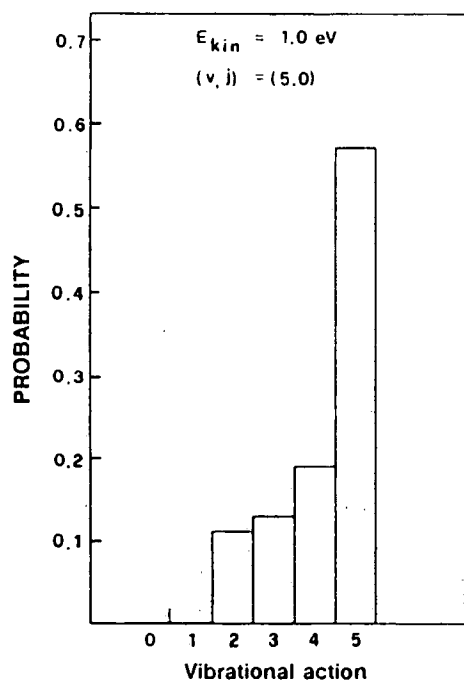


Fig. 11. Deactivation probability of vibrationally excited deuterium molecules colliding with copper surfaces, as a function of final vibrational quantum number.

are possible for the high lying vibrational levels. This is illustrated in Fig. 10, which shows the tunnelling probability for H₂ on Cu as a function of vibrational quantum number at different translational temperatures. These probabilities have been obtained by integrating the values reported in Ref. [24] over a Maxwell velocity distribution function.

Figure 11 [25] shows the final vibrational distribution of D₂ in the initial rotovibrational state, $j = 0$ and $v = 5$, impinging on the copper surface with an initial translational energy of 1 eV. In this case (high translational temperature) D₂ is deactivated. These results agree with those obtained by Hiskes and Karo for the H₂/Fe system; they found similar results for very small translational temperatures of molecules.

5. CONCLUSIONS

We have shown the dependence of several elementary processes, involving H₂/D₂ vibrationally excited states, on the vibrational quantum number. This is the first step on the way to an understanding of the role of vibrationally excited H₂/D₂ molecules in edge plasmas. For a complete understanding, it is necessary to solve appropriate equations for the vibrational distribution of H₂/D₂ as well as for the energy distribution functions of electrons and heavy particles. This kind of problem was solved by our group for low energy plasmas sustained by the electric field and by electron beams. In principle, an extension of these codes to edge plasmas is possible, even though it is not obvious.

ACKNOWLEDGEMENTS

The authors thank M. Bacal, G. Billing, P. Cives, R. Caporusso, P. De Felice, A. Laganà, C. Gorse and M. Wadehra for useful discussions.

The Italian National Research Council and the Progetto Finalizzato Chimica Fine II are acknowledged for supporting this research. One of the authors (R.C.) also thanks the Italian Ministry of Education (MURST 90).

REFERENCES

- [1] JANEV, R.K., in Phenomena in Ionized Gases (Proc. 19th Int. Conf. Belgrade, 1989), Faculty of Physics, University of Belgrade (1989) 264.
- [2] HARRISON, M.F.A., in Atomic Processes in Electron-Ion and Ion-Ion Collisions, Nato Asi Series B145, Plenum Press, New York (1985).

- [3] CACCIATORE, M., CAPITELLI, M., DILONARDO, M., Chem. Phys. **34** (1978) 193; CACCIATORE, M., CAPITELLI, M., GORSE, C., J. Phys., D **13** (1980) 575; CACCIATORE, M., CAPITELLI, M., Chem. Phys. **55** (1981) 67.
- [4] GORSE, C., CAPITELLI, M., BRETAGNE, J., BACAL, M., Chem. Phys. **93** (1985) 1; GORSE, C., CAPITELLI, M., BACAL, M., BRETAGNE, J., LAGANA, A., Chem. Phys. **117** (1987) 177.
- [5] SCHULTZ, G.J., ASUNDI, R.K., Phys. Rev. **158** (1967) 25; ERHARDT, H., LANGHANS, L., LINDNER, F., TAYLOR, H.S., Phys. Rev. **173** (1968) 222; ALLAN, M., WONG, S.F., Phys. Rev. Lett. **41** (1978) 1791; ALLAN, M., J. Phys., B **18** (1985) L451; POPOVIC, D., Meas. Sci. Technol. **1** (1990) 1041.
- [6] BARDSLEY, J.N., WADEHRA, J.M., Phys. Rev. **20** (1979) 1398; WADEHRA, J.M., Phys. Rev. **29** (1984) 106; ATEMS, D.E., WADEHRA, J.M., in Production and Neutralization of Negative Ions and Beams (Proc. 5th Int. Symp. Brookhaven, 1989), AIP Conf. Proc. 210 (1990).
- [7] GAUYACQ, J.P., J. Phys., B **18** (1985) 1859.
- [8] DOMCKE, W., MUNDEL, C., CEDERBAUM, L.S., Comments At. Mol. Phys. **20** (1987) 293; MUNDEL, C., BERMAN, M., DOMCKE, W., Phys. Rev., A **32** (1985) 181.
- [9] HISKES, J.R., J. Appl. Phys. **51** (1980) 4592.
- [10] CELIBERTO, R., CIVES, P., CACCIATORE, M., CAPITELLI, M., LAMANNA, U.T., Chem. Phys. Lett. **169** (1990) 69.
- [11] WADEHRA, J.M. (Wayne State University), personal communication, 1984.
- [12] MARX, J., LEBEHOT, A., CAMPARGUE, R., Phys. Rev. **46** (1985) 102.
- [13] CACCIATORE, M., CAPITELLI, M., CELIBERTO, R., CIVES, P., GORSE, C., in Production and Neutralization of Negative Ions and Beams (Proc. 5th Int. Symp. Brookhaven, 1989), AIP Conf. Proc. 210 (1990).
- [14] BACAL, M., SKINNER, D., Comments At. Mol. Phys. **23** (1990) 283.
- [15] CELIBERTO, R., CACCIATORE, M., CAPITELLI, M., GORSE, C., Chem. Phys. **133** (1989) 355.
- [16] CELIBERTO, R., CAPITELLI, M., CACCIATORE, M., Chem. Phys. **140** (1990) 209.
- [17] PEEK, J.M., Phys. Rev. **154** (1967) 52.
- [18] DUNN, G.H., Van ZYL, B., Phys. Rev. **154** (1967) 40.
- [19] CELIBERTO, R. (Bari University), unpublished results, 1991.
- [20] CACCIATORE, M., CAPITELLI, M., BILLING, G.D., Chem. Phys. Lett. **157** (1989) 305; CACCIATORE, M., BILLING, G.D., State-to-state vibration-translation and vibration-vibration rate constants in H₂-H₂ and HD-HD collisions, to be published in J. Phys. Chem.
- [21] CACCIATORE, M., CAPORUSSO, R. (CNR Centro Chimica Plasmi, Bari University), personal communication, 1991.
- [22] LAGANA, A., in Non-Equilibrium Processes in Partially Ionized Gases, Plenum Press, New York (1990).
- [23] HISKES, J.R., KARO, A.M., J. Appl. Phys. **56** (1984) 1927.
- [24] CACCIATORE, M., CAPITELLI, M., BILLING, G.D., Surf. Sci. **227** (1989) 391; CACCIATORE, M., BILLING, G.D., Surf. Sci. **232** (1990) 35.
- [25] CACCIATORE, M., De FELICE, P., unpublished results.

ASSESSMENT OF ION-ATOM COLLISION DATA FOR MAGNETIC FUSION PLASMA EDGE MODELLING

R.A. PHANEUF
Controlled Fusion Atomic Data Center,
Physics Division,
Oak Ridge National Laboratory,
Oak Ridge, Tennessee,
United States of America

ABSTRACT. Cross-section data for ion-atom collision processes which play important roles in the edge plasma of magnetically confined fusion devices are surveyed and reviewed. The species considered include H, He, Li, Be, B, C, O, Ne, Al, Si, Ar, Ti, Cr, Fe, Ni, Cu, Mo, W and their ions. The most important ion-atom collision processes occurring in the edge plasma are charge exchange reactions. Excitation and ionization processes are also considered. The scope is limited to atomic species and to collision velocities corresponding to plasma ion temperatures in the range 2-200 eV. Sources of evaluated or recommended data are presented where possible, and deficiencies in the database are indicated.

This paper is dedicated to the memory of Clarence F. Barnett, founder of the Controlled Fusion Atomic Data Center of the Oak Ridge National Laboratory. 'Barney' devoted his professional career to the promotion of effective communication between the atomic and fusion research communities, and was still actively engaged in this mission at the time of his death in 1989. The data compilation upon which he was working, entitled Collisions of H, H₂, He and Li atoms and ions with atoms and molecules, was published in August 1990 as part of the Atomic Data for Fusion series, popularly known as 'the Redbooks'. This compilation is a source for some of the data assessment presented in this paper. Barney's critical insights, guidance and dedication will be sorely missed by the Data Center and by the fusion research community.

1. INTRODUCTION

The edge region of magnetically confined fusion plasmas has received considerable attention [1, 2] because of its pivotal role in insulating the high temperature core plasma from the vacuum vessel. This interest has been intensified by mounting evidence that the quality of confinement of the hot plasma core depends critically on subtle details of the edge or scrape-off plasma [2, 3]. Gas puffing, pellet injection and particle recycling from material surfaces (vessel walls, limiters and divertor plates) are the primary sources of neutral particles in the plasma edge [2-4]. Thus, atomic processes involving neutral hydrogen, helium (in ignited D-T plasmas), carbon, oxygen and metallic impurities play an important role in the particle, energy and ionization balance in the edge plasma. This region is characterized in general by relatively low ion and electron temperatures (2-200 eV) and moderate to high particle densities (10^{12} - 10^{15} cm⁻³). Molecules and molecular ions also play a role [1], but collisions involving them are excluded from the present discussion;

these are addressed specifically in other articles in this volume.

Initial surveys of the relative importance of the various atomic reactions occurring in the edge plasma were performed by Janev et al. [5, 6]. More recent assessments of atomic and molecular data requirements and the available database for modelling and diagnostics of the edge plasma were made by Tawara and Phaneuf [7] and by Janev et al. [8].

Although electron impact processes are by far the most frequent and dominant in the edge plasma, heavy particle collisions (particularly charge exchange reactions) may also have a significant effect on particle transport and cooling [1, 8]. While the atomic database for reactions occurring in the hotter core plasma or in energetic neutral beam heating has grown substantially in recent years [9], relatively less attention was paid to such processes at the lower collision energies which prevail in the edge region. This is due to the difficulty in reliably extending experimental measurements for heavy particle collisions down to energies in the eV range and also, from a theoretical standpoint, to the

need for elaborate quantum mechanical approaches to address the dynamics of such collisions with a high degree of confidence.

2. SCOPE OF THE SURVEY

In this report, the available cross-section data for a number of ion-atom collision processes which are important for both modelling and diagnostics of the edge plasma are surveyed and reviewed. In the relevant velocity range, the most important processes involve charge exchange, association, electron detachment and, to a lesser degree, impact excitation. The species considered include H, He, Li, Be, B, C, O, Ne, Al, Si, Ar, Ti, Cr, Fe, Ni, Cu, Mo, W and their ions [8]. Atoms and ions of hydrogen isotopes are considered to be the primary plasma constituents, as are those of He, which will constitute the ash of ignited D-T plasmas and will be abundant in the edge plasma. All other species are classified as impurities, for which the maximum charge state considered is +10. Ne, Ar and Li are included because they are frequently introduced for plasma diagnostic purposes.

The reaction rate — the product of the concentrations of the two reactants and the rate coefficient for the process of interest — has been chosen to serve as a rough measure of the relative importance of a given reaction and pair of reactants. The reaction rate for a specific reaction represents the total number of such reactions which take place per unit volume per unit time in the plasma. Thus, in general, reactions involving two primary plasma constituents will be more important than reactions involving one primary species and one impurity species, which will in turn be more important than those involving two impurity species. Of course, other factors may also mitigate the relative importance of one reaction compared to another, for example its effect on the ionization balance, cooling and transport of particles or on specific diagnostic measurements. The concentrations of different species may also vary significantly in different plasma devices or in different operating regimes in the same device.

During the past five to ten years, considerable effort has been devoted on an international scale to the compilation, assessment and recommendation of atomic collision data for fusion relevant processes. Of particular significance to the present survey are reports from the Princeton group [5, 6], the Nagoya Data Center [10–13], the JAERI Data Center [13–17], the ORNL Controlled Fusion Atomic Data Center [18–22], the JILA Information Center [23] and the Ruhr University [24]. The

IAEA Atomic and Molecular Data Unit has co-ordinated a recent assessment of the carbon and oxygen collision database for fusion applications [25]. A number of the reactions covered in the present survey are included in a recently published volume of recommended data by C.F. Barnett [19].

3. GENERAL CONSIDERATIONS FOR HEAVY PARTICLE COLLISIONS

Because electrons have a much higher velocity than heavy particles at the same temperature, electron collisions with heavy particles occur much more frequently than collisions between heavy particles. Thus, to be of comparable importance, a particular collision process between heavy particles must have a larger cross-section to compensate for the reduced collision frequency. Because of the relatively low temperatures in the edge region, the lower ionization stages are predominant. Therefore, collisions of atoms and impurity ions in the lower ionization stages play a significant role in the dynamics of the edge plasma.

Inelastic processes may be generally classified with regard to whether they are endothermic, resonant or exothermic. Endothermic processes have a finite threshold energy, usually of the order of several eV to several tens of eV for the species present in the edge. For such processes, the cross-section decreases with decreasing energy, becoming exponentially small at the lowest energies. Resonant or exothermic processes, on the other hand, are characterized by cross-sections which often increase with decreasing energy, and these may play an important role at the lower temperatures prevailing in the edge plasma.

Figure 1, taken from a report by Tawara et al. [10], compares cross-sections for the production of various excited states of H by both charge exchange and proton impact excitation, as well as the cross-section for proton impact ionization of H. This figure serves to illustrate both the typical availability of data for different processes and the behaviour of the corresponding cross-sections for the $H^+ + H$ collision system. While data are not available for processes other than total electron capture at collision energies below 1 keV/amu, it is apparent that all of these reactions will have cross-sections which are many orders of magnitude smaller than that for total capture in the low energy region appropriate to the edge plasma. It should be noted that, at these energies, electron capture goes almost exclusively into the 1s ground state (i.e. the total cross-section at low energies is the same as that for resonant capture into the 1s state).

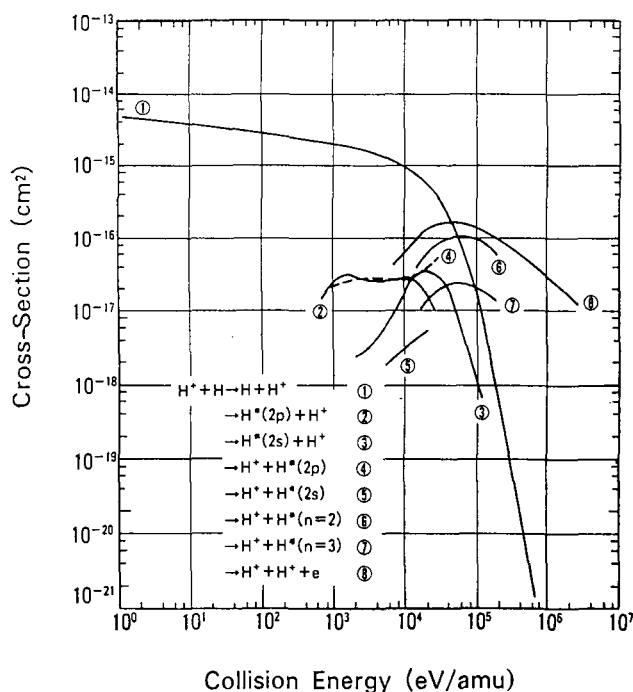


FIG. 1. Cross-sections for inelastic processes resulting from $H^+ + H$ collisions, taken from the compilation of Tawara et al. [10].

4. CHARGE EXCHANGE COLLISIONS

Because of the relatively large density of neutral particles, charge exchange (electron capture) reactions are by far the dominant inelastic collision processes between heavy particles in the edge plasma. Such reactions generally proceed via avoided crossings of the curves for the potential energy, and only those which are either resonant or exothermic have appreciable cross-sections at energies corresponding to the edge temperature range (2–200 eV). Such temperatures are nonetheless still sufficiently high to produce appreciable impurity ion concentrations in relatively high charge states. Ionization stages up to He-like ones will be strongly populated by C and O impurities in the edge, and heavier impurities such as Fe and Ni will have appreciable populations in charge states as high as 10.

Of particular importance are symmetric charge exchange reactions, which are exactly resonant, and charge exchange reactions involving multiply ionized plasma impurities. The latter are generally exothermic by several eV to several tens of eV, populating excited levels of the once less charged product ion, with relatively large cross-sections ($> 10^{-15}$ cm²) at low energies. These excited products decay radiatively, cooling the plasma and providing useful diagnostic information.

Table I presents a survey of the available data for total charge exchange cross-sections (i.e. summed over all final states) at three different relative collision energies characteristic of the edge plasma (2, 20 and 200 eV/amu), together with estimated uncertainties. Experimental total charge exchange cross-section data are generally obtained by measuring the fraction of ions in a beam whose charge has changed as a function of the gas target thickness (i.e. product of gas density and target cell length). Theoretical calculations in this energy region are generally based on a coupled atomic or molecular state approach. The available evaluated data are included in Table I, as indicated. References are given to the latest available source of evaluated or compiled data, and the reader is referred to those publications for references to the original research articles. In a few cases, where newer data have become available, a reference to the specific source is given. The lack of an entry for a reaction at a given energy signifies a lack of data or a serious inconsistency in the available data. In some cases, the data were extrapolated over a small fraction of their energy range where the energy dependence was weak or clearly suggested, or an interpolation was made between sets of data in different energy ranges. These values are given in parentheses. The accuracies listed in Table I are based on a judgement of the overall quality and consistency of the available data and of the methods employed to obtain them. Cross-section data are available at higher energies for many relevant reactions which are not included in Table I. For such data, the reader is referred to the more extensive data compilations [6, 10–26].

The selection of specific reactant combinations for inclusion in Table I is based on a consideration of the relative abundances of the elements in a typical plasma, as discussed in Section 2. Hydrogen (H, D and T) and helium (in an ignited D–T plasma) atoms and ions are considered to be primary plasma constituents; ions and atoms of all other elements are considered to be secondary constituents (impurities), with correspondingly lower particle densities in the edge. The most important reactions included are those involving two primary constituents (H and He atoms or ions). The next level of importance includes reactions involving a primary constituent and an impurity constituent. Reactions involving two impurity constituents have been excluded from Table I. For all the ion–atom reactions considered in this report, collisions involving the isotopes H, D or T may be assumed to have identical cross-sections at the same relative velocity (i.e. the same energy in eV/amu). Isotopic effects are expected to be significant only at much lower collision energies.

TABLE I. EDGE PLASMA ION-ATOM TOTAL CHARGE EXCHANGE CROSS-SECTIONS

Reaction	Cross Section (cm ²)*			Status [#]	Accuracy ^{&}	Reference
	E=2 eV/amu	20 eV/amu	200 eV/amu			
H ⁺ + H → H + H ⁺	3.8×10	2.9×10 ⁻¹⁵	2.2×10 ⁻¹⁵	ev	A A A	19
H ⁺ + He → He + H ⁺	X	X	2.5×10 ⁻²⁰	ev	X X C	19
H ⁺ + He → H ⁻ + He ²⁺	X	X	(6×10 ⁻²³)	ev	X X E	19
H ⁺ + Li → H + Li ⁺	X	(3×10 ⁻¹⁸)	1.6×10 ⁻¹⁶	ev	X E C	19,28
H ⁺ + Ne → H + Ne ⁺	X	X	8×10 ⁻²¹	co	X X E	16
H ⁺ + Ar → H + Ar ⁺	X	X	4×10 ⁻¹⁷	co	X X D	16
H ⁻ + H → H + H ⁻	1.3×10 ⁻¹⁴	9.0×10 ⁻¹⁵	4.2×10 ⁻¹⁵	ev	C C C	19
He ⁺ + H → He + H ⁺	X	X	2.5×10 ⁻¹⁷	ev,nd	X X D	19,42
He ⁺ + He → He + He ⁺	2.1×10 ⁻¹⁵	1.5×10 ⁻¹⁵	1.1×10 ⁻¹⁵	ev	B B B	19
He ⁺ + Li → He + Li ⁺	X	X	3.3×10 ⁻¹⁵	ev	X X C	19
He ⁺ + Ne → He + Ne ⁺	X	(5×10 ⁻¹⁸)	8×10 ⁻¹⁷	co,nd	X D C	15,29
He ⁺ + Ar → He + Ar ⁺	X	2×10 ⁻¹⁶	2.5×10 ⁻¹⁶	co	X E E	15
He ²⁺ + H → He ⁺ + H ⁺	X	X	3.1×10 ⁻¹⁸	ev	X X C	19
He ²⁺ + He → He ⁺ + He ⁺	2.2×10 ⁻²⁰	2.2×10 ⁻¹⁹	3.0×10 ⁻¹⁸	ev	B B B	19
He ²⁺ + He → He + He ²⁺	(5×10 ⁻¹⁶)	4.1×10 ⁻¹⁶	3.2×10 ⁻¹⁶	ev	C B B	19
He ²⁺ + Li → He ⁺ + Li ⁺	X	X	7.0×10 ⁻¹⁵	ev	X X C	19
Be ⁴⁺ + H → Be ³⁺ + H ⁺	X	X	2.1×10 ⁻¹⁵	nd	X X C	43
Be ⁴⁺ + He → Be ³⁺ + He ⁺	X	X	(2.5×10 ⁻¹⁶)	co	X X D	24
B ⁵⁺ + H → B ⁴⁺ + H ⁺	X	X	1.3×10 ⁻¹⁵	nd	X X C	43
C ⁺ + H → C + H ⁺	X	(5×10 ⁻¹⁷)	1.4×10 ⁻¹⁶	ev	X C B	18,21
C ²⁺ + H → C ⁺ + H ⁺	5.1×10 ⁻¹⁹	3.2×10 ⁻¹⁷	3.7×10 ⁻¹⁶	ev	C B B	18,21
C ²⁺ + He → C ⁺ + He ⁺	5.9×10 ⁻¹⁷	3.5×10 ⁻¹⁶	6.0×10 ⁻¹⁶	ev	C C C	18,21
C ³⁺ + H → C ²⁺ + H ⁺	2.1×10 ⁻¹⁵	1.0×10 ⁻¹⁵	5.2×10 ⁻¹⁶	ev	B B B	18,21
C ³⁺ + He → C ²⁺ + He ⁺	3.2×10 ⁻¹⁶	1.1×10 ⁻¹⁵	1.8×10 ⁻¹⁵	ev	D D D	18,21
C ⁴⁺ + H → C ³⁺ + H ⁺	1.1×10 ⁻¹⁵	1.4×10 ⁻¹⁵	3.0×10 ⁻¹⁵	ev	C B B	18,21
C ⁴⁺ + He → C ³⁺ + He ⁺	X	(8×10 ⁻¹⁸)	4.4×10 ⁻¹⁷	ev	X C C	18,21
C ⁴⁺ + He → C ²⁺ + He ²⁺	X	(4×10 ⁻¹⁷)	3.4×10 ⁻¹⁶	ev	X C B	18,21

*Cross sections in parentheses represent an extrapolation or interpolation of existing data.

[#]"ev" denotes evaluated data, "co" denotes data compilation, "sc" denotes scaling formula, "nd" indicates newer data available (reference given).

[&]Accuracy: A+ <3% A <10% B 10-25% C 25-50% D 50-100% E >100%

TABLE I. (cont.)

Reaction	Cross Section (cm ²)*			Status [#]	Accuracy ^{&}	Reference
	E=2 eV/amu	20 eV/amu	200 eV/amu			
C ⁵⁺ + H → C ⁴⁺ + H ⁺	6.0×10 ⁻¹⁵	3.3×10 ⁻¹⁵	2.1×10 ⁻¹⁵	ev	C C B	18,21
C ⁵⁺ + He → C ⁴⁺ + He ⁺	X	X	(1×10 ⁻¹⁵)	ev	X X C	18,21
C ⁶⁺ + H → C ⁵⁺ + H ⁺	2.4×10 ⁻¹⁸	6.0×10 ⁻¹⁷	1.4×10 ⁻¹⁵	ev	C C B	18,21
C ⁶⁺ + He → C ⁵⁺ + He ⁺	X	X	4.4×10 ⁻¹⁶	ev	X X C	18,21
O ⁺ + H → O + H ⁺	1.5×10 ⁻¹⁵	1.2×10 ⁻¹⁵	9.1×10 ⁻¹⁵	ev	B B B	18,21
O ⁺ + He → O + He ⁺	2.4×10 ⁻¹⁷	3.9×10 ⁻¹⁷	8.0×10 ⁻¹⁷	ev	D D D	18,21
O ²⁺ + H → O ⁺ + H ⁺	8.5×10 ⁻¹⁶	6.4×10 ⁻¹⁶	3.4×10 ⁻¹⁶	ev	D D C	18,21
O ²⁺ + He → O ⁺ + He ⁺	4.6×10 ⁻¹⁶	1.1×10 ⁻¹⁵	1.2×10 ⁻¹⁵	ev	C C C	18,21
O ³⁺ + H → O ²⁺ + H ⁺	6.3×10 ⁻¹⁵	3.7×10 ⁻¹⁵	2.9×10 ⁻¹⁵	ev	C C B	18,21
O ³⁺ + He → O ²⁺ + He ⁺	2.6×10 ⁻¹⁶	1.6×10 ⁻¹⁶	1.6×10 ⁻¹⁶	ev	E E E	18,21
O ⁴⁺ + H → O ³⁺ + H ⁺	1.9×10 ⁻¹⁶	9.6×10 ⁻¹⁶	3.2×10 ⁻¹⁵	ev	C C B	18,21
O ⁴⁺ + He → O ³⁺ + He ⁺	1.8×10 ⁻¹⁶	1.4×10 ⁻¹⁶	3.1×10 ⁻¹⁶	ev	D D D	18,21
O ⁵⁺ + H → O ⁴⁺ + H ⁺	4.0×10 ⁻¹⁵	8.8×10 ⁻¹⁵	4.5×10 ⁻¹⁵	ev,nd	D C B	18,21,30
O ⁵⁺ + He → O ⁴⁺ + He ⁺	X	X	(3×10 ⁻¹⁵)	ev	X X C	18,21
O ⁶⁺ + H → O ⁵⁺ + H ⁺	X	X	3.6×10 ⁻¹⁵	ev	X X B	18,21
O ⁶⁺ + He → O ⁵⁺ + He ⁺	X	X	(9×10 ⁻¹⁶)	ev	X X D	18,21
O ⁷⁺ + H → O ⁶⁺ + H ⁺	X	(5×10 ⁻¹⁵)	5.0×10 ⁻¹⁵	ev	X C B	18,21
O ⁷⁺ + He → O ⁶⁺ + He ⁺	X	X	(9×10 ⁻¹⁶)	ev	X X D	18,21
O ⁸⁺ + H → O ⁷⁺ + H ⁺	X	X	2.0×10 ⁻¹⁵	ev	X X B	18,21
O ⁸⁺ + He → O ⁷⁺ + He ⁺	X	X	(2×10 ⁻¹⁵)	ev	X X D	18,21
Ne ⁺ + He → Ne + He ⁺	X	(5×10 ⁻¹⁹)	(3×10 ⁻¹⁷)	co	X E E	24
Ne ²⁺ + H → Ne ⁺ + H ⁺	X	(2×10 ⁻¹⁷)	5×10 ⁻¹⁷	co,nd	X D D	13,35
Ne ²⁺ + He → Ne ⁺ + He ⁺	4×10 ⁻²⁰	1.4×10 ⁻¹⁷	2.5×10 ⁻¹⁷	co	C B B	24
Ne ²⁺ + He → Ne + He ²⁺	X	X	3.5×10 ⁻¹⁸	co	X X B	24

*Cross sections in parentheses represent an extrapolation or interpolation of existing data.

[#]"ev" denotes evaluated data, "co" denotes data compilation, "sc" denotes scaling formula, "nd" indicates newer data available (reference given).

[&]Accuracy: A+ <3% A <10% B 10-25% C 25-50% D 50-100% E >100%

TABLE I. (cont.)

Reaction	Cross Section (cm ²)*			Status [#]	Accuracy ^{&}	Reference
	E=2 eV/amu	20 eV/amu	200 eV/amu			
Ne ³⁺ + H → Ne ²⁺ + H ⁺	4×10 ⁻¹⁵	(3×10 ⁻¹⁵)	1.8×10 ⁻¹⁵	co,nd	D D C	13,35,36,37,40
Ne ³⁺ + He → Ne ²⁺ + He ⁺	X	(2.2×10 ⁻¹⁶)	1.2×10 ⁻¹⁶	co	X C C	24
Ne ³⁺ + He → Ne ⁺ + He ²⁺	X	X	1.0×10 ⁻¹⁷	co	X X B	24
Ne ⁴⁺ + H → Ne ³⁺ + H ⁺	X	(1×10 ⁻¹⁵)	1.8×10 ⁻¹⁵	co,nd	X D B	13,35,37
Ne ⁴⁺ + He → Ne ³⁺ + He ⁺	X	X	1.7×10 ⁻¹⁵	co	X X B	24
Ne ⁴⁺ + He → Ne ²⁺ + He ²⁺	X	X	8×10 ⁻¹⁷	co	X X C	24
Ne ⁵⁺ + H → Ne ⁴⁺ + H ⁺	X	X	2.5×10 ⁻¹⁵	co,nd	X X C	13,35
Ne ⁵⁺ + He → Ne ⁴⁺ + He ⁺	X	(1×10 ⁻¹⁵)	1.6×10 ⁻¹⁵	co	X C B	24
Ne ⁶⁺ + H → Ne ⁵⁺ + H ⁺	X	X	1.3×10 ⁻¹⁵	nd	X X C	35
Ne ⁶⁺ + He → Ne ⁵⁺ + He ⁺	X	(9×10 ⁻¹⁶)	1.2×10 ⁻¹⁵	co	X C B	24
Ne ⁷⁺ + H → Ne ⁶⁺ + H ⁺	X	X	(3×10 ⁻¹⁵)	nd	X X C	35
Ne ⁷⁺ + He → Ne ⁶⁺ + He ⁺	X	(2×10 ⁻¹⁵)	2×10 ⁻¹⁵	co	X C C	24
Ne ⁸⁺ + H → Ne ⁷⁺ + H ⁺	X	X	(8×10 ⁻¹⁵)	co	X X D	13
Ne ⁸⁺ + He → Ne ⁷⁺ + He ⁺	X	(2×10 ⁻¹⁵)	2×10 ⁻¹⁵	co	X C B	24
Ne ⁹⁺ + H → Ne ⁸⁺ + H ⁺	X	X	7.3×10 ⁻¹⁵	co,nd	X X B	13,39
Ne ¹⁰⁺ + H → Ne ⁹⁺ + H ⁺	X	X	(6×10 ⁻¹⁵)	co,nd	X X C	13,38,39
Al ²⁺ + H → Al ⁺ + H ⁺	X	5×10 ⁻¹⁷	3.5×10 ⁻¹⁶	co	X C C	24
Al ²⁺ + He → Al ⁺ + He ⁺	X	X	2×10 ⁻¹⁶	co	X X E	24
Al ³⁺ + H → Al ²⁺ + H ⁺	X	(1.5×10 ⁻¹⁵)	X	co	X D X	24
Al ³⁺ + He → Al ²⁺ + He ⁺	X	(1×10 ⁻¹⁷)	3×10 ⁻¹⁷	co	X E D	24
Al ³⁺ + He → Al ⁺ + He ²⁺	X	X	(3×10 ⁻¹⁷)	co	X X E	24
Al ⁴⁺ + H → Al ³⁺ + H ⁺	X	(4×10 ⁻¹⁵)	(4×10 ⁻¹⁵)	co	X C C	24
Al ⁴⁺ + He → Al ³⁺ + He ⁺	X	(4×10 ⁻¹⁶)	(2×10 ⁻¹⁵)	co	X E D	24
Al ⁴⁺ + He → Al ²⁺ + He ²⁺	X	X	(4×10 ⁻¹⁶)	co	X X E	24
Al ⁵⁺ + H → Al ⁴⁺ + H ⁺	X	(4×10 ⁻¹⁵)	(4×10 ⁻¹⁵)	co	X C C	24

*Cross sections in parentheses represent an extrapolation or interpolation of existing data.

[#]"ev" denotes evaluated data, "co" denotes data compilation, "sc" denotes scaling formula, "nd" indicates newer data available (reference given).

[&]Accuracy: A+ <3% A <10% B 10-25% C 25-50% D 50-100% E >100%

TABLE I. (cont.)

Reaction	Cross Section (cm ²)*			Status [#]	Accuracy ^{&}	Reference
	E=2 eV/amu	20 eV/amu	200 eV/amu			
Al ⁵⁺ + He → Al ⁴⁺ + He ⁺	X	X	1.2×10 ⁻¹⁵	co	X X B	24
Al ⁵⁺ + He → Al ³⁺ + He ²⁺	X	X	3×10 ⁻¹⁶	co	X X C	24
Al ⁶⁺ + H → Al ⁵⁺ + H ⁺	X	(4×10 ⁻¹⁵)	(4×10 ⁻¹⁵)	co	X C C	24
Al ⁷⁺ + H → Al ⁶⁺ + H ⁺	X	(8×10 ⁻¹⁵)	(8×10 ⁻¹⁵)	co	X C C	24
Al ⁸⁺ + H → Al ⁷⁺ + H ⁺	X	(7×10 ⁻¹⁵)	(7×10 ⁻¹⁵)	co	X C C	24
Al ⁹⁺ + H → Al ⁸⁺ + H ⁺	X	(8×10 ⁻¹⁵)	(8×10 ⁻¹⁵)	co	X C C	24
Al ¹⁰⁺ + H → Al ⁹⁺ + H ⁺	X	(9×10 ⁻¹⁵)	(9×10 ⁻¹⁵)	co	X C C	24
Si ⁴⁺ + He → Si ³⁺ + He ⁺	1.9×10 ⁻¹⁵	1.2×10 ⁻¹⁵	1×10 ⁻¹⁵	co	C C D	24
Ar ⁺ + He → Ar + He ⁺	6×10 ⁻¹⁹	(8×10 ⁻¹⁷)	(2×10 ⁻¹⁶)	co	C E E	24
Ar ²⁺ + H → Ar ⁺ + H ⁺	X	(7×10 ⁻¹⁸)	1.3×10 ⁻¹⁶	co	X D B	13
Ar ²⁺ + He → Ar ⁺ + He ⁺	5×10 ⁻¹⁶	3×10 ⁻¹⁶	4×10 ⁻¹⁶	co	C B B	24
Ar ²⁺ + He → Ar + He ²⁺	X	X	6×10 ⁻¹⁹	co	X X C	24
Ar ³⁺ + H → Ar ²⁺ + H ⁺	X	X	(2.5×10 ⁻¹⁵)	co	X X C	13
Ar ³⁺ + He → Ar ²⁺ + He ⁺	5.5×10 ⁻¹⁷	1.0×10 ⁻¹⁶	5×10 ⁻¹⁶	co	B B C	24
Ar ³⁺ + He → Ar ⁺ + He ²⁺	X	X	3×10 ⁻¹⁸	co	X X C	24
Ar ⁴⁺ + H → Ar ³⁺ + H ⁺	X	(3×10 ⁻¹⁵)	4.0×10 ⁻¹⁵	co	X C B	13
Ar ⁴⁺ + He → Ar ³⁺ + He ⁺	(1×10 ⁻¹⁵)	1.0×10 ⁻¹⁵	8×10 ⁻¹⁶	co	C B B	24
Ar ⁴⁺ + He → Ar ³⁺ + He ²⁺ + e	X	X	(1.2×10 ⁻¹⁷)	co	X X D	24
Ar ⁴⁺ + He → Ar ²⁺ + He ²⁺	X	X	3×10 ⁻¹⁷	co	X X B	24
Ar ⁵⁺ + H → Ar ⁴⁺ + H ⁺	X	X	(4.4×10 ⁻¹⁵)	co	X X C	13
Ar ⁵⁺ + He → Ar ⁴⁺ + He ⁺	X	2.0×10 ⁻¹⁵	1.9×10 ⁻¹⁵	co	X B B	24
Ar ⁵⁺ + He → Ar ⁴⁺ + He ²⁺ + e	X	X	(3×10 ⁻¹⁷)	co	X X D	24
Ar ⁵⁺ + He → Ar ³⁺ + He ²⁺	X	1.4×10 ⁻¹⁶	1.8×10 ⁻¹⁶	co	X C C	24

*Cross sections in parentheses represent an extrapolation or interpolation of existing data.

[#]"ev" denotes evaluated data, "co" denotes data compilation, "sc" denotes scaling formula, "nd" indicates newer data available (reference given).

[&]Accuracy: A+ <3% A <10% B 10-25% C 25-50% D 50-100% E >100%

TABLE I. (cont.)

Reaction	Cross Section (cm ²)*			Status [#]	Accuracy ^{&}	Reference
	E=2 eV/amu	20 eV/amu	200 eV/amu			
Ar ⁶⁺ + H → Ar ⁵⁺ + H ⁺	X	X	4.5×10 ⁻¹⁵	co	X X B	13
Ar ⁶⁺ + He → Ar ⁵⁺ + He ⁺	X	2.0×10 ⁻¹⁵	2.2×10 ⁻¹⁵	co	X B B	24
Ar ⁶⁺ + He → Ar ⁵⁺ + He ²⁺ + e	X	X	(3.5×10 ⁻¹⁷)	co	X X D	24
Ar ⁶⁺ + He → Ar ⁴⁺ + He ²⁺	X	3.5×10 ⁻¹⁶	8×10 ⁻¹⁶	co	X C C	24
Ar ⁷⁺ + H → Ar ⁶⁺ + H ⁺	X	X	5.3×10 ⁻¹⁵	co	X X B	13
Ar ⁷⁺ + He → Ar ⁶⁺ + He ⁺	X	(2×10 ⁻¹⁵)	2×10 ⁻¹⁵	co	X C B	24
Ar ⁷⁺ + He → Ar ⁶⁺ + He ²⁺ + e	X	X	(4×10 ⁻¹⁷)	co	X X D	24
Ar ⁷⁺ + He → Ar ⁵⁺ + He ²⁺	X	2×10 ⁻¹⁶	5×10 ⁻¹⁶	co	X C C	24
Ar ⁸⁺ + He → Ar ⁷⁺ + He ⁺	X	1.5×10 ⁻¹⁵	1.7×10 ⁻¹⁵	co	X C B	24
Ar ⁸⁺ + He → Ar ⁶⁺ + He ²⁺	X	X	4×10 ⁻¹⁶	co	X X C	24
Ar ⁹⁺ + He → Ar ⁸⁺ + He ⁺	X	X	2.1×10 ⁻¹⁵	co	X X B	24
Ar ⁹⁺ + He → Ar ⁷⁺ + He ²⁺	X	X	8×10 ⁻¹⁷	co	X X C	24
Ar ¹⁰⁺ + He → Ar ⁹⁺ + He ⁺	X	(3×10 ⁻¹⁵)	(3×10 ⁻¹⁵)	co	X C C	24
Ti ²⁺ + H → Ti ⁺ + H ⁺	X	X	3.5×10 ⁻¹⁷	co	X X B	13
Fe ²⁺ + He → Fe ⁺ + He ⁺	X	X	(5×10 ⁻¹⁸)	co	X X C	24
Fe ³⁺ + H → Fe ²⁺ + H ⁺	X	4.4×10 ⁻¹⁵	X	co	X B X	13
Fe ³⁺ + He → Fe ²⁺ + He ⁺	X	X	2×10 ⁻¹⁶	co	E E E	24
Fe ⁴⁺ + H → Fe ³⁺ + H ⁺	X	2.1×10 ⁻¹⁵	X	co	X B X	13
Fe ⁵⁺ + H → Fe ⁴⁺ + H ⁺	4.8×10 ⁻¹⁵	4.8×10 ⁻¹⁵	5.0×10 ⁻¹⁵	co,sc	B B B	13,20
Fe ⁵⁺ + He → Fe ⁴⁺ + He ⁺	2.0×10 ⁻¹⁵	1.7×10 ⁻¹⁵	1.5×10 ⁻¹⁵	sc	D D D	20
Fe ⁶⁺ + H → Fe ⁵⁺ + H ⁺	7.3×10 ⁻¹⁵	5.7×10 ⁻¹⁵	5.7×10 ⁻¹⁵	co,sc	D B C	13,20
Fe ⁶⁺ + He → Fe ⁵⁺ + He ⁺	2.4×10 ⁻¹⁵	2.1×10 ⁻¹⁵	1.8×10 ⁻¹⁵	sc	D D D	20
Fe ⁷⁺ + H → Fe ⁶⁺ + H ⁺	8.6×10 ⁻¹⁵	7.0×10 ⁻¹⁵	6.6×10 ⁻¹⁵	co,sc	D B B	13,20
Fe ⁷⁺ + He → Fe ⁶⁺ + He ⁺	2.8×10 ⁻¹⁵	2.5×10 ⁻¹⁵	2.2×10 ⁻¹⁵	sc	D D D	20

*Cross sections in parentheses represent an extrapolation or interpolation of existing data.

[#]"ev" denotes evaluated data, "co" denotes data compilation, "sc" denotes scaling formula, "nd" indicates newer data available (reference given).

[&]Accuracy: A+ <3% A <10% B 10-25% C 25-50% D 50-100% E >100%

TABLE I. (cont.)

Reaction	Cross Section (cm ²)*			Status*	Accuracy ^{&}	Reference
	E=2 eV/amu	20 eV/amu	200 eV/amu			
Fe ⁸⁺ + H → Fe ⁷⁺ + H ⁺	9.8×10 ⁻¹⁵	8.7×10 ⁻¹⁵	7.6×10 ⁻¹⁵	co,sc	D C B	13,20
Fe ⁸⁺ + He → Fe ⁷⁺ + He ⁺	3.2×10 ⁻¹⁵	2.8×10 ⁻¹⁵	2.5×10 ⁻¹⁵	sc	D D D	20
Fe ⁹⁺ + H → Fe ⁸⁺ + H ⁺	1.1×10 ⁻¹⁴	9.8×10 ⁻¹⁵	8.6×10 ⁻¹⁵	co,sc	D C B	13,20
Fe ⁹⁺ + He → Fe ⁸⁺ + He ⁺	3.6×10 ⁻¹⁵	3.2×10 ⁻¹⁵	2.8×10 ⁻¹⁵	sc	D D D	20
Fe ¹⁰⁺ + H → Fe ⁹⁺ + H ⁺	1.2×10 ⁻¹⁴	1.1×10 ⁻¹⁴	9.6×10 ⁻¹⁵	co,sc	D C B	13,20
Fe ¹⁰⁺ + He → Fe ⁹⁺ + He ⁺	4.0×10 ⁻¹⁵	3.5×10 ⁻¹⁵	3.1×10 ⁻¹⁵	sc	D D D	20

*Cross sections in parentheses represent an extrapolation or interpolation of existing data.

"ev" denotes evaluated data, "co" denotes data compilation, "sc" denotes scaling formula, "nd" indicates newer data available (reference given).

[&]Accuracy: A+ <3% A <10% B 10-25% C 25-50% D 50-100% E >100%

Evaluated total cross-section data are available for C^{q+} and O^{q+} ions colliding with H and He atoms [18, 21], and for a number of reactions involving H, He and Li atoms and ions [6, 19]. Total cross-sections for electron capture by heavier impurities (such as partially stripped Fe ions) from H and He have been measured over a wide energy range, and these cross-sections have been well characterized using analytical scaling formulas based on theoretical considerations [20]

$$\sigma(q, E) = \frac{A q \ln(B\sqrt{q}/E)}{1 + CE^2/q + D(E/\sqrt{q})^{4.5}} \quad (1)$$

where σ is the cross-section in cm², q is the initial ionic charge, E is the collision energy in keV/nucleon, and A , B , C and D are adjustable parameters, whose values are given below. Parameters A , B , C and D in Eq. (1):

Target	A	B	C
H	5.967 × 10 ⁻¹⁷	5.870 × 10 ⁵	1.913 × 10 ⁻⁷
H ₂	5.707 × 10 ⁻¹⁷	5.283 × 10 ⁴	7.800 × 10 ⁻⁴
He	1.818 × 10 ⁻¹⁷	1.856 × 10 ⁶	2.753 × 10 ⁻⁴
Target	D	RMS deviation	
H	1.383 × 10 ⁻⁷	13%	
H ₂	2.721 × 10 ⁻⁸	15%	
He	1.370 × 10 ⁻⁹	70%	

These scaling formulas have been shown to be reliable for Fe^{q+} + H collisions to within 20–25% for charge states with $q > 4$, and are estimated to be within 50–80% for Fe^{q+} + He collisions. These same formulas (and cross-section values in Table I) can be used for collisions of other partially stripped heavy ions with H and He, with an estimated accuracy of 50–80% [20].

Charge exchange collisions of impurities with metastable H and He are expected from theoretical considerations to have significantly larger cross-sections than those for ground state atoms, and to populate more highly excited states [26, 27]. Although such processes are important for spectroscopic diagnostics [27], almost no data are available at the low energies relevant to the edge plasma.

Table II contains cross-section data for electron capture into specific quantum states. The criteria for selection of reactions are the same as those for Table I. The data for collisions involving H⁺, He⁺ and He²⁺ are taken primarily from the recent compilation of Barnett [19]. While such state selective data are available for a large number of important reactions, very few cross-section measurements or calculations extend down to the lower energies relevant to the edge plasma. In fact, many of the tabulated cross-sections are based on extrapolations of the available data and have correspondingly large uncertainties.

In contrast, partial cross-sections for populating specific excited product states are available for many charge exchange reactions involving C^{q+} and O^{q+} ions

TABLE II. EDGE PLASMA STATE SELECTIVE CHARGE EXCHANGE CROSS-SECTIONS

Reaction	Cross Section (cm ²)*			Status*	Accuracy ^{&}	Reference
	E=2 eV/amu	20 eV/amu	200 eV/amu			
H ⁺ + H → H(2s) + H ⁺	X	X	(8×10 ⁻²⁰)	ev	X X E	6,19
H ⁺ + H → H(2p) + H ⁺	X	1×10 ⁻¹⁹	3×10 ⁻¹⁸	ev	X E E	6,19
H ⁺ + H(n=2) → H(n=2) + H ⁺	2×10 ⁻¹⁴	1×10 ⁻¹⁴	8×10 ⁻¹⁵	sc	E E E	6
H ⁺ + H(n=3) → H(n=3) + H ⁺	8×10 ⁻¹⁴	6×10 ⁻¹⁴	4×10 ⁻¹⁴	sc	E E E	6
H ⁺ + He → H(2p) + He ⁺	X	X	(1×10 ⁻²¹)	ev	X X E	19
H ⁺ + He → H(3s) + He ⁺	X	X	(4×10 ⁻²⁰)	ev	X X E	19
H ⁺ + He → H(3p) + He ⁺	X	X	(2×10 ⁻²⁰)	ev	X X E	19
H ⁺ + Li → H(2s) + Li ⁺	X	X	(2×10 ⁻¹⁶)	ev	X X E	19
H ⁺ + Li → H(2p) + Li ⁺	X	X	(4×10 ⁻¹⁶)	ev	X X E	19
He ⁺ + H → He(1s2s) + H ⁺	X	X	2.5×10 ⁻¹⁷	nd	X X C	42
He ⁺ + He → He(m) + He ⁺	X	3×10 ⁻¹⁹	3×10 ⁻¹⁸	ev	X C C	19
He ⁺ + He → He(2 ¹ P) + He ⁺	X	X	(1×10 ⁻¹⁸)	ev	X X E	19
He ⁺ + He → He(3 ¹ P) + He ⁺	X	X	(2×10 ⁻¹⁹)	ev	X X E	19
He ⁺ + He → He(3 ³ P) + He ⁺	X	X	2×10 ⁻¹⁹	ev	X X C	19
He ⁺ + He → He(3 ³ D) + He ⁺	X	X	1.3×10 ⁻¹⁸	ev	X X C	19
He ⁺ + He → He(4 ³ S) + He ⁺	X	X	(5×10 ⁻²⁰)	ev	X X E	19
He ⁺ + He → He(4 ³ P) + He ⁺	X	X	3×10 ⁻²⁰	ev	X X C	19
He ⁺ + He → He(4 ³ D) + He ⁺	X	X	2.5×10 ⁻¹⁹	ev	X X C	19
He ²⁺ + H → He ⁺ (2s) + H ⁺	X	(5×10 ⁻²⁴)	5.2×10 ⁻¹⁹	ev	X E E	19
He ²⁺ + H → He ⁺ (2p) + H ⁺	X	X	(1.4×10 ⁻¹⁷)	ev	X X D	19
He ²⁺ + He → He ⁺ (2s) + H ⁺	X	X	(2×10 ⁻¹⁸)	ev	X X E	19
He ²⁺ + Li → He ⁺ (3p) + He ⁺	X	X	(7×10 ⁻¹⁵)	ev	X X C	19,24
He ²⁺ + Li → He ⁺ (4p) + He ⁺	X	X	(1×10 ⁻¹⁶)	ev	X X E	19
Be ⁴⁺ + H → Be ³⁺ (n=2) + H ⁺	X	X	4×10 ⁻¹⁷	nd	X X C	43
Be ⁴⁺ + H → Be ³⁺ (n=3) + H ⁺	X	X	2.0×10 ⁻¹⁵	nd	X X C	43
B ⁵⁺ + H → B ⁴⁺ (n=3) + H ⁺	X	X	3.0×10 ⁻¹⁶	nd	X X C	43
B ⁵⁺ + H → B ⁴⁺ (n=4) + H ⁺	X	X	9.5×10 ⁻¹⁶	nd	X X C	43
B ⁵⁺ + H → B ⁴⁺ (n=5) + H ⁺	X	X	1×10 ⁻¹⁷	nd	X X C	43
C ²⁺ + H → C ⁺ (2s ² 2p ² P) + H ⁺	5×10 ⁻¹⁹	X	X	co	E X X	11
C ²⁺ + H → C ⁺ (2s2p ² D) + H ⁺	3×10 ⁻²⁴	X	X	co	E X X	11

*Cross sections in parentheses represent an extrapolation or interpolation of existing data.

[#]"ev" denotes evaluated data, "co" denotes data compilation, "sc" denotes scaling formula, "nd" indicates newer data available (reference given).

[&]Accuracy: A+ <3% A <10% B 10-25% C 25-50% D 50-100% E >100%

TABLE II. (cont.)

Reaction	Cross Section (cm ²)*			Status [#]	Accuracy ^{&}	Reference
	E=2 eV/amu	20 eV/amu	200 eV/amu			
C ³⁺ + H → C ²⁺ (2s3s ³ S) + H ⁺	2×10 ⁻¹⁵	8×10 ⁻¹⁶	3×10 ⁻¹⁶	co,nd	D C B	11,31,32
C ³⁺ + H → C ²⁺ (2p ² 1S) + H ⁺	2×10 ⁻¹⁶	3×10 ⁻¹⁶	1.8×10 ⁻¹⁶	co,nd	D C B	11,32
C ³⁺ + H → C ²⁺ (2s3p) + H ⁺	5×10 ⁻¹⁸	2×10 ⁻¹⁷	3×10 ⁻¹⁷	co,nd	E D C	11,31,32
C ³⁺ + H → C ²⁺ (2s3d) + H ⁺	X	X	3×10 ⁻¹⁷	co,nd	X X C	11,32
C ⁴⁺ + H → C ³⁺ (3s) + H ⁺	X	X	4×10 ⁻¹⁶	co,nd	X X C	11,33,34
C ⁴⁺ + H → C ³⁺ (3p) + H ⁺	2×10 ⁻¹⁷	9×10 ⁻¹⁶	3×10 ⁻¹⁵	co,nd	E D C	11,33,34
C ⁴⁺ + H → C ³⁺ (3d) + H ⁺	X	5×10 ⁻¹⁶	3×10 ⁻¹⁶	co,nd	X D C	11,33,34
C ⁶⁺ + H → C ⁵⁺ (4s) + H ⁺	X	1×10 ⁻¹⁷	1×10 ⁻¹⁶	co,nd	X D D	11,33
C ⁶⁺ + H → C ⁵⁺ (4p) + H ⁺	X	(4×10 ⁻¹⁷)	3×10 ⁻¹⁶	co,nd	X E D	11,33
C ⁶⁺ + H → C ⁵⁺ (4d) + H ⁺	(1×10 ⁻¹⁸)	3×10 ⁻¹⁷	4×10 ⁻¹⁶	co,nd	E D C	11,33
C ⁶⁺ + H → C ⁵⁺ (4f) + H ⁺	X	3×10 ⁻¹⁷	9×10 ⁻¹⁶	co,nd	X E C	11,33
C ⁶⁺ + He → C ⁵⁺ (3s) + He ⁺	X	X	1.5×10 ⁻¹⁶	co	X X C	11
C ⁶⁺ + He → C ⁵⁺ (3p) + He ⁺	X	X	1×10 ⁻¹⁶	co	X X C	11
C ⁶⁺ + He → C ⁵⁺ (3d) + He ⁺	X	X	3×10 ⁻¹⁶	co	X X E	11
O ²⁺ + H → O ⁺ (2s2p ⁴ P) + H ⁺	8×10 ⁻¹⁶	(8×10 ⁻¹⁶)	X	co	D D X	11
O ²⁺ + He → O ⁺ (2p ³ 2D) + He ⁺	2×10 ⁻¹⁷	2×10 ⁻¹⁶	3×10 ⁻¹⁶	co	D D D	11,24
O ²⁺ + He → O ⁺ (2p ³ 2P) + He ⁺	8×10 ⁻¹⁶	1.1×10 ⁻¹⁵	8×10 ⁻¹⁶	co	C C C	11,24
O ³⁺ + H → O ²⁺ (2p3p ³ D) + H ⁺	4×10 ⁻¹⁶	2.5×10 ⁻¹⁶	1.4×10 ⁻¹⁶	co	D D X	11
O ³⁺ + H → O ²⁺ (2p3p ¹ P) + H ⁺	9×10 ⁻¹⁶	9×10 ⁻¹⁶	4×10 ⁻¹⁶	co	C C C	11
O ³⁺ + H → O ²⁺ (2p3p ³ S) + H ⁺	2×10 ⁻¹⁶	2×10 ⁻¹⁶	2×10 ⁻¹⁶	co	E E E	11
O ³⁺ + H → O ²⁺ (2p3s ¹ P) + H ⁺	2×10 ⁻¹⁷	1×10 ⁻¹⁶	2×10 ⁻¹⁶	co	D D D	11
O ³⁺ + H → O ²⁺ (2p3s ³ P) + H ⁺	2×10 ⁻¹⁷	X	X	co	D D D	11
O ⁶⁺ + H → O ⁵⁺ (4s) + H ⁺	X	X	4×10 ⁻¹⁶	co,nd	X X D	11,33
O ⁶⁺ + H → O ⁵⁺ (4p) + H ⁺	X	X	1.7×10 ⁻¹⁶	co,nd	X X D	11,33
O ⁶⁺ + H → O ⁵⁺ (4d) + H ⁺	X	X	9×10 ⁻¹⁶	co,nd	X X E	11,33
O ⁶⁺ + H → O ⁵⁺ (4f) + H ⁺	X	X	1.2×10 ⁻¹⁵	co,nd	X X C	11,33
O ⁶⁺ + He → O ⁵⁺ (3s) + He ⁺	X	X	8×10 ⁻¹⁶	co	X X D	11
O ⁶⁺ + He → O ⁵⁺ (3p) + He ⁺	X	X	2×10 ⁻¹⁶	co	X X E	11
O ⁶⁺ + He → O ⁵⁺ (3d) + He ⁺	X	X	4×10 ⁻¹⁶	co	X X E	11
O ⁸⁺ + H → O ⁷⁺ (5s) + H ⁺	X	X	1.2×10 ⁻¹⁶	co	X X C	11

*Cross sections in parentheses represent an extrapolation or interpolation of existing data.

[#]"ev" denotes evaluated data, "co" denotes data compilation, "sc" denotes scaling formula, "nd" indicates newer data available (reference given).

[&]Accuracy: A+ <3% A <10% B 10-25% C 25-50% D 50-100% E >100%

TABLE II. (cont.)

Reaction	Cross Section (cm ²)*			Status*	Accuracy ^{&}	Reference
	E=2 eV/amu	20 eV/amu	200 eV/amu			
O ⁸⁺ + H → O ⁷⁺ (5p) + H ⁺	X	X	4×10 ⁻¹⁶	co	X X C	11
O ⁸⁺ + H → O ⁷⁺ (5d) + H ⁺	X	X	4×10 ⁻¹⁶	co	X X C	11
O ⁸⁺ + H → O ⁷⁺ (5f) + H ⁺	X	X	4×10 ⁻¹⁶	co	X X C	11
O ⁸⁺ + H → O ⁷⁺ (5g) + H ⁺	X	X	1×10 ⁻¹⁵	co	X X D	11
Ne ³⁺ + H → Ne ²⁺ (3s) + H ⁺	1×10 ⁻¹⁵	1×10 ⁻¹⁵	2.7×10 ⁻¹⁶	nd	D D B	36,37,40
Ne ³⁺ + H → Ne ²⁺ (3p) + H ⁺	3×10 ⁻¹⁵	2×10 ⁻¹⁵	1.5×10 ⁻¹⁵	nd	D D B	36,37,40
Ne ⁴⁺ + H → Ne ³⁺ (3p) + H ⁺	X	X	2×10 ⁻¹⁶	nd	X X C	37,41
Ne ⁴⁺ + H → Ne ³⁺ (3d) + H ⁺	X	X	1.6×10 ⁻¹⁵	nd	X X C	37,41
Ne ⁵⁺ + H → Ne ⁴⁺ (4s ³ P) + H ⁺	X	X	(5×10 ⁻¹⁶)	nd	X X C	41
Ne ⁵⁺ + H → Ne ⁴⁺ (4s ¹ P) + H ⁺	X	X	(2.0×10 ⁻¹⁵)	nd	X X C	41
Ne ⁶⁺ + H → Ne ⁵⁺ (4s) + H ⁺	X	X	(1.0×10 ⁻¹⁵)	nd	X X C	41
Ne ⁶⁺ + H → Ne ⁵⁺ (4p,4d) + H ⁺	X	X	(3×10 ⁻¹⁶)	nd	X X C	41
Ne ⁷⁺ + H → Ne ⁶⁺ (5s,5p) + H ⁺	X	X	1.6×10 ⁻¹⁵	nd	X X C	41
Ne ⁷⁺ + H → Ne ⁶⁺ (5d) + H ⁺	X	X	1.4×10 ⁻¹⁵	nd	X X C	41
Si ⁴⁺ + He → Si ³⁺ (3s) + He ⁺	8×10 ⁻²⁰	5×10 ⁻¹⁷	6×10 ⁻¹⁶	co	C C C	24
Ar ³⁺ + He → Ar ²⁺ (3p ³ 4s) + He ⁺	X	X	3.5×10 ⁻¹⁶	co	X X C	24
Ar ³⁺ + He → Ar ²⁺ (3p ⁴) + He ⁺	X	X	1×10 ⁻¹⁶	co	X X C	24
Ar ³⁺ + He → Ar ²⁺ (3s3p ⁵) + He ⁺	X	X	5×10 ⁻¹⁷	co	X X C	24
Ar ⁴⁺ + H → Ar ³⁺ (4s) + H ⁺	X	X	3×10 ⁻¹⁶	nd	X X C	37,41
Ar ⁴⁺ + H → Ar ³⁺ (4p) + H ⁺	X	2×10 ⁻¹⁶	3.5×10 ⁻¹⁵	nd	X D C	37,41
Ar ⁴⁺ + H → Ar ³⁺ (3d) + H ⁺	X	X	(1×10 ⁻¹⁶)	nd	X X C	37,41
Ar ⁵⁺ + H → Ar ⁴⁺ (4p) + H ⁺	X	X	4.5×10 ⁻¹⁶	nd	X X C	37,41
Ar ⁵⁺ + H → Ar ⁴⁺ (4d) + H ⁺	X	X	1.6×10 ⁻¹⁵	nd	X X C	37,41
Ar ⁵⁺ + H → Ar ⁴⁺ (4f) + H ⁺	X	X	1.0×10 ⁻¹⁵	nd	X X C	37,41
Ar ⁵⁺ + He → Ar ⁴⁺ (3p4s) + He ⁺	X	X	3×10 ⁻¹⁶	co	X X C	24
Ar ⁶⁺ + H → Ar ⁵⁺ (4f) + H ⁺	X	X	(1.0×10 ⁻¹⁵)	nd	X X C	41

*Cross sections in parentheses represent an extrapolation or interpolation of existing data.

#"ev" denotes evaluated data, "co" denotes data compilation, "sc" denotes scaling formula, "nd" indicates newer data available (reference given).

&Accuracy: A+ <3% A <10% B 10-25% C 25-50% D 50-100% E >100%

TABLE II. (cont.)

Reaction	Cross Section (cm ²)*			Status [#]	Accuracy ^{&}	Reference
	E=2 eV/amu	20 eV/amu	200 eV/amu			
Ar ⁶⁺ + H → Ar ⁵⁺ (5s) + H ⁺	X	X	(1.3×10 ⁻¹⁵)	nd	X X C	41
Ar ⁶⁺ + H → Ar ⁵⁺ (5p) + H ⁺	X	X	(1.9×10 ⁻¹⁵)	nd	X X C	41
Ar ⁶⁺ + H → Ar ⁵⁺ (5d) + H ⁺	X	X	(8×10 ⁻¹⁶)	nd	X X C	41
Ar ⁶⁺ + He → Ar ⁵⁺ (3d) + He ⁺	X	X	2.8×10 ⁻¹⁶	co	X X C	24
Ar ⁶⁺ + He → Ar ⁵⁺ (4s) + He ⁺	X	1×10 ⁻¹⁵	1.1×10 ⁻¹⁵	co	X B B	24
Ar ⁶⁺ + He → Ar ⁵⁺ (4p) + He ⁺	X	1.2×10 ⁻¹⁵	1.0×10 ⁻¹⁵	co	X C B	24
Ar ⁷⁺ + H → Ar ⁶⁺ (5p) + H ⁺	X	X	(1.0×10 ⁻¹⁵)	nd	X X C	41
Ar ⁷⁺ + H → Ar ⁶⁺ (5d) + H ⁺	X	X	(3.6×10 ⁻¹⁵)	nd	X X C	41
Ar ⁷⁺ + H → Ar ⁶⁺ (5f) + H ⁺	X	X	(7×10 ⁻¹⁶)	nd	X X C	41
Ar ⁸⁺ + H → Ar ⁷⁺ (5d,5f) + H ⁺	X	X	(5×10 ⁻¹⁶)	nd	X X C	41
Ar ⁸⁺ + H → Ar ⁷⁺ (6s,6p) + H ⁺	X	X	(6×10 ⁻¹⁵)	nd	X X C	41
Ar ⁸⁺ + He → Ar ⁷⁺ (4d) + He ⁺	X	6.4×10 ⁻¹⁶	5.4×10 ⁻¹⁶	co	X C C	24
Ar ⁸⁺ + He → Ar ⁷⁺ (4f) + He ⁺	X	2.3×10 ⁻¹⁵	1.9×10 ⁻¹⁵	co	X C C	24

*Cross sections in parentheses represent an extrapolation or interpolation of existing data.

[#]"ev" denotes evaluated data, "co" denotes data compilation, "sc" denotes scaling formula, "nd" indicates newer data available (reference given).

[&]Accuracy: A+ <3% A <10% B 10-25% C 25-50% D 50-100% E >100%

[11], although, for most reactions, only theoretical data are available at energies below 1 keV/amu. Some significant discrepancies exist between the different coupled state calculations, especially for the non-dominant reaction channels, where the choice of an atomic or molecular set of basis functions has a significant effect on the predicted cross-section. The accuracies listed in Table II reflect such discrepancies and also the level of consistency with experimental data, where available (usually at somewhat higher energies). The latter are based on both optical and translational energy spectroscopy techniques. Experimental and theoretical data were reviewed in 1985 by Janev and Winter [26], and data for C^{q+} and O^{q+} colliding with H, H₂ and He were compiled in 1987 by Tawara [11]. More recent results are contained in the topical report on carbon and oxygen collision data [25]. Extensive compilations of both total and state selective charge exchange cross-section data for collisions of all atoms and ions with helium were published recently [24]. The state selective data for Ar^{q+} + He have been taken from this compilation; the data for

Ne^{q+} + H and Ar^{q+} + H collisions have been taken directly from the literature.

5. EXCITATION AND IONIZATION COLLISIONS

Ion impact excitation and ionization are endothermic processes, and few data are available for these reactions at the collision energies relevant to the plasma edge. However, the corresponding cross-sections also decrease rapidly with decreasing collision energy below several keV/amu and become negligibly small at edge relevant energies. Cross-sections for electron impact excitation, on the other hand, tend to be largest at electron energies in the range 10–100 eV. Thus, direct electronic excitation occurs predominantly by electron impact in the edge plasma [1, 8].

Evaluated data for a number of impact excitation reactions involving H, He and Li atoms and ions are included in the recent compilation of Barnett [19]. However, only a small fraction of the ion-atom

TABLE III. EDGE PLASMA ION-ATOM EXCITATION CROSS-SECTIONS

Reaction	Cross Section (cm ²)* E=200 eV/amu	Status [#]	Accuracy ^{&}	Reference
H ⁺ + He(1 ¹ S) → H ⁺ + He(2 ¹ P)	3×10 ⁻¹⁹	sc	E	6
H ⁺ + Li(2s) → H ⁺ + Li(2p)	(6×10 ⁻¹⁶)	ev	E	19
He ⁺ + H(1s) → He ⁺ + H(2p)	2.2×10 ⁻¹⁷	ev	C	19
He ⁺ + He(1 ¹ S) → He ⁺ + He(3 ³ P)	(2.2×10 ⁻¹⁹)	ev	E	19
He ⁺ + He(1 ¹ S) → He ⁺ + He(3 ³ D)	(1.6×10 ⁻¹⁸)	ev	E	19
He ⁺ + He(1 ¹ S) → He ⁺ + He(4 ¹ S)	(3×10 ⁻²¹)	ev	E	19
He ⁺ + He(1 ¹ S) → He ⁺ + He(4 ¹ D)	(8×10 ⁻²⁰)	ev	E	19
He ⁺ + He(1 ¹ S) → He ⁺ + He(4 ³ P)	(2×10 ⁻²⁰)	ev	E	19
He ⁺ + He(1 ¹ S) → He ⁺ + He(4 ³ D)	(3×10 ⁻¹⁹)	ev	E	19
He ⁺ + Li(2s) → He ⁺ + Li(2p)	(2×10 ⁻¹⁶)	ev	D	19
He ²⁺ + Li(2s) → He ²⁺ + Li(2p)	6.4×10 ⁻¹⁷	sc	E	19

*Cross sections in parentheses represent an extrapolation or interpolation of existing data.

[#]"ev" denotes evaluated data, "co" denotes data compilation, "sc" denotes scaling formula, "nd" indicates newer data available (reference given).

[&]Accuracy: A+ <3% A <10% B 10-25% C 25-50% D 50-100% E >100%

excitation cross-sections extend to collision energies below 1 keV/amu. These are summarized in Table III, where most of the cross-section values result from some extrapolation of the existing data and therefore have large uncertainties. As noted above, these cross-sections are in general relatively small ($< 10^{-18}$ cm²) at these low energies. Janev et al. [6] have systematically applied analytical scaling formulas based on theoretical considerations in order to estimate cross-sections and rate coefficients at the lowest energies for a large number of reactions occurring in H-He plasmas. These are included in Table III when they are consistent with the evaluated data at higher energies. No reliable data were found for ionization by heavy particle impact at energies relevant to the edge plasma, except for detachment from negative ions, which is considered in Section 6.

6. DETACHMENT AND ASSOCIATION COLLISIONS

The presence and role of negative ions in the plasma edge have yet to be determined. Collisional electron detachment from negative ions is an endoergic process,

but the binding energies (electron affinities) are often sufficiently small that cross-sections are still appreciable (and measurable) at collision energies relevant to the edge plasma. Associative detachment collisions of negative ions with neutral atoms are characterized by large cross-sections, which may increase with decreasing collision energy. Data for these two processes are collected in Table IV.

7. SUMMARY

It is clear from the present survey and analysis that charge exchange reactions are by far the dominant ion-atom collision processes in the plasma edge. While some experimental and/or theoretical data are available for most important charge exchange reactions between primary plasma constituents (H and He atoms and ions), only in a relatively few cases do these data extend to the lower energies relevant to the plasma edge. Therefore, much of the needed data must be estimated by extrapolation or by use of scaling formulas and, thus, these data have large uncertainties.

TABLE IV. EDGE PLASMA DETACHMENT AND ASSOCIATION CROSS-SECTIONS

Reaction	Cross Section (cm ²)*			Status*	Accuracy ^{&}	Reference
	E=2 eV/amu	20 eV/amu	200 eV/amu			
H ⁻ + H → H + H + e	4×10 ⁻¹⁶	1.3×10 ⁻¹⁵	1.3×10 ⁻¹⁵	ev	C	6,19
H ⁻ + He → H + He + e	1.3×10 ⁻¹⁶	3.2×10 ⁻¹⁶	4.5×10 ⁻¹⁶	ev	B	19
H ⁻ + H → H ₂ + e	9×10 ⁻¹⁶	5.6×10 ⁻¹⁶	3.8×10 ⁻¹⁶	ev	C	6
He ⁻ + He → He + He + e	X	X	1.3×10 ⁻¹⁵	ev	B	19
Li ⁻ + He → Li + He + e	X	X	4.6×10 ⁻¹⁶	ev	B	19
O ⁻ + He → O + He + e	X	X	5.5×10 ⁻¹⁶	co	B	44

*Cross sections in parentheses represent an extrapolation or interpolation of existing data.

#"ev" denotes evaluated data, "co" denotes data compilation, "sc" denotes scaling formula, "nd" indicates newer data available (reference given).

[&]Accuracy: A+ <3% A <10% B 10-25% C 25-50% D 50-100% E >100%

The relevant database for charge exchange collisions involving C and O impurity ions is more complete; this is due to a strong research emphasis on collisions of highly charged ions during the past decade. Total cross-section data are available for almost all reactions, and state selective data are available for some, at least at the higher energies prevailing in the edge region. Total and state selective electron capture cross-section data are also available for most reactions of Ne^{q+} and Ar^{q+} ions with H and He, although usually not at the lower energies relevant to the edge region. Estimates of total electron capture cross-sections for heavier impurity ions such as iron are available from scaling formulas, but they are reliable only for charge states with $q > 4$. State selective data for such processes are virtually non-existent at the relevant energies.

Data for direct excitation in ion-atom collisions are extremely sparse at edge relevant energies, and are virtually non-existent for ionization. These processes are, however, of lesser importance in the edge, because the cross-sections become very small ($< 10^{-17}$ cm²) at such low energies, at least for the lower ion charge states colliding with ground state atoms. Some data are available for electron detachment from negative ions, which may have an appreciable cross-section at low energies. The presence and role of negative ions in the plasma edge have yet to be ascertained.

ACKNOWLEDGEMENTS

The author is grateful to Dr. R.K. Janev for valuable comments on this manuscript, as well as to participants of the IAEA Specialists Meeting on the Review of the Status of Atomic and Molecular Data for Fusion Edge Plasma Studies, September 1989, for valuable discussions which motivated the present survey. The author is also indebted to many colleagues for preparing the comprehensive data compilations cited in the References which served as convenient sources of much of the data presented in this survey.

This work was sponsored by the Office of Fusion Energy of the United States Department of Energy, under Contract No. DE-AC05-84OR21400 with Martin Marietta Energy Systems, Inc.

REFERENCES

- [1] HARRISON, M.F.A., in *Physics of Plasma-Wall Interactions in Controlled Fusion* (POST, D.E., BEHRISCH, R., Eds), Plenum Press, New York (1986) 281.
- [2] STANGEBY, P.C., McCracken, G.M., *Nucl. Fusion* **30** (1990) 1225.
- [3] CRANDALL, D.H., *Nucl. Instrum. Methods Phys. Res., Sect. B* **27** (1987) 475.

- [4] HEIFETZ, D.M., in *Physics of Plasma-Wall Interactions in Controlled Fusion* (POST, D.E., BEHRISCH, R., Eds), Plenum Press, New York (1986) 695.
- [5] JANEV, R.K., POST, D.E., LANGER, W.D., EVANS, K., HEIFETZ, D.B., WEISHEIT, J.C., *J. Nucl. Mater.* **121** (1984) 10.
- [6] JANEV, R.K., LANGER, W.D., EVANS, K., Jr., POST, D.E., Jr., *Elementary Processes in Hydrogen-Helium Plasmas*, Springer Series on Atoms and Plasmas, Vol. 4, Springer-Verlag, Heidelberg (1987).
- [7] TAWARA, H., PHANEUF, R.A., *Comments At. Mol. Phys.* **21** (1988) 177.
- [8] JANEV, R.K., HARRISON, M.F.A., DRAWIN, H.W., *Nucl. Fusion* **29** (1989) 109.
- [9] JANEV, R.K., KATSONIS, K., *Nucl. Fusion* **27** (1987) 1493.
- [10] TAWARA, H., ITIKAWA, Y., ITOH, Y., et al., *Atomic Data Involving Hydrogens Relevant to Edge Plasmas*, Rep. IPPJ-AM-46, Institute of Plasma Physics, Nagoya University, Nagoya (1986).
- [11] TAWARA, H., *Total and Partial Cross Sections for Electron Capture for C^{9+} ($q = 6-2$) and O^{9+} ($q = 8-2$) Ions in Collisions with H, H_2 and He Atoms*, Rep. IPPJ-AM-56, Institute of Plasma Physics, Nagoya University, Nagoya (1987).
- [12] TAWARA, H., KATO, T., NAKAI, Y., *Cross Sections for Charge Transfers of Highly Ionized Ions in Hydrogen Atoms*, Rep. IPPJ-AM-30, Institute of Plasma Physics, Nagoya University, Nagoya (1983).
- [13] TAWARA, H., KATO, T., NAKAI, Y., *At. Data Nucl. Data Tables* **32** (1985) 235.
- [14] NAKAI, Y., SHIRAI, T., TABATA, T., ITO, R., *At. Data Nucl. Data Tables* **37** (1987) 69.
- [15] NAKAI, Y., KIKUCHI, A., SHIRAI, T., SATAKA, M., *Data on Collisions of Helium Atoms and Ions with Atoms and Molecules: Cross Sections for Charge Transfer of He^{2+} , He^+ , He and He^- with He, Ne, Ar, Kr and Xe*, Rep. JAERI-M 84-069, Japan Atomic Energy Research Institute, Tokyo (1984).
- [16] NAKAI, Y., KIKUCHI, A., SHIRAI, T., SATAKA, M., *Data on Collisions of Hydrogen Atoms and Ions with Atoms and Molecules: Cross Sections for Charge Transfer of H, H^+ and H^- with He, Ne, Ar, Kr and Xe*, Rep. JAERI-M 83-143, Japan Atomic Energy Research Institute, Tokyo (1983).
- [17] SATAKA, M., SHIRAI, T., KIKUCHI, A., NAKAI, Y., *Ionization Cross Section for Ion-Atom and Ion-Molecule Collisions: Ionization Cross Sections for H^+ , H_2^+ , He^+ and He^{++} incident on H, H_2 and He*, Rep. JAERI-M 9310, Japan Atomic Energy Research Institute, Tokyo (1981).
- [18] PHANEUF, R.A., JANEV, R.K., PINDZOLA, M.S., *Collisions of Carbon and Oxygen Ions with Electrons, H, H_2 and He*, *Atomic Data for Fusion*, Vol. 5, Rep. ORNL-6090, Oak Ridge National Laboratory, Oak Ridge, TN (1987).
- [19] BARNETT, C.F., *Collisions of H, H_2 , He and Li Atoms and Ions with Atoms and Molecules*, *Atomic Data for Fusion*, Vol. 1, Rep. ORNL-6086, Oak Ridge National Laboratory, Oak Ridge, TN (1990).
- [20] PHANEUF, R.A., JANEV, R.K., HUNTER, H.T., in *Recommended Data on Atomic Collision Processes Involving Iron and its Ions*, *Nucl. Fusion Special Supplement* (1987) 7.
- [21] JANEV, R.K., PHANEUF, R.A., HUNTER, H.T., *At. Data Nucl. Data Tables* **40** (1988) 249.
- [22] BARNETT, C.F., RAY, J.A., RICCI, E., WILKER, M.I., GILBODY, H.B., *Atomic Data for Controlled Fusion Research*, Rep. ORNL-5206, Oak Ridge National Laboratory, Oak Ridge, TN (1977).
- [23] JANEV, R.K., GALLAGHER, J.W., BRANSDEN, B.H., *Evaluated Theoretical Cross-Section Data for Charge Exchange of Multiply Charged Ions with Atoms*, Rep. No. 25, JILA Information Center, Univ. of Colorado, Boulder, CO (1984); see also *J. Phys. Chem. Ref. Data* **12** (1983) 829; **12** (1983) 873; **13** (1984) 1199.
- [24] WU, W.K., HUBER, B.A., WIESEMANN, K., *At. Data Nucl. Data Tables* **40** (1988) 57; **42** (1989) 157.
- [25] JANEV, R.K. (Ed.), *Carbon and Oxygen Collision Data for Fusion Plasma Research*, *Phys. Scr.* **T28** (1989) (Proc. IAEA Top. Mtg Vienna, 1988).
- [26] JANEV, R.K., WINTER, H., *Phys. Rep.* **117** (1985) 265.
- [27] ISLER, R.C., OLSON, R.E., *Phys. Rev.*, A **37** (1988) 3399.
- [28] TABATA, T., ITO, R., NAKAI, Y., SHIRAI, T., SATAKA, M., SUGUIRA, T., *Nucl. Instrum. Methods Phys. Res., Sect. B* **31** (1988) 375.
- [29] MARTINEZ, H., CISNEROS, C., de URQUIJO, J., ALVAREZ, I., *Phys. Rev.*, A **38** (1988) 5914.
- [30] HAVENER, C.C., HUQ, M.S., KRAUSE, H.F., SCHULZ, P.A., PHANEUF, R.A., *Phys. Rev.*, A **39** (1989) 1725.
- [31] WILKIE, F.G., McCULLOUGH, R.W., GILBODY, H.B., *J. Phys.*, B **19** (1986) 239.
- [32] OPRADOLCE, L., BENMEURAIEM, L., MCCARROLL, R., PIACENTINI, R.D., *J. Phys.*, B **21** (1988) 503.
- [33] HAREL, C., JOUIN, H., *J. Phys.*, B **21** (1988) 859.
- [34] BAPTIST, R., BONNET, J.J., BONNEFOY, M., et al., *Nucl. Instrum. Methods Phys. Res., Sect. B* **23** (1987) 123.
- [35] CAN, C., GRAY, T.J., VARGHESE, S.L., HALL, J.M., TUNNELL, L.N., *Phys. Rev.*, A **31** (1985) 72.
- [36] HEIL, T.G., BUTLER, S.E., DALGARNO, A., *Phys. Rev.*, A **27** (1983) 2365.
- [37] AFROSIMOV, V.V., BARASH, D.F., BASALAEV, A.A., LOZHKIN, K.O., PANOV, M.N., in *Physics of Electronic and Atomic Collisions* (Proc. 15th Int. Conf. Brighton, 1987); *Abstracts of Contributed Papers*, Queen's University, Belfast (1987) 533.
- [38] BENDAHMAN, M., BLIMAN, S., DOUSSON, S., et al., *J. Phys. (Paris)* **46** (1985) 561.
- [39] MEYER, F.W., HOWALD, A.M., HAVENER, C.C., PHANEUF, R.A., *Phys. Rev.*, A **32** (1985) 3310.
- [40] WILSON, S.M., McCULLOUGH, R.W., GILBODY, H.B., *J. Phys.*, B **21** (1988) 1027.
- [41] GIESE, J.P., COCKE, C.L., WAGGONER, W., TUNNELL, L.N., VARGHESE, S.L., *Phys. Rev.*, A **34** (1986) 3770.
- [42] ERREA, L.F., MENDEZ, L., RIERA, A., *Z. Phys.*, D **14** (1989) 229.
- [43] FRITSCH, W., LIN, C.D., *Phys. Rev.*, A **29** (1984) 3039.
- [44] RAHMAN, F., HIRD, B., *At. Data Nucl. Data Tables* **35** (1986) 123.

EXTENDED SCALING OF CROSS-SECTIONS FOR THE IONIZATION OF H, H₂ AND He BY MULTIPLY CHARGED IONS

T. TABATA, R. ITO
Research Institute for Advanced
Science and Technology,
University of Osaka Prefecture,
Sakai, Osaka,
Japan

T. SHIRAI, Y. NAKAI*
Tokai Research Establishment,
Japan Atomic Energy Research Institute,
Tokai-mura, Ibaraki-ken,
Japan

H.T. HUNTER, R.A. PHANEUF
Oak Ridge National Laboratory,
Oak Ridge, Tennessee,
United States of America

ABSTRACT. An analytic cross-section formula is given for the impact ionization of H, H₂ and He by multiply charged ions. The formula is expressed as a modified Bethe cross-section for ionization by protons, multiplied by the square of the ionic charge and an analytic scaling factor. This scaling factor behaves as E^ν at low energies, where E represents the projectile energy and ν is approximately equal to 0.9. The values of adjustable parameters in the formula were determined by least squares fits to the experimental data collected from the literature. The lowest projectile energy of the available data is 6 keV/amu and the root mean square deviation of all data from the analytic formula is 21%.

1. INTRODUCTION

Knowledge of the cross-sections for the impact ionization of H, H₂ and He by multiply charged ions is important in thermonuclear fusion research. Janev et al. [1] provided recommended values of the cross-sections for the incident ions of C^{q+} and O^{q+} ($1 \leq q \leq Z$, where Z is the atomic number) as well as Chebyshev polynomial fits to these data. The ranges to which these fits are applicable, defined by the minimum energy E_{\min} and the maximum energy E_{\max} , are as follows: $E_{\min} = 7-70$ keV/amu and $E_{\max} = 10-22$ MeV/amu. For estimates of unknown cross-sections for different species of incident ions and for wider ranges of projectile energy, it is often more useful to have an analytic scaling formula with asymptotic behaviour which is based on physical considerations.

* Present address: Laser Atomic Separation Engineering Research Association of Japan, Tokai-mura, Ibaraki-ken 319-11, Japan.

Gillespie [2, 3] proposed such an analytic scaling formula for projectile charge q and collision energy E . This formula is applicable to various ions with charge q greater than $Z/2$ and in the following energy ranges: $E \geq 30$ keV/amu for H targets, $E \geq 40$ keV/amu for H₂ targets and $E \geq 80$ keV/amu for He targets. In the present work, we have modified Gillespie's formula to extend its applicability to a wider range of q and to lower energy.

2. FORMULATION

Gillespie's expression σ_G for the ionization cross-section is given by

$$\sigma_G = q^2 f(q, \beta) \sigma_B(\beta) \quad (1)$$

where $f(q, \beta)$ is given by

$$f(q, \beta) = \exp[-\lambda(q^{1/2} \alpha/\beta)^2] \quad (2)$$

λ is a constant for a given target species, α is the fine structure constant, β is the ratio of the speed of the incident ion to the speed of light, and $\sigma_B(\beta)$ is the Bethe cross-section for ionization by protons, written as

$$\sigma_B(\beta) = 4\pi a_0^2 (\alpha^2/\beta^2) (M^2 \{\ln[\beta^2/(1-\beta^2)] - \beta^2\} + C + (\alpha^2/\beta^2)\gamma) \quad (3)$$

where a_0 is the Bohr radius ($4\pi a_0^2 = 3.52 \times 10^{-16} \text{ cm}^2$), and the symbols M , C and γ denote constants for a given target species.

Equation (1) is not applicable to the energy range below the maximum of the Bethe cross-section (around 30, 40 and 80 keV/amu for H, H₂ and He targets, respectively) because of a fall-off at lower energies which is much more rapid than that shown by the available data. To extend the region of applicability, we modify both the Bethe cross-section and the function $f(q,\beta)$, expressing the ionization cross-section σ by

$$\sigma = q^2 F(q,\beta) \sigma_{MB}(\beta) \quad (4)$$

where

$$F(q,\beta) = g(q,\beta) / [(\alpha^2/\beta^2)\kappa + g(q,\beta)] \quad (5)$$

with

$$g(q,\beta) = \Lambda(1/q)^\mu (\beta^2/\alpha^2)^\nu \quad (6)$$

$\sigma_{MB}(\beta)$ is a modified Bethe cross-section for ionization by protons, written as

$$\sigma_{MB}(\beta) = 4\pi a_0^2 (\alpha^2/\beta^2) \times (M^2 \{\ln[\beta^2/(1-\beta^2) + \Delta] - \beta^2\} + C) \quad (7)$$

The symbol Λ in Eq. (6) denotes a constant for a given target species (defined identically equal to unity for H targets), and Δ in Eq. (7) denotes a small constant (1.35×10^{-5}). The symbols κ , μ and ν in Eqs (5) and (6) denote constants which are independent of the target species.

On the basis of an examination of the available data, the constant Δ has been introduced to prevent the right hand side of Eq. (7) from dropping too rapidly at the lowest energies considered. For the same reason, the term $(\alpha^2/\beta^2)\gamma$ (γ being negative) present in the Bethe cross-section σ_B has been omitted in Eq. (7). The effects of these modifications are negligible at high energies.

We use the following relation, which is applicable to non-relativistic energies:

$$\beta^2/\alpha^2 = E/25 \quad (E \text{ in keV/amu}) \quad (8)$$

For the constants M and C , the values used by Gillespie [3, 4] (see Table I) are retained in the present work.

The values of κ , Λ , μ and ν have been determined by least squares fits of Eq. (4) to available experimental data [4-16]. For H₂ targets, we have only considered the data for non-dissociative ionization. The number of data points used are given in Table II. The lowest energy covered by the experimental data was 9.4 keV/amu for H targets, 10 keV/amu for H₂ targets and 6 keV/amu for He targets.

In the least squares fit, we have used the two-step method provided by the code ALESQ [17]. This method was developed to fit a function to those data whose dependent variable changes by more than a few orders of magnitude. In the first step, the logarithm of the fitting function is fitted to the logarithm of the

TABLE I. VALUES OF M^2 AND C IN THE MODIFIED BETHE CROSS-SECTION σ_{BM}

Target	M^2	C
H	0.283	4.04
H ₂	0.721	9.06
He	0.489	5.52

TABLE II. NUMBER N OF EXPERIMENTAL AND RECOMMENDED DATA AND ROOT MEAN SQUARE DEVIATION δ_{rms} OF THE DATA FROM THE PRESENT ANALYTIC EXPRESSION

Target	Experimental data		Recommended data	
	N	δ_{rms} (%)	N	δ_{rms} (%)
H	254	20	188	20
H ₂	205	22	181	24
He	115	23	159	18
Overall	574	21	528	21

TABLE III. VALUES OF THE PARAMETERS κ , Λ , μ AND ν DETERMINED IN THE ANALYTIC EXPRESSION, OPTIMIZED FOR THE EXPERIMENTAL DATA

Constant	Value
κ	2.188
Λ for H	1
for H ₂	0.514
for He	0.1950
μ	1.587
ν	0.921

data with a uniform weight. When a number of data at a given value of the abscissa show a scatter, we expect that the function obtained gives a value close to the arithmetic mean of the data. However, the result of the logarithmic fit tends to be smaller than the arithmetic mean (see Ref. [17] for a detailed explanation). In the second step of the two-step method, this effect is removed by using a non-logarithmic fit, with the weights inversely proportional to the values of the fitting function obtained in the first step.

3. RESULTS AND DISCUSSION

The values of the constants determined in Eqs (2) and (3) are given in Table III. To give a measure of the goodness of fit, the root mean square deviation δ_{rms} of the data from the expression has been evaluated for the experimental data used and also for the recommended data for the incident ions of C^{q+} and O^{q+} [1]. The results are shown in Table II. The value of δ_{rms} of all the data is 21% for both the experimental and the recommended data.

In Figs 1 and 2, the experimental data [4–15] and the recommended data [1] for the ionization cross-section divided by $q^2\sigma_{\text{MB}}$ are plotted as a function of $(\beta^2/\alpha^2)g(q,\beta)$ and are compared with the corresponding quantity $F(q,\beta)$ in Eq. (5). It can be seen that the present scaling of the data is less reliable at low energies; note that the values of Eq. (4) for H₂ targets at the lowest energies deviate to an exceptionally large degree (about a factor of ten) from some of the recommended data. However, Eq. (4) is free from the sudden fall-off that Gillespie's formula [2, 3] predicts for energies below the maximum of the Bethe cross-

section. Figure 1 indicates that even at these energies (down to 6 keV/amu — the lowest energy of the available data), Eq.(4) gives approximations to the experimental data which are generally reliable to within a factor of two.

The function $F(q,\beta)$ given by Eq. (5) and also the right hand side of Eq. (4) behave approximately as E^ν at low energies. In Gillespie's cross-section formulas [2, 3], a similar function is given (Eq. (2)). While a

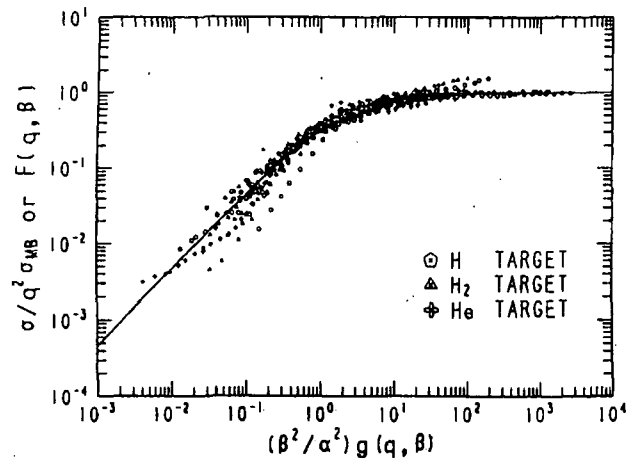


FIG. 1. Experimental cross-sections σ for impact ionization of H, H₂ and He by multiply charged ions, divided by the q^2 -scaled modified Bethe cross-section for ionization by protons, plotted as a function of $(\beta^2/\alpha^2)g(q,\beta)$. The data are taken from Refs [4–16]. The ion species of the data are: H⁺, Li⁽¹⁻³⁾⁺, C⁽²⁻⁶⁾⁺, N⁽²⁻⁵⁾⁺, O⁽²⁻⁶⁾⁺ and Ar⁽³⁻⁹⁾⁺ for H targets; H⁺, He²⁺, Li⁽¹⁻³⁾⁺, C⁽²⁻⁴⁾⁺, N⁽²⁻⁵⁾⁺ and O⁽²⁻⁵⁾⁺ for H₂ targets; and H⁺, He²⁺, Li³⁺, C⁽⁴⁻⁶⁾⁺ and O⁽³⁻⁸⁾⁺ for He targets. The curve represents Eq. (5).

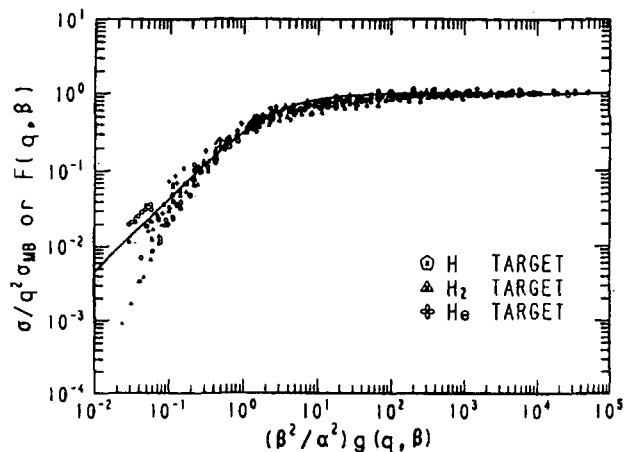


FIG. 2. Recommended cross-sections σ for impact ionization of H, H₂ and He by C^{q+} and O^{q+} ions, divided by the q^2 -scaled modified Bethe cross-section for ionization by protons, plotted as a function of $(\beta^2/\alpha^2)g(q,\beta)$. The data are taken from Ref. [1]. The curve represents Eq. (5).

low energy behaviour of the cross-section as expressed by Eq. (2) was suggested by Janev and Presnyakov [18], a behaviour expressed by E^p was assumed by Rudd et al. [19] in fitting experimental data for ionization by proton impact. We have compared the use of Eqs (2) and (5) for scaling and found that the available data are better described by Eq. (4).

4. SUMMARY

We have given an analytic expression for the impact ionization of H, H₂ and He by multiply charged ions. This expression is a modification of earlier scaling formulas, intended to better represent the low energy behaviour of the cross-section, and describes the available experimental data with a root mean square deviation of 21%.

ACKNOWLEDGEMENTS

The present research was organized and inspired by Dr. M. Ishii, Chairman of the research committee on atomic and molecular data of the Japan Atomic Energy Research Institute, to whom the authors owe special thanks.

This work was partly supported by the US-Japan Fusion Co-operation Programme and by the Office of Magnetic Fusion Energy of the United States Department of Energy.

REFERENCES

- [1] JANEV, R., PHANEUF, R.A., HUNTER, H.T., *At. Data Nucl. Data Tables* **40** (1988) 249.
- [2] GILLESPIE, G.H., *J. Phys.*, **B 15** (1982) L729.
- [3] GILLESPIE, G.H., *Phys. Lett.*, **A 93** (1983) 327.
- [4] HAUGEN, H.K., ANDERSEN, L.H., HVELPLUND, P., KNUDSEN, H., *Phys. Rev.*, **A 26** (1982) 1950.
- [5] HVELPLUND, P., HAUGEN, H.K., KNUDSEN, H., *Phys. Rev.*, **A 22** (1980) 1930.
- [6] SCHLACHTER, A.S., BERKNER, K.H., GRAHAM, W.G., et al., *Phys. Rev.*, **A 23** (1981) 2331.
- [7] SCHLACHTER, A.S., BERKNER, K.H., GRAHAM, W.G., PYLE, R.V., STEARNS, J.W., TANIS, J.A., *Phys. Rev.*, **A 24** (1981) 1110.
- [8] SHAH, M.B., GILBODY, H.B., *J. Phys.*, **B 14** (1981) 2361.
- [9] SHAH, M.B., GILBODY, H.B., *J. Phys.*, **B 14** (1981) 2831.
- [10] SHAH, M.B., GILBODY, H.B., *J. Phys.*, **B 15** (1982) 413.
- [11] SHAH, M.B., GILBODY, H.B., *J. Phys.*, **B 15** (1982) 3441.
- [12] SHAH, M.B., GILBODY, H.B., *J. Phys.*, **B 16** (1983) 4395.
- [13] SHAH, M.B., GILBODY, H.B., *J. Phys.*, **B 18** (1985) 899.
- [14] SHAH, M.B., ELLIOTT, D.S., GILBODY, H.B., *J. Phys.*, **B 20** (1987) 2481.
- [15] SHAH, M.B., McCALLION, P., GILBODY, H.B., *J. Phys.*, **B 22** (1989) 3037.
- [16] SHAH, M.B., McCALLION, P., GILBODY, H.B., *J. Phys.*, **B 22** (1989) 3983.
- [17] ITO, R., TABATA, T., ALESQ — A Code for Nonlinear Least-Squares Fit and TSOLV — A Code for Nonlinear Best Approximation, Tech. Rep. No. 4, Radiation Centre, Osaka Prefecture (1984).
- [18] JANEV, R.K., PRESNYAKOV, L.P., *Phys. Rep.* **70** (1981) 1.
- [19] RUDD, M.E., KIM, Y.-K., MADISON, D.H., GALLAGHER, J.W., *Rev. Mod. Phys.* **57** (1985) 965.

ION-MOLECULE COLLISION PROCESSES RELEVANT TO FUSION EDGE PLASMAS

P. REINIG, M. ZIMMER, F. LINDER

Department of Physics,
University of Kaiserslautern,
Kaiserslautern, Germany

ABSTRACT. A survey is presented on the existing database for ion-molecule collision processes relevant to fusion edge plasmas. The scope of the survey is limited to hydrogen and helium species, which form the main plasma constituents. In accordance with the energy range of interest (about 1–200 eV), the data have been mainly collected from low energy beam experiments. The experimental methods used are briefly discussed and characterized with respect to their strengths and weaknesses. The survey of data is divided into the following categories: (1) reactive collisions, with total cross-sections, state selective measurements and product distributions; (2) energy transfer collisions; and (3) negative ion collisions. Conclusions are drawn with regard to further work to be done on this subject.

1. INTRODUCTION

Recent experiments on large tokamaks have shown that the processes taking place at the plasma edge may have a crucial influence on the central plasma parameters, and there is strong evidence that the edge plasma conditions decisively affect the overall plasma performance. These observations have stimulated increased interest in understanding the physics of the edge plasma in a more fundamental way. However, the existing atomic and molecular database was found to be by far insufficient to meet the needs of edge plasma modelling and diagnostics [1].

The edge plasma is characterized by temperatures of about 1–200 eV and particle densities in the range 10^{12} – 10^{15} cm⁻³. The dominant constituents will always be the hydrogen isotopes. In an ignited D-T plasma, helium must also be considered as an important species. In addition to these primary constituents, there is a large number of possible impurities. These include carbon and oxygen compounds, in particular hydrocarbons and carbon oxides, various metallic (and related) impurities originating from structural materials (Ti, V, Cr, Fe, Ni, Cu, Al, Ta, Mo, W, Be, B, Si) and several diagnostic species (Li, Ne, Ar). The relative abundance of these impurities in the edge plasma is typically between 0.1 and 10%. Detailed estimates can be found in Ref. [1].

The range of collision processes relevant to edge plasma studies is extremely wide. Because of the low plasma temperatures, there are neutral particles with high densities and significant amounts of molecular species. This, combined with the large variety of constituents, makes the collision physics of the edge plasma very complex. This complexity is further increased by

the fact that the plasma conditions are usually such that a collisional-radiative treatment is required, i.e. multi-step processes involving collisions of excited species are important. Quantitative modelling of the edge plasma is therefore a formidable task and, as a prerequisite, a sufficiently complete database of the atomic and molecular processes is needed.

2. SCOPE OF THE SURVEY

In this paper, we are concerned with heavy particle collisions relevant to fusion edge plasmas, with special emphasis on ion-molecule collisions. We consider only singly charged ions and, with the exception of a few cases, we discuss only molecular systems, i.e. at least one of the reactants will usually be a molecule. Other types of processes (electron collisions, ion-atom collisions, collisions involving multiply charged ions) are specifically addressed in other papers of this volume.

The energy range of interest is approximately 1–200 eV. In view of the enormous number of possible combinations of reactants, the scope of the article must be drastically limited. As regards the selection of systems, we have chosen to include only the primary constituents, i.e. hydrogen and helium. We are aware that we miss some of the most interesting parts of the edge plasma physics by this limited choice, but the available space forces us to make this selection. It becomes immediately clear that even the inclusion of a few of the major impurity species (e.g. carbon and oxygen) would expand the list of possible processes in such a way that they become intractable.

Regarding the types of processes to be considered, we treat mainly those processes which are expected to have sizeable cross-sections at edge relevant energies. For the present systems, these are primarily charge transfer and particle interchange reactions. However, we also consider collisional dissociation of molecular ions and energy transfer collisions (momentum transfer, rotational and vibrational excitation). On the other hand, we do not take into account electronic excitation and ionization induced by ion impact, since these are highly endothermic processes which are generally found to have very small cross-sections in the present range of collision energies. A special case are negative ion collisions, which are briefly discussed in this paper. The binding energy of the extra electron is usually small (0.75 eV for H^-) so that collisional electron detachment is one of the most important processes in negative ion collisions; this process is therefore included in the present discussion.

As regards the different classes of data, we want to stress that present scattering experiments not only include the range of sub-eV collision energies but also provide a wealth of detailed information on the collision process which goes far beyond the determination of total cross-sections. Such detailed data include the dependence of cross-sections on specific reactant states, state resolved differential cross-sections, partial cross-sections for specific product states as well as the complete energy and angular distributions of the reaction products. Therefore, a considerable part of this paper is used to illustrate some of these more recent developments.

The present compilation is mainly based on experimental data. Theoretical work is considered only in some special cases; wider inclusion of theoretical results is beyond the scope of this article. In accordance with the collision energy range relevant to the edge plasma, the experimental data are mainly collected from low energy beam experiments. Different types of such experiments must be distinguished, and some of the main characteristics are discussed in Section 3. Swarm-type experiments are not included, except for a few special cases. Beam experiments in the keV range are also outside the scope of this article, except if their energy range overlaps with the present range of edge relevant energies.

It should be pointed out that the present article mainly gives a survey of the existing data. A full evaluation, leading to complete sets of recommended data, must be left for future work. It should also be mentioned that there is already a considerable number of data compilations in this field [1, 2]. However, most of these com-

pilations concentrate on higher collision energies and are restricted to total cross-sections. For this survey, we have mainly used the original literature, but we also refer to existing data reports. Of particular relevance are the reports by Janev et al. [3], Phelps [4], Barnett [5], Tawara et al. [6, 7] and Nakai et al. [8].

3. EXPERIMENTAL METHODS

In low energy beam experiments, ion-molecule reactions are usually studied by detecting the slow product ions; at higher energies, it is also possible to use fast neutral detection (FND) in studying processes such as charge transfer or electron detachment. The traditional method in this field is the ion beam gas cell (IBGC) method, which largely originated from mass spectrometry. A mass selected ion beam of variable energy is injected into a gas filled reaction chamber and the resulting product ions are measured using a variety of detection methods. We discuss first the determination of total cross-sections in these measurements. For completeness, we mention that a gas beam is sometimes used instead of a reaction chamber; however, this is of no importance for the following discussion.

For measurements of total cross-sections in IBGC experiments, two basically different methods must be distinguished. In the first method, sometimes called the condenser method and denoted by SID (slow ion detection) in the following tables, the total of all slow product ions is collected on some plate, grid or cylinder structure for which very different geometries are used. Electric fields, sometimes in conjunction with a magnetic field, are applied in order to ensure saturation in the collection efficiency. The fact that no mass analysis is provided in this method certainly poses a problem. However, for processes where there is no doubt about the identity of the product ions, for example in the case of simple charge transfer reactions, this method can give absolute total cross-sections which are quite reliable.

In the second method, often called tandem mass spectrometry (TMS), a second mass spectrometer is used to analyse the product ions by their masses. Two different geometries are typically used in TMS instruments: the transverse geometry, in which the product ions are extracted perpendicularly to the direction of the primary beam, and the longitudinal geometry, in which the extraction occurs along the axis of the primary beam. The first version discriminates against products with appreciable momentum transfer in the forward direction, whereas the reverse is the case in the second configuration. In favourable cases, depend-

ing on the kinematics, the reaction mechanism and the type of instrument used, the collection efficiency may come close to unity. In general, however, the energy and angular distribution of the product ions is a priori unknown so that relatively large uncertainties can arise from insufficient and inaccurately known collection efficiencies. Absolute total cross-sections obtained with this method should therefore be regarded with caution.

This problem has been overcome to a large extent with the development of the guided beam (GB) technique. Not only can this method be used for very low collision energies, but it also has a high sensitivity and, most importantly, a guaranteed product collection efficiency of nearly unity. Absolute total cross-sections can therefore be measured with high accuracy, and the overall properties of this technique make it the ideal method for this type of measurement in the field of low energy ion-molecule reactions. A full description of this technique including more recent advances is given in Ref. [9].

Another powerful method in this field is the merged beam (MB) technique. By merging two fast beams co-axially and by varying their relative velocity, a broad range of centre of mass collision energies down to extremely low energies becomes accessible and a high centre of mass energy resolution can be obtained. The reaction products are contained in a relatively narrow cone of laboratory angles and can therefore be easily collected with high efficiency, thus enabling the determination of total reaction cross-sections. For absolute measurements, a careful study of the spatial beam overlap along the reaction path is necessary.

A further important and unique feature of the MB technique is the fact that the neutral reactants are usually formed by charge transfer of the corresponding ions. This allows the production of neutral reactant beams for a wide range of chemical systems. In many cases it is equally easy to produce beams of chemically unstable species (e.g. atomic and molecular radicals) as it is to produce beams of closed shell stable molecules (e.g. H_2). On the other hand, it is important to realize that reactant molecules prepared in this way are very likely to be formed in vibrationally excited states. This has to be kept in mind when cross-section data obtained by the MB technique are compared with results from other experiments.

So far, we have concentrated on the determination of absolute total cross-sections. Now we proceed to the discussion of other data classes such as product distributions and differential cross-sections. Within certain limits, all the above methods can also be used to obtain information on the energy and angular distributions of

the reaction products. However, the predestinated method for providing the most detailed information in this respect is the crossed beam (CB) technique. In present day CB experiments, a mass and energy selected ion beam is crossed with a supersonic nozzle beam of the target gas. Both beams are well collimated and can be made nearly monoenergetic. Because of the supersonic nozzle expansion, the internal state distribution of the neutral reactant molecules corresponds to a very low temperature. The kinematically well defined conditions of a CB experiment permit measurements with high resolution in energy and angle. The product analysis is performed using a rotatable detector with mass and energy analysis. The energy resolution is generally sufficient to perform state resolved measurements. In favourable cases, individual rotational transitions can be resolved.

Simultaneously with the improvements in resolution, the development of the CB technique has reached the state that it is now possible to carry out measurements down to collision energies of the order of 0.1 eV, so that the full energy range relevant to edge plasma studies can be covered. Both elastic and inelastic as well as reactive collisions can be studied. The measurements provide very detailed and complete data, such as product and state specific differential cross-sections, angle integrated partial cross-sections, and finally total cross-sections summed over all product states. However, it is important to stress that cross-sections have to be determined in absolute units in order to be useful in practical applications. This point has often been neglected in CB measurements. In the following, we briefly outline several possibilities for making absolute measurements in CB experiments. We expect that these methods will be used more extensively in future work.

Direct determination of absolute differential cross-sections based on the relation

$$I_s = \frac{d\sigma}{d\Omega} \cdot n l I_0 \cdot \Delta\Omega \quad (1)$$

is generally difficult, since it is not easy to obtain an accurate measure for the effective value of $n l$ for which the absolute gas beam density and the overlap integral of the two beams must be known. Therefore, one has to rely on other methods. One possible procedure is the following. All product and state specific differential cross-sections are first measured in relative units, then the data are integrated over angles, summed over product states and finally normalized to a total cross-section which is known in absolute units from other measure-

ments. In this way, the whole set of detailed cross-sections can be put on an absolute scale. Concerning absolute total cross-sections needed for normalization, it is often possible to combine information from different sources covering the whole energy range from thermal energies up to the keV region. An example of a case in which this method has been applied in full detail can be found in an earlier paper from our group [10].

Another well known possibility is normalization to theory. The experimental data, again in the form of state specific differential cross-sections, are first measured in relative units. Then a detailed comparison with theory is performed. If good agreement between all details of the data is achieved, one can be confident that reliable absolute cross-sections are obtained by normalizing the experimental data with regard to theory. This method has been extensively used in the case of $H^+ + H_2$ energy transfer collisions which will be discussed later in this paper (see Section 4.2). It should be emphasized, however, that the application of this method is more problematic at low energies. At higher energies, relatively simple scattering approximations (e.g. Born approximation) can often be used to normalize the experimental data. For low energy collisions and in particular for molecular collision systems, a much more elaborate theoretical treatment is needed. The applicability of the method is therefore expected to be limited to relatively simple collision systems.

The third and probably most attractive method consists of using simple ion-atom scattering systems as secondary standards for absolute cross-section measurements in CB experiments. Examples of such systems are $H^+ + He$, $He^+ + He$ and $H^- + He$; these systems are well known, both experimentally and theoretically, are easy to handle experimentally and are therefore convenient to use for this purpose. To avoid a rather lengthy discussion, which would be necessary to justify the details of the method, we refer to electron scattering work [11] in which similar techniques have been used already for some time. The principle of the method is to compare the scattering intensity I_S of the collision system under study with that of a suitable reference system. Under certain conditions, which are discussed in detail in Ref. [11], the beam overlap integrals of the two systems will cancel, to a good approximation, and the differential cross-section in question can be obtained in absolute units through the relation

$$\left(\frac{d\sigma}{d\Omega}\right)_X = \frac{I_{SX}}{I_{SR}} \cdot \frac{n_R}{n_X} \cdot \left(\frac{d\sigma}{d\Omega}\right)_R \quad (2)$$

where the index R indicates the reference system and the index X the system under study. The relative target

gas densities n_R and n_X are quite accurately known in the present case, since the technology of supersonic nozzle beams is highly developed and the properties of these beams are well understood [12]. This method has recently been employed by our group in studies of $H^- + H_2(D_2)$ reactions using $H^- + He$ as a reference system [13]. Some results are reported later in this paper (see Section 4.3).

Concluding the discussion of CB experiments, we can say that all types of processes (elastic, inelastic, reactive) can be studied with this method in the relevant energy range. We have emphasized the importance of making absolute measurements. All classes of data needed for edge plasma modelling can be obtained in great detail. It must be realized, however, that these measurements are very time consuming so that, in practice, the number of such studies will be limited. The majority of processes will be studied by other techniques with which total cross-sections and rate coefficients are more readily obtained than in CB experiments.

This overview of experimental methods is far from being complete. We have pointed out some characteristics of those methods which are of main importance in the following survey of data. A very important class of experiments, which we have not discussed here, are measurements with state selected reactants. Several methods, such as state selective photoionization (SSPI), photoelectron product ion coincidence (PEPICO) and resonance enhanced multiphoton ionization (REMPI), have been used in the study of systems relevant to the discussion of the present paper. The results of these studies are surveyed in Section 4.1.2. The data with state resolved products have been obtained mainly by time of flight analysis or using electrostatic energy selectors. Optical methods, which can be very powerful in this respect, are of less importance for the present systems and processes.

We have intentionally refrained from giving extensive references in this section, since all experimental methods used are quoted explicitly in the following compilation of original work.

4. SURVEY OF DATA

The following survey of data is divided into five categories and is mainly given in the form of tables. As already stated, a full evaluation of the data is outside the scope of this article. A few examples are illustrated by figures.

TABLE I. REACTIVE COLLISIONS (TOTAL CROSS-SECTIONS)

Reaction	Collision energy ^{a)} [eV]	Method ^{b)}	Reference	Comments ^{c)}
$H^+ + H_2 \rightarrow H + H_2^+$	2 - 10 42 - 1300 ✓ 33 - 600 33 - 270 45 - 700 130 - 1600	IBGC (TMS) CB (FND) IBGC (TMS) IBGC (SID) IBGC (SID) IBGC (SID)	17 18 19 20 21 22	1 (below 40eV) 2 (above 40eV) 12 in [3 - 8]
$H^+ + D_2 \rightarrow H + D_2^+$	2 - 8 2 - 7.5 2 - 12 2 - 80	IBGC (TMS) IBGC (TMS) GB IBGC (TMS)	17 23 24, 25 26	3, 4
$H^+ + D_2 \rightarrow D + HD^+$	2 - 8 2 - 7.5 2 - 12 2 - 80	IBGC (TMS) IBGC (TMS) GB IBGC (TMS)	17 23 24, 25 26	3, 4
$H^+ + D_2 \rightarrow D^+ + HD$ ($D^+ + H + D$)	2 - 8 1.7 - 7.5 0.3 - 12 0.3 - 80	IBGC (TMS) IBGC (TMS) GB IBGC (TMS)	17 23, 27 24, 25 26	3, 4
$D^+ + H_2 \rightarrow H + HD^+$	2 - 7.5 2 - 9	IBGC (TMS) GB	17 25	3, 4
$D^+ + H_2 \rightarrow H^+ + HD$ ($H^+ + H + D$)	1 - 8 2 - 9	IBGC (TMS) GB	17 25	3, 4
$D^+ + HD \rightarrow D + HD^+$	2 - 9 2 - 6	IBGC (TMS) IBGC (TMS)	17 23, 27	1
$D^+ + HD \rightarrow H + D_2^+$	2 - 9 2 - 6	IBGC (TMS) IBGC (TMS)	17 23, 27	1
$D^+ + HD \rightarrow H^+ + D_2$	1.5 - 6 0.8 - 6	IBGC (TMS) IBGC (TMS)	17 23, 27	1
$D^+ + D_2 \rightarrow D + D_2^+$	2 - 10 2 - 6 2 - 11 43 - 270	IBGC (TMS) IBGC (TMS) GB IBGC (SID)	17 27 25 28	3, 4
$H_2^+ + H \rightarrow H_2 + H^+$	~ 0.04 33 - 4600	ICR CB (SID, TMS)	29 30	-
$D_2^+ + D \rightarrow D_2 + D^+$	~ 0.04	ICR	29	-
$H_2^+ + D \rightarrow HD^+ + H$	0.05 - 5	MB	31	-
$H_2^+ + H_2 \rightarrow H_2 + H_2^+$	0.5 - 22 2 - 200 2.5 - 50 5 - 2200 25 - 450 25 - 1000 30 - 2500 35 - 500 35 - 500 50 - 2200 50 - 400	SSMS IBGC (SID) IBGC (TMS) IBGC (SID) IBGC (TMS) IBGC (SID) IBGC (SID) IBGC (SID) IBGC (SID) IBGC (SID) IBGC (SID) IBGC (SID)	32 20 ✓ 33 34 ✓ 19 35 ✓ 36 21 37 22 38	1 (below 5eV) 5 (below 5eV) 12 in [3 - 6]

TABLE I. (cont.)

Reaction	Collision energy ^a [eV]	Method ^b	Reference	Comments ^c
<i>CX</i> } $H_2^+ + D_2 \rightarrow H_2 + D_2^+$ $D_2^+ + H_2 \rightarrow D_2 + H_2^+$ $D_2^+ + D_2 \rightarrow D_2 + D_2^+$	170 - 670 85 - 330 2 - 200 25 - 1000	IBGC (SID) IBGC (SID) IBGC (SID) IBGC (SID)	37 37 28 35, 39	2
$H_2^+ + H_2 \rightarrow H_3^+ + H$	0.01 - 7 0.1 - 5 0.2 - 3 0.3 - 5 0.7 - 8.5 0.7 - 7.5	MB MB SCC IBGC (TMS) IBGC (TMS) SSMS	40 41 42 43 33 32	3, 6, 7 12 in [3 - 6]
$HD^+ + D_2 \rightarrow HD_2^+ + D$ $\rightarrow D_3^+ + H$	0.01 - 8	MB	44	6
$D_2^+ + HD \rightarrow HD_2^+ + D$ $\rightarrow D_3^+ + H$	0.01 - 8	MB	44	6
$D_2^+ + D_2 \rightarrow D_3^+ + D$	0.3 - 8	ICR, SCC	5	12 in [5]
$H_2^+ + H_2 \rightarrow H^+ + \text{products}$	1 - 50 1.5 - 5 5 - 50 50 - 1000	IBGC (TMS) SSMS IBGC (TMS) IBGC (TMS)	45 32 33 46	2 (except 33) 12 in [4, 5]
$D_2^+ + D_2 \rightarrow D^+ + \text{products}$	1 - 50 50 - 1000	IBGC (TMS) IBGC (TMS)	47 46	
$H_3^+ + D_2 \rightarrow HD_2^+ + H_2$	0.01 - 11	MB	48	6
$H_3^+ + H_2 \rightarrow \text{fast } H^+, H_2^+$ $H_3^+(D_3^+) + H_2 \rightarrow \text{slow } H^+, H_2^+$	40 - 200 40 - 200 (25 - 125)	IBGC (TMS) IBGC (SID, TMS)	49 50	12 in [4 - 6]
$H_3^+(D_3^+) + D_2 \rightarrow \text{slow } D^+, D_2^+$	57 - 280 (40 - 200)	IBGC (SID, TMS)	50	
$H_2^+ + He \rightarrow HeH^+ + H$	0.05 - 12 0.7 - 3 0.7 - 14 1 - 6	MB IBGC (TMS) CB (TMS) GB	51 43 52 53, 54	2 12 in [5]
$H_2^+ + He \rightarrow H^+ + \text{products}$	0.5 - 6 3 - 65	GB IBGC (TMS)	53, 54 45	2 (except 53)
$HD^+ + He \rightarrow H^+ + \text{products}$ $\rightarrow D^+ + \text{products}$	2.3 - 28	IBGC (TMS)	55	
$D_2^+ + He \rightarrow D^+ + \text{products}$	5 - 50	IBGC (TMS)	47	
$He^+ + H_2 \rightarrow He + H_2^+$	0.03 - 57 50 - 300	IBGC (TMS) IBGC (TMS)	56 19	1, 8
<i>CX</i> $He^+ + H_2 \rightarrow He + H + H^+$	0.1 - 7.2 0.1 - 50 6.7 - 16 33 - 800 50 - 300 330 - 1000	IBGC (TMS) IBGC (TMS) IBGC (TMS) IBGC (SID) IBGC (TMS) IBGC (FND)	57 58 59 22 19 60	1, 5, 8 12 in [3, 5, 7]

TABLE I. (cont.)

Reaction	Collision energy ^a [eV]	Method ^b	Reference	Comments ^c
✓ CT $\text{He}^+ + \text{D}_2 \rightarrow \text{He} + \text{D} + \text{D}^+$	0.1 - 50	IBGC (TMS)	58	9
✓ CT $\text{He}^+ + \text{HD} \rightarrow \text{He} + \text{D} + \text{H}^+$ $\rightarrow \text{He} + \text{H} + \text{D}^+$	0.2 - 7.2 5 - 20	IBGC (TMS) IBGC (TMS)	57 59	10
✓ $\text{He}^+ + \text{H}_2 \rightarrow \text{HeH}^+ + \text{H}$	0.1 - 30	IBGC (TMS)	58	2, 11
✓ $\text{He}^+ + \text{D}_2 \rightarrow \text{HeD}^+ + \text{D}$	0.1 - 50 0.1 - 30	GB IBGC (TMS)	61 58	
✓ $\text{He}^+ + \text{HD} \rightarrow \text{HeH}^+ + \text{D}$ $\rightarrow \text{HeD}^+ + \text{H}$	0.1 - 50	GB	61	
✓ $\text{HeH}^+ + \text{H} \rightarrow \text{H}_2^+ + \text{He}$	~0.04	ICR	29	2
✓ $\text{HeH}^+ + \text{H}_2 \rightarrow \text{H}_3^+ + \text{He}$	0.2 - 4 ~0.04	CB (TMS) ICR	52 62	

^a All energies are given as centre-of-mass (cm) collision energies.

^b CB — crossed beams
MB — merged beams
ICR — ion cyclotron resonance
SSMS — single-stage mass spectrometer
SID — slow ion detection (without mass analysis of reaction products)
TMS — tandem mass spectrometer (including mass analysis of reaction products)

IBGC — ion beam gas cell experiment
GB — guided beam technique
SSC — single collision chamber
FND — fast neutral detection

^c Comments:

1 — Data have large uncertainties
2 — Fair agreement between different measurements
3 — Large discrepancies between different measurements
4 — GB data are recommended
5 — Controversial recommendations in different data compilations
6 — MB studies imply neutral reactant molecules in vibrationally excited states (in contrast to IBGC experiments)

7 — All data compilations apparently recommend MB data
8 — Very small cross-section at low eV energies ($\sim 10^{-19} \text{ cm}^2$)
9 — Experimental data in relative units only
10 — Cross-section of comparable magnitude as for $\text{He}^+ - \text{H}_2$ system
11 — Data of Jones et al. [58] in relative units only
12 — Evaluated/recommended data in Ref. [x]

4.1. Reactive collisions

4.1.1. Total cross-sections

Table I gives a summary of total cross-section measurements for reactive collisions. The system $\text{H}^+ + \text{H}_2$ (including isotopic variants) has been studied extensively. The first entries of Table I refer to charge transfer (CT) and particle interchange (PI) reactions for this system. In most cases, there are large discrepancies (up to factors of 30) between different measurements at low eV energies. As already discussed in Section 3, the IBGC-TMS measurements are generally not reliable because of problems of collection efficiency. The GB results are the recommended data. The uncertainty of these data is estimated to be 10% or better [25]. In those cases where GB data are not

available, the existing data must be regarded as very uncertain.

Figure 1 illustrates the present situation for the $\text{H}^+ + \text{H}_2$ CT reaction. Above 400 eV, there is fair agreement between different measurements. As representative data, the most recent results of Gealy and Van Zyl [18] are shown. The data below 40 eV have large uncertainties. The only experimental data available for this energy range are the IBGC-TMS results of Holliday et al. [17]. The three sets of recommended data [3-5] deviate from each other considerably around 10 eV. Also included in Fig. 1 are theoretical values at 20 eV from Niedner et al. [77] and Baer et al. [78]. In particular the value of Baer et al. appears to be rather high.

Figure 2 shows the corresponding situation for the CT reaction in $\text{D}^+ + \text{D}_2$. In this case, GB results are

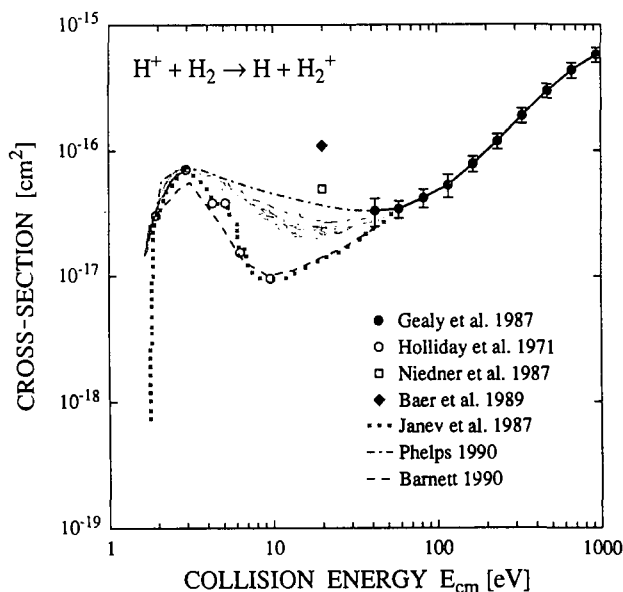


FIG. 1. Total cross-section for the charge transfer reaction $H^+ + H_2 \rightarrow H + H_2^+$. The data are from Gealy and Van Zyl [18], Holliday et al. [17], Niedner et al. [77], Baer et al. [78], Janev et al. [3], Phelps [4] and Barnett [5].

available [25] and they clearly represent the recommended data. The discrepancies between different low eV measurements, which become evident in this figure, are typical of the situation for other $H^+ + H_2$ reactions listed in Table I. At higher energies, the only existing data are those of Cramer and Marcus [28]. They have been obtained with the IBGC-SID method and should therefore be quite reliable. This is supported by the fact that the corresponding results for $H^+ + H_2$ obtained by Cramer [20] are in very good agreement with the other measurements in this energy range. The cross-sections for the different isotopic systems do not simply scale with the velocity of the reactants, which indicates that charge transfer in ion-molecule systems is a more complex process (involving internal degrees of freedom) compared to ion-atom systems.

For the $H_2^+ + H_2$ system, the different measurements for the CT reaction are generally in fair agreement with each other (within a factor of two). At energies below 5 eV, it is not clear whether the sharp decrease of the CT cross-section observed in some cases is due to competition with the PI reaction $H_3^+ + H$. Experiments and the different data compilations [3-6] are controversial on this point.

For the PI reaction $H_2^+ + H_2 \rightarrow H_3^+ + H$, the results obtained by different methods show significant differences. All measurements give essentially the same energy dependence of the cross-section, but the absolute values differ by a factor of three. The MB data are

systematically lower. Whether this is due to the fact that in the MB studies, in contrast to the other methods, the H_2 reactant molecules are in vibrationally excited states (which may inhibit the reaction, as observed for vibrationally excited H_2^+) or whether simply experimental errors are involved is not clear. All data compilations apparently have adopted the MB data.

For collision induced dissociation (CID) of H_2^+ , the situation at low energies is also not completely clear. Recent compilations of recommended data [4, 5] are mainly based on the results of Tunitskij et al. [45] and Zhurkin et al. [46, 47]. There are strong indications, however, that these cross-sections may be too low. The measurements of Vance and Bailey [33] for $H_2^+ + H_2$ as well as those of Schlier [53] for $H_2^+ + He$ give considerably larger values (about a factor of six in both cases). Furthermore, the state selective measurements (see Table II) indicate a strong dependence of the CID cross-section on the vibrational state of the H_2^+ ion. Taking an appropriate average over the full distribution of H_2^+ vibrational states, Guyon et al. [66] find excellent agreement with the data of Vance and Bailey in the case of $H_2^+ + H_2$. The same tendency is observed in the case of $H_2^+ + He$ [54]. Evidently, the vibrational state population of the H_2^+ ion plays an important role in CID processes, and it seems difficult to compare different experimental results, if the internal state population is unknown.

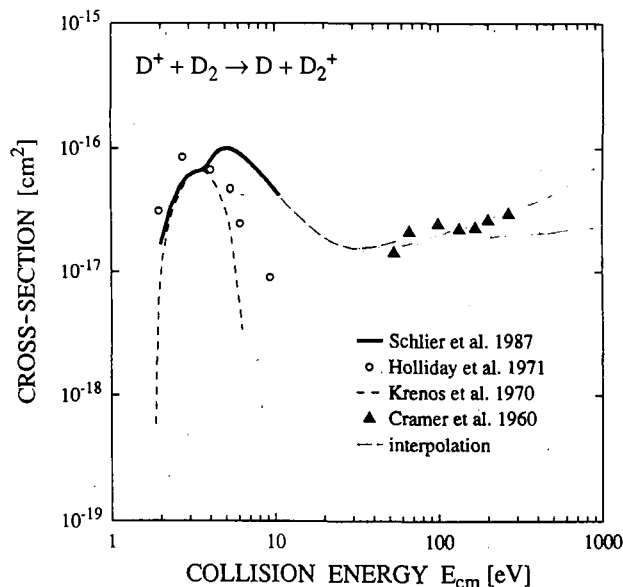


FIG. 2. Total cross-section for the charge transfer reaction $D^+ + D_2 \rightarrow D + D_2^+$. The data are from Schlier et al. [25], Holliday et al. [17], Krenos and Wolfgang [27] and Cramer and Marcus [28].

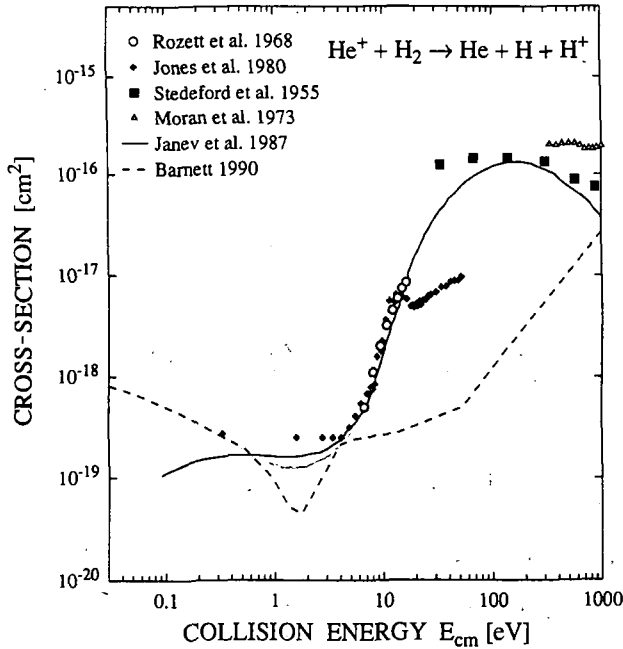


FIG. 3. Total cross-section for the dissociative charge transfer reaction $\text{He}^+ + \text{H}_2 \rightarrow \text{He} + \text{H} + \text{H}^+$. The data are from Rozett and Koski [59], Jones et al. [58], Stedeford and Hasted [22], Moran and Conrads [60], Janev et al. [3] and Barnett [5].

The H_3^+ ion must be expected to be an abundant species under edge plasma conditions. Phelps [4] has recently attempted to give a compilation of cross-section data for various $\text{H}_3^+ + \text{H}_2$ collision processes. He finds that the database for this collision system is extremely sparse. In particular, the information for the energy range 1–1000 eV is almost totally based on extrapolations from low or high energies. More work on the collisional behaviour of H_3^+ for edge relevant energies is clearly needed.

A rather confusing situation is found for the CT reaction in $\text{He}^+ + \text{H}_2$ collisions at energies below about 1000 eV (see Fig. 3). There seems to be general agreement that dissociative CT is the dominant process. However, the data are in a very unsatisfactory state. Figure 3 shows four sets of experimental data and two sets of recommended data. The data of Jones et al. [58] are in relative units and have been normalized to the data of Rozett and Koski [59] in the region of overlap. This leads, however, to a severe disagreement with the measurements of Stedeford and Hasted [22] in the 30–50 eV region. It is also evident that the two sets of recommended data are completely different from each other.

Measurements of optical emissions resulting from $\text{He}^+ + \text{H}_2$ collisions (listed in Table II and shown in Figs 4 and 5) can help to shed some light on this

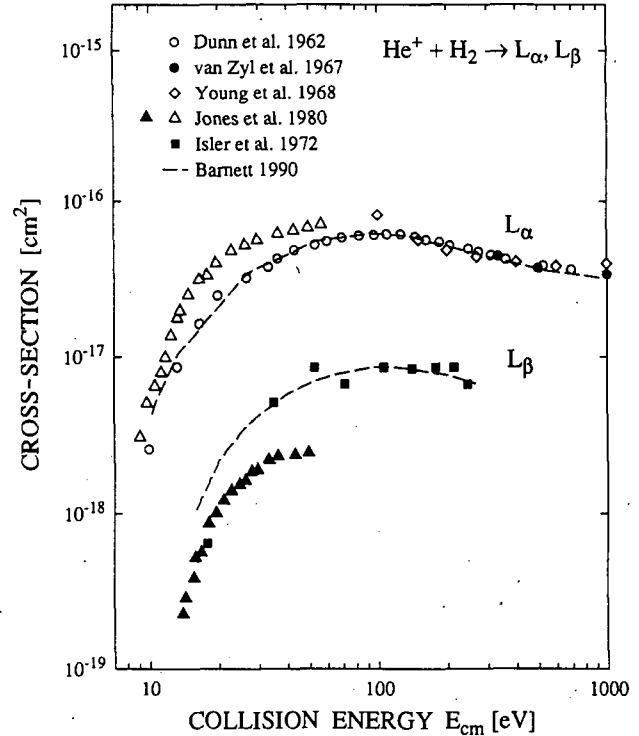


FIG. 4. Total cross-sections for Lyman- α (L_α) and Lyman- β (L_β) emission in $\text{He}^+ + \text{H}_2$ collisions. The data are from Dunn et al. [80], Van Zyl et al. [84], Young et al. [85], Jones et al. [58], Isler and Nathan [79] and Barnett [5].

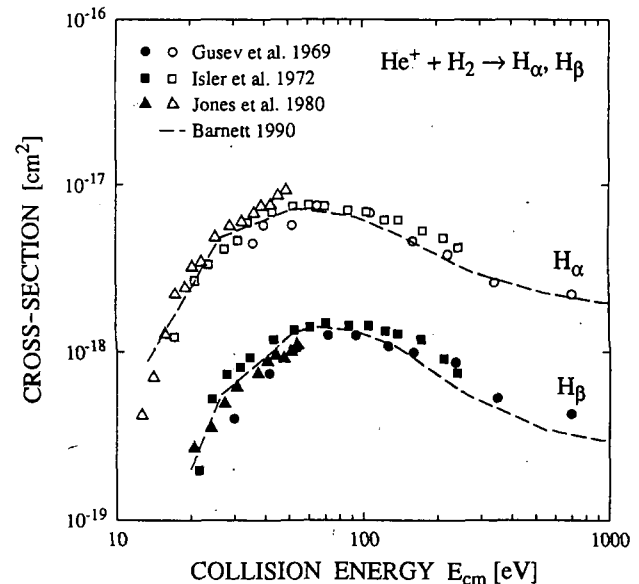


FIG. 5. Total cross-sections for Balmer- α (H_α) and Balmer- β (H_β) emission in $\text{He}^+ + \text{H}_2$ collisions. The data are from Gusev et al. [81], Isler and Nathan [79], Jones et al. [58] and Barnett [5].

TABLE II. REACTIVE COLLISIONS (STATE SELECTIVE MEASUREMENTS)

Reaction ^a	Collision energy ^b [eV]	Method ^c	Reference	Comments ^d
$H_2^+(v, j) + H_2 \rightarrow H_2 + H_2^+$ $v=0, j=0, 1, 2$	2 - 4	SSPI - CB	63	1
$H_2^+(v_1) + H_2 \rightarrow H_2 + H_2^+(v_2')$ $v_1=0, 1; v_2'=0, 1, 2$	2 - 16	SSPI - CB	64	2
$H_2^+(v) + H_2 \rightarrow H_2 + H_2^+$ $v=0-4$ $v=0-5$ $v=0-10$	2 - 200 4 - 500 4 - 16	SSPI - CB PEPICO - CB PEPICO - CB	63 65 66	3, 4, 5
$D_2^+(v) + H_2 \rightarrow D_2 + H_2^+$ $v=0$ $v=0-10$	0.2 - 3 4	SSPI - GB PEPICO - CB	67 66	3, 7
$H_2^+(v) + H_2 \rightarrow H_3^+ + H$ $v=0-8$ $v=0-4$ $v=0-3$ $v=0-5$	~0.04 ~0.04 - 15 0.1 - 1 ~1	PEPICO - SCC SSPI - GB PEPICO - SCC SSPI - SCC	68 69 70 71	3, 4, 6
$H_2^+(v) + D_2 \rightarrow HD_2^+ + H$ $v=0-4$	0.2 - 6	SSPI - GB	67	3, 4
$D_2^+(v) + H_2 \rightarrow HD_2^+ + H$ $v=0-4$	0.2 - 6	SSPI - GB	67	3, 4
$D_2^+(v) + D_2 \rightarrow D_3^+ + D$ $v=0-12$	~0.04	PEPICO - SCC	68	3
$H_2^+(v) + H_2 \rightarrow H^+ + \text{products}$ $v=0-10$	4 - 16	PEPICO - CB	66	3, 6
$D_2^+(v) + H_2 \rightarrow H^+ + \text{products}$ $\rightarrow D^+ + \text{products}$ $v=0-10$	4	PEPICO - CB	66	
$D_2^+(v) + HD \rightarrow H^+ + \text{products}$ $\rightarrow D^+ + \text{products}$ $v=0-4$	1 - 8	SSPI - GB	67	
$H_2^+(v) + He \rightarrow HeH^+ + H$ $v=0-8$ $v=0-5$ $v=0-4$ $v=0-4$ $v=0-6$	~0.04 ~0.04 - 7 0.4 - 3 1 - 8 3.1	PEPICO - SCC SSPI - SSC PEPICO - IBGC SSPI - GB PEPICO - CB	68 72 73, 74 75 76	3, 4, 6
$HD^+(v) + He \rightarrow HeH^+ + D$ $\rightarrow HeD^+ + H$ $v=0-4$	1 - 8	SSPI - GB	75	
$H_2^+(v) + He \rightarrow H^+ + H + He$ $v=0-5$ $v=0-6$	~0.04 - 7 3.1	SSPI - SCC PEPICO - CB	72 76	
$H^+ + H_2 \rightarrow H + H_2^+(v)$ $v=0-3$	20	CB - TOF	77, 78	8

TABLE II. (cont.)

Reaction ^a	Collision energy ^b [eV]	Method ^c	Reference	Comments ^d
$\text{He}^+ + \text{H}_2 \rightarrow \text{He} + \text{H}^+ + \text{H}^*(n\text{l})$	5 - 50	IBGC - OES	58	6, 9 10 in [5]
	10 - 230	IBGC - OES	79	
	10 - 670	IBGC - OES	80	
	30 - 10000	IBGC - OES	81, 82	
$\text{He}^+ + \text{D}_2 \rightarrow \text{He} + \text{D}^+ + \text{D}^*(n\text{l})$	5 - 80	IBGC - OES	58	
$\text{He}^+ + \text{H}_2 \rightarrow \text{He}^*(1\text{snl}) + \text{products}$	23 - 230	IBGC - OES	79	
	30 - 10000	IBGC - OES	82, 83	

^a The neutral reactant molecule is always in the ground vibrational state $v = 0$. The product states are usually unknown unless stated otherwise.

^b All energies are given as centre-of-mass (cm) collision energies.

^c SSPI — state selective photoionization TOF — time of flight measurement

PEPICO — photoelectron product ion coincidence OES — optical emission spectroscopy

Other notations as in Table I

^d Comments:

1 — The measured cross-section shows no dependence on rotational state of reactant ion

2 — Final state analysis of product ions by chemical detection method

3 — Marked/strong dependence on vibrational state of reactant ion

4 — The observed vibrational state dependence varies with collision energy

5 — Considerable discrepancies between different measurements

6 — Fair agreement between different measurements

7 — The measured $v = 0$ cross-sections differ by a factor of two

8 — Final state analysis of product ions by time of flight spectroscopy of neutral H atoms

9 — Final state analysis by detection of spectral line emission (Lyman series, Balmer series, various HeI lines)

10 — Evaluated/recommended data in Ref. [x]

problem. The different measurements for Lyman and Balmer emissions are in reasonable agreement with each other. Furthermore, there is general agreement that these optical line emissions are to be attributed to dissociative CT in the $\text{He}^+ + \text{H}_2$ collision process leading to electronically excited $\text{H}^*(n\text{l})$ atoms. The 2p state and the nl states with $n \geq 3$ are observed in optical emission, whereas the contribution of the 2s state remains unknown. The data shown in Figs 4 and 5 strongly support the measurements of Stedeford and Hasted [22] and the recommended data of Janev et al. [3] for the total dissociative CT cross-section in $\text{He}^+ + \text{H}_2$ collisions. The data given by Barnett [5] should be revised. Additional measurements, in particular on kinetic energy distributions of the H^+ product ions, would be helpful to clarify the situation.

4.1.2. State selective measurements

Table II gives a compilation of measurements with state selected reactants. Also included are some measurements with state resolved products.

Although pioneering work with state selected reactants began more than 20 years ago, more systematic studies have only been carried out in recent years. The experimental methods used are the SSPI and PEPICO

techniques. Within the present selection of collision systems, the H_2^+ molecular ion is the only species for which state selective measurements have been performed. Nevertheless, it is one of the most important species in the edge plasma.

There is one experiment in which rotationally state selected H_2^+ ions have been used. The measured cross-section shows no dependence on the rotational state of the reactant ion. All other experiments are concerned with the vibrational state dependence of the cross-sections.

The $\text{H}_2^+ + \text{H}_2$ CT reaction shows a quite pronounced dependence on the H_2^+ vibrational state (up to a factor of four in the range $v = 0-10$). In addition, the observed vibrational state dependence is found to vary significantly with the collision energy. It should be noted that the results of different groups are not fully consistent with each other for this reaction.

The vibrational dependence of the PI reaction $\text{H}_2^+ + \text{H}_2 \rightarrow \text{H}_3^+ + \text{H}$ appears to be somewhat weaker, although it is still significant. Again, the character of the dependence varies with the collision energy. At thermal energies, for example, the cross-section decreases by about 20% in the range $v = 0-8$, whereas at a collision energy of 3 eV the cross-section increases by about 60% in the range $v = 0-3$.

TABLE III. REACTIVE COLLISIONS (PRODUCT DISTRIBUTIONS)

Reaction	Collision energy ^a [eV]	Method ^b	Reference	Comments ^c
$H^+ + H_2 \rightarrow H + H_2^+(v)$	20	CB	77, 78	1, 3, 5
$H^+ + D_2 \rightarrow D^+ + HD(v, j)$ $\rightarrow D^+ + HD$	0.4 - 5.2 4.0 - 5.6	IBGC CB	86, 87 23	2, 3, 5 2, 5
$H^+ + D_2 \rightarrow D + HD^+$	2 - 5	IBGC	25, 87	6
$D^+ + H_2 \rightarrow H + HD^+$	1 - 5	MB	88	2, 7
$D^+ + HD \rightarrow D + HD^+$ $\rightarrow H + D_2^+$ $\rightarrow H^+ + D_2$	1.5 - 5.5	CB	23	1, 5
$D^+ + D_2 \rightarrow D + D_2^+$	2.8 - 4.6	CB	23	1
$H_2^+ + D \rightarrow HD^+ + H$	1 - 10	MB	88	2, 7
$H_2^+ + H_2 \rightarrow H_3^+ + H$	0.002 - 2 0.5 - 10 8 - 10	MB MB MB	40 89 90	2, 7 2, 7 2, 7
$H_2^+(v) + H_2 \rightarrow H_3^+ + H$	2	REMPI - SB	91	1, 4
$H_2^+ + D_2 \rightarrow HD_2^+ + H$	0.5 - 10 0.9 - 4.0 1.0 - 4.6	MB CB CB	89 92 93	2, 7 1 1
$H_2^+ + D_2 \rightarrow H_2D^+ + D$	1.0 - 4.0	CB	93	1
$HD^+ + D_2 \rightarrow HD_2^+ + D$ $\rightarrow D_3^+ + H$	0.002 - 3	MB	44	1
$D_2^+ + H_2 \rightarrow HD_2^+ + H$	0.5 - 6 0.7 - 3.4 0.7 - 5	MB CB IBGC	89 93 94	2, 7 1 2
$D_2^+ + H_2 \rightarrow H_2D^+ + D$	0.7 - 5	IBGC	94	2
$D_2^+(v) + H_2 \rightarrow HD_2^+ + H$	1.3	REMPI - SB	91	1, 4
$D_2^+ + HD \rightarrow HD_2^+ + D$ $\rightarrow D_3^+ + H$	0.002 - 3	MB	44	1
$D_2^+ + D_2 \rightarrow D_3^+ + D$	1 - 7.5	IBGC	94	2
$H_2^+(v) + H_2 \rightarrow H^+ + \text{products}$	6	PEPICO - CB	66, 95	2, 4, 5
$D_2^+(v) + H_2 \rightarrow H^+ + \text{products}$ $\rightarrow D^+ + \text{products}$	4	PEPICO - CB	66, 95	2, 4, 5
$H_3^+ + D_2 \rightarrow HD_2^+ + H_2$	0.002 - 11 0.1 - 11 0.2 - 8.2	MB MB CB	48 96 97	1 2, 7 1
$D_3^+ + H_2 \rightarrow H_2D^+ + D_2$	0.2 - 2.4	CB	97	1
$H_3^+ + H_2 \rightarrow \text{fast } H^+, H_2^+$	40 - 200	IBGC	49	1

TABLE III. (cont.)

Reaction	Collision energy ^a [eV]	Method ^b	Reference	Comments ^c
$H_2^+ + He \rightarrow HeH^+ + H$	0.05 - 12	MB	51	2, 7
	0.5 - 4.0	CB	98, 99	1, 5
	1.2 - 8.4	IBGC	100	2
$H_2^+(v) + He \rightarrow HeH^+ + H$	3.1	PEPICO - CB	76, 101	2, 4, 5
$H_2^+ + He \rightarrow H^+ + H + He$	3 - 5	CB	102	1, 5
$D_2^+ + He \rightarrow D^+ + D + He$	3 - 5	CB	102	1, 5
$H_2^+(v) + He \rightarrow H^+ + H + He$	3.1	PEPICO - CB	76, 101	2, 4, 5

^a All energies are given as centre-of-mass (cm) collision energies.

^b REMPI — resonance enhanced multiphoton ionization SB — single-beam experiment
Other notations as in Tables I and II

^c Comments:

- 1 — Energy and angular distributions
- 2 — Mainly energy distributions
- 3 — State resolved measurements
- 4 — State selected reactants

- 5 — Detailed comparison with theory
- 6 — Only very limited data
- 7 — Data of limited value for the present purpose (measured laboratory energy distributions have not been fully evaluated)

The CID process shows a very strong dependence on the H_2^+ vibrational state. For $H_2^+ + H_2$, the cross-section increases by a factor of seven in the range $v = 0-6$ (at 4 eV collision energy), whereas for $H_2^+ + He$ the increase amounts to a factor of 24 in the same range of vibrational levels (at 3 eV collision energy). This strong dependence on the initial vibrational state of the reactant ion may be one reason for the rather large discrepancies in the measured total cross-sections, as already mentioned before. It also makes clear once more that knowledge of the internal state distribution of the reactants is very important for edge plasma modelling.

The reaction $H_2^+ + He \rightarrow HeH^+ + H$ shows a very peculiar behaviour. At a collision energy of 1 eV, the cross-section increases dramatically with the vibrational energy of the reactant ion (by a factor of 30 in the range $v = 0-4$). With increasing collision energy, the vibrational dependence becomes weaker until, above 5 eV, the cross-section becomes essentially independent of the vibrational state. Note that the reaction has an endothermicity of 0.80 eV.

4.1.3. Product distributions

Table III gives an overview on measurements of product distributions for reactive collisions. The results

have been obtained with different techniques (IBGC, CB, MB).

In nearly all of the cases, the purpose of these measurements has been to study details of the reaction mechanisms rather than to determine absolute cross-sections. The measurements are therefore normally in relative units. It is possible, however, to put the data on an absolute scale, which can be done in different ways. If the energy and angular distributions of the products (often given in the form of contour plots) are sufficiently complete, they can be integrated over product energies and angles and then be normalized to an absolute total cross-section, which is often known from other experiments. In this way, all the detailed information contained in the differential measurements can be given in absolute units.

Another, very attractive, possibility consists of developing a quantitative theory directly in parallel with the differential scattering experiments. The collision process can thus be studied in great detail by both theory and experiment (this goes far beyond the possibilities in connection with the total cross-section). If satisfactory agreement is obtained, the absolute scales can be derived from theory. This method has been successfully used in a number of cases, in particular for smaller collision systems such as $H^+ + H_2$ and $H_2^+ + He$. It is important, however, that additional experimental

TABLE IV. ENERGY TRANSFER COLLISIONS

Collision system	Type of data ^a	Collision energy ^b [eV]	Method ^c	Reference	Comments ^d		
H ⁺ + H ₂	$\sigma_m(E)$	0.1 - 6000	DE	4	1		
	$\sigma_{0j}(E)$	j = 0 → 2 j = 1 → 3	DE	4	2		
	$\sigma_v(E)$	v = 0 → 1 v = 0 → 2 v = 0 → 3	DE	4	3		
experiment	$P_{0j}(\Theta)$	j = 0 → 0 - 20 j = 1 → 1 - 17	CB	103	6 in [126, 127]		
	$P_{0j}(\Theta)$	j = 1 → 3 - 7	CB	104, 105	6 in [119, 121]		
	$P_{vj}(\Theta)$	v = 0 → 1 j = 1 → 1 - 5	CB	103	--		
	$P_{vj}(\Theta)$	v = 0 → 1 j = 1 → 3 - 7	CB	105	6 in [119]		
	$(d\sigma/d\Omega)_v(E)$	v = 0 → 1 - 4	IBGC	106, 107	4, 6 in [115]		
	$(d\sigma/d\Omega)_v(\Theta)$	v = 0 → 0 - 2 v = 0 → 0 - 3 v = 0 → 0 - 6	10 10 - 20 20	IBGC CB CB	108, 109 105, 110 77	5, 6 in [112] 5, 6 in [120] 5, 6 in [78, 128]	
	$P_v(\Theta)$	v = 0 → 0 - 4 v = 0 → 0 - 3	4 - 16 4.7 - 20	IBGC CB	109 104, 105, 110, 111	6 in [112] 6 in [110, 119 - 121]	
theory I	$(d\sigma/d\Omega)_v(\Theta)$	v = 0 → 0 - 3 v = 0 → 0 - 2	CTC CTC, SCPT	112 113	8 7		
	$\sigma_v(E)$	v = 0 → 0 - 3 v = 0 → 1 - 4 v = 0 → 1 - 3	CTC SCSA CTC	112 114 115, 116	8 7 8		
	theory II	$(d\sigma/d\Omega)_v(\Theta)$	v = 0 → 0 - 4 v = 0 → 0 - 3 v = 0 → 0 - 3	10 - 40 16 - 25 4.7 - 10	QMIPA QMIPA IOSVR	117 118 119	8 8 8
$\sigma_v(E)$		v = 0 → 1 - 3 v = 0 → 1 - 3 v = 0 → 0 - 3	10 - 600 10 - 200 4.7 - 10	QMIPA QMIPA IOSVR	117 118 119	8 8 8	
$(d\sigma/d\Omega)_{vj}(\Theta)$		j = 0 → 0 - 3 j = 1 → 1 - 7	10	IOSVR	119	8	
$\sigma_{vj}(E)$		v = 0 → 0 - 3 j = 0 → 0 - 10 j = 1 → 1 - 11	4.7 - 10	IOSVR	119	8	
theory III		$(d\sigma/d\Omega)_v(\Theta)$	v = 0 → 0 - 3	10	IOSVR	120	9
		$\sigma_v(E)$	v = 0 → 0 - 3	4.7 - 10	IOSVR	120 - 122	9
		$(d\sigma/d\Omega)_{0j}(\Theta)$	j = 0 → 0 - 6 j = 1 → 3 - 7	4.7 - 6 4.7	IOSVR	121	9
	$\sigma_{0j}(E)$	j = 1 → 1 - 11	4.7	IOSVR	121, 122	9	
	$\sigma_{vj}(E)$	v = 0 → 0 - 2 j = 0 → 0 - 10 j = 1 → 1 - 11	6	IOSVR	121, 122	9	

TABLE IV. (cont.)

Collision system	Type of data ^a	Collision energy ^b [eV]	Method ^c	Reference	Comments ^d
H ⁺ + HD	P _v (Θ) v = 0 → 0 - 4	9 - 21	IBGC	109	6 in [112]
	(dσ/dΩ) _v (Θ) v = 0 → 0 - 3	10	CTC	112	8
	σ _v (E) v = 0 → 0 - 3	10	CTC	112	8
H ⁺ + D ₂	P _v (Θ) v = 0 → 0 - 5	4 - 10	IBGC	109	6 in [112]
	(dσ/dΩ) _v (Θ) v = 0 → 0 - 3	10	CTC	112	8
	σ _v (E) v = 0 → 0 - 3	10	CTC	112	8
D ⁺ + H ₂	(dσ/dΩ) _v (E) v = 0 → 1 - 4	20 - 1600	IBGC	107	4, 6 in [115]
	σ _v (E) v = 0 → 1 - 3	35 - 1000	CTC	115	8
H ₂ ⁺ + H ₂	σ _v (E) v = 0 → 1 excitation of H ₂ ⁺	1.2 - 6000	DE	4	3
	(dσ/dΩ) _v (E) v = 0 → 1 - 3 excitation of H ₂	70 - 400	IBGC	106	4
	(dσ/dΩ) _v (E) Δv = -1, -2, -3 deexcitation of H ₂ ⁺	70 - 400	IBGC	123	4
H ₃ ⁺ + H ₂	σ _m (E)	0.1 - 6000	DE	4	1
He ⁺ + H ₂	(dσ/dΩ) _v (Θ) v = 0 → 0 - 5	170	CB	124	5
H ⁻ + H ₂	σ _m (E)	0.1 - 6000	DE	4	1
	(dσ/dΩ) _v (E) v = 0 → 1 - 2	20 - 120	CB	125	4

^a σ_m — momentum transfer cross-section; σ_{0j} — integral cross-section for individual rotational transitions in the vibrational ground state v = 0; σ_{vj} — integral cross-section for individual rotational-vibrational transitions; σ_v — integral cross-section for vibrational transitions (summed and averaged over final and initial rotational states, respectively); (dσ/dΩ)_{0j}, (dσ/dΩ)_{vj}, (dσ/dΩ)_v — corresponding differential cross-sections; P_{0j}, P_{vj}, P_v — corresponding transition probabilities [P_α = (dσ/dΩ)_α/Σ_α(dσ/dΩ)_α].

^b All energies are given as centre-of-mass (cm) collision energies.

^c DE — data evaluation combining different sources of information
 CB — crossed beam experiment
 IBGC — ion beam gas cell experiment
 CTC — classical trajectory calculation
 SCPT — semi-classical (time dependent) perturbation theory

SCSA — semi-classical (rotationally and vibrationally) sudden approximation
 QMIPA — quantum mechanical impact parameter approach
 IOSVR — infinite order sudden vib-rotor calculations (IOS for rotation, 'exact' close coupling for vibration)

^d Comments:

- 1 — Data largely based on extrapolation and/or interpolation (with relatively large uncertainties)
- 2 — Data based on very limited experimental data
- 3 — Data mainly based on theory
- 4 — Partial cross-sections for forward scattering

- 5 — Experimental data in relative units, normalized to theory
- 6 — Detailed comparison with theory in Ref. [x]
- 7 — Calculations based on DIMZO potential surface
- 8 — Calculations based on Giese-Gentry fit potential surface
- 9 — Calculations based on complete ab initio CI potential surface

checks can be made. As discussed in Section 3, simple ion-atom scattering systems can be used as secondary standards for directly measuring absolute differential cross-sections in CB experiments. This method will certainly find more extensive application in future experiments. If all methods are combined, there will be plenty of possibilities to cross-check the data so that a comprehensive and reliable picture can finally be obtained.

4.2. Energy transfer collisions

Table IV summarizes the available information on energy transfer collisions. We have included the data recently evaluated by Phelps [4]. The main part of Table IV refers to original work.

From among the systems taken into consideration, there is only one system — H⁺ + H₂ including isotopic variants — which has been studied rather extensively.

TABLE V. NEGATIVE ION COLLISIONS

Reaction	Type of data ^a	Collision energy ^b [eV]	Method ^c	Reference	Comments ^d
$H^- + H \rightarrow H + \text{products}$	$\sigma(E)$	32 - 10 ³ 200 - 10 ⁴ 500 - 10 ⁵	CB (FND) CB (SID, DED) IBGC (FND)	18 129 130	1, 2 13 in [5]
	$I_n(\Theta)$	70 - 670	CB (FND, TOF)	131	3
$H^- + H \rightarrow H + H^-$	$\sigma(E)$	4 - 200 20 - 5000	CB (SID) CB (SID)	132 129	2, 3 12 in [159, 160]
	$I_n(\Theta)$	70 - 200	CB (FND, TOF)	131	3
$H^- + H \rightarrow H + H + e$ $\rightarrow H_2 + e$	$\sigma(E)$	2 - 200 50 - 150 200 - 10 ⁴	CB (DED) CB (FND, TOF) CB (DED)	132 131 129	2, 3, 4 12 in [160 - 165]
	$I_n(\Theta)$	70 - 200	CB (FND, TOF)	131	3
$H^- + H_2 \rightarrow H + H_2 + e$	$\sigma(E)$	1 - 200 3 - 260 7 - 1700 42 - 1300 130 - 6700	IBGC (DED) IBGC (DED) IBGC (DED) CB (FND) IBGC (BAM)	133 134, 135 136 18 137, 138	3, 5, 6 13 in [4, 5]
	$I_n(\Theta)$	20 - 60 200 - 400	CB (FND) CB (FND)	152 139, 140	3
	$I_e(\epsilon, \Theta)$	7 - 2700	CB (DEES)	141, 142	-
$H^- + D_2 \rightarrow HD + D^-$	$\sigma(E)$	0.3 - 3 0.5 - 10 2 - 9	CB IBGC (TMS) IBGC (SID)	143 144 133	7
	$\sigma(E)$	0.5 - 10	IBGC (TMS)	144	8
	$D^- + H_2 \leftrightarrow HD + H^-$				
$H^- + D_2 \rightarrow H + D + D^-$ $D^- + D_2 \rightarrow D + D + D^-$	$\sigma(E)$	9 - 200	IBGC (SID)	133	9
$H^- + He \rightarrow H + He + e$	$\sigma(E)$	2 - 10 ⁷ 2 - 200 3 - 280 80 - 1300 160 - 8000	RA IBGC (DED) IBGC (DED) IBGC (DED) IBGC (BAM)	145, 146 147, 148 149 150 137, 138	3, 10, 11 12 in [166] 13 in [5]
	$I_n(\Theta)$	30 - 150 70 - 1200 400 - 1600	CB (FND) CB (FND) IBGC (FND)	151, 152 153 154	2, 3
	$I_e(\epsilon, \Theta)$	2 - 200 8 - 3200 80 - 400 160 - 8000	CB (DEES) CB (DEES) CB (FND, TOF) IBGC (DEES)	155 141, 142 153, 156 157, 158	2, 3

^a $\sigma(E)$ — total cross-section; $I_n(\Theta)$ — angular distributions of fast neutrals; $I_e(\epsilon, \Theta)$ — energy and angular distributions of detached electrons.

^b All energies are given as centre-of-mass (cm) collision energies.

^c FND — fast neutral detection

SID — slow ion detection

DED — detached electron detection

TOF — time of flight measurement

For the other systems listed in Table IV ($H_2^+ + H_2$, $He^+ + H_2$, $H^- + H_2$), only very limited information is available. Concerning the work on $H^+ + H_2$, the compilation in Table IV is organized in the following way. In the first group, the original experiments are listed. The following three groups (theory I-III) reflect the development of the theoretical calculations at various stages of elaboration. The last groups give complementary results for other isotopic variants of the $H^+ + H_2$ system.

The first calculations, listed under theory I, were based on very approximate or semi-empirical potential surfaces, and relatively simple (classical or semi-classical) scattering approximations were used. In the next step (theory II), the treatment of the collision dynamics was further elaborated on a quantum mechanical basis, which finally resulted in the development of the IOSVR approximation [119]. However, the calculations were still based on the semi-empirical fit potential originally derived by Giese and Gentry [112], and the comparison with experiment was still unsatisfactory. It was only after Schinke and co-workers [120, 121] calculated a new ab initio potential surface which extended over a sufficiently large configuration space of the H_3^+ system (theory III) that they were able to show that theory and experiment could be brought into full quantitative agreement.

The present example of $H^+ + H_2$ energy transfer collisions clearly shows the importance of combining theory and experiment in a joint effort. The experimental measurements are normally restricted to a limited range of energies and angles. Once the theory is developed and tested against the experimental results, the calculations can provide the full description of the processes and the complete set of data needed for modelling can be obtained. In the present case, such calculations are still pending.

4.3. Negative ion collisions

Table V presents a collection of data for negative ion collisions. It has yet to be ascertained if negative ions play a significant role in the edge plasma. One can expect, however, that the H^- ion is a relatively abundant species, at least in the regions of lower temperature. Therefore, it appears appropriate to consider collision processes of H^- with the main neutral constituents, i.e. H , H_2 and He ; it is understood that the discussion includes all different combinations of hydrogen isotopes.

The most important collision processes in the edge relevant energy range are resonant charge transfer, electron detachment and particle interchange reactions. The two former processes have been widely studied and are rather well documented. In addition to total cross-sections, data on product distributions are also included in Table V. In contrast, only little information is available on particle interchange reactions.

In our laboratory we have recently performed an experimental study of low energy $H^- + H_2$ (D_2) collisions using the CB technique [143]. Various processes, including elastic, inelastic and reactive scattering, have been studied. The data obtained by these measurements are suited to demonstrate the present possibilities of a high resolution CB experiment. The measurements reach down to impact energies of 0.3 eV in the laboratory system. The primary results are rotationally and vibrationally state resolved differential cross-sections which are directly obtained in absolute units using $H^- + He$ as a reference system. These data can then be integrated over angles and summed over product states, which finally yields total cross-sections for specific product channels. As an example of these measurements, the total cross-section for the particle interchange reaction $H^- + D_2 \rightarrow HD + D^-$ is shown in Fig. 6. Also shown are the results previously reported by Michels and

DEES — detached electron energy spectra

RA — review article

BAM — beam attenuation method

Other notations as in Tables I-IV

^d Comments:

- | | |
|---|--|
| 1 — These measurements represent essentially the sum of charge transfer and electron detachment | 7 — Data are presented in Fig. 6 (see text) |
| 2 — Good/fair agreement between different measurements | 8 — These data probably have large uncertainties (see text) |
| 3 — Measurements have been performed for different isotopic combinations | 9 — The SID signal is tentatively assigned to dissociative charge transfer for this energy range |
| 4 — At energies $E \leq 2$ eV, associative detachment becomes the dominant channel | 10 — Fair agreement between more recent measurements |
| 5 — Considerable discrepancies between different measurements at low energies | 11 — Data of Huq et al. [148] are recommended for the low energy region |
| 6 — Data of Huq et al. [133] are recommended for the low energy region | 12 — Theoretical results in Ref. [x] |
| | 13 — Evaluated/recommended data in Ref. [x] |

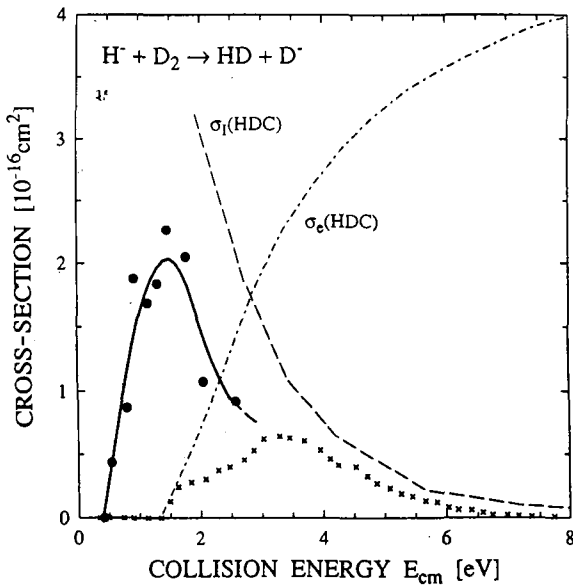


FIG. 6. Total cross-section for the particle interchange reaction $H^- + D_2 \rightarrow HD + D^-$. Full circles and solid line: Zimmer and Linder [143]; crosses: Michels and Paulson [144]. The curves σ_e (HDC) and σ_i (HDC) represent the total cross-sections for electron detachment and for slow ion production, respectively, measured by Huq et al. [133].

Paulson [144]. The discrepancy observed at energies below 3 eV must presumably be attributed to transmission and collection efficiency problems in their TMS instrument. This is supported by measurements of Huq et al. [133], which are also included in Fig. 6 for comparison. The curve σ_e gives the total electron detachment cross-section, whereas σ_i represents the total cross-section for slow ion production. It must be mentioned that Huq et al. could not distinguish between H^- and D^- products, since no mass analysis was provided in their experiment. Nevertheless, the main portion of σ_i can be attributed to D^- products resulting from the reaction $H^- + D_2 \rightarrow HD + D^-$. However, at the lowest energies measured, the SID signal probably contains a certain fraction of H^- ions resulting from large angle elastic and inelastic scattering, so that σ_i must be regarded as an upper limit for the particle interchange cross-section. In any case, the results shown in Fig. 6 nicely demonstrate the competition between reactive scattering and electron detachment in negative ion collisions.

Finally, we mention that collision processes involving H^-/D^- ions, in particular production and destruction processes of these ions in hydrogen discharges, are extensively discussed in connection with the development of H^-/D^- volume sources [14–16].

5. SUMMARY AND CONCLUSIONS

The range of collision processes relevant to fusion edge plasmas is extremely wide. The present article is concerned with ion–molecule collisions in the energy range 1–200 eV. For reasons of available space, the subject has been limited to collision systems involving hydrogen and helium — the main plasma constituents. Both reactive and energy transfer collisions are considered. Besides total cross-sections, the present survey also includes more specific classes of data (state selective cross-sections, product distributions, etc.) which are needed for edge plasma modelling.

In accordance with the energy range of interest, the data have been collected mainly from low energy beam experiments. The different experimental methods used in this field have been discussed briefly and their individual strengths and weaknesses characterized. The importance of making absolute measurements is emphasized.

Several conclusions can be drawn from the present survey. Although only systems with hydrogen and helium — the most elementary constituents of the edge plasma — are considered, there are still significant gaps and, in some cases, large uncertainties in the database for edge relevant energies. Even for very fundamental processes such as charge transfer in $H^+ + H_2$ and $He^+ + H_2$, the data are in a quite unsatisfactory state. With the available experimental techniques, it should be possible to aim at a 10% confidence level of the cross-section data.

A point of particular importance is the strong dependence on the initial reactant states observed for some processes. As a consequence, at least an approximate knowledge of the internal state distribution of the reactants seems necessary for edge plasma modelling. Systematic studies with state selected reactants have only begun and, within the range of the present systems, the only existing measurements are those for the H_2^+ molecular ion. Corresponding measurements for the H_2 neutral molecule in well defined excited states are not available at the present time.

In some cases, the combination of theory and experiment has proved very successful. The experimental measurements are normally restricted to a certain range of experimental parameters. Once the theory is checked against the experimental results, the full picture of the processes and the complete set of data can be derived from the theoretical calculations. Another aspect is the range of systems and processes. Also in this respect are the experiments often confronted with serious limitations. The required procedure is to develop and test

theoretical methods against experiment for certain prototype cases. Once this is done, the methods can be extended and applied to systems and processes which are difficult to access experimentally. The hydrogen and helium systems treated in this paper should be particularly suitable for this type of work. One should keep in mind, however, that molecular collision systems are far more complex than ion-atom systems.

Further work on the present subject is clearly needed. We suggest that such work should proceed along the following lines. The scope has to be widened to include a broader range of collision systems which are important in edge plasma studies. Information from swarm type experiments and low keV beam experiments should be taken into account; this can serve as an additional consistency check on either end of the present energy range. The most important point, however, is that more experiments be performed at edge relevant energies. As demonstrated in this paper, the required experimental methods are available. The experiments should be connected with theory as closely as possible, as outlined above. It is evident from the discussion that substantial effort is still needed to provide a sufficiently complete and reliable database for edge plasma modelling.

ACKNOWLEDGEMENTS

The authors would like to thank Dr. R.K. Janev for valuable advice and encouragement. This article was motivated by the IAEA Specialists Meeting on Review of the Status of Atomic and Molecular Data for Fusion Edge Plasma Studies (Vienna, September 1989). Further input came from the IAEA First Research Co-ordination Meeting on this topic (Vienna, September 1990). Thanks are due to the participants of these meetings for valuable discussions.

The work at the University of Kaiserslautern has been supported by the Deutsche Forschungsgemeinschaft under SFB 91.

REFERENCES

- [1] JANEV, R.K., HARRISON, M.F.A., DRAWIN, H.W., Nucl. Fusion **29** (1989) 109.
- [2] TAWARA, H., PHANEUF, R.A., Comments At. Mol. Phys. **21** (1988) 177.
- [3] JANEV, R.K., LANGER, W.D., EVANS, K., POST, D.E., Elementary Processes in Hydrogen-Helium Plasmas, Springer Verlag, Heidelberg (1987).
- [4] PHELPS, A.V., J. Phys. Chem. Ref. Data **19** (1990) 653.
- [5] BARNETT, C.F., Collisions of H, H₂, He and Li Atoms and Ions with Atoms and Molecules, Atomic Data for Fusion, Vol. 1, Rep. ORNL-6086, Oak Ridge National Laboratory, Oak Ridge, TN (1990).
- [6] TAWARA, H., ITIKAWA, Y., ITOH, Y., et al., Atomic Data Involving Hydrogens Relevant to Edge Plasmas, Rep. IPPJ-AM-46, Institute of Plasma Physics, Nagoya University (1986).
- [7] TAWARA, H., KATO, T., NAKAI, Y., At. Data Nucl. Data Tables **32** (1985) 235.
- [8] NAKAI, Y., SHIRAI, T., TABATA, T., ITO, R., At. Data Nucl. Data Tables **37** (1987) 69.
- [9] GERLICH, D., in State-Selected and State-to-State Ion-Molecule Reaction Dynamics: Experiment, Part I, to be published in Adv. Chem. Phys.
- [10] BISCHOF, G., LINDER, F., Z. Phys., D **1** (1986) 303.
- [11] NICKEL, J.C., ZETNER, P.W., SHEN, G., TRAJMAR, S., J. Phys., E: Sci. Instrum. **22** (1989) 730.
- [12] MILLER, D.R., in Atomic and Molecular Beam Methods, Oxford University Press, Oxford (1988).
- [13] MÜLLER, H., ZIMMER, M., LINDER, F., State-resolved measurements of rotational excitation in H⁻-H₂ collisions at low eV energies, to be published in J. Phys., B; ZIMMER, M., LINDER, F., Crossed-beam study of the H⁻ + D₂ → HD(v') + D⁻ rearrangement reaction in the collision energy range 0.3-3 eV, to be published in J. Phys., B.
- [14] BACAL, M., Phys. Scr. **T2/2** (1982) 467.
- [15] BACAL, M., Nucl. Instrum. Methods B **37&38** (1989) 28.
- [16] BACAL, M., SKINNER, D.A., Comments At. Mol. Phys. **23** (1990) 283.
- [17] HOLLIDAY, M.G., MUCKERMAN, J.T., FRIEDMAN, L., J. Chem. Phys. **54** (1971) 1058.
- [18] GEALY, M.W., VAN ZYL, B., Phys. Rev., A **36** (1987) 3091.
- [19] GUSTAFSSON, E., LINDHOLM, E., Ark. Fysik **18** (1960) 219.
- [20] CRAMER, W.H., J. Chem. Phys. **35** (1961) 836.
- [21] KOOPMAN, D.W., Phys. Rev. **154** (1967) 79.
- [22] STEDEFORD, J.B.H., HASTED, J.B., Proc. R. Soc. London, Ser. A., Math. Phys. **227** (1955) 466.
- [23] KRENOS, J.R., PRESTON, R.K., WOLFGANG, R., TULLY, J.C., J. Chem. Phys. **60** (1974) 1634.
- [24] OCHS, G., TELOY, E., J. Chem. Phys. **61** (1974) 4930.
- [25] SCHLIER, Ch., NOWOTNY, U., TELOY, E., Chem. Phys. **111** (1987) 401.
- [26] MAIER, W.B., II, J. Chem. Phys. **54** (1971) 2732.
- [27] KRENOS, J.R., WOLFGANG, R., J. Chem. Phys. **52** (1970) 5961.
- [28] CRAMER, W.H., MARCUS, A.B., J. Chem. Phys. **32** (1960) 186.
- [29] KARPAS, Z., ANICICH, V., HUNTRESS, W.T., J. Chem. Phys. **70** (1979) 2877.
- [30] FITE, W.L., BRACKMANN, R.T., SNOW, W.R., Phys. Rev. **112** (1958) 1161.
- [31] WENDELL, K.L., ROL, P.K., J. Chem. Phys. **61** (1974) 2059.
- [32] MORAN, T.F., ROBERTS, J.R., J. Chem. Phys. **49** (1968) 3411.
- [33] VANCE, D.W., BAILEY, T.L., J. Chem. Phys. **44** (1966) 486.

- [34] GILBODY, H.B., HASTED, J.B., Proc. R. Soc. London, Ser. A, Math. Phys. **238** (1956) 334.
- [35] ROTHWELL, H.L., VAN ZYL, B., AMME, R.C., J. Chem. Phys. **61** (1974) 3851.
- [36] NODA, N., J. Phys. Soc. Jpn. **43** (1977) 1021.
- [37] HAYDEN, H.C., AMME, R.C., Phys. Rev. **172** (1968) 104.
- [38] GHOSH, S.N., SHERIDAN, W.F., J. Chem. Phys. **26** (1957) 480.
- [39] STOCKER, R.N., NEUMANN, H., J. Chem. Phys. **61** (1974) 3852.
- [40] GENTRY, W.R., McCLURE, D.J., DOUGLASS, C.H., Rev. Sci. Instrum. **46** (1975) 367.
- [41] NEYNABER, R.H., TRUJILLO, S.M., Phys. Rev. **167** (1968) 63.
- [42] SPECHT, L.T., FOSTER, K.D., MUSCHLITZ, E.E., J. Chem. Phys. **63** (1975) 1582.
- [43] GIESE, C.F., MAIER, W.B., II, J. Chem. Phys. **39** (1963) 739.
- [44] DOUGLASS, C.H., McCLURE, D.J., GENTRY, W.R., J. Chem. Phys. **67** (1977) 4931.
- [45] TUNITSKIJ, N.N., ZHURKIN, E.S., KAMINSKIJ, V.A., TIKHOMIROV, M.V., Sov. Phys. - Tech. Phys. **15** (1971) 1652.
- [46] ZHURKIN, E.S., KAMINSKIJ, V.A., TIKHOMIROV, M.V., TUNITSKIJ, N.N., Sov. Phys. - Tech. Phys. **18** (1973) 259.
- [47] ZHURKIN, E.S., TIKHOMIROV, M.V., TUNITSKIJ, N.N., Sov. Phys. - Tech. Phys. **16** (1971) 495.
- [48] DOUGLASS, C.H., RINGER, G., GENTRY, W.R., J. Chem. Phys. **76** (1982) 2423.
- [49] LANGE, G., HUBER, B., WIESEMANN, K., Z. Phys., A **281** (1977) 21.
- [50] HUBER, B., SCHULZ, U., WIESEMANN, K., Phys. Lett., A **79** (1980) 58.
- [51] NEYNABER, R.H., MAGNUSON, G.D., J. Chem. Phys. **59** (1973) 825.
- [52] RUTHERFORD, J.A., VROOM, D.A., J. Chem. Phys. **58** (1973) 4076.
- [53] SCHLIER, Ch., cited in Ref. [54].
- [54] SCHNEIDER, F., HAVEMANN, U., ZÜLICHE, L., HERMAN, Z., Chem. Phys. Lett. **48** (1977) 439.
- [55] ROZETT, R.W., KOSKI, W.S., J. Chem. Phys. **49** (1968) 2691.
- [56] WU, R.L.C., HOPPER, D.G., Chem. Phys. **57** (1981) 385.
- [57] HOPPER, D.G., WU, R.L.C., Chem. Phys. Lett. **81** (1981) 230.
- [58] JONES, E.G., WU, R.L.C., HUGHES, B.M., TIERNAN, T.O., HOPPER, D.G., J. Chem. Phys. **73** (1980) 5631.
- [59] ROZETT, R.W., KOSKI, W.S., J. Chem. Phys. **48** (1968) 533.
- [60] MORAN, T.F., CONRADS, R.J., J. Chem. Phys. **58** (1973) 3793.
- [61] ERVIN, K.M., ARMENTROUT, P.B., J. Chem. Phys. **86** (1987) 6240.
- [62] THEARD, L.P., HUNTRESS, W.T., J. Chem. Phys. **60** (1974) 2840.
- [63] LIAO, C.L., LIAO, C.X., NG, C.Y., J. Chem. Phys. **81** (1984) 5672.
- [64] LIAO, C.L., NG, C.Y., J. Chem. Phys. **84** (1986) 197.
- [65] CAMPBELL, F.M., BROWNING, R., LATIMER, C.J., J. Phys., B **14** (1981) 3493.
- [66] GUYON, P.M., BAER, T., COLE, S.K., GOVERS, R.T., Chem. Phys. **119** (1988) 145.
- [67] ANDERSON, S.L., HOULE, F.A., GERLICH, D., LEE, Y.T., J. Chem. Phys. **75** (1981) 2153.
- [68] VAN PIJKEREN, D., BOLTJES, E., VAN ECK, J., NIEHAUS, A., Chem. Phys. **91** (1984) 293.
- [69] SHAO, J.D., NG, C.Y., J. Chem. Phys. **84** (1986) 4317.
- [70] KOYANO, I., TANAKA, K., J. Chem. Phys. **72** (1980) 4858.
- [71] CHUPKA, W.A., RUSSELL, M.E., REFAEY, K., J. Chem. Phys. **48** (1968) 1518.
- [72] CHUPKA, W.A., RUSSELL, M.E., J. Chem. Phys. **49** (1968) 5426; CHUPKA, W.A., BERKOWITZ, J., RUSSELL, M.E., Abstr. VI. ICPEAC, MIT Press, Cambridge, MA (1969) 71.
- [73] BAER, M., SUZUKI, S., TANAKA, K., et al., Phys. Rev., A **34** (1986) 1748.
- [74] HERMAN, Z., KOYANO, I., J. Chem. Soc. Faraday Trans. **83** (1987) 127.
- [75] TURNER, T., DUTUIT, O., LEE, Y.T., J. Chem. Phys. **81** (1984) 3475.
- [76] GOVERS, T.R., GUYON, P.M., Chem. Phys. **113** (1987) 425.
- [77] NIEDNER, G., NOLL, M., TOENNIES, J.P., SCHLIER, Ch., J. Chem. Phys. **87** (1987) 2685.
- [78] BAER, M., NIEDNER-SCHATTEBURG, G., TOENNIES, J.P., J. Chem. Phys. **91** (1989) 4169.
- [79] ISLER, R.C., NATHAN, R.D., Phys. Rev., A **6** (1972) 1036.
- [80] DUNN, G.H., GEBALLE, R., PRETZER, D., Phys. Rev. **128** (1962) 2200.
- [81] GUSEV, V.A., POLYAKOVA, G.N., ERKO, V.F., FOGEL, Ya.M., ZATS, A.V., Abstr. VI. ICPEAC, MIT Press, Cambridge, MA (1969) 809.
- [82] POLYAKOVA, G.N., GUSEV, V.A., ERKO, V.F., FOGEL, Ya.M., ZATS, A.V., Sov. Phys. - JETP **31** (1970) 637.
- [83] POLYAKOVA, G.N., ERKO, V.F., ZATS, A.V., Opt. Spectrosc. **29** (1970) 219.
- [84] VAN ZYL, B., JAECKS, D., PRETZER, D., GEBALLE, R., Phys. Rev. **158** (1967) 29.
- [85] YOUNG, R.A., STEBBINGS, R.F., MCGOWAN, J.W., Phys. Rev. **171** (1968) 85.
- [86] TELOY, E., in *Electronic and Atomic Collisions*, North-Holland, Amsterdam (1978) 591.
- [87] GERLICH, D., *Reaktionen von Protonen mit Wasserstoff bei Stossenergien von 0.4 eV bis 10 eV*, PhD Thesis, University of Freiburg (1977).
- [88] LEES, A.B., ROL, P.K., J. Chem. Phys. **63** (1975) 2461.
- [89] LEES, A.B., ROL, P.K., J. Chem. Phys. **61** (1974) 4444.
- [90] GENTRY, W.R., RINGER, G., J. Chem. Phys. **67** (1977) 5398.
- [91] POLLARD, J.E., LICHTIN, D.A., COHEN, R.B., Chem. Phys. Lett. **152** (1988) 171.
- [92] HIERL, P.M., HERMAN, Z., Chem. Phys. **50** (1980) 249.
- [93] KRENOS, J.R., LEHMANN, K.K., TULLY, J.C., HIERL, P.M., SMITH, G.P., Chem. Phys. **16** (1976) 109.



- [94] DOVERSPIKE, L.D., CHAMPION, R.L., *J. Chem. Phys.* **46** (1967) 4718.
- [95] EAKER, C.W., SCHATZ, G.C., *J. Chem. Phys.* **89** (1988) 6713.
- [96] LEES, A.B., ROL, P.K., *J. Chem. Phys.* **63** (1975) 5077.
- [97] VESTAL, M.L., BLAKLEY, C.R., RYAN, P.W., FUTRELL, J.H., *J. Chem. Phys.* **64** (1976) 2094.
- [98] SCHNEIDER, F., HAVEMANN, U., ZÜLICHE, L., PACÁK, V., BIRKINSHAW, K., HERMAN, Z., *Chem. Phys. Lett.* **37** (1976) 323.
- [99] PACÁK, V., HAVEMANN, U., HERMAN, Z., SCHNEIDER, F., ZÜLICHE, L., *Chem. Phys. Lett.* **49** (1977) 273.
- [100] LEVENTHAL, J.J., *J. Chem. Phys.* **54** (1971) 3279; **58** (1973) 4710.
- [101] SIZUN, M., GISLASON, E.A., *J. Chem. Phys.* **91** (1989) 4603.
- [102] HAVEMANN, U., PACÁK, V., HERMAN, Z., SCHNEIDER, F., ZUHRT, Ch., ZÜLICHE, L., *Chem. Phys.* **28** (1978) 147.
- [103] RUDOLPH, K., TOENNIES, J.P., *J. Chem. Phys.* **65** (1976) 4483.
- [104] SCHMIDT, H., HERMANN, V., LINDER, F., *J. Chem. Phys.* **69** (1978) 2734.
- [105] HERMANN, V., SCHMIDT, H., LINDER, F., *J. Phys.*, **B 11** (1978) 493.
- [106] MOORE, J.H., DOERING, J.P., *Phys. Rev. Lett.* **23** (1969) 564.
- [107] HERRERO, F.A., DOERING, J.P., *Phys. Rev.*, **A 5** (1972) 702.
- [108] UDSETH, H., GIESE, C.F., GENTRY, W.R., *J. Chem. Phys.* **54** (1971) 3642.
- [109] UDSETH, H., GIESE, C.F., GENTRY, W.R., *Phys. Rev.*, **A 8** (1973) 2483.
- [110] SCHINKE, R., KRÜGER, H., HERMANN, V., SCHMIDT, H., LINDER, F., *J. Chem. Phys.* **67** (1977) 1187.
- [111] SCHMIDT, H., HERMANN, V., LINDER, F., *Chem. Phys. Lett.* **41** (1976) 365.
- [112] GIESE, C.F., GENTRY, W.R., *Phys. Rev.*, **A 10** (1974) 2156.
- [113] COLLINS, F.S., PRESTON, R.K., CROSS, R.J., *Chem. Phys. Lett.* **25** (1974) 608.
- [114] COLLINS, F.S., CROSS, R.J., *J. Chem. Phys.* **65** (1976) 644.
- [115] GENTRY, W.R., GIESE, C.F., *Phys. Rev.*, **A 11** (1975) 90.
- [116] SKODJE, R.T., GENTRY, W.R., GIESE, C.F., *J. Chem. Phys.* **65** (1976) 5532.
- [117] KRÜGER, H., SCHINKE, R., *J. Chem. Phys.* **66** (1977) 5087.
- [118] SCHINKE, R., *Chem. Phys.* **24** (1977) 379.
- [119] SCHINKE, R., McGUIRE, P., *Chem. Phys.* **31** (1978) 391.
- [120] SCHINKE, R., DUPUIS, M., LESTER, W.A., *J. Chem. Phys.* **72** (1980) 3909.
- [121] SCHINKE, R., *J. Chem. Phys.* **72** (1980) 3916.
- [122] LINDER, F., in *Electronic and Atomic Collisions*, North-Holland, Amsterdam (1980) 535.
- [123] HERRERO, F.A., DOERING, J.P., *Phys. Rev. Lett.* **29** (1972) 609.
- [124] LEBÉHOT, A., CAMPARGUE, R., *J. Phys.*, **B 15** (1982) 1711.
- [125] HEGE, U., LINDER, F., *Z. Phys.*, **A 320** (1985) 95.
- [126] McGUIRE, P., *J. Chem. Phys.* **65** (1976) 3275.
- [127] McGUIRE, P., RUDOLPH, K., TOENNIES, J.P., *J. Chem. Phys.* **65** (1976) 5522.
- [128] BAER, M., NIEDNER, G., TOENNIES, J.P., *J. Chem. Phys.* **88** (1988) 1461.
- [129] HUMMER, D.G., STEBBINGS, R.F., FITE, W.L., BRANSCOMB, L.M., *Phys. Rev.* **119** (1960) 668.
- [130] GEDDES, J., HILL, J., SHAH, M.B., GOFFE, T.V., GILBODY, H.B., *J. Phys.*, **B 13** (1980) 319.
- [131] ESAULOV, V.A., *J. Phys.*, **B 13** (1980) 4039.
- [132] HUELS, M.A., CHAMPION, R.L., DOVERSPIKE, L.D., WANG, Y., *Phys. Rev.*, **A 41** (1990) 4809.
- [133] HUQ, M.S., DOVERSPIKE, L.D., CHAMPION, R.L., *Phys. Rev.*, **A 27** (1983) 2831.
- [134] MUSCHLITZ, E.E., BAILEY, T.L., SIMONS, J.H., *J. Chem. Phys.* **24** (1956) 1202.
- [135] MUSCHLITZ, E.E., BAILEY, T.L., SIMONS, J.H., *J. Chem. Phys.* **26** (1957) 711.
- [136] HASTED, J.B., SMITH, R.A., *Proc. R. Soc. London, Ser. A, Math. Phys.* **235** (1956) 349.
- [137] RISLEY, J.S., GEBALLE, R., *Phys. Rev.*, **A 9** (1974) 2485.
- [138] RISLEY, J.S., *Phys. Rev.*, **A 10** (1974) 731.
- [139] TUAN, V.N., ESAULOV, V.A., *J. Phys.*, **B 15** (1982) L 95.
- [140] TUAN, V.N., ESAULOV, V.A., GAUYACQ, J.P., HERZENBERG, A., *J. Phys.*, **B 18** (1985) 721.
- [141] MONTMAGNON, J.L., ESAULOV, V.A., GROUARD, J.P., et al., *J. Phys.*, **B 16** (1983) L 143.
- [142] ESAULOV, V.A., GROUARD, J.P., HALL, R.I., et al., *J. Phys.*, **B 17** (1984) 1855.
- [143] See Ref. [13].
- [144] MICHELS, H.H., PAULSON, J.F., in *Potential Energy Surfaces and Dynamics Calculations*, Plenum Press, New York (1981) 535.
- [145] RISLEY, J.S., in *Electronic and Atomic Collisions*, North-Holland, Amsterdam (1980) 619.
- [146] RISLEY, J.S., *Comments At. Mol. Phys.* **12** (1983) 215.
- [147] CHAMPION, R.L., DOVERSPIKE, L.D., LAM, S.K., *Phys. Rev.*, **A 13** (1976) 617.
- [148] HUQ, M.S., DOVERSPIKE, L.D., CHAMPION, R.L., ESAULOV, V.A., *J. Phys.*, **B 15** (1982) 951.
- [149] BAILEY, T.L., MAY, C.J., MUSCHLITZ, E.E., *J. Chem. Phys.* **26** (1957) 1446.
- [150] HASTED, J.B., *Proc. R. Soc. London, Ser. A, Math. Phys.* **212** (1952) 235.
- [151] HEGE, U., ITOH, Y., LINDER, F., *J. Phys.*, **B 18** (1985) 2705.
- [152] HEGE, U., *Elektronen-Detachment und Schwingungsanregung bei H⁻/D⁻ Stossprozessen*, PhD Thesis, University of Kaiserslautern (1984).
- [153] ESAULOV, V.A., DHUICQ, D., GAUYACQ, J.P., *J. Phys.*, **B 11** (1978) 1049.
- [154] Van der LEEUW, P.E., TIP, A., KOOT, W., KLEYN, A.W., LOS, J., *Chem. Phys.* **101** (1986) 183.
- [155] ITOH, Y., HEGE, U., LINDER, F., *J. Phys.*, **B 20** (1987) 3437.

- [156] TUAN, V.N., GAUYACQ, J.P., ESAULOV, V.A.,
J. Phys., B **16** (1983) L 95.
- [157] GEBALLE, R., RISLEY, J.S., Abstr. VIII. ICPEAC,
Belgrade (1973) 834.
- [158] RISLEY, J.S., in *Atomic Physics*, Vol. 4, Plenum Press,
New York (1975) 487.
- [159] DALGARNO, A., McDOWELL, M.R.C., *Proc. Phys.
Soc.*, A **69** (1956) 615.
- [160] BARDSLEY, J.N., *Proc. Phys. Soc.* **91** (1967) 300.
- [161] BROWNE, J.C., DALGARNO, A., *J. Phys.*, B **2** (1969)
885.
- [162] DALGARNO, A., BROWNE, J.C., *Astrophys. J.* **149**
(1967) 231.
- [163] JANEV, R.K., *Astron. Astrophys.* **35** (1974) 161.
- [164] BIENIEK, R.J., DALGARNO, A., *Astrophys. J.* **228** (1979)
635.
- [165] BIENIEK, R.J., *J. Phys.*, B **13** (1980) 4405; **14** (1981)
1707.
- [166] GAUYACQ, J.P., *J. Phys.*, B **13** (1980) 4417.

RADIATIVE LOSSES AND ELECTRON COOLING RATES FOR CARBON AND OXYGEN PLASMA IMPURITIES

X. BONNIN, R. MARCHAND

Energie et matériaux,
Institut national de la recherche scientifique,
Université du Québec,
Varenes, Quebec, Canada

R.K. JANEV

Division of Physical and Chemical Sciences,
International Atomic Energy Agency,
Vienna

ABSTRACT. Radiative loss and electron cooling rates are calculated for carbon and oxygen ions under conditions relevant to fusion plasmas. Both rates are based on the most recent recommended atomic data. A modified coronal model which includes the effects of metastable states is described and used in the calculations.

1. INTRODUCTION

Radiative losses can represent a significant contribution to the local power balance and the total energy losses in present tokamaks [1–8]. They should also play an important role in physics and design of future reactors, especially in the plasma edge and divertor regions. For example, line radiation by light impurities in the edge region could help distribute the exhausted power over a large area of the neutralizer plates and, thus, alleviate the erosion problem in the divertor [9]. The presence of heavy impurities in the core, however, will always be detrimental. In addition to diluting the fuel there, strong line radiation by not fully stripped ions will make the conditions required for ignition more difficult to achieve [10–13]. With the design of the next generation machines (ITER) entering its final phase, it is important that the plasma transport models used in this design be equipped with the best available atomic rates. These considerations have recently stimulated much interest in the construction of models for the calculation of atomic and molecular processes and the establishment of atomic databases required in fusion energy research. Over the years, the models have ranged in complexity from the simple average ion approach with semi-empirical rates [14] to detailed calculations using recommended data [15–21]. Although the formalism required for an accurate calculation of

the rates is well established, the effort in computing such rates is still very much in progress. This evolution is tied to the completeness of the atomic data at any given time, and to the continuing efforts to add new and more accurate data to the existing databases.

In this paper we present calculation results for radiative losses and electron cooling rates of carbon and oxygen impurity ions under conditions relevant to tokamak edge plasmas. Our calculations are based on the most recent available recommended atomic data. We also use a modified coronal approximation to account for long lived metastable states.

2. RADIATIVE LOSS AND COOLING RATES

2.1. Generalities

The radiative loss rate is the rate at which energy is lost by radiation, per unit plasma volume, in an optically thin plasma. This loss mechanism is directly measurable experimentally with bolometers. Radiative losses also enter the balance equation for the total (thermal plus ionization) plasma energy [22]. The cooling rate, on the other hand, represents the rate at which electron thermal energy is lost by inelastic collisions with atoms or ions. This process is not measurable directly. It appears as a loss term in the balance equation for the electron thermal energy.

More precisely, the radiative power loss P_r includes the following contributions:

- line radiation associated with the radiative cascade which follows collisional excitation, recombination (dielectronic, radiative and three-body) and charge transfer,
- continuum radiation associated with radiative recombination, and
- bremsstrahlung.

We note that for the densities of interest to tokamak plasmas, three-body recombination is usually negligible. It is mentioned here for completeness.

The electron cooling rate P_e accounts for the following contributions:

- collisional excitation and de-excitation,
- ionization,
- dielectronic, radiative and three-body recombination, and
- bremsstrahlung.

A precise definition of these various contributions follows.

2.2. Definitions

We now give precise definitions for the radiative loss and cooling rates in terms of elementary atomic processes. We start by considering a general definition, valid over a wide range of plasma densities and temperatures. A simpler and more tractable definition, based on a modified coronal approximation, is then presented.

2.2.1. General case

We assume a single ion species of nuclear charge Z and ionization stages i ranging from 0 for neutral to Z for fully ionized. We also assume that the medium is optically thin to all photons radiated. The extension of the definitions to account for multiple ion species is straightforward. The inclusion of opacity effects, however, would considerably increase the complexity of the problem. These effects are not considered here for simplicity. The radiative loss rate P_r and the electron cooling rate P_e are given by

$$P_r = \sum_{i\alpha} n_{i\alpha} \left\{ \sum_{\beta} A_{\alpha\beta}^i \epsilon_{\beta\alpha}^i + n_e \sum_{\beta} \int d^3v \left(\frac{1}{2} Mv^2 + \epsilon_{\beta}^{i-1} + \epsilon_{0\alpha}^i \right) v \sigma_{rr,\alpha\beta}^i(v) f(\vec{v}) + n_e B_{\alpha}^i \right\} \quad (1)$$

$$P_e = \sum_{i\alpha} n_e n_{i\alpha} \left\{ \sum_{\beta} X_{\alpha\beta}^i \epsilon_{\alpha\beta}^i + S_{\alpha}^i \epsilon_{\alpha}^i + \sum_{\beta} \int d^3v \frac{1}{2} Mv^2 v \sigma_{rr,\alpha\beta}^i(v) f(\vec{v}) + \sum_{\beta\gamma} \int d^3v \frac{1}{2} Mv^2 v \sigma_{dr,\alpha\beta\gamma}^i(v) f(\vec{v}) - \sum_{\beta} n_e \int d^3v (\epsilon_{\beta}^{i-1} + \epsilon_{0\alpha}^i) v \sigma_{tb,\alpha\beta}^i(v) f(\vec{v}) + B_{\alpha}^i \right\} \quad (2)$$

In these equations, $f(\vec{v})$ is a Maxwellian electron distribution function normalized such that its integral over velocities is equal to unity, n_e is the electron density and $n_{i\alpha}$ is the density of impurity in quantum state α in stage i . The coefficient $A_{\alpha\beta}^i$ is the transition probability for the transition $\alpha \rightarrow \beta$, $\sigma_{rr,\alpha\beta}^i$ is the cross-section for radiative recombination into state β of stage $i-1$, from stage i in state α , B_{α}^i is the rate of bremsstrahlung associated with stage i in state α , $X_{\alpha\beta}^i$ is the excitation rate for the transition $\alpha \rightarrow \beta$, S_{α}^i is the ionization rate from state α , $\sigma_{dr,\alpha\beta\gamma}^i$ is the cross-section for dielectronic recombination into the Rydberg state γ of ionization stage $i-1$, associated with a core transition to state β , from an ion initially in state α of stage i , and $\sigma_{tb,\alpha\beta}^i$ is the cross-section for three-body recombination into state β of stage $i-1$ from stage i in state α . The ionization energy of an ion in stage i , in quantum state α , is represented by ϵ_{α}^i . The excitation energy for the transition $\alpha \rightarrow \beta$ in stage i is $\epsilon_{\alpha\beta}^i$. In these expressions, subscript zero refers to the ground state. In Eqs (1) and (2), the densities $n_{i\alpha}$ are assumed to be known. These densities are obtained in practice by solving a large set of equations in which the states of the various possible ionization stages are all coupled by ionization, excitation, radiative decay, recombination (dielectronic, radiative and three-body) and charge transfer processes. Methods for approximately calculating these densities have been described, for example, in Refs [16, 19–21].

2.2.2. Modified coronal model, with metastable state effects

We now briefly describe the model used in the calculation of the radiative loss and cooling rates. The method of calculation is similar to the familiar coronal approximation [15], with the exception that it accounts for the effect of metastable states when such states exist. We recall that in the usual coronal approximation the plasma is assumed to be optically thin and of sufficiently low density so that all excited states (including the metastable ones) decay radiatively to the ground state

on a time-scale which is much shorter than any collisional time-scale. The present calculations, on the other hand, are based on the following assumptions:

(1) There may be long lived metastable states for which the largest transition probability is smaller than, or comparable to, the largest collisional rate to the ground state or to other metastable states. In practice, all excited states which cannot decay radiatively to a lower energy state via an optically allowed transition will be treated as long lived metastables.

(2) For metastable states, the relative densities $n_{i\alpha}$ for a given ionization stage i are determined by:

- collisional (de)excitation between the ground state and metastable states,
- possible (slow) radiative decay,
- ionization from the ground state and metastable states, and
- excitation from the ground state and metastable states to non-metastable states, followed by radiative cascade back to the ground state or to metastable states.

(3) Multistep processes are neglected for excited non-metastable states.

(4) Recombination, whether radiative or dielectronic, from metastable states may take place. When the recombined ion is in an excited state, it decays instantaneously to its ground state.

(5) For the relatively low densities of interest to tokamak plasmas, three-body recombination is neglected.

In this model, the relative populations $n_{i\alpha}$ of the background state and the metastable states of a given ionization stage i are not affected by recombination from the upper ionization stage, or by the different rates at which recombination takes place from the different states α of stage i . This assumption is motivated by the fact that recombination is generally a slow process. Our calculations using that model will be valid, provided that P_r is dominated by excitation and that P_e is dominated by excitation plus ionization. Our model effectively reduces to the standard coronal approximation for impurities in a strongly recombining regime. In practice, the conditions encountered in the edge and divertor regions of tokamaks correspond to impurities in an ionization regime, and recombination is indeed slow compared with ionization and excitation. In this model, the expression for P_r is

$$P_r = \sum_i \left\{ \sum_{\beta\alpha} n_{i\beta} A_{\beta\alpha}^i \epsilon_{\alpha\beta}^i + \sum_{\alpha\beta\delta} n_{i\alpha} \int d^3v \epsilon_{\delta}^{i-1} v \sigma_{dr,\alpha\beta\delta}^i(v) f(\vec{v}) \right.$$

$$\left. + \sum_{\alpha\beta} n_{i\alpha} \int d^3v \left(\frac{1}{2} M v^2 + \epsilon_{0\alpha}^i + \epsilon_{0\beta}^{i-1} \right) v \sigma_{tr,\alpha\beta}^i(v) f(\vec{v}) + n_H \sum_{\alpha\beta} n_{i\alpha} T_{\alpha\beta}^i \epsilon_{0\beta}^{i-1} + \sum_{\alpha} n_{i\alpha} B_{\alpha}^i \right\} \quad (3)$$

where n_H is the density of neutral hydrogen and $T_{\alpha\beta}^i$ is the rate of charge transfer between neutral hydrogen and an impurity initially in state α of stage i , resulting in stage $i-1$ in state β . The expression for P_e is the same as that given in Eq. (2). The density $n_{i\alpha}$ of states α for a given ionization stage i is obtained by solving the following set of equations:

$$\frac{dn_{i\alpha}}{dt} = \sum_{\beta} [-(A_{\alpha\beta}^i + X_{\alpha\beta}^i)n_{i\alpha} + (A_{\beta\alpha}^i + X_{\beta\alpha}^i)n_{i\beta}] - S_{\alpha}^i n_{i\alpha} + \delta_{0\alpha}^i \sum_{\beta} S_{\beta}^i n_{i\beta} = 0 \quad (4)$$

with the normalization

$$\sum_{\substack{\text{ground state} \\ \text{and metastables}}} n_{i\alpha} = n_i \quad (5)$$

In Eq. (4), the rates S_{α} and $X_{\alpha\beta}$ are assumed to vanish whenever α corresponds to a non-metastable state, in order to be consistent with our neglect of multistep effects from non-metastable states. Also, the last summation on the left hand side of Eq. (4) has been introduced to ensure the existence of a non-trivial solution. Physically, this term means that particles lost by ionization are instantaneously fed back into the ground state. This assumption is somewhat arbitrary. It could have been replaced, for example, by substituting

$$\delta_{0\alpha}^i \sum_{\beta} S_{\beta}^i n_{i\beta} \rightarrow \lambda n_{i\alpha} \quad (6)$$

on the right hand side of Eq. (4), which would correspond to a uniform exponential decay $\exp(-\lambda t)$ for all states of ionization stage i . The exact form of this term should be of little consequence in the final result, provided the rates of excitation $X_{\alpha\beta}^i$ are much larger than the rates of ionization S_{α}^i .

2.2.3. Standard coronal approximation

It will be instructive to compare our results with those obtained in the standard coronal approximation (see Section 4). We recall that in this approximation, the plasma density is assumed to be low, and even metastable states are assumed to decay radiatively to the ground state on a time-scale which is much shorter

than any collisional time-scale. As a result, all collisional processes proceed from the ground state, and multistep processes are negligible. With these assumptions, the expressions for the rates are

$$\begin{aligned}
 P_r = & \sum_i n_{i0} \left\{ n_e \sum_{\alpha} X_{0\alpha}^i \epsilon_{0\alpha}^i \right. \\
 & + n_e \sum_{\alpha} \int d^3v \left(\frac{1}{2} Mv^2 + \epsilon_0^{i-1} \right) v \sigma_{rr,0\alpha}^i(v) f(\vec{v}) \\
 & + n_e \sum_{\alpha\beta} \int d^3v \epsilon_{0\beta}^{i-1} v \sigma_{dr,0\alpha\beta}^i(v) f(\vec{v}) \\
 & \left. + n_H \sum_{\alpha} T_{0\alpha}^i \epsilon_{0\alpha}^{i-1} + n_e B_0^i \right\} \quad (7)
 \end{aligned}$$

$$\begin{aligned}
 P_e = & \sum_i n_e n_{i0} \left\{ \sum_{\alpha} X_{0\alpha}^i \epsilon_{0\alpha}^i + S_0^i \epsilon_0^i \right. \\
 & + \sum_{\alpha} \int d^3v \frac{1}{2} Mv^2 v \sigma_{rr,0\alpha}^i(v) f(\vec{v}) \\
 & \left. + \sum_{\alpha\beta} \int d^3v \frac{1}{2} Mv^2 v \sigma_{dr,0\alpha\beta}^i(v) f(\vec{v}) + B_0^i \right\} \quad (8)
 \end{aligned}$$

We note that, consistent with the low density assumed in the coronal approximation, three-body recombination has been neglected in this definition of P_e .

2.2.4. Steady ionization balance

In the calculation of radiative losses it is customary to consider impurities under so-called steady state [14] or steady ionization [19] balance. This condition will also be considered in Section 4. A given ion species is at steady ionization balance when the rate at which any given ionization stage is lost by ionization and recombination is exactly balanced by the rate at which it is populated by recombination and ionization of neighbouring stages. After some simple algebra, this condition proves to be equivalent to the requirement that the rate at which any stage i ionizes be equal to the rate at which stage $i+1$ recombines. Considering the model of Section 2.2.2 for the purposes of the discussion, this is translated mathematically as

$$\begin{aligned}
 n_i \sum_{\alpha} \frac{n_{i\alpha}}{n_i} S_{\alpha}^i &= n_{i+1} \sum_{\alpha} \frac{n_{i+1\alpha}}{n_{i+1}} \\
 &\times \left(\sum_{\beta} R_{rr,\alpha\beta}^{i+1} + \sum_{\beta\delta} D_{dr,\alpha\beta\delta}^{i+1} + n_H \sum_{\beta} T_{\alpha\beta}^{i+1} \right) \quad (9)
 \end{aligned}$$

where $R_{rr,\alpha\beta}^{i+1}$ is the rate of radiative recombination into state β of stage i , from state α of stage $i+1$, and $D_{dr,\alpha\beta\delta}^{i+1}$ is the rate of dielectronic recombination into state δ of

stage i , from state α of stage $i+1$, associated with a core excitation to state β . The densities $n_{i\alpha}$ are determined in terms of the total density n_i of particles in ionization stage i by Eqs (4) and (5). This constitutes a set of recursive equations for n_i , which can readily be solved for a given total impurity density.

It is important to stress that steady ionization balance is not implied by a steady state solution of the plasma transport equation. Because of transport and recycling, the actual distribution of ionization stages may differ significantly from that of the steady ionization balance computed with the local plasma density and temperature [1, 22–24]. This is why atomic loss rates must be known for individual ionization stages when modelling tokamak plasmas. Following Ref. [15], we call radiative loss and electron cooling functions, respectively, the radiative loss and cooling rates divided by the electron density and the total ion density. Similarly, the radiative loss and cooling coefficients are defined as the radiative loss and cooling functions calculated for ions in a single ionization stage i .

3. ATOMIC DATABASE

Whenever possible, we use recommended data for the atomic processes involved in the power loss functions. When no recommended data are available, semi-empirical data are used. In the next sections we briefly review the sources of the data used for excitation, ionization, radiative and dielectric recombination, and the transition probabilities. The contribution from charge transfer recombination has been included in Eqs (7) and (9) for completeness. This process will now be neglected for simplicity, because of the dependence of the charge transfer rate on the neutral hydrogen density, in addition to the electron density. We stress, however, that charge transfer can be important in many fusion plasma studies [25–27]. The various quantum states considered in the calculations for carbon and oxygen ions are listed in the Appendix.

3.1. Excitation

Most of the excitation rates used in this work are those recommended by Phaneuf et al. [28]. For certain transitions not considered by these authors, the rates of Itikawa et al. [29] have been used. For helium-like ions the rates recently recommended by Kato and Nakazaki [30], and for O V those recommended by Kato et al. [31] have been used. For C IV and O VI the excitation rates from the ground state to the autoionizing states

are those of Itikawa et al. [32]. We note that the cross-sections in these references have been fitted over a finite energy interval, with analytic expressions which did not ensure correct extrapolation outside the interval. This circumstance has forced us to construct new fits to the data for several forbidden transitions, in order to extend the rates to higher temperatures. For neutral oxygen, we use the cross-sections recently compiled by Laher and Gilmore [33] and by Itikawa and Ichimura [34].

For most ionization stages considered in this calculation, none of the excited states taken into account are autoionizing. The three exceptions are C IV, O I and O IV, for which transitions from the ground state to autoionizing states are considered. In the calculation of the loss terms, the excitation rates to these states are multiplied by the branching ratio for radiative decay. Autoionization from Auger states is already accounted for in the recommended ionization cross-sections [35].

Use is made of semi-empirical excitation rates [14] for transitions from the ground state or the metastable states to hydrogenic energy levels with large principal quantum numbers. Specifically, this is used for transitions towards levels $n = n_0 + 1$, up to $n = 10$, where n_0 is the largest principal quantum number of an excited state for which recommended data are available.

3.2. Ionization

Ionization rates from the ground state are calculated from analytic integration of the cross-sections recommended by Lennon et al. [35]. Ionization from metastable states is calculated with the Lotz semi-empirical formula [36]. Specifically, the cross-section from an energy level n containing q_n electrons is assumed to be

$$\sigma_n = a q_n \frac{\ln(E/I_n)}{E I_n} \quad (10)$$

where $a = 4 \times 10^{-14} \text{ cm}^2 (\text{eV})^2$, E is energy of the incident electron and I_n is the ionization energy from energy level n , both expressed in units of eV.

3.3. Radiative recombination

Radiative recombination from the ground state is calculated so as to reproduce recommended total recombination rates. The rates of radiative recombination to specific states are first calculated from approximate scaled hydrogenic formulas [14]. All rates are then multiplied by a constant which is chosen such that the normalized rates correctly reproduce the recommended rate for total radiative recombination. The total recombination rates used are those calculated by Aldrovandi

and Péquignot [37] for all ionization stages, with the exception of C III, for which we used the rates calculated by Datz and Dittner [38]. No recommended data have been found for radiative recombination from metastable states. For these, the rates are calculated from scaled hydrogenic expressions.

3.4. Dielectronic recombination

As for radiative recombination, the rates of dielectronic recombination are calculated empirically and, when possible, normalized so as to reproduce recommended rates for specific groups of transitions [38–44]. There are five possibilities for grouping the transitions, corresponding to five possible levels of normalization:

- (a) total rates, including $\Delta n = 0$ (so-called mode B) transitions and $\Delta n > 0$ (mode A) transitions,
- (b) total specific Δn (typically $\Delta n = 0$ and $\Delta n = 1$) transitions,
- (c) total $\Delta n > 0$ transitions,
- (d) transition to a specific state, and
- (e) total transitions to autoionizing states.

Ideally, recommended rates should be used for the various individual transitions possible (case (d)). When such detailed data are not available, the preferred normalization options are (b) and then (c).

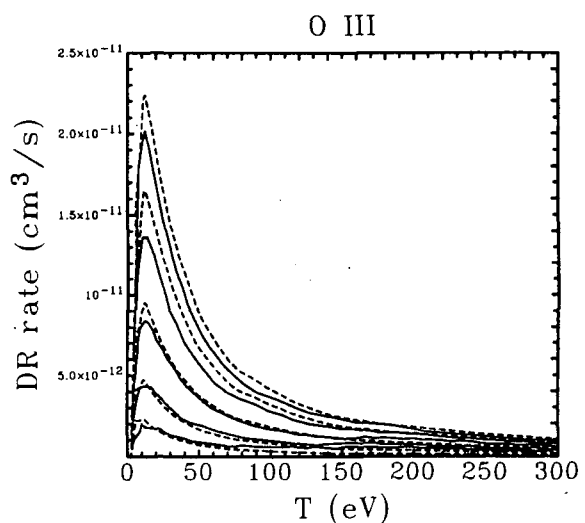


FIG. 1. Comparison between the finite density rates of dielectronic recombination obtained from empirically scaled recommended rates (dashed lines) and those calculated by Roszman [44] (solid lines) for O III. For the densities, the range considered is from 10^{12} m^{-3} (higher curves) to 10^{20} m^{-3} (lower curves), in increments of 10^2 .

When those are not available, scaling is done from the total recombination rate (case (a)). In one instance (recombination from the metastable state of C V), no recommended data have been found and purely semi-empirical rates are used.

The recommended dielectronic recombination rates considered here have been calculated in the zero density limit. At finite densities, the rates are reduced by so-called collisional interruption or thermal equilibration of the Rydberg states with the continuum. Unfortunately, none of the calculations considered offered a simple method to account for this effect. We have accounted for the weak density and temperature dependence of the rates in an ad hoc way, by multiplying the normalized rates by empirical correction factors for $\Delta n \neq 0$ and $\Delta n = 0$ transitions. These factors have the same form as in Ref. [14], but their numerical coefficients are obtained by fitting to available density dependent rates [44]. Figure 1 shows a comparison between the finite density recombination rates obtained with this method and those calculated by Roszman [44] for O III.

3.5. Transition probabilities

Most transition probabilities used in the calculations have been provided by Wiese and Fuhr [45] and by Wiese et al. [46]. For forbidden transitions in hydrogen- and helium-like ions, we use the transition probabilities calculated by Drake [47, 48]. For helium- and beryllium-like ions, these are complemented by the transition probabilities of Shevelko et al. [49]. For beryllium-like ions, we also use the transition probabilities of Dufton et al. [50].

4. RESULTS

4.1. Effect of metastable states

Most previous calculations of the radiative loss and cooling rates have been made in the coronal approximation briefly described in Section 2.2.3. The method of calculation used here is different from the standard coronal approximation in that it accounts for long lived metastable states. We therefore start this section with an assessment of the effect of metastable states. Unless stated otherwise, the electron density assumed in all the calculations is 10^{20} m^{-3} .

Figures 2 and 3 show the radiative loss and cooling coefficients for selected ions of oxygen as a function of temperature, computed with (solid line) and without (dashed line) metastable state effects. In those figures,

we express the loss coefficients in units of attowatts $\cdot \text{m}^3$. This is related to the more familiar units of $\text{erg} \cdot \text{cm}^3/\text{s}$ by $1 \text{ aW} = 10^{-5} \text{ erg} \cdot \text{cm}^3/\text{s}$. Significant differences are found in both figures. These results are representative of the differences between the coefficients computed for carbon ions with and without metastables. For both carbon and oxygen, the coronal coefficients computed for helium- and hydrogen-like ions are close to those

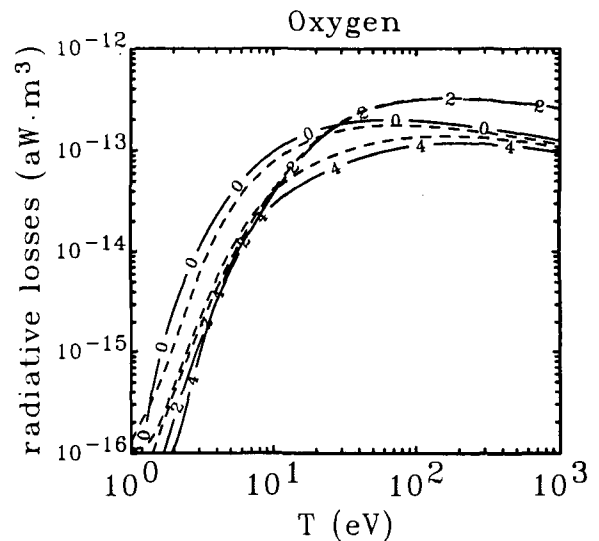


FIG. 2. Radiative loss coefficients computed for selected ionization stages of oxygen as a function of temperature, with (solid lines) and without (dashed lines) metastable effects. The numbers on the curves refer to the charges of the ions. Unless stated otherwise, the electron density assumed in the calculations is 10^{20} m^{-3} . We recall that $1 \text{ aW} = 10^{-18} \text{ W}$.

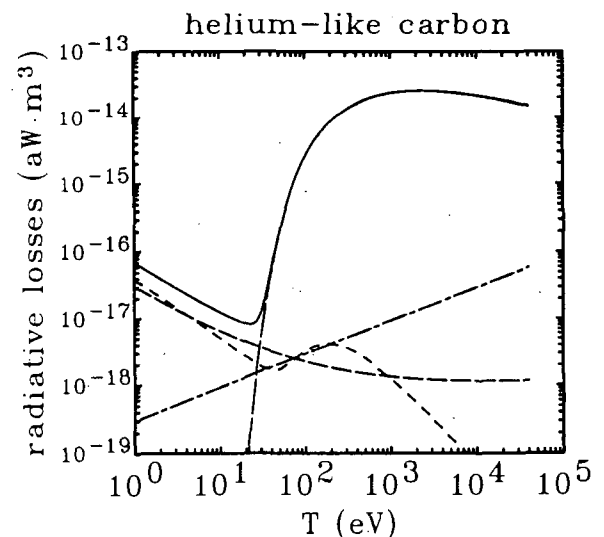


FIG. 3. Radiative loss coefficients computed for helium-like carbon as a function of temperature, with metastable effects. The various contributions are as described in Section 4.2.

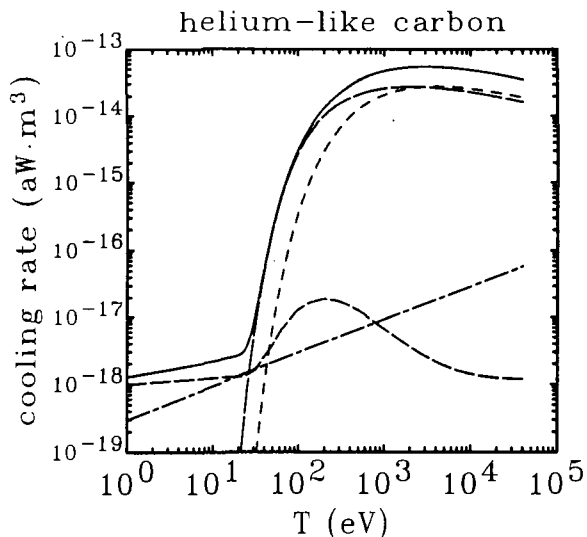


FIG. 4. Cooling coefficients computed for helium-like carbon as a function of temperature, with metastable effects. The various contributions are as described in Section 4.2.

computed with metastable states. This is because of the large radiative transition probability from metastable states in these ionization stages [47, 48].

4.2. Radiative loss and cooling coefficients

Figures 3 and 4 give the radiative loss and cooling coefficients calculated for helium-like carbon. For radiative losses, we distinguish between the following contributions:

- (a) line radiation associated with excitation by direct collisional impact and dielectronic recombination (long dashes),
- (b) bremsstrahlung (alternating long and short dashes),
- (c) continuum radiation associated with radiative recombination (medium dashes), and
- (d) radiative cascade following radiative and dielectronic recombinations (short dashes).

In the calculation of electron cooling rates, the following contributions are considered:

- (a) excitation by direct collisional impact or associated with dielectronic recombination, minus collisional de-excitation from metastable states (long dashes),
- (b) bremsstrahlung (alternating long and short dashes),
- (c) loss of electron kinetic energy associated with radiative and dielectronic recombinations (medium dashes), and
- (d) ionization (short dashes).

The total power loss coefficients are shown as solid curves.

The rates shown in Figs 3 and 4 are characterized by two distinct regimes. At low temperature, P_r is dominated by radiative cascade and continuum radiation, while P_e is dominated by the rate at which recombining electrons lose their kinetic energy. In this case, P_r is always larger than P_e and the difference between P_r and P_e increases as the temperature decreases. At higher temperatures, the various contributions are approximately of the same proportions as for the lower ionization stages. The largest differences between P_r and P_e are found for fully ionized ions when recombination is dominant (when $T \leq 1$ keV). As pointed out in Section 2.3.4, the approximate model used here to account for metastable states is only valid when recombination does not contribute significantly to the loss rates. This condition breaks down for the higher ionization stages, at low temperatures. In this case, our model effectively reduces to the usual coronal model which ignores the effect of metastable states.

For ionization stages below helium-like ones, radiative loss rates are dominated by line radiation. Electron cooling rates are dominated by excitation and, at higher temperatures, also by ionization. As a result, P_r and P_e generally have comparable numerical values, except at higher temperatures, where $P_e > P_r$.

Figures 5 to 8 show the total radiative loss and cooling coefficients computed for the various ionization stages of carbon and oxygen. The logarithm of the loss coefficients for fully stripped ions and ionization stages below

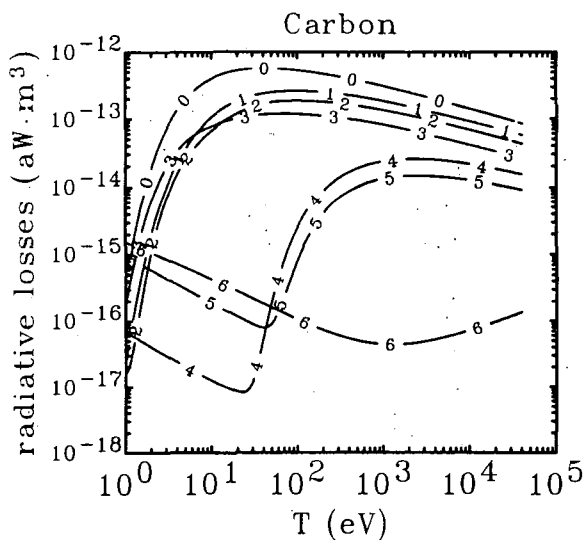


FIG. 5. Radiative loss coefficients computed for carbon as a function of temperature, with metastable effects.

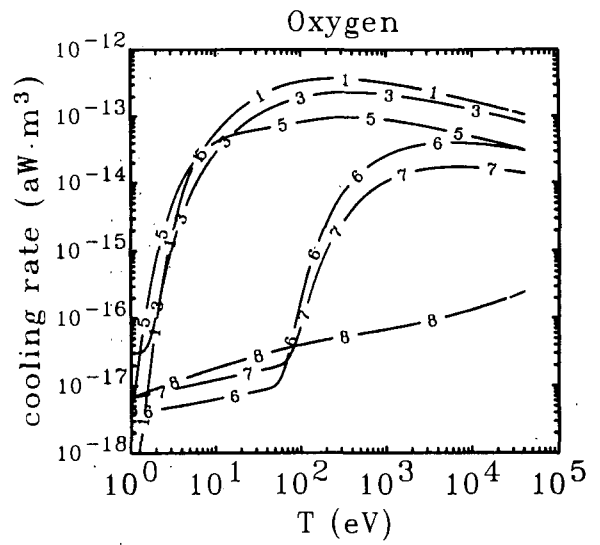
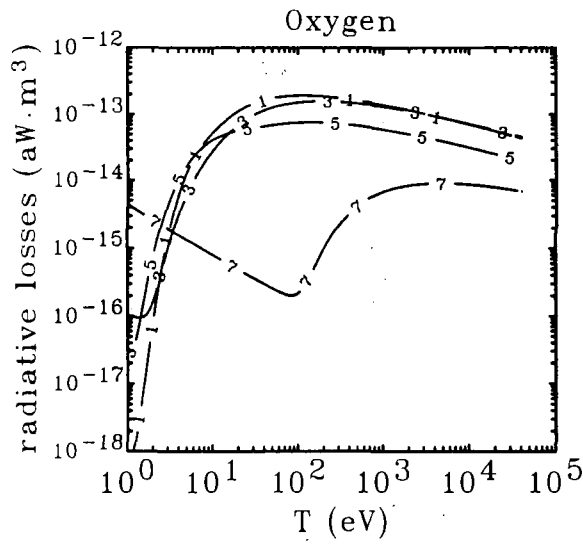
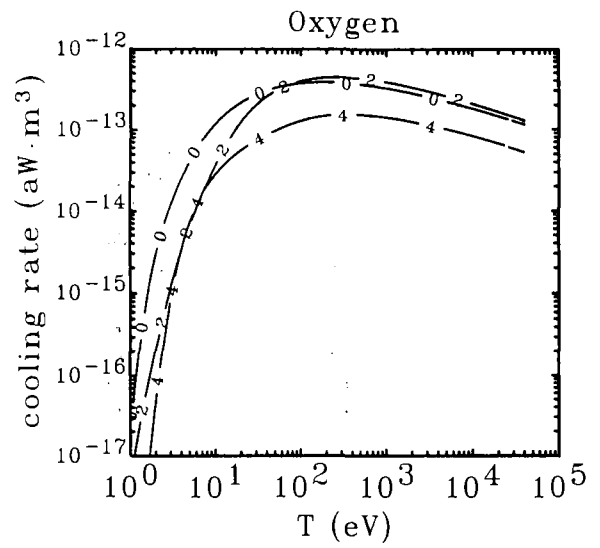
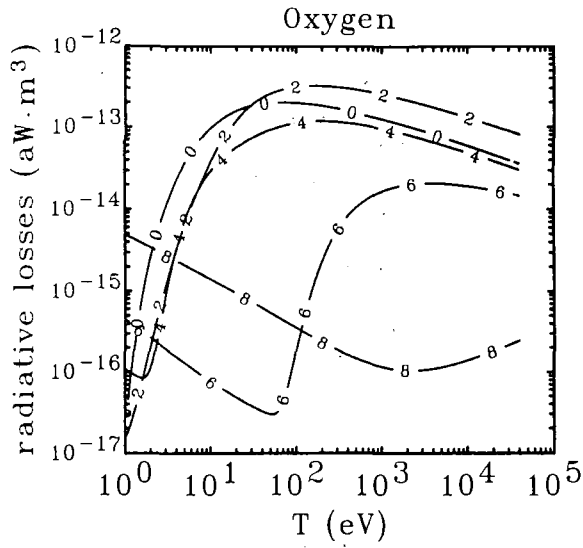


FIG. 6. Radiative loss coefficients computed for oxygen as a function of temperature, with metastable effects.

FIG. 8. Electron cooling coefficients computed for oxygen as a function of temperature, with metastable effects.

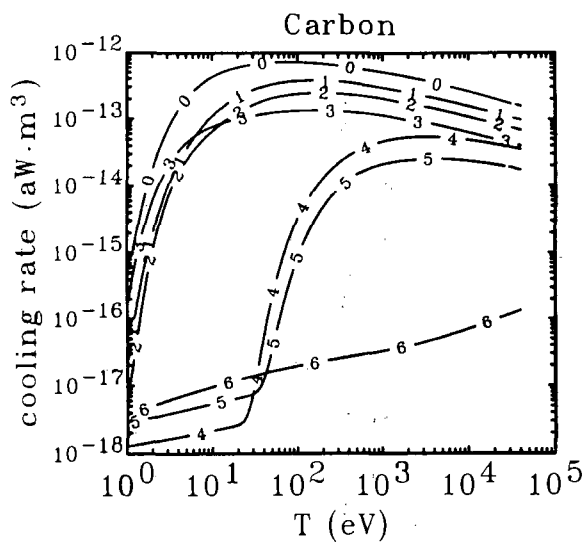


FIG. 7. Electron cooling coefficients computed for carbon as a function of temperature, with metastable effects.

helium-like ones have been fitted with Legendre polynomials as follows:

$$\ln P_{e,r} = \sum_{n=0}^8 a_n P_n(x) \quad (11)$$

where

$$x = 2 \frac{\ln(T/T_{\min})}{\ln(T_{\max}/T_{\min})} - 1 \quad (12)$$

with $T_{\min} = 1 \text{ eV}$ and $T_{\max} = 40 \text{ keV}$. The values of fitting parameters are given in Tables I and II. The loss coefficients for He-like and H-like ions have a more complex structure and cannot be accurately fitted by Eq. (11). The computed values of these loss coefficients are given in Table III in the temperature range from 1 eV to 40 keV.

TABLE I. FITTING COEFFICIENTS FOR THE LOGARITHM OF THE RADIATIVE LOSS COEFFICIENTS OF VARIOUS IONIZATION STAGES OF CARBON AND OXYGEN*

	a_0	a_1	a_2	a_3	a_4	a_5	a_6	a_7	a_8
C I	-29.0857	-0.3167	-0.9483	0.3165	-0.1005	0.0903	-0.0155	-0.0281	-0.0147
C II	-30.0174	0.5288	-1.3700	0.4437	-0.1217	0.1495	-0.0380	-0.0545	-0.0187
C III	-30.3632	0.6041	-1.3089	0.5854	-0.5821	-0.2083	0.2757	0.2232	0.0306
C IV	-30.4756	-0.1081	-0.9179	0.3028	-0.2015	-0.0210	0.0911	0.0404	-0.0048
C VII	-36.4669	-1.7297	1.8894	0.1651	-0.5557	-0.0335	0.1477	0.0521	0.0051
O I	-30.2674	0.2046	-1.2971	0.2587	0.1915	0.5571	-0.2401	-0.3361	-0.0805
O II	-30.5716	1.0148	-1.4157	1.2187	-1.5248	-1.4183	0.8163	1.0666	0.2165
O III	-30.4477	1.8595	-2.1637	0.8668	-0.4176	0.0819	0.0105	0.0520	0.0202
O IV	-30.8952	1.5659	-1.7529	1.1959	-1.0351	-1.1830	0.4316	0.8623	0.2108
O V	-31.0988	1.2828	-1.5970	1.5099	-1.3846	-2.0325	0.6849	1.3678	0.3256
O VI	-31.0177	0.3422	-1.0452	0.7626	-0.7759	-0.9719	0.4448	0.6638	0.1351
O VIII	-35.4920	-2.1429	1.6597	0.5067	-0.4796	-0.1786	0.1115	0.0683	0.0097

* The electron density assumed in the calculations is 10^{20} m^{-3} .

TABLE II. FITTING COEFFICIENTS FOR THE LOGARITHM OF THE COOLING RATE COEFFICIENTS OF VARIOUS IONIZATION STAGES OF CARBON AND OXYGEN*

	a_0	a_1	a_2	a_3	a_4	a_5	a_6	a_7	a_8
C I	-28.7559	0.0838	-1.0770	0.3315	-0.0979	0.0728	-0.0042	-0.0232	-0.0146
C II	-29.7154	0.8818	-1.5441	0.4860	-0.1255	0.1674	-0.0287	-0.0723	-0.0244
C III	-30.1159	0.9469	-1.4850	0.5382	-0.4184	-0.0282	0.1989	0.0780	-0.0058
C IV	-30.2594	0.2293	-1.0145	0.2443	-0.0851	-0.0341	0.0531	0.0295	-0.0063
C VII	-38.3682	1.5004	0.1820	0.3174	-0.1334	-0.1024	0.0334	0.0305	0.0049
O I	-29.6098	0.9236	-1.5412	0.2911	0.2025	0.5059	-0.2191	-0.3180	-0.0781
O II	-30.0679	1.6647	-1.8646	1.0360	-0.9754	-0.7770	0.5210	0.5828	0.1012
O III	-30.1892	2.2141	-2.3886	0.7652	-0.1512	0.3539	-0.1171	-0.1590	-0.0314
O IV	-30.5901	1.9964	-1.8877	1.3297	-1.2487	-1.5806	0.6410	1.1010	0.2526
O V	-30.8154	1.6358	-1.5374	1.5421	-1.8515	-2.3613	1.0922	1.6194	0.3453
O VI	-30.7775	0.7172	-1.3649	0.4202	0.0972	-0.3054	-0.0317	0.1390	0.0222
O VIII	-37.7059	1.5126	0.0067	0.3525	-0.0213	-0.1040	-0.0063	0.0161	0.0035

* The electron density assumed in the calculations is 10^{20} m^{-3} .

4.3. Loss functions computed for steady ionization balance

The radiative and cooling rates computed for carbon and oxygen at steady ionization balance are given in Figs 9–12. The various contributions considered for the radiative power loss and electron cooling rate functions are as described in the previous section. In Fig. 13 we show the corresponding effective ion charges as a

function of electron temperature, where the effective charge is defined as

$$Z_{\text{eff}} = \frac{\sum_i i^2 n_i}{\sum_i i n_i} \quad (13)$$

The radiative loss functions calculated at steady ionization balance show a too complex structure to be approximated accurately with a simple analytic fit. The values of loss functions at various electron temperatures in the range 1 eV–40 keV are given in Table IV.

TABLE III. RADIATIVE LOSS AND COOLING RATE COEFFICIENTS COMPUTED AT VARIOUS ELECTRON TEMPERATURES FOR HELIUM- AND HYDROGEN-LIKE CARBON AND OXYGEN IONS*

T (eV)	Radiative losses (aW · m ³)				Cooling rates (aW · m ³)			
	C V	C VI	O VII	O VIII	C V	C VI	O VII	O VIII
1.00	6.985 × 10 ⁻¹⁷	9.614 × 10 ⁻¹⁶	4.551 × 10 ⁻¹⁶	4.352 × 10 ⁻¹⁵	1.279 × 10 ⁻¹⁸	2.799 × 10 ⁻¹⁸	3.793 × 10 ⁻¹⁸	6.6266 × 10 ⁻¹⁸
1.70	4.591 × 10 ⁻¹⁷	6.575 × 10 ⁻¹⁶	2.993 × 10 ⁻¹⁶	2.941 × 10 ⁻¹⁵	1.435 × 10 ⁻¹⁸	3.259 × 10 ⁻¹⁸	4.268 × 10 ⁻¹⁸	7.6510 × 10 ⁻¹⁸
2.89	3.046 × 10 ⁻¹⁷	4.503 × 10 ⁻¹⁶	1.977 × 10 ⁻¹⁶	1.988 × 10 ⁻¹⁵	1.614 × 10 ⁻¹⁸	3.789 × 10 ⁻¹⁸	4.802 × 10 ⁻¹⁸	8.8212 × 10 ⁻¹⁸
4.90	2.053 × 10 ⁻¹⁷	3.091 × 10 ⁻¹⁶	1.315 × 10 ⁻¹⁶	1.346 × 10 ⁻¹⁵	1.822 × 10 ⁻¹⁸	4.403 × 10 ⁻¹⁸	5.406 × 10 ⁻¹⁸	1.0158 × 10 ⁻¹⁷
8.33	1.420 × 10 ⁻¹⁷	2.131 × 10 ⁻¹⁶	8.857 × 10 ⁻¹⁷	9.135 × 10 ⁻¹⁶	2.068 × 10 ⁻¹⁸	5.116 × 10 ⁻¹⁸	6.098 × 10 ⁻¹⁸	1.1688 × 10 ⁻¹⁷
14.1	1.024 × 10 ⁻¹⁷	1.479 × 10 ⁻¹⁶	6.082 × 10 ⁻¹⁷	6.221 × 10 ⁻¹⁶	2.364 × 10 ⁻¹⁸	5.949 × 10 ⁻¹⁸	6.902 × 10 ⁻¹⁸	1.3452 × 10 ⁻¹⁷
24.0	8.317 × 10 ⁻¹⁸	1.038 × 10 ⁻¹⁶	4.310 × 10 ⁻¹⁷	4.263 × 10 ⁻¹⁶	3.256 × 10 ⁻¹⁸	6.941 × 10 ⁻¹⁸	7.850 × 10 ⁻¹⁸	1.5499 × 10 ⁻¹⁷
40.8	6.207 × 10 ⁻¹⁷	7.974 × 10 ⁻¹⁷	3.210 × 10 ⁻¹⁷	2.951 × 10 ⁻¹⁶	6.346 × 10 ⁻¹⁷	1.365 × 10 ⁻¹⁷	9.054 × 10 ⁻¹⁸	1.7902 × 10 ⁻¹⁷
69.3	8.301 × 10 ⁻¹⁶	2.286 × 10 ⁻¹⁶	4.043 × 10 ⁻¹⁷	2.118 × 10 ⁻¹⁶	9.863 × 10 ⁻¹⁶	1.903 × 10 ⁻¹⁶	2.606 × 10 ⁻¹⁷	2.4600 × 10 ⁻¹⁷
117.7	3.700 × 10 ⁻¹⁵	1.318 × 10 ⁻¹⁵	3.942 × 10 ⁻¹⁶	2.749 × 10 ⁻¹⁶	4.983 × 10 ⁻¹⁵	1.434 × 10 ⁻¹⁵	4.090 × 10 ⁻¹⁶	1.4989 × 10 ⁻¹⁶
200.0	8.739 × 10 ⁻¹⁵	4.031 × 10 ⁻¹⁵	2.329 × 10 ⁻¹⁵	9.764 × 10 ⁻¹⁶	1.326 × 10 ⁻¹⁴	4.919 × 10 ⁻¹⁵	2.606 × 10 ⁻¹⁵	9.6129 × 10 ⁻¹⁶
339.7	1.461 × 10 ⁻¹⁴	7.642 × 10 ⁻¹⁵	6.563 × 10 ⁻¹⁵	2.649 × 10 ⁻¹⁵	2.466 × 10 ⁻¹⁴	1.037 × 10 ⁻¹⁴	8.157 × 10 ⁻¹⁵	3.1239 × 10 ⁻¹⁵
577.1	1.987 × 10 ⁻¹⁴	1.093 × 10 ⁻¹⁴	1.169 × 10 ⁻¹⁴	4.830 × 10 ⁻¹⁵	3.663 × 10 ⁻¹⁴	1.627 × 10 ⁻¹⁴	1.643 × 10 ⁻¹⁴	6.5611 × 10 ⁻¹⁵
980.3	2.348 × 10 ⁻¹⁴	1.325 × 10 ⁻¹⁴	1.619 × 10 ⁻¹⁴	6.781 × 10 ⁻¹⁵	4.642 × 10 ⁻¹⁴	2.118 × 10 ⁻¹⁴	2.558 × 10 ⁻¹⁴	1.0410 × 10 ⁻¹⁴
1665	2.525 × 10 ⁻¹⁴	1.436 × 10 ⁻¹⁴	1.925 × 10 ⁻¹⁴	8.157 × 10 ⁻¹⁵	5.254 × 10 ⁻¹⁴	2.431 × 10 ⁻¹⁴	3.344 × 10 ⁻¹⁴	1.3761 × 10 ⁻¹⁴
2828	2.539 × 10 ⁻¹⁴	1.456 × 10 ⁻¹⁴	2.065 × 10 ⁻¹⁴	8.895 × 10 ⁻¹⁵	5.476 × 10 ⁻¹⁴	2.565 × 10 ⁻¹⁴	3.855 × 10 ⁻¹⁴	1.6054 × 10 ⁻¹⁴
4804	2.429 × 10 ⁻¹⁴	1.407 × 10 ⁻¹⁴	2.065 × 10 ⁻¹⁴	9.072 × 10 ⁻¹⁵	5.370 × 10 ⁻¹⁴	2.547 × 10 ⁻¹⁴	4.059 × 10 ⁻¹⁴	1.7153 × 10 ⁻¹⁴
8161	2.239 × 10 ⁻¹⁴	1.312 × 10 ⁻¹⁴	1.968 × 10 ⁻¹⁴	8.821 × 10 ⁻¹⁵	5.037 × 10 ⁻¹⁴	2.420 × 10 ⁻¹⁴	4.010 × 10 ⁻¹⁴	1.7208 × 10 ⁻¹⁴
13863	2.007 × 10 ⁻¹⁴	1.191 × 10 ⁻¹⁴	1.818 × 10 ⁻¹⁴	8.277 × 10 ⁻¹⁵	4.572 × 10 ⁻¹⁴	2.225 × 10 ⁻¹⁴	3.788 × 10 ⁻¹⁴	1.6489 × 10 ⁻¹⁴
23548	1.763 × 10 ⁻¹⁴	1.059 × 10 ⁻¹⁴	1.643 × 10 ⁻¹⁴	7.565 × 10 ⁻¹⁵	4.049 × 10 ⁻¹⁴	1.996 × 10 ⁻¹⁴	3.466 × 10 ⁻¹⁴	1.5276 × 10 ⁻¹⁴
40000	1.523 × 10 ⁻¹⁴	9.265 × 10 ⁻¹⁵	1.462 × 10 ⁻¹⁴	6.782 × 10 ⁻¹⁵	3.520 × 10 ⁻¹⁴	1.757 × 10 ⁻¹⁴	3.099 × 10 ⁻¹⁴	1.3803 × 10 ⁻¹⁴

* The electron density assumed in the calculations is 10²⁰ m⁻³.

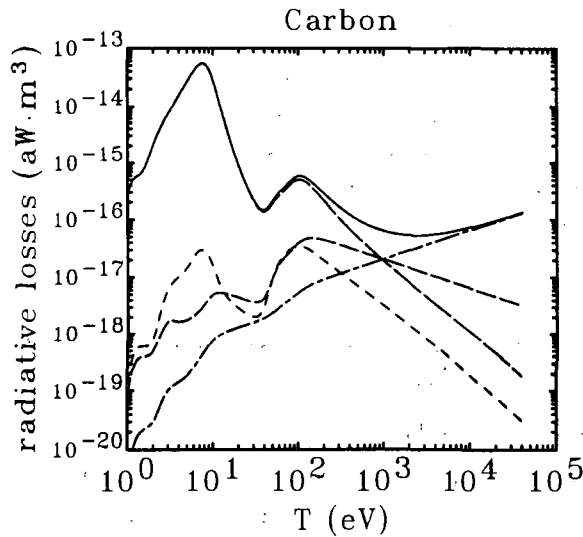


FIG. 9. Radiative loss functions as a function of temperature, for carbon at steady ionization balance. The various contributions shown are as in Fig. 3.

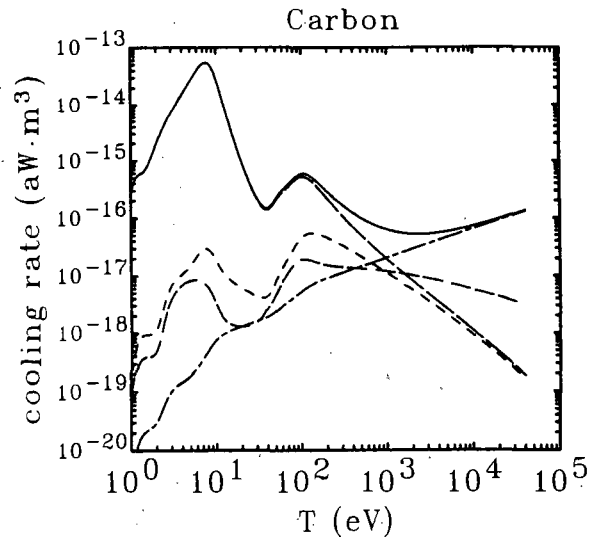


FIG. 10. Electron cooling functions as a function of temperature, for carbon at steady ionization balance. The various contributions shown are as in Fig. 4.

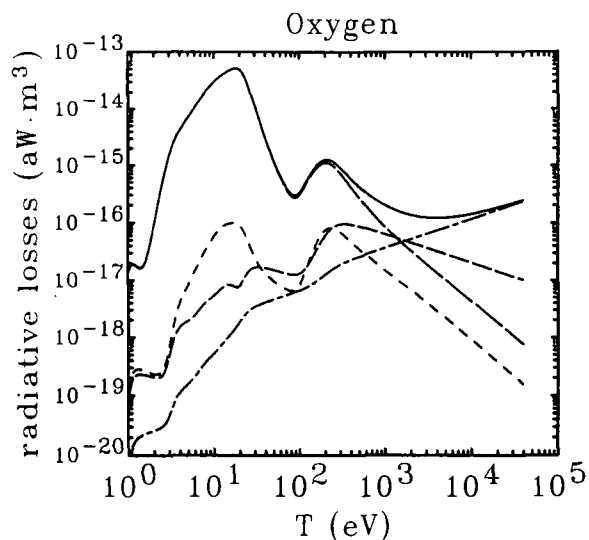


FIG. 11. Radiative loss functions as a function of temperature, for oxygen steady ionization balance. The various contributions shown are as in Fig. 3.

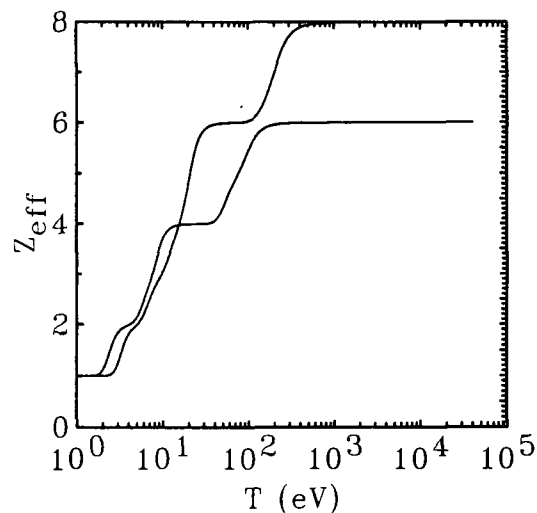


FIG. 13. Effective ion charges of carbon and oxygen ions as a function of electron temperature, computed at steady ionization balance.

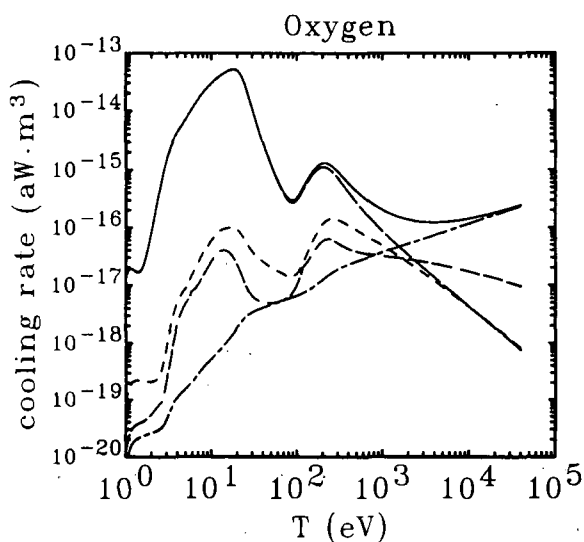


FIG. 12. Electron cooling functions as a function of temperature, for oxygen at steady ionization balance. The various contributions shown are as in Fig. 4.

4.4. Sensitivity of results to the electron density

Unless stated otherwise, the results presented here are for an electron density of 10^{20} m^{-3} . Because of the weak density dependence of dielectronic recombination rates and because of the small but finite transition probability of metastable states, we expect our results to show some sensitivity to the electron density. This point has been examined by varying the electron density

TABLE IV. VALUES OF THE RADIATIVE COOLING FUNCTION (in units of $\text{aW} \cdot \text{m}^3$) COMPUTED AT VARIOUS ELECTRON TEMPERATURES FOR CARBON AND OXYGEN IMPURITIES AT STEADY IONIZATION BALANCE*

T (eV)	Carbon	Oxygen
1.00	2.720×10^{-16}	1.291×10^{-17}
1.70	1.063×10^{-15}	2.847×10^{-17}
2.89	6.720×10^{-15}	1.173×10^{-15}
4.90	2.539×10^{-14}	6.778×10^{-15}
8.33	5.073×10^{-14}	2.173×10^{-14}
14.1	4.551×10^{-15}	4.465×10^{-14}
24.0	4.448×10^{-16}	3.133×10^{-14}
40.8	1.502×10^{-16}	2.740×10^{-15}
69.3	3.812×10^{-16}	4.268×10^{-16}
117.7	5.615×10^{-16}	4.906×10^{-16}
200.0	2.848×10^{-16}	1.261×10^{-15}
339.7	1.454×10^{-16}	7.504×10^{-16}
577.1	8.879×10^{-17}	3.518×10^{-16}
980.3	6.433×10^{-17}	2.063×10^{-16}
1665	5.458×10^{-17}	1.483×10^{-16}
2828	5.347×10^{-17}	1.265×10^{-16}
4804	5.842×10^{-17}	1.242×10^{-16}
8161	6.865×10^{-17}	1.358×10^{-16}
13863	8.435×10^{-17}	1.596×10^{-16}
23548	1.063×10^{-16}	1.959×10^{-16}
40000	1.360×10^{-16}	2.467×10^{-16}

* The electron density assumed in the calculations is 10^{20} m^{-3} .

in the range 10^{16} to 10^{20} m^{-3} . The computed rates were found to be nearly independent of the density in that range. This weak sensitivity has been confirmed independently by Clark and Abdallah [51]. At higher densities, however, the rate coefficients become more sensitive to the electron density. It then becomes necessary to account for multistep processes, not only for transitions involving metastable states but also for transitions between all excited states.

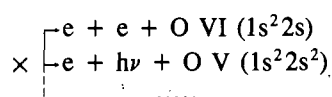
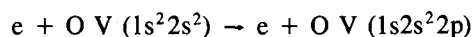
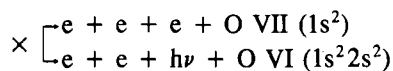
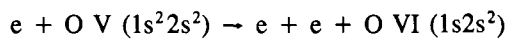
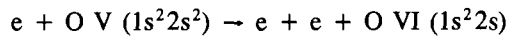
5. CONCLUSION

Radiative loss and electron cooling rates have been calculated for carbon and oxygen impurity ions, for plasma conditions of relevance to fusion. These rates have been calculated with the most recent recommended atomic data available. The radiative loss function enters the total energy balance. The electron cooling rate enters the electron thermal energy balance. The two rates are equal under steady ionization balance conditions. They may differ significantly under non-steady conditions.

A simple method has been used to calculate loss rates while approximately accounting for the effects of metastable states. The importance of metastable states has been assessed by making comparisons with results obtained in the standard coronal approximation. For both radiative losses and electron cooling rates, significant differences have been found. We stress that such calculations are contingent upon the availability and accuracy of data for a wealth of atomic processes. We would like to conclude with a short list of processes for which more accurate or detailed data would be desirable. These are:

(a) *Excitation.* When metastable states are taken into account, excitations to higher states become significant. In practice, these would correspond to transitions with Δn up to two, from the ground state.

(b) *Ionization.* Recommended data for the ionization cross-sections typically account for a number of processes. For example,



Because these processes have different energy thresholds, they will contribute differently to the radiative losses and electron cooling rates. Accurate cross-sections and, when appropriate, Auger rates and branching ratios are therefore required for each process.

(c) *Dielectronic recombination.* Cross-sections for dielectronic recombination corresponding to specific transitions are required. The results presented here have relied largely on scaled hydrogenic rates that were normalized to reproduce recommended total recombination rates. Accurate calculations with finite density effects are also needed.

(d) *Radiative recombination.* Detailed cross-sections for radiative recombination to specific states are needed. This includes recombination into metastable states, from ions initially in the ground state or the metastable states.

(e) *Transition probabilities.* Some transition probabilities needed to calculate the relative populations of the ground state and the metastable states are missing and had to be evaluated from scaled hydrogenic values. Transition probabilities are also required for forbidden transitions from metastable states.

REFERENCES

- [1] TFR Group, Nucl. Fusion **15** (1975) 1053.
- [2] BAGDASAROV, A.A., BERLIZOV, A.B., VASIN, N.L., et al., in Plasma Physics and Controlled Nuclear Fusion Research 1978 (Proc. 7th Int. Conf. Innsbruck, 1978), Vol. 1, IAEA, Vienna (1979) 35.
- [3] EUBANK, H., GOLDSTON, R.J., ARUNASALAM, V., et al., *ibid.*, p. 167.
- [4] BARTIROMO, R., BRUSATI, M., BURATTI, P., et al., in Plasma Physics and Controlled Nuclear Fusion Research 1984 (Proc. 8th Int. Conf. Brussels, 1980), Vol. 1, IAEA, Vienna (1981) 43.
- [5] EFTHIMION, P.C., BRETZ, N., BELL, M., et al., in Plasma Physics and Controlled Nuclear Fusion Research 1984 (Proc. 10th Int. Conf. London, 1984), Vol. 1, IAEA, Vienna (1985) 29.
- [6] KEILHACKER, M., FUSSMAN, G., von GIERKE, G., et al., *ibid.*, p. 71.
- [7] JET Team (presented by P.H. Rebut), in Plasma Physics and Controlled Nuclear Fusion Research 1986 (Proc. 11th Int. Conf. Kyoto, 1986), Vol. 1, IAEA, Vienna (1987) 31.
- [8] NISHITANI, T., ITAMI, K., NAGASHIMA, K., et al., Nucl. Fusion **30** (1990) 1095.
- [9] POST, D., in Plasma Physics and Controlled Nuclear Fusion Research 1990 (Proc. 13th Int. Conf. Washington, DC, 1990), Vol. 3, IAEA, Vienna (1991) 239.
- [10] MEADE, D.M., Nucl. Fusion **14** (1974) 289.

- [11] JENSEN, R.V., POST, D.E., GRASBERGER, W.H., TARTER, C.B., LOKKE, W.A., *Nucl. Fusion* **17** (1977) 1187.
- [12] REITER, D., WOLF, G.H., KEVER, H., *Nucl. Fusion* **30** (1990) 2141.
- [13] BEHRISCH, R., PROZESKY, V., *Nucl. Fusion* **30** (1990) 2166.
- [14] POST, D.E., JENSEN, R.V., TARTER, C.B., GRASBERGER, W.H., LOKKE, W.A., *At. Data Nucl. Data Tables* **20** (1977) 397.
- [15] SUMMERS, H.P., McWHIRTER, R.W.P., *J. Phys., B* **12** (1979) 2387.
- [16] SUMMERS, H.P., HOOPER, M.B., *Plasma Phys.* **25** (1983) 1331.
- [17] McWHIRTER, R.W.P., SUMMERS, H.P., *Appl. At. Coll. Phys.* **2** (1984) 51.
- [18] KEANE, C., SKINNER, C.H., *Phys. Rev., A* **33** (1986) 4179.
- [19] BATES, D.R., KINGSTON, A.E., McWHIRTER, R.W.P., *Proc. R. Soc. London, Ser. A* **267** (1962) 297.
- [20] SUMMERS, H.P., *Mon. Not. R. Astron. Soc.* **178** (1977) 131.
- [21] LEE, Y.T., *J. Quant. Spectrosc. Radiat. Transfer* **38** (1987) 131.
- [22] IGITKHANOV, Yu.L., KUKUSHKIN, A.S., PIGAROV, A.Yu., PISTUNOVICH, V.I., POZHAROV, V.A., in *Plasma Physics and Controlled Nuclear Fusion Research 1984* (Proc. 10th Int. Conf. London, 1984), Vol. 2, IAEA, Vienna (1985) 113.
- [23] HULSE, R., *Nucl. Technol./Fusion* **3** (1983) 259.
- [24] BRETON, C., De MICHELIS, C., MATTIOLI, M., *Nucl. Fusion* **16** (1976) 891.
- [25] HARRISON, M.F.A., in *Physics of Plasma-Wall Interactions in Controlled Fusion* (POST, D.E., BEHRISCH, R., Eds), Plenum Press, New York and London (1986) 281.
- [26] HULSE, R.A., POST, D.E., MIKKELSEN, D.R., *J. Phys., B* **13** (1980) 3895.
- [27] SUMMERS, H.P., THOMAS, P., GIANNELLA, R., et al., *J. Phys.* **4** (1991) C1-191.
- [28] PHANEUF, R.A., JANEV, R.K., PINDZOLA, M.S., "Collisions of carbon and oxygen ions with electrons, H, H₂ and He", *Atomic Data for Fusion*, Vol. 5, Rep. ORNL-6090, Oak Ridge National Laboratory, Oak Ridge, TN (1987).
- [29] ITIKAWA, Y., HARA, S., KATO, T., et al., *At. Data Nucl. Data Tables* **33** (1985) 149.
- [30] KATO, T., NAKAZAKI, S., *At. Data Nucl. Data Tables* **42** (1989) 313.
- [31] KATO, T., LANG, J., BERRINGTON, K.E., *At. Data Nucl. Data Tables* **44** (1990) 133.
- [32] ITIKAWA, Y., SAKIMOTO, K., NAKAZAKI, S., *Phys. Rev., A* **36** (1987) 1088.
- [33] LAHER, R.R., GILMORE, F.R., *J. Phys. Chem. Ref. Data* **19** (1990) 277.
- [34] ITIKAWA, Y., ICHIMURA, A., *J. Phys. Chem. Ref. Data* **19** (1990) 637.
- [35] LENNON, M.A., BELL, K.L., GILBODY, H.B., et al., *J. Phys. Chem. Ref. Data* **17** (1988) 1285.
- [36] LOTZ, W., *Z. Phys.* **206** (1967) 205.
- [37] ALDROVANDI, S.M.V., PÉQUIGNOT, D., *Astron. Astrophys.* **25** (1973) 137.
- [38] DATZ, S., DITTNER, P.F., *Z. Phys., D* **10** (1988) 187.
- [39] BADNELL, N.R., *J. Phys., B* (London) **20** (1987) 2081.
- [40] BADNELL, N.R., *J. Phys., B* (London) **21** (1988) 749.
- [41] BADNELL, N.R., *Phys. Scr., T* **28** (1989) 33.
- [42] GRIFFIN, D.C., *Phys. Scr., T* **28** (1989) 17.
- [43] HAHN, Y., *Phys. Scr., T* **28** (1989) 25.
- [44] ROSZMAN, L.J., *Phys. Scr., T* **28** (1989) 36.
- [45] WIESE, W.L., FUHR, J.R. (National Institute of Standards and Technology, Gaithersburg Labs), personal communication, 1991.
- [46] WIESE, W.L., SMITH, M.W., GLENNON, B.M., *Atomic Transition Probabilities, Vol. 1., Hydrogen through Neon, Natl. Standard Ref. Data Ser. Natl. Bur. Stand. (U.S.)* **4**, US Government Printing Office, Washington, DC (1966).
- [47] DRAKE, G.W.F., *Phys. Rev., A* **34** (1986) 2871.
- [48] DRAKE, G.W.F., *Phys. Rev., A* **3** (1971) 908.
- [49] SHEVELKO, V.P., VAINSHTEIN, L.A., YUKOV, E.A., *Phys. Scr., T* **28** (1989) 39.
- [50] DUFTON, P.L., BERRINGTON, K.A., BURKE, P.G., KINGSTON, A.E., *Astron. Astrophys.* **62** (1978) 111.
- [51] CLARK, R.E.H., ABDALLAH, J. (LANL), personal communication, 1992.

Appendix

LIST OF STATES CONSIDERED IN THE CALCULATIONS

In this Appendix, we list the states considered in the calculation, for which recommended data are available. The ground state and the metastable and autoionizing states are identified at the right of the corresponding rows. For each state we also give the energy and degeneracy. The energy is defined such that an ion in its ground state has an energy equal to minus its ionization energy.

C I

State index	Energy (eV)	Degeneracy	Configuration
1	-11.264	9	$1s^2 2s^2 2p^2 \ ^3P$ ground

C II

State index	Energy (eV)	Degeneracy	Configuration
1	-24.376	6	$1s^2 2s^2 2p \ ^2P$ ground
2	-19.046	12	$2s 2p^2 \ ^4P$ metastable
3	-15.086	10	$\ ^2D$
4	-12.416	2	$\ ^2S$
5	-10.666	6	$\ ^2P$
6	-9.926	2	$2s^2 3s \ ^2S$
7	-8.046	6	$3p \ ^2P$
8	-6.326	10	$3d \ ^2D$

C III

State index	Energy (eV)	Degeneracy	Configuration
1	-47.864	1	$1s^2 2s^2 \ ^1S$ ground
2	-41.364	9	$2s 2p \ ^3P$ metastable
3	-35.174	3	$\ ^1P$
4	-30.824	9	$2p^2 \ ^3P$
5	-29.774	5	$\ ^1D$
6	-25.234	1	$\ ^1S$
7	-18.334	3	$2s 3s \ ^3S$
8	-17.224	1	$\ ^1S$
9	-15.764	3	$3p \ ^1P$
10	-15.664	9	$\ ^3P$
11	-14.384	15	$3d \ ^3D$
12	-13.584	5	$\ ^1D$

C IV

State index	Energy (eV)	Degeneracy	Configuration
1	-64.476	2	$1s^2 2s \ ^2S$ ground
2	-56.476	6	$2p \ ^2P$
3	-26.926	2	$3s \ ^2S$
4	-24.796	6	$3p \ ^2P$
5	-24.196	10	$3d \ ^2D$
6	229.135	2	$1s 2s^2 \ ^2S$ autoionizing
7	232.400	12	$2s 2p \ ^4P$
8	237.298	6	$2s(^1S) 2p \ ^2P$
9	242.332	6	$2s(^3S) 2p \ ^2P$

RADIATIVE LOSSES AND ELECTRON COOLING RATES FOR C AND O IMPURITIES

C V

State index	Energy (eV)	Degeneracy	Configuration
1	-391.986	1	1s ² ¹ S ground
2	-93.036	3	1s2s ³ S metastable
3	-87.586	1	¹ S metastable
4	-87.586	9	1s2p ³ P
5	-84.086	3	¹ P
6	-45.833	3	1s3s ³ S
7	-44.850	1	¹ S
8	-38.466	9	1s3p ³ P
9	-37.686	15	1s3d ³ D
10	-37.679	3	¹ D
11	-37.486	3	1s3p ¹ P

C VI

State index	Energy (eV)	Degeneracy	Configuration
1	-489.84	2	1s ground
2	-122.34	2	2s metastable
3	-122.34	6	2p
4	-54.44	2	3s
5	-54.34	6	3p
6	-54.24	10	3d
7	-30.44	2	4s
8	-30.44	6	4p
9	-30.44	10	4d
10	-30.44	14	4f
11	-19.44	6	5p

O I

State index	Energy (eV)	Degeneracy	Configuration
1	-13.618	9	1s ² 2s ² 2p ⁴ ³ P ground
2	-11.651	5	¹ D metastable
3	-9.428	1	¹ S metastable
4	-4.472	5	2p ³ (⁴ S)3s ⁵ S metastable
5	-4.097	3	³ S
6	-2.878	15	3p ³ P
7	-2.628	9	³ P
8	-1.778	5	4s ⁵ S
9	-1.688	3	³ S
10	-1.538	25	3d ⁵ D
11	-1.528	15	³ D
12	-1.328	15	4p ³ P
13	-1.258	9	³ P
14	-1.078	15	(² D)3s ³ D
15	-0.888	5	¹ D
16	-0.868	25	(⁴ S)4d ⁵ D
17	-0.858	15	¹ D
18	0.502	9	(² P)3s ³ P autoionizing
19	0.742	3	¹ P
20	1.552	15	(² D)4d ³ D
21	1.602	5	¹ D
22	1.672	9	3d ³ P
23	1.742	3	³ S
24	1.742	15	³ D
25	2.042	9	2s2p ⁵ ³ P

O I (cont.)

26	2.492	9	$2s^2 2p^3 ({}^2D) 4d {}^3P$
27	3.282	3	$({}^2P) 4s {}^1P$
28	3.472	9	$3d {}^3P$
29	3.472	15	3D
30	3.472	21	3F
31	4.152	21	$4d {}^3F$

O II

State index	Energy (eV)	Degeneracy	Configuration
1	-35.108	4	$1s^2 2s^2 2p^3 {}^4S$ ground
2	-31.784	10	2D metastable
3	-30.092	6	2P metastable
4	-20.242	12	$2s 2p^4 {}^4P$
5	-12.127	12	$2s^2 2p^2 3s {}^4P$

O III

State index	Energy (eV)	Degeneracy	Configuration
1	-54.886	9	$1s^2 2s^2 2p^2 {}^3P$ ground
2	-52.369	5	1D metastable
3	-49.556	1	1S metastable
4	-47.436	5	$2s 2p^3 {}^5S$ metastable
5	-40.026	14	3D
6	-37.256	9	3P
7	-31.726	5	1D
8	-30.486	3	3S
9	-28.826	3	1P

O IV

State index	Energy (eV)	Degeneracy	Configuration
1	-77.394	6	$1s^2 2s^2 2p {}^2P$ ground
2	-68.577	12	$2s 2p^2 {}^4P$ metastable
3	-61.684	10	2D
4	-57.044	2	2S
5	-55.034	6	2P
6	-33.054	2	$2s^2 3s {}^2S$
7	-25.374	10	$3d {}^2D$

O V

State index	Energy (eV)	Degeneracy	Configuration
1	-113.873	1	$1s^2 2s^2 {}^1S$ ground
2	-103.673	9	$2s 2p {}^3P$ metastable
3	-94.193	3	1P
4	-87.373	9	$2p^2 {}^3P$
5	-85.373	5	1D
6	-78.183	1	1S
7	-46.053	3	$2s 3s {}^3S$
8	-44.303	1	1S
9	-41.883	3	$3p {}^1P$
10	-41.603	9	3P
11	-39.383	15	$3d {}^3D$
12	-37.943	5	1D

RADIATIVE LOSSES AND ELECTRON COOLING RATES FOR C AND O IMPURITIES

O VI

State index	Energy (eV)	Degeneracy	Configuration
1	-138.080	2	$1s^2 2s^2 S$ ground
2	-126.100	6	$2p^2 P$
3	-58.730	2	$3s^2 S$
4	-55.480	6	$3p^2 P$
5	-54.440	10	$3d^2 D$
6	414.311	2	$1s2s^2 S$ autoionizing
7	418.393	12	$2s2p^4 P$
8	426.556	6	$2s(^1S)2p^2 P$
9	432.816	6	$2s(^3S)2p^2 P$

O VII

State index	Energy (eV)	Degeneracy	Configuration
1	-739.114	1	$1s^2 ^1S$ ground
2	-178.114	3	$1s2s^3 S$ metastable
3	-170.514	9	$2p^3 P$
4	-170.414	1	$2s^1 S$ metastable
5	-165.214	3	$2p^1 P$
6	-77.214	3	$3s^3 S$
7	-75.114	9	$3p^3 P$
8	-75.014	1	$3s^1 S$
9	-74.014	15	$3d^3 D$
10	-73.914	5	$3d^1 D$
11	-73.514	3	$3p^1 P$
12	-45.484	9	$4p^3 P$
13	-44.804	5	$4d^1 D$
14	-43.460	1	$4s^1 S$
15	-42.763	3	$4p^1 P$
16	-42.756	15	$4d^3 D$
17	-30.109	5	$5d^1 D$
18	-28.222	1	$5s^1 S$
19	-27.873	3	$5p^1 P$
20	-27.654	9	$^3 P$
21	-27.654	15	$5d^3 D$
22	-19.949	1	$6s^1 S$
23	-19.775	3	$6p^1 P$

O VIII

State index	Energy (eV)	Degeneracy	Configuration
1	-870.272	2	$1s$ ground
2	-216.772	2	$2s$ metastable
3	-216.672	6	$2p$
4	-96.672	2	$3s$
5	-96.672	6	$3p$
6	-96.672	10	$3d$
7	-54.384	2	$4s$
8	-54.384	6	$4p$
9	-54.384	10	$4d$
10	-54.384	14	$4f$

HOW TO ORDER IAEA PUBLICATIONS

An exclusive sales agent for IAEA publications, to whom all orders and inquiries should be addressed, has been appointed for the following countries:

CANADA
UNITED STATES OF AMERICA UNIPUB, 4611-F Assembly Drive, Lanham, MD 20706-4391, USA

In the following countries IAEA publications may be purchased from the sales agents or booksellers listed or through major local booksellers. Payment can be made in local currency or with UNESCO coupons.

ARGENTINA Comisión Nacional de Energía Atómica, Avenida del Libertador 8250, RA-1429 Buenos Aires

AUSTRALIA Hunter Publications, 58 A Gipps Street, Collingwood, Victoria 3066

BELGIUM Service Courrier UNESCO, 202, Avenue du Roi, B-1060 Brussels

CHILE Comisión Chilena de Energía Nuclear, Venta de Publicaciones, Amunategui 95, Casilla 188-D, Santiago

CHINA IAEA Publications in Chinese:
China Nuclear Energy Industry Corporation, Translation Section, P.O. Box 2103, Beijing
IAEA Publications other than in Chinese:
China National Publications Import & Export Corporation, Deutsche Abteilung, P.O. Box 88, Beijing

CZECHOSLOVAKIA S.N.T.L., Mikulandska 4, CS-116 86 Prague 1
Alfa, Publishers, Hurbanovo námestie 3, CS-815 89 Bratislava

FRANCE Office International de Documentation et Librairie, 48, rue Gay-Lussac, F-75240 Paris Cedex 05

HUNGARY Kultura, Hungarian Foreign Trading Company, P.O. Box 149, H-1389 Budapest 62

INDIA Oxford Book and Stationery Co., 17, Park Street, Calcutta-700 016
Oxford Book and Stationery Co., Scindia House, New Delhi-110 001

ISRAEL YOZMOT (1989) Ltd, P.O. Box 56055, Tel Aviv 61560

ITALY Libreria Scientifica, Dott. Lucio de Biasio "aeiou", Via Meravigli 16, I-20123 Milan

JAPAN Maruzen Company, Ltd, P.O. Box 5050, 100-31 Tokyo International

PAKISTAN Mirza Book Agency, 65, Shahrah Quaid-e-Azam, P.O. Box 729, Lahore 3

POLAND Ars Polona-Ruch, Centrala Handlu Zagranicznego, Krakowskie Przedmiescie 7, PL-00-068 Warsaw

ROMANIA Ilexim, P.O. Box 136-137, Bucharest

RUSSIAN FEDERATION Mezhdunarodnaya Kniga, Smolenskaya-Sennaya 32-34, Moscow G-200

SOUTH AFRICA Van Schaik Bookstore (Pty) Ltd, P.O. Box 724, Pretoria 0001

SPAIN Díaz de Santos, Lagasca 95, E-28006 Madrid
Díaz de Santos, Balmes 417, E-08022 Barcelona

SWEDEN AB Fritzes Kungl. Hovbokhandel, Fredsgatan 2, P.O. Box 16356, S-103 27 Stockholm

UNITED KINGDOM HMSO, Publications Centre, Agency Section, 51 Nine Elms Lane, London SW8 5DR

YUGOSLAVIA Jugoslavenska Knjiga, Terazije 27, P.O. Box 36, YU-11001 Belgrade

Orders from countries where sales agents have not yet been appointed and requests for information should be addressed directly to:



**Division of Publications
International Atomic Energy Agency
Wagramerstrasse 5, P.O. Box 100, A-1400 Vienna, Austria**

INFORMATION FOR AUTHORS

General

NUCLEAR FUSION (NF) publishes papers, letters and critical reviews on theoretical and experimental aspects of controlled thermonuclear fusion research and comments on these contributions. Appropriate scientific summaries of major international conferences and workshops are also considered for publication.

Manuscripts, which may be submitted in Chinese, English, French, Russian or Spanish, will be published in English. For a manuscript submitted in a language other than English, a translation into English of technical terms should be provided. Manuscripts must be submitted in triplicate and typewritten double spaced on good quality standard size paper. All copies should include the main text, an abstract, tables, references, figures, captions and appendices, as appropriate. One set of glossy prints or reproducible transparencies of the figures should also be provided. *Final manuscript versions may be submitted in camera-ready form or on diskettes (see NF's Note for Authors, available on request from the NF Office).*

Every manuscript submitted must be accompanied by a disclaimer stating that the paper has not been published and is not being considered for publication elsewhere. If no copyright is claimed by the authors, the IAEA automatically owns the copyright of the paper.

Authors will receive proofs of the text of accepted manuscripts. Proofs of figures are sent only if requested. Rejected manuscripts will not be returned unless this is expressly requested within six weeks of rejection.

Fifty reprints are provided free of charge; additional reprints may be ordered at the time the author returns the proofs. Manuscripts and correspondence should be addressed to: The Editor, NUCLEAR FUSION, International Atomic Energy Agency, Wagramerstrasse 5, P.O. Box 100, A-1400 Vienna, Austria.

Manuscript preparation

Authors are referred to any recent issue of NF for examples of *format* and *style*.

All submitted articles should be *concise* and written in a *clear style*. The description of the methods used, either theoretical or experimental, should be given in detail only when such methods are new. Exhaustive description of previous or related work is not appropriate. If a laboratory report is used as the basis for a manuscript, it should be checked and rewritten for journal presentation.

Titles should be as concise as possible but sufficiently informative to describe the subject of the paper.

Abstracts must briefly summarize the contents of the article. They should state the principal objectives, mention the methodology employed, summarize the results (emphasizing the new findings) and present the main conclusions. They should be concise and self-contained so that they can be used by the International Nuclear Information System (INIS) and other abstracting systems without changes. General, well known information should be avoided in the abstract and accommodated in the introduction.

Letters to NF are either short communications of new approaches and developments or research notes. As a rule, they should be no longer than ten typewritten double spaced standard pages, including references and figures.

Guidelines for *bibliographical citations* can be found in issues 2, 3 and 4 of NF 28 (1988). In short, references should be accurately described in sufficient detail for easy identification. In the text, they should be indicated consecutively by Arabic numerals in square brackets. All references should be listed on a separate page at the end of the text. In this list, the names of all authors (or, if there are more than six, of the first three authors plus 'et al.') or else the corporate author (e.g. TFR GROUP) should be given. All unpublished material, e.g. laboratory reports, doctoral theses or papers in proceedings that have not yet been published, should be cited with full titles, place and year; citations of reports should also contain laboratory prefix and number, date of issue, etc. References to periodicals should contain the name of the journal, volume number, page number and year of publication; the title of the article is not needed. References to books should contain the full title of the book, names of editors (if any), name and location of the publisher, year of publication and page number (if appropriate). References to personal communications should be avoided if possible. For journal citations use the list of abbreviations given in "IAEA-INIS-11, INIS: Authority List for Journal Titles". Russian names should be transliterated according to "IAEA-INIS-10, INIS: Transliteration Rules for Selected Non-Roman Characters". Examples of the style followed by NF for references are:

REFERENCES

- [1] KAYE, S.M., GOLDSTON, R.J., Nucl. Fusion 25 (1985) 65.
- [2] MIODUSZEWSKI, P.K., SIMPKINS, J.E., EDMONDS, P.H., et al., J. Nucl. Mater. 128 & 129 (1984) 884.
- [3] TRUBNIKOV, B.A., in Problems of Plasma Theory, Vol. 1 (LEONTOVICH, M.A., Ed.), Gosatomizdat, Moscow (1963) 98 (in Russian). [English translation: Reviews of Plasma Physics, Vol. 1, Consultants Bureau, New York (1965) 105.]
- [4] UCKAN, N.A., SHEFFIELD, J., in Tokamak Startup (KNOEPFEL, H., Ed.), Plenum Press, New York (1986) 45.
- [5] JT-60 TEAM: ABE, T., AIKAWA, H., AKAOKA, H., et al., in Plasma Physics and Controlled Nuclear Fusion Research 1986 (Proc. 11th Int. Conf. Kyoto, 1986), Vol. 1, IAEA, Vienna (1987) 11.
- [6] TFR GROUP, in Controlled Fusion and Plasma Physics (Proc. 11th Eur. Conf. Aachen, 1983), Vol. 7D, Part II, European Physical Society (1983) 493.
- [7] KOVRIZHNYKH, L.M., Transport Processes in Toroidal Magnetic Traps, Internal Rep. IC/70/86, International Centre for Theoretical Physics, Trieste (1970).
- [8] MARKLIN, G., MHD Stability of the Spheromak, PhD Thesis, Univ. of Maryland, College Park (1983).
- [9] TUBBING, B.J.D., LOPES CARDOZO, N.J., VAN DER WIEL, M.J., Tokamak heat transport, A study of heat pulse propagation in JET, submitted to Nucl. Fusion.
- [10] YAMADA, H., KUSANO, K., KAMADA, Y., UTSUMI, M., YOSHIDA, Z., INOUE, N., Observation of ultra-low q equilibrium, to be published in Nucl. Fusion.

All figures should be on separate sheets and numbered consecutively with Arabic numerals, e.g. Fig. 1. A separate list of captions must be provided (see also General above).

Tables must carry a heading and be numbered consecutively with Roman numerals in the order in which they are mentioned in the text, e.g. Table II. Footnotes to tables should be indicated by raised letters (not numbers or asterisks) and set immediately below the table itself. Tables should be typed clearly for possible direct reproduction.

Footnotes to the text should be numbered consecutively with raised Arabic numerals; excessive use of footnotes should be avoided.

All equations should be typed as carefully as possible, with unavailable Greek letters and other symbols clearly inserted by hand so that formulas may be reproduced without retyping. Specifically:

- (1) To eliminate confusion between symbols with similar appearance (e.g. between ones, eils and primes), make them as distinct as possible, if necessary marking them clearly by hand. In manuscripts with handwritten formulas, all further sources of confusion (such as n's and u's, u's and v's, e's and l's, J's and I's) should also be marked.
- (2) Indicate a vector by an arrow on top rather than by bold face lettering.
- (3) Tensors of second rank should bear two arrows on top; if higher rank tensors are required, choose an appropriate symbol and explain it.
- (4) Indicate the normal algebraic product by simple juxtaposition of symbols, i.e. without multiplication sign (\times).
- (5) Write scalar products of vectors with a raised point, e.g. $\vec{A} \cdot \vec{B}$.
- (6) Use the multiplication sign (\times) solely to designate: (i) a vector product, (ii) an algebraic (but not a scalar) product in the case where an equation has to be split over two lines, and (iii) in expressions like $3 \text{ cm} \times 3 \text{ cm}$ or $2 \times 10^6 \text{ cm}$.
- (7) The nabla operator (∇) does not carry an arrow.
- (8) When equations are split over two or more lines, place operational signs only at the beginning of each new line, not at the end of the preceding line (except at the end of a page). For direct reproduction of an equation, the length of the lines should not exceed 9 cm.
- (9) Where it is impossible to split long fractions over two lines, use negative exponents; similarly, replace root signs by fractional exponents where appropriate.
- (10) Do not use symbols, abbreviations and formulations that are recognizable only in a particular language.

Use SI units as far as possible; where this is not possible, please give the appropriate conversion factor.